GAMMA SPECTROSCOPIC STUDIES IN ^{45}Sc, ^{45}Ti, ^{46}Ti, ^{57}Co and ^{71}As

THESIS SUBMITTED TO THE DEPARTMENT OF PHYSICS,
UNIVERSITY OF DACCA, FOR THE DEGREE OF
DOCTOR OF PHILOSOPHY

384984

Dhaka University Library
384984

DIGITIZED

MD. MIZANUR RAHMAN

ঢাকা
বিশ্ববিদ্যালয়
গ্রন্থাগার

DACCA
JUNE, 1979

Physics

CONTENTS

		Page
ABSTRACT		
ACKNOWLEDGEMENTS		
CHAPTER-1	INTRODUCTION	1
CHAPTER-2	THE DOPPLER-SHIFT-ATTENUATION METHOD AND THEORY OF SLOWING DOWN	
2.1	Introduction	12
2.2	The Doppler shift of a gamma ray	13
2.3	Formula for attenuation factor $F(\tau)$	14
2.4	The LSS theory and the slowing down process	16
2.5	The electronic stopping	19
2.6	The nuclear stopping	20
2.7	The deflection	21
2.8.	Calculation of attenuation factor $F(\tau)$	23
2.9	The analysis	28
2.10	Accuracy of the theory of slowing down	29
2.11	Other treatments of ion-atom collisions	32
2.12	Limitations and uncertainties	33
CHAPTER-3	EXPERIMENTAL PROCEDURE	
3.1	Principle of measurement	36
3.2	The target chamber	39
3.3	The electronics	42
3.4	Determination of the mean value of $\cos\theta$	44
3.5	The experiment in general	47

384984

ঢাকা
বিশ্ববিদ্যালয়
গ্রন্থাগার

		Page
3.6	Target preparation	51
3.7	Analyses of spectra	51
3.8	Calculation of weighted mean	53
CHAPTER-4	LIFETIME MEASUREMENTS IN ^{46}Ti	
4.1	Introduction	54
4.2	The experiment	56
4.3	Analysis	58
4.4	Results and discussions	64
CHAPTER-5	LIFETIME MEASUREMENTS IN ^{45}Sc	
5.1	Introduction	69
5.2	The initial velocity	71
5.3	Calculation of averaged attenuation factor $\widetilde{F(\tau)}$ vs. τ curve for recoiling nuclei having undefined initial velocity	73
5.4	The experiment	78
5.5	Analyses	80
5.6	Results and discussions	82
CHAPTER-6	LIFETIME MEASUREMENTS IN ^{45}Ti	
6.1	Introduction	91
6.2	The experiment and analyses	92
6.3	Results and discussions	93
CHAPTER-7	LEVEL SCHEME AND LIFETIME MEASUREMENTS FOR ^{71}As	
7.1	Level scheme	
7.1.1	Introduction	96

384984

Dhaka University Institutional Repository

		Page
7.1.2	Experimental procedure	97
7.1.3	The electronic set-up	100
7.1.4	Efficiency calibration of Ge(Li)detector	101
7.1.5	Energy calibration	102
7.1.6	Results and discussions	103
7.2	Lifetime measurements in ^{71}As	
7.2.1	Introduction	112
7.2.2	Experimental procedure	112
7.2.3	Density of germanium dioxide	112
7.2.4	Results and discussions	113
CHAPTER-8	LEVEL SCHEMES AND GAMMA-RAY ANGULAR DISTRIBUTION MEASUREMENTS IN ^{57}Co	
8.1	Introduction	115
8.2	Experimental procedure	124
8.3	Efficiency calibration	126
8.4	Energy calibration	126
8.5	Results and discussion	127
8.5.1	Level scheme in ^{57}Co	127
8.5.2	Gamma-ray angular distribution and spin assignments	140
8.5.3	General remarks	142
CHAPTER-9	CONCLUSIONS	147
REFERENCES		

Dhaka University Institutional Repository

ABSTRACT

The Doppler-shift-attenuation (DSA) method has been used to determine the lifetimes of the levels in ^{46}Ti, ^{45}Sc and ^{45}Ti by (p,γ), $(p,p'\gamma)$ and $(p,n\gamma)$ reactions respectively on ^{45}Sc target.

A target chamber with two-target arrangement has been used in lifetime measurements to avoid the problem of gain drift. The lifetimes of the long-lived states determined from the present measurements agree quite well with the previous measurements, although these long lifetimes are close to the limit where the use of DSA method is no longer possible. This agreement demonstrates that the two-target arrangement is very useful for DSA work.

Calibrated attenuation function $F(\tau)$ versus lifetime τ curves with correction factor $f_e = f_n = 0.9$ have been used for the extraction of lifetimes. To take into account of the undefined kinematics and Q-value dependence, the averaged attenuation factor $\widetilde{F(\tau)}$ were calculated from the above calibrated attenuation factor for extraction of lifetimes in ^{45}Sc and ^{45}Ti.

Lifetimes of 12 states and limit for one state in ^{46}Ti have been determined from the (p,γ) reaction on ^{45}Sc. The lifetimes (in fs) of the levels (keV) in ^{46}Ti as obtained in this work are: 889.2(6000^{+9000}_{-2500}); 2009.8(2200 ± 400); 2961.8(240 ± 10); 3058.6(3900^{+2700}_{-1300}); 3168.0(275^{+45}_{-35});

Dhaka University Institutional Repository

3235.7(42^{+10}_{-4}); 3298.8(1390±155); 3441.7(> 2500); 3569.4 (302±35); 3571.7(280^{+25}_{-20}); 3723.9(85±5); 3845(15±5) and 3905.6(55^{+20}_{-13}). The discrepancies in lifetimes in ^{46}Ti between two previous works seem to have been removed from the present measurements. The B (E2) values and the transition strengths $|M|^2_{W.u.}$ for the members of the ground state band, namely the $6^+_1 \rightarrow 4^+_1$, $4^+_1 \rightarrow 2^+_1$ and $2^+_1 \rightarrow 0^+_1$ transitions in ^{46}Ti have been obtained. The B(γ L) values and transition strengths have been obtained for some other levels also.

A complete set of lifetimes of 18 levels in ^{45}Sc up to E_x = 2778 keV has been obtained for the first time from the present measurements of the ^{45}Sc(p,p'γ) reaction. The lifetimes (in fs) of the levels (keV) in ^{45}Sc as obtained in this work are: 376(5100±800); 543(7600±1300); 720(313±70); 939(> 3800); 974(3600±500); 1067(380±70); 1237 (2400±150); 1303(3250^{+1200}_{-650}); 1409(385±20); 1662(150±10); 1800(110^{+15}_{-8}); 2092(< 10); 2151(400^{+160}_{-110}); 2303(250±25); 2352(52±3); 2531(30±7); 2590(15±7) and 2778(< 25). The present lifetime values of the 543, 939, 974, 1303 and 1800 keV states are in good agreement with the results obtained from ^{42}Ca(α,pγ)^{45}Sc reaction by Toulemonde et al. Lifetimes of other levels in ^{45}Sc agree quite well with previous works except for a few levels as measured by Schulte et al. and Rust et al. from (p,γ) and (p,p'γ) reactions respectively. But since the lifetime values determined in the present work for the 543, 720, 974, 1237, 1409, 1662, 1800 and 2092 keV

Dhaka University Institutional Repository

levels are in good agreement with those obtained by resonance fluorescence data, present values for other levels should be regarded as reliable.

The E2 transition probabilities for the ground state transitions of the 5 multiplet states of 376($3/2^-$),720($5/2^-$), 1237($11/2^-$), 1409($7/2^-$) and 1662($9/2^-$) keV in ^{45}Sc have been obtained and are compared with previous measurements. Transition strengths have been calculated for other levels also.

Lifetimes of 5 levels in ^{45}Ti have been determined from the ^{45}Sc(p,nγ) reaction. The lifetimes (in fs) of the levels (keV) in ^{45}Ti as obtained in this work are: 744(9000^{+6600}_{-1650}); 1226(3700^{+1250}_{-800}); 1353(125 ± 6); 1468(720 ± 100) and 1521(31 ± 5). It was possible to check the mean lifetimes for the 744 and 1226 keV levels given by the only other measurement of Blasi *et al.* which is found to be in agreement with the present results; prior to Blasi *et al.* only lower limit of lifetime for these two levels were given by other authors. Except for the 1521 keV level results agree quite well with the previous works. Transition strengths have been calculated for the 744, 1226 and 1521 keV levels assuming pure multipole radiation.

Information on the ^{71}As nucleus is meagre. The Ge(Li) - NaI(Tl) coincidence spectra and γ-ray singles spectra from the ^{70}Ge(p,γ)^{71}As reaction have been measured

Dhaka University Institutional Repository

at E_p = 2.8 MeV. A decay scheme for ^{71}As up to E_x=2874 keV is proposed. A previously known level at 510 keV is found to be a doublet; the second member has an energy of 506 keV. A new level at 1192 keV is assigned tentatively. Lifetimes of 10 levels in ^{71}As have been determined for the first time. Transition strengths have been calculated using the present lifetime values.

Angular distribution of the γ-rays have been measured and decay schemes have been constructed from the ^{56}Fe(p,γ)^{57}Co reaction for resonances at E_p = 1248, 1652 and 2065 keV. The γ-decay and energy of 31 levels in ^{57}Co are found to agree fairly well with those of previous workers. A level at 3534 keV is assigned tentatively. Some transitions from the low-lying and resonance levels have been observed new. The decay scheme of the 2065 keV proton resonance has been studied for the first time. The spins of the 7253, 7650 and 2065 keV resonant states corresponding to the E_p = 1248, 1652 and 2065 keV resonances have been assigned as 3/2.

Dhaka University Institutional Repository

ACKNOWLEDGEMENTS

It is a great pleasure for me to express my heartfelt gratitude to Professor H.M. Sen Gupta for his kind supervision, guidance and constant help during the work. I express my deep sense of gratitude to Professor Dr. F. Rauch for his invaluable help, numerous useful discussions and encouragement during the measurement of lifetimes at Frankfurt, West Germany.

I am thankful to Professors A.K.M. Siddiq and M. Hussain, Dacca University and Mr. A.H.M. Habibul Islam, Director, Atomic Energy Centre, Dacca for providing me with facilities for work. Thanks are due to Mrs. Sofia Khatun, Dr. M.A. Rahman, Dr. M.A. Awal and Mr. N.I. Molla for their invaluable help at different stages of the work. I thank Mr. H. Reza for preparing targets and the personnel of the Van de Graaff accelerator and the Computer Division, Atomic Energy Centre, Dacca for helpful co-operation.

I am thankful to Professor Dr. E. Schopper, Director, Institut für Kernphysik, University of Frankfurt, for providing me with the facilities at the Institute. Thanks are due to Dr. H.P. Nottrodt, for his help and discussions during the work on lifetime measurements. The help of Mr. P. Hübener and Mr. G. Glas is acknowledged. I thank Dr. Waldschmidt and Mr. J. Doppner for preparing targets. I also thank the personnel of the Van de Graaff accelerator and UNIVAC 1108 computer at the Institute and University respectively.

I am grateful to the DAAD authorities for the financial support during my stay at Frankfurt, West Germany.

Dhaka University Institutional Repository

CHAPTER-1

INTRODUCTION

In addition to the ground state, nuclei also exist in excited states for a measurable period of time. The excited nuclei decay to the states of lower energy by the emission of, say, gamma radiation. The lifetime of a nuclear excited state can be defined as the mean time during which a nucleus exists in that state before it decays to a state of lower energy. An attempt is now made to describe the importance of the measurements of nuclear lifetimes and the sensitivity of nuclear lifetimes on the nuclear structure. The lifetimes of excited nuclear states have their relations to the electromagnetic properties of nuclei. The electromagnetic interactions within nuclei offer a useful and detailed source of information about the structure of nuclei.

The electromagnetic transition probability depends strongly on the wave functions of the initial and final states. The mean lifetime τ of a nuclear state is equal to the reciprocal of the transition probability. A measurement of lifetimes thus helps one to test the wave functions of a particular nuclear model. Nuclear models have been constructed to understand the properties of nuclei. These models are to be verified by experimental data for their validity. One can use the electromagnetic transition probability for this purpose. The extreme single-particle

Dhaka University Institutional Repository

shell model is a simple model. In this model a single-particle transition is considered. That means it is assumed that the radiation arises from the transition of a single nucleon from one orbital state to another. The measured transition probability can be conveniently expressed in single-particle units.

A brief review of the theory of multipole radiation with respect to transitions between nuclear states is given below to outline the relation and sensitivity of nuclear lifetimes to the nuclear structure. The description is independent of any particular nuclear model. We refer to a review paper by Siegbahn[1] for details.

Let us consider an electromagnetic radiation emitted by a transition from an initial state i to a final state f. Let us also consider that the initial and final states are specified by $(J_i\ \pi_i)$ and $(J_f\ \pi_f)$ respectively. J and π are the angular momentum and parity respectively. The allowed multipolarities are governed by the relation:

$$\left|J_i - J_f\right| \leq L \leq \left|J_i + J_f\right| \qquad (1\text{-}1)$$

and

$$\Delta\pi = (-1)^L \text{ for electric multipole (EL)}$$

$$\Delta\pi = (-1)^{L+1} \text{ for magnetic multipole (ML)}$$

where $\Delta\pi$ is the change in parity in going from the state i

Dhaka University Institutional Repository

to the state f. For an electromagnetic decay the transition probability for a gamma transition of multipolarity L from an excited state i to the final state f is expressed as (ref. 1)

$$T(\sigma L; i \rightarrow f) = \frac{8\pi(L+1)}{L\left[(2L+1)!!\right]^2} \frac{1}{\hbar}\left(\frac{E}{\hbar c}\right)^{2L+1} B(\sigma L; J_i \rightarrow J_f) \quad (1\text{-}2)$$

where E_γ is the gamma ray energy and $(2L+1)!! = 1.3.5...(2L+1)$, $B(\sigma L; J_i \rightarrow J_f)$ is the reduced transition probability and is defined by

$$B = \sum_{M_f \mu} \left| \langle J_f M_f | M^\sigma (L\mu) | J_i M_i \rangle \right|^2 \quad (1\text{-}3)$$

The quantities M_i, M_f and μ are the Z components of J_i, J_f and L respectively. The operator $M^\sigma (L\mu)$ is the multipole operator which causes the transition via the emission of the corresponding multipole radiation. By the index σ is referred to the electric or magnetic character of the radiation. It may be seen that the transition probability is proportional to the square of an electromagnetic matrix element. The squared matrix element in the expression (1-3) contains the nuclear structure information. It is thus required to experimentally measure the transition probability $T(\sigma L; i \rightarrow f)$ to obtain B, the reduced transition probability connecting the initial state i to the final state f. When a gamma decay of multipolarity L is the only decay mode, then the lifetime of the initial state is directly related to the transition probability $T(\sigma L; i \rightarrow f)$.

Dhaka University Institutional Repository

A transition can, in fact, involve radiation of all multipolarities governed by the selection rules given by relation (1-1). If the wave functions of the initial and final states are known then the transition probability can be calculated with the help of the expressions (1-2) and (1-3). It can be shown from these calculations that the lowest allowed multipole order has the largest probability. That is the electromagnetic interaction decreases rapidly with increasing L and as a result only the lowest allowed L for the electric and magnetic multipoles are important. Sometimes a mixture of M1-E2 polarities is also present. When a multipole mixing ratio occurs, the corresponding δ^2 must be determined in order to obtain both transition probabilities separately. The mixing ratio is defined by

$$\delta^2 = \frac{T(M1;\ i \rightarrow f)}{T(E2;\ i \rightarrow f)} \qquad (1\text{-}4)$$

A measured lifetime τ can be used to test the calculated transition probability according to the following expression

$$\frac{1}{\tau} = T = \sum_L (1+\alpha(L))\ T(\sigma L;\ i \rightarrow f) \qquad (1\text{-}5)$$

In the above expression T is the total transition probability for a given initial state i and is the sum over the lowest multipole order L. The factor $(1+\alpha(L))$ is the internal conversion effect and $\alpha(L)$ is the total conversion coefficient corresponding to the 2^L - pole radiation.

Dhaka University Institutional Repository

The total transition probability T is the quantity which is determined in a lifetime measurement of a given excited state. It is thus possible to obtain reduced transition probability from lifetime measurement.

The subject of the measurement of nuclear lifetimes has been reviewed by several authors [2-5]. Nuclear lifetimes are generally short and cannot be measured by mechanical means. There are different methods for the measurement of lifetimes of nuclear states. Each method has specific advantages and applicability and is suitable for a particular region of lifetime. The indirect techniques used for the determination of lifetime are: Resonance fluorescence method, capture cross-section measurements, Coulomb excitation, inelastic electron scattering and inelastic particle scattering. The microwave and channeling techniques are among the direct techniques. Fossan and Warburton [5] have described in details the other very popular direct methods with the regions of application. The three direct methods are: Delayed coincidence method, recoil distance method (RDM) and Doppler-shift attenuation (DSA) method. These three direct methods can be applied favourably in the following lifetime regions approximately:

$\tau > 10^{-10}$ sec. for electronic timing

5×10^{-12} sec $< \tau < 10^{-10}$ sec. for RDM method

$\tau < 5\times10^{-12}$ sec. for DSA method

Dhaka University Institutional Repository

A substantial fraction of nuclear states occurs in nature that have lifetimes in the range of approximately 10^{-11} to 10^{-15} sec. Thus because of its applicability to many nuclear states, the DSA method is being currently popularly used to determine the lifetimes of nuclear states. In the present measurements the DSA method has been used to determine the lifetimes of excited states in ^{46}Ti, ^{45}Sc, ^{45}Ti and ^{71}As.

The description of the early developments of DSA techniques with the help of NaI(Tl) detectors has been given by Devons [6] in 1954. In those days this method could be applied only to a limited number of cases because of the very poor resolution of the NaI(Tl) detectors. The other measurements [7-8], heavy ion work of Litherland et al. [9] and developments of Warburton et al. [10] are significant works with NaI(Tl) detectors. With the introduction of the Ge(Li) detectors with an improved resolution of 2 to 3 keV, the DSA method has become a favourite method for the measurement of short lifetimes.

Studies of nuclear lifetimes using the DSA method have been discussed in detail by several authors [11-15]. The concept of Dopplershift is utilised in the Doppler-shift attenuation method. The Doppler-shift can be defined as the velocity dependent change in energy. In this method a level is first excited by a nuclear reaction which decays with

Dhaka University Institutional Repository

emission of γ-rays. Since the excited nuclei are moving when they decay, there is a shift in energy of the emitted gamma rays. These shifts depend on the velocity of the recoiling nuclei just at the time of emission of the gamma rays. So the mean lifetime τ of a decaying state can be obtained if a time scale can be derived from the slowing down time of the recoiling nuclei in the stopping medium. For this purpose one has to calculate the attenuation factor $F(\tau)$ versus lifetime τ curve.

In the present measurements the calculation of the theoretical ratio $F(\tau)$ between the observed Doppler-shift ΔE_γ^{obs} and the maximum shift ΔE_γ^{max} has been performed by using the dimensionless variables formulated by Lindhard et al. [16-18] and the expressions for multiple scattering given by Blaugrund [19]. The Doppler-shift attenuation method, the theory of slowing down and the calculation of the theoretical attenuation factor $F(\tau)$ are described in chapter 2.

Doppler-shift attenuation measurements are based on the energy difference of the gamma ray peaks observed at two different angles. For this purpose many hours of runs are necessary for the measurement of gamma ray spectra. Consequently there is a serious problem of electronic gain drift. Now in the measurements of very short lifetimes peak positions should be determined accurately. But the

Dhaka University Institutional Repository

gain drift gives wrong information on the measured lifetimes. To get rid of this disturbing problem of gain drift a target chamber with two-target arrangement has been used in the present measurements. This target chamber makes it possible to measure the gamma-ray spectra at both the forward and backward angles simultaneously. Experimental arrangements with similar idea have been used by two other authors [20-21]. Detailed description of the two-target arrangement together with the experimental set-up are given in chapter 3.

Lifetimes in ^{46}Ti have been measured in several previous experiments [22-24]. There are discrepancies in the results obtained by these authors. In the present measurement the reaction ^{45}Sc(p,γ)^{46}Ti has been investigated to determine the lifetimes in ^{46}Ti by the Doppler-shift attenuation method. A calibration of the stopping process in ^{45}Sc was necessary since this might influence the accuracy of the lifetimes in ^{46}Ti. The calibration of the F(τ) curve was obtained by measuring the lifetimes of the 720, 1237, 1409, 1662 and 2092 keV levels in ^{45}Sc by (p,p'γ) measurements and comparing these results with resonance fluorescence data [25] for the same levels. A correction factor of f = 0.9 was found to fit well and was used for F(τ) curve calculations. The ^{45}Sc(p,p'γ) measurements are described in chapter 5. An attempt has been made in the ^{45}Sc(p,γ) experiment to remove the discrepancies among the various previous measurements. The other purpose was to obtain a complete set

Dhaka University Institutional Repository

of lifetimes upto an excitation energy of 4.0 MeV and to obtain electromagnetic decay properties for this nucleus. The results are discussed in chapter 4.

In the (p,γ) reaction the attenuation factor $F(\tau)$ has been calculated considering the velocity of the center of mass as the initial velocity of the recoiling nuclei. But in a $(p,p'\gamma)$ reaction the initial velocity is the resultant of the velocity of the center of mass and the velocity of the recoiling nuclei in the center of mass system which is caused by the emission of the inelastic proton. The inelastic scattering of protons causes a range of initial velocities for the recoiling nuclei. Thus it was necessary to have an average over all initial velocities using the angular correlation function as the weighting factor. To consider this factor the averaged attenuation factor $\widetilde{F(\tau)}$ has been calculated according to Moazed et al. [11]. This is described in the beginning of chapter 5.

The lifetimes of levels in ^{45}Sc have been determined by a few authors [25, 25a, 26-29]. For some of these levels there exist discrepancies among the various measurements. For other levels only one measurement is available until now. In the present measurement the levels in ^{45}Sc were populated by the $^{45}Sc(p,p'\gamma)$ reaction at E_p=3.0 and 4.5 MeV to determine lifetimes by DSA method. The objective of the present measurements were the following : an attempt to remove the discrepancies in

Dhaka University Institutional Repository

the previous measurements, to obtain a complete set of lifetimes up to an excitation energy of about 3.0 MeV, to check the values of those states for which only a single measurement is available and to calculate the reduced transition probabilities and transition strengths from the measured lifetimes. The results are discussed in chapter 5.

Lifetimes in ^{45}Ti have been previously measured by Zuk et al. [30], Iyengar et al. [31] and Blasi et al. [31a]. During the measurements of ^{45}Sc(p,p'γ) reaction at E_p=4.5 MeV the levels in ^{45}Ti were simultaneously populated by ^{45}Sc(p,nγ) reaction which afforded the opportunity to determine lifetimes of 5 levels in ^{45}Ti. The results are discussed in chapter 6.

Information on the nucleus ^{71}As is meagre. Broman and Rosner [32] obtained 10 levels and Betts et al. [33] obtained 27 levels from their (^{3}He,d) work. Energy levels are not usually accurately given in the (^{3}He,d) reaction. Hundelshausen [34] proposed a decay scheme of only 5 levels up to an excitation energy of 1265 keV from the ^{71}Se (β^-) decay work. During our measurements Heits et al. [35] have reported information on the level schemes of this nucleus from the ^{69}Gd(α,2n)^{71}As reaction. Because of the large angular momentum in the incoming channel in this reaction, mostly the high-spin states were populated. Liu et al. [36] studied the level scheme up to 2947 keV by the (p,γ) reaction on ^{70}Ge. The low-lying low-spin states and their decay schemes are not well established and lifetimes are

Dhaka University Institutional Repository

not known at all. Thus the present measurements were carried out using the $^{70}Ge(p,)^{71}As$ reaction to obtain more information on the ^{71}As nucleus including lifetimes. Results are discussed in chapter 7.

Angular distribution measurements of -radiation from an excited nucleus yield valuable information on multipole mixing ratios and nuclear level spins. Such measurements have been done on many targets. The properties of the proton-capture states in ^{57}Co have been studied by several authors through $^{56}Fe(p,\gamma)^{57}Co$ reaction. Discrepancy exists in the spin assignments for some of the resonance levels in ^{57}Co and assignments for other levels have not been done. Discrepancy also exists in the level schemes obtained by different (p,γ) measurements and also among (p,γ), $(^{3}He,d)$, $(p,n\gamma)$ and other measurements as summarised in Nuclear Data Sheets [37]. The present angular distribution measurements were carried out to obtain spin values of resonance levels at E_p=1248, 1652 and 2065 keV through $^{56}Fe(p,\gamma)^{57}Co$ reaction. The level and decay schemes with branching ratios have also been constructed from the spectra at 90° and 55° at all the above three resonances. This is given in chapter 8.

Dhaka University Institutional Repository

CHAPTER-2

THE DSA METHOD AND THE THEORY OF SLOWING DOWN

2.1 Introduction

The principle of the Doppler effect has been utilised in nuclear physics to determine the lifetimes of excited states of nuclei. According to this effect the energy of the electromagnetic radiation emitted from a moving source is different from what would be measured if the source were at rest i.e. there is a shift in energy of the emitted gamma rays. In the Doppler-shift attenuation (DSA) method these shifts in the energy of the emitted gamma rays from nuclei in motion are measured. After a nuclear reaction the excited nuclei are slowed down in the target material itself or in the backing material. Then the shifts in the energy of these moving nuclei depend on the velocity at the time of gamma emission. Thus the DSA method compares the decay time of the nuclei with the slowing down time of the nuclei in the medium through which they are moving. To know the time dependence of slowing down one has to calculate the attenuation factor $F(\tau)$ versus lifetime τ curve.

The main experimental requirement of the Doppler-shift attenuation technique is the production of a unidirectional and monoenergetic beam of excited nuclei with a certain velocity from a nuclear reaction. This is achieved by the bombardment of a suitable target with particles accelerated with the aid of an accelerator. Mean lifetimes of nuclear excited states

Dhaka University Institutional Repository

between 10^{-15} sec and 10^{-11} sec can be measured by this method. Lifetimes of many nuclear states lie in this region. So this method is suitably applied for lifetime determination.

2.2 The Doppler-shift of a gamma ray

Let us consider an excited nucleus N moving with a velocity v(t), as shown in fig. 2.1. Let us also suppose a gamma transition between an initial state E_i and a final state E_f. So the energy of the emitted gamma ray is given by

$$E_{\gamma_0} = E_i - E_f$$

Since the nucleus is in motion, the gamma-ray energy emitted in the decay is also susceptible to Doppler-shift. So the

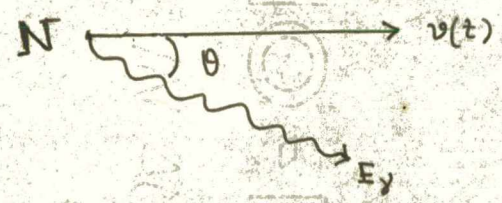

Fig. 2.1. An excited nucleus N moving with a velocity v(t) emits a gamma ray of energy E_γ at an angle θ relative to the direction of motion.

shifted gamma-ray energy emitted from the excited moving nucleus at an angle θ relative to the direction of the recoiling nuclei and moving with a velocity v(t) is given in the laboratory system as

$$E_\gamma = \frac{E_{\gamma_0}(1+(v(t)/c)\cos\theta)}{(1-(v(t)/c)^2)^{1/2}}$$

where c is the velocity of light and E_{γ_0} is the unshifted γ-ray

Dhaka University Institutional Repository

energy that would be observed if the nuclei decayed at rest. If we neglect the relativistic effects, that means if $v \ll c$, then the above expression simplifies to

$$E_\gamma = E_{\gamma_0}(1+(v(t)/c)\cos\theta) \qquad (2\text{-}1)$$

The difference between the shifted and the unshifted γ-ray energy i.e. the observed Doppler-shift is expressed as

$$\overline{\Delta E_\gamma^{obs.}} = E_{\gamma_0}\frac{v(t)}{c}\cos\theta$$

After a nuclear reaction the gamma rays are measured at two different angles θ_1 and θ_2. The above expression is then

$$\overline{\Delta E_\gamma^{obs.}} = E_{\gamma_0}\frac{v(t)}{c}(\cos\theta_1 - \cos\theta_2) \qquad (2\text{-}2)$$

Extraction of lifetimes from the Doppler-shift depends on the knowledge of the velocity of the nucleus as a function of time after the nucleus has been excited. A measured Doppler-shift establishes the velocity and so the time at which the nucleus decays. The time dependence is known from the calculation of the attenuation factor.

2.3. Formula for attenuation factor

Let us consider a nuclear reaction which produces a monoenergetic and unidirectional beam of excited nuclei all with initial velocity v_0 at time $t=0$ and that they decay with a mean lifetime τ by emission of gamma rays whose unshifted energy is given by E_{γ_0}. As the nuclei slow down in the stopping medium, which may be the target material itself, their rate

Dhaka University Institutional Repository

of decay is given by the radioactive decay law as

$$\frac{d}{dt} N(t) = -\frac{N_0}{\tau} e^{-t/\tau} \qquad (2\text{-}3)$$

where N(t) is the number of nuclei that have not decayed in time t and N_0 is the initial number of nuclei. The fraction of nuclei which decays between time t and (t+dt) is given by relation (2-3). The average shift can be obtained by multiplying these fractions of nuclei with the shift given by relation (2-2) and integrating over all time i.e. all decays. The average measured Doppler shift is expressed as

$$\overline{\Delta E_\gamma^{obs.}} = \frac{E_{\gamma_0}(\cos\theta_1 - \cos\theta_2)}{c\tau} \int_0^\infty \overline{v(t)}\, e^{-t/\tau} dt \qquad (2\text{-}4)$$

where $\overline{v(t)}$ is the average velocity at time t. The maximum possible shift that would be observed if all the nuclei decayed at velocity $v(t) = v_0$ can be obtained from reaction kinematics. The maximum possible shift is given by

$$\Delta E_\gamma^{max} = E_{\gamma_0}(v_0/c)(\cos\theta_1 - \cos\theta_2) \qquad (2\text{-}5)$$

The ratio of the observed shift to maximum shift is called the attenuation factor and is given by the relation

$$F(\tau) = \frac{1}{v_0\tau} \overline{v(t)}\, e^{-t/\tau} dt \qquad (2\text{-}6)$$

The expression (2-6) has been modified by Blaugrund [19] to take into account the average change in the direction of the recoiling nuclei as a result of the multiple ion-atom collisions and

Dhaka University Institutional Repository

the expression is given by

$$F(\tau) = \frac{1}{v_0 \tau} \int_0^{\infty} \overline{v(t)}\ \overline{\cos \phi(t)}\ e^{-t/\tau} dt \qquad (2\text{-}7)$$

and the observed shift is given by

$$\overline{\Delta E_\gamma} = E_{\gamma_0} 1/c\ \overline{v(t)}\ \overline{\cos \phi(t)}\ (\cos \theta_1 - \cos \theta_2) \qquad (2\text{-}8)$$

The Blaugrund [19] approximation is discussed in section (2-7). In order to evaluate the mean lifetime τ of a nuclear excited state from the observed Doppler shift, the attenuation factor must be calculated using the slowing down theory of Lindhard, Scharff and Schiøtt [16-18] (LSS theory) and Blaugrund [19] approximation.

2.4. The LSS theory and the slowing down process

Extraction of lifetimes is possible only when the velocity of the nuclei in the slowing down medium is known as a function of time. The function $\overline{v(t)}$ in relation (2-7) can be obtained only when the stopping power dE/dx for the recoiling nuclei in the stopping medium is known. Sometimes this time dependence is available from range experiments [38-41]. But because of the meagre experimental information one has to apply the theory of Lindhard *et al.* [16-18] to obtain the theoretical estimate for the stopping power dE/dx.

An ion moving with a velocity v(t) is slowed down in matter by collisions with atoms. The ion-atom interaction

Dhaka University Institutional Repository

depends on the velocity of the moving ion. When the velocity is high the influence of atomic and ionic electrons is negligible and the interaction is Coulomb potential causing only the Rutherford scattering. At low velocity, screening of the nuclear charge comes into account which results in a screened Coulomb force. In DSA measurements the velocities of the recoiling nuclei are generally low ($v/c \sim 0.1\%$). Therefore the discussions here will be limited to collisions with low velocities. At low velocities there are two mechanisms which are important for the slowing down of the moving nuclei:

a) Excitation and ejection of electrons by inelastic process. In this process the kinetic energy of the moving ion is decreased in exciting and ejecting electrons but there is no deflection of the ion from the original direction of motion because of the negligible mass of the electrons compared to the mass of the ion. This process is the electronic stopping.

b) In the elastic collision the ion loses its kinetic energy in transferring energy to translational motion of an atom as a whole and is also deflected from the original direction of motion. This process is the nuclear stopping.

The stopping cross-section S is an important quantity in the slowing down process and can be defined as the energy loss per scattering centre. It is given by

$$S = dE/dx \; 1/N = \int T(\theta) \, d\sigma \, (T(\theta)) \qquad (2\text{-}9)$$

where dE/dx is the energy loss per unit length, N is the number

Dhaka University Institutional Repository

of scattering centres per unit volume and $d\sigma$ is the differential cross-section for an energy transfer $T(\theta)$ to atoms and atomic electrons for scattering angle θ.

The most comprehensive treatment of the slowing down process is given by Lindhhard, Scharff and Schiøtt [16] (LSS). They have described the slowing down of moving ions in amorphous matter and treated the electronic stopping and nuclear stopping separately. Since the energy loss to electrons has also to do with atoms, the description is an approximate one. For collisions at low velocities one has to know electron distribution in atomic space. Lindhard et al. [16-18] have used the distribution given by the Thomas-Fermi model for the atoms. In this model the electrons are considered as a degenerate gas, the total charge is taken as continuous and it is supposed that there is equilibrium between the charge of the nucleus and the charge of the gas. These authors [16-18] have introduced dimensionless quantities for the convenience of calculation given by

$$\rho = \frac{4\pi a^2 N A_1 A_2}{(A_1+A_2)^2} X, \quad \varepsilon = \frac{a A_2}{z_1 z_2 e^2 (A_1+A_2)} E \qquad (2\text{-}10)$$

where ρ and ε are the dimensionless parameters proportional to the path length X and energy E. The subscripts 1 and 2 refer to the moving ion and the atoms of the stopping medium respectively. In these expressions .

$$a = 0.8853 \frac{h^2}{me^2} (z_1^{2/3} + z_2^{2/3})^{-1/2},$$

Dhaka University Institutional Repository

m and e are the mass and charge of an electron, z is the atomic number, A the atomic mass, N the number of atoms per unit volume, E the kinetic energy of the moving ion and X the length of the path. Lindhard et al. [16] defined the stopping power as

$$d\varepsilon/d\rho = (d\varepsilon/d\rho)_e + (d\varepsilon/d\rho)_n \qquad (2\text{-}11)$$

where $(d\varepsilon/d\rho)_e$ is the specific energy loss due to collisions with electrons and $(d\varepsilon/d\rho)_n$ is the specific energy loss due to collisions with atoms.

At low velocities of the recoiling nuclei ($v/c \leq 0.35\%$), the energy loss is dominated by nuclear stopping. At higher velocities ($v/c > 1.5\%$), the relative importance of the nuclear stopping decreases and electronic stopping process becomes more important. The velocity region $v/c \doteq 0.5\text{-}1.5\%$ is a common one for DSA measurements by p, d, t, ^{3}He and ^{4}He beams. In this energy region both the processes of energy loss are important.

2.5. The electronic stopping

Electronic stopping is the completely dominating process in the slowing down of atoms with high velocity. The electronic stopping increases with increasing velocity of the ion reaching a maximum at the recoil velocity $v = v_0 z_1^{2/3}$ where $v_0 = c/137$ is the velocity of the ion in the first Bohr orbit. For velocities $v < v_0 z_1^{2/3}$ Lindhard and Scharff [17] have given

Dhaka University Institutional Repository

electronic stopping cross-section as

$$S_e = \xi_e 8\pi e^2 a_0 z_1 z_2 (z_1^{2/3} + z_2^{2/3})^{-3/2} \, v/v_0 \qquad (2\text{-}12)$$

where $a_0 = \frac{h^2}{me^2}$ and $\xi_e = z_1^{1/6}$

The relation is an approximate one.

In the region of $v/c < 1.5\%$, the electronic stopping is well represented by a linear dependence on velocity. Making use of relation (2-12) the specific energy loss due to electronic stopping is given by

$$(d\varepsilon/d\rho)_e = k \quad ^{1/2} \qquad (2\text{-}13)$$

with. $$k = \xi_e \frac{0.0793 \, z_1^{1/2} z_2^{1/2} (A_1+A_2)^{3/2}}{(z_1^{2/3}+z_2^{2/3})^{3/4} A_1^{3/2} A_2^{1/2}} \qquad (2\text{-}14)$$

2.6. The nuclear stopping

The nuclear stopping has been described by Lindhard et al.[16,18]. The scattering cross-section in the screened potential for the ion-atom interaction can be obtained by using an extrapolated perturbation method for classical scattering. The universal differential scattering cross-section arrived at is given by

$$d\sigma = \frac{\pi a^2 \, dt \, f(t^{1/2})}{2 \, t^{3/2}.} \qquad (2\text{-}15)$$

Dhaka University Institutional Repository

with $t^{1/2} = \varepsilon \sin \theta$. The function $f(t^{1/2})$ is determined by the kind of screening function occuring in the scattering potential. The values of function $f(t^{1/2})$ is given in ref. 16. With the help of relations (2-9), (2-10) and (2-15) the nuclear stopping cross-section can be written as

$$S_n = \frac{1}{\varepsilon} \int_0^{\varepsilon} f(x)dx \qquad (2\text{-}16)$$

The nuclear stopping power has been calculated according to Thomas-Fermi model given in ref. 42. In fig. 2.2 is shown the stopping cross-sections according to LSS-theory [16]. The abscissa is $\varepsilon^{1/2}$ i.e. proportional to velocity. The full drawn curve is the nuclear stopping $(d\varepsilon/d\rho)_n$ according to LSS-theory. The dot-and-dash line is the electronic stopping cross-section $k\varepsilon^{1/2}$. The value of k has been calculated for the particular case of ^{46}Ti nuclei recoiling in ^{45}Sc stopping medium as investigated in the present experiment.

2.7. The deflection

In sections 2.4, 2.5 and 2.6 has been described how the energy loss of the moving ions occurs. However the recoiling nuclei do not travel in the same direction in the stopping medium. Rather due to the multiple collisions of the recoiling nuclei with the atoms of the stopping medium, the direction of motion of the nuclei is changed by a scattering angle Ø in the lab. system

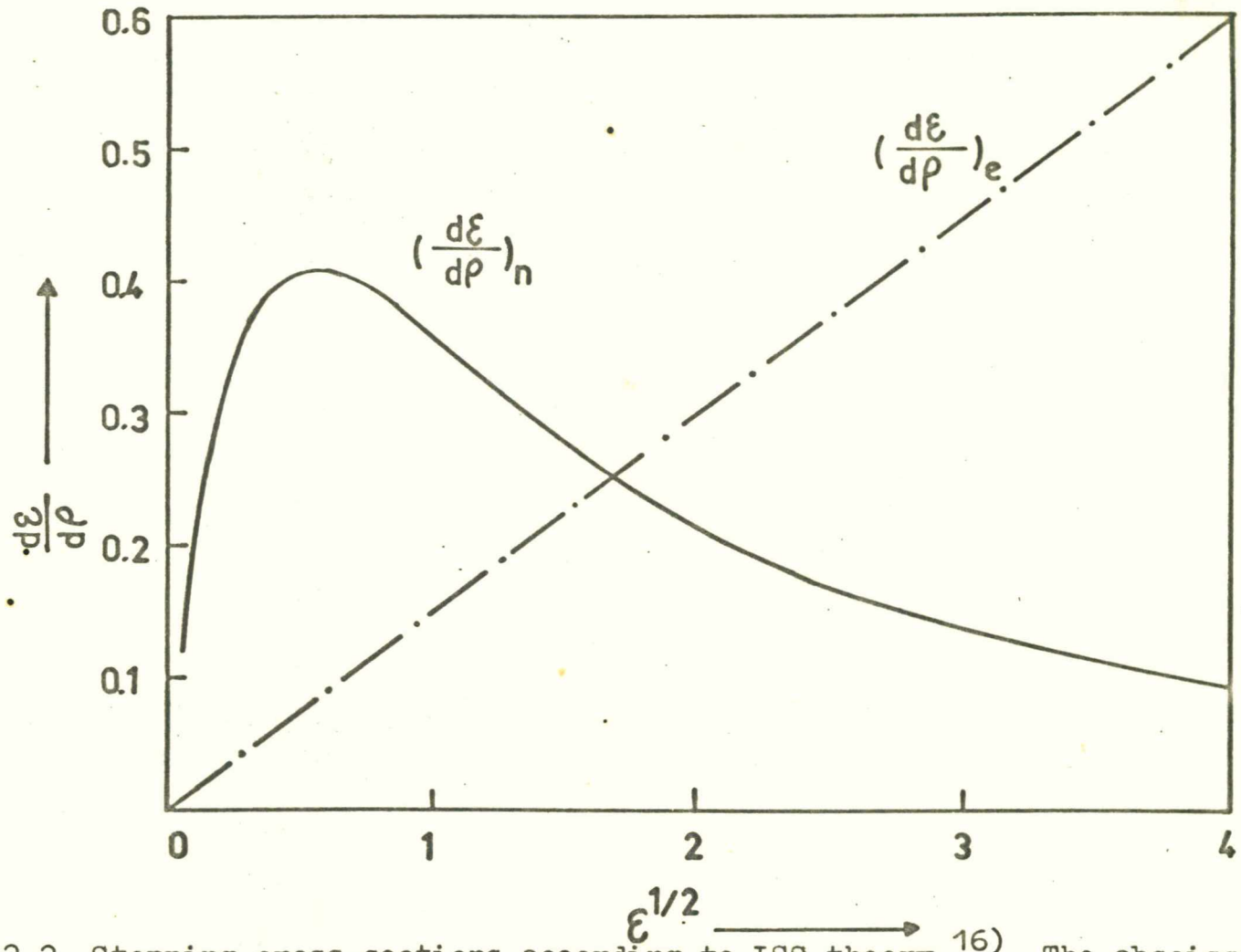

Fig. 2.2 Stopping cross-sections according to LSS-theory [16]. The abscissa is the reduced energy $\varepsilon^{1/2}$ i.e. proportional to velocity. The ordinate is the stopping cross-sections. The full drawn curve is the nuclear stopping cross-section. The dot and dash line is the electronic stopping cross-section, $k\,\varepsilon^{1/2}$. The value of k was calculated for ^{46}Ti nuclei recoiling in ^{45}Sc and was found to be 0.15.

Dhaka University Institutional Repository

Dhaka University Institutional Repository

(fig. 2.3) and consequently the Doppler-shift is changed by a factor of cos Ø. So when the DSA method is applied, the

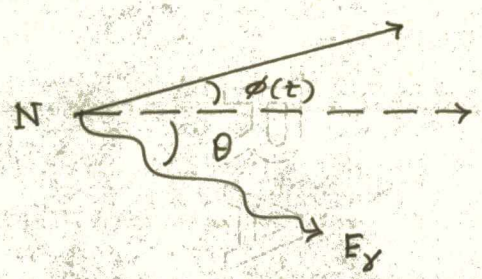

Fig. 2.3 The direction of motion of the recoiling nucleus N changes by a scattering angle Ø in the lab. system due to multiple ion-atom collision.

deflection of the recoiling nuclei from the original direction of motion has to be taken into consideration in order to account for the attenuation of the Doppler-shift. Thus the term $\overline{v(t)}$ in equation (2-6) requires to be replaced by $\overline{v(t)\cos Ø}$ which is the average projected velocity and $\overline{\cos Ø(t)}$ is the average cosine of the angles through which the recoiling nuclei have been scattered in time t. The term $\overline{\cos Ø(t)}$ has to be calculated as a function of time. Since the stopping of the ion involves many discrete collisions, an accurate evaluation of the process requires a statistical treatment such as Monte Carlo method, which is time consuming. However Blaugrund [19] has made an approximation. The essential point of Blaugrund treatment is the approximation

$$\overline{v(t)\cos Ø(t)} \simeq \overline{v(t)}\;\overline{\cos Ø(t)}.$$

Dhaka University Institutional Repository

Using formula (2-15) Blaugrund [19] has derived an expression for the deflection cos Ø(t). The derivation is based on the multiple-scattering theory developed by Goudsmit and Saunderson [42] and extended by Lewis [43]. The theory makes no distinction between the centre of mass angle and laboratory system because the recoil was assumed to be small. Blaugrund [19] generalised it for colliding particles having comparable masses and arrived at

$$\overline{\cos \phi(t)} = \exp(-\,1/2\; r\, G(r) I) \qquad (2\text{-}17)$$

where $r = A_2/A_1$ and $I = \int_{\varepsilon}^{\varepsilon_0} \frac{S_n}{\varepsilon(S_n+S_e)}\, d$

G(r) is given as a power series in r in ref. 19.

2.8. Calculation of attenuation curve

The DSA method compares the decay time of the recoiling nuclei with the slowing down time of the nuclei in the stopping medium. That means one has to know the time dependence of slowing down. In the present work the attenuation curve has been calculated according to ISS [16-18] theory and Blaugrund approximation [19] to evaluate the mean lifetimes of nuclear states from the observed Doppler-shift. The procedure of calculation is given below.

According to relation (2-7) the attenuation factor $F(\tau)$ is defined by

$$F(\tau) = \frac{1}{v_0 \tau} \int_0^{\infty} \overline{v(t)\, \cos \phi(t)}\; e^{-t(v)/\tau}\, dt$$

Dhaka University Institutional Repository

For the solution of the above integral a transformation of the variable $t \rightarrow v$ is made. So the above equation can be written as

$$F(\tau) = \frac{1}{v_0 \tau} \int_0^{\infty} v \, \overline{\cos \phi(v,v_0)} \, e^{-t(v)/\tau} \frac{dt}{dv} \, dv \qquad (2\text{-}18)$$

The quantities $\frac{dt}{dv}$, $t(v)$ and $\overline{\cos \phi(v,v_0)}$ are required to express as a function of velocity. The initial velocity v_0 is obtained from the reaction kinematics. In the following expressions index 1 is used for the recoiling nuclei and index 2 (or 2_i) for the atoms of the stopping medium. The kinetic energy of the recoils is given by

$$E_{kin.} = \frac{M_1}{2} v(t)^2 \qquad (2\text{-}19)$$

after time t, $$\frac{dE_{kin.}}{dt} = M_1 v(t) \frac{dv(t)}{dt} \qquad (2\text{-}20)$$

But $$v(t) = \frac{dx(t)}{dt}$$

So $$\frac{dt}{dv} = M_1 \frac{dx}{dt} \frac{1}{\frac{dE_{kin.}}{dt}} = M_1 \frac{1}{\frac{dE_{kin}}{dx}(v)} \qquad (2\text{-}21)$$

and integrating, $$t(v) = M_1 \int_v^{v_0} \frac{1}{\frac{dE_{kin.}}{dx}(v)} \, dv \qquad (2\text{-}22)$$

Using equations (2-21) and (2-21), equation (2-18) can

Dhaka University Institutional Repository

be rewritten as

$$F(\tau) = \frac{M_1}{\tau v_0}\int_0^{v_0} \frac{1}{\left|\frac{dE}{dx}(v)\right|} \exp -\left\{\frac{M_1}{\tau}\int_v^{v_0} \frac{1}{\frac{dE}{dx}(v)} dv\right\} v \overline{\cos \phi(v,v_0)}\, dv \quad (2\text{-}23)$$

It is seen from equation (2-23) that $F(\tau)$ can be calculated if the energy loss of the recoiling nuclei is known.

The energy loss calculated according to LSS [16-18] has been described in sections 2.4, 2.5 and 2.6. LSS used the dimensionless quantities ε and ρ (relations 2-10) for the energy and path length. The total energy loss is the sum of $(d\varepsilon/d\rho)_e$, the electronic energy loss, and $(d\varepsilon/d\rho)_n$, the nuclear energy loss and is given by

$$d\varepsilon/d\rho = f_e\, d\varepsilon/d\rho\big|_e + f_n\, d\varepsilon/d\rho\big|_n \quad (2\text{-}24)$$

where f_e and f_n are the correction factors for electronic and nuclear parts, respectively.

The stopping medium may have different kinds of atoms. So the energy loss is then

$$\frac{dE}{dx} = \sum_{i=1}^{N} \left(\frac{dE}{dx}\right)_i \quad (2\text{-}25)$$

Using the absolute values and equation (2-13), the electronic energy loss is given by

$$\left.\frac{dE}{dx}\right|_e^i = 8.7285 \times 10^{-3}\, N_i v \frac{z_1^{7/6}\, z_{2i}}{(z_1^{2/3}+z_{2,i}^{2/3})^{3/2}} \left(\frac{MeV}{\mu}\right) \quad (2\text{-}26)$$

Dhaka University Institutional Repository

where $(N_i) = 10^{22}/cm^3$ and $(v) = 10^8$ cm/s.

A good approximation by Engelbertink et al.[44] for the LSS nuclear stopping is

$$\left(\frac{d\varepsilon}{d\rho}\right)_n = -0.2 \log_{10}\left\{\frac{\varepsilon^{1.125}}{70.0} + \frac{0.002}{\varepsilon^{0.815}}\right\} \qquad (2\text{-}27)$$

so that

$$\left.\frac{dE}{dx}\right|_n^i = -0.2\, C_{2,i} \log_{10}\left(2.3879\times10^{-5} W_i^{1.215} + \frac{0.1458}{W_i^{0.815}}\right)\left(\frac{MeV}{\mu}\right) \qquad (2\text{-}28)$$

where $W_i = A_1 C_i v^2$,

$$C_i = 3.2533\times10^4 \frac{A_{2,i}}{z_1 z_{2,i}(A_1+A_{2,i})(z_1^{2/3}+z_{2,i}^{2/3})^{1/2}}\left(\frac{1}{MeV}\right)$$

$$C_{2,i} = 1.8096\times10^6 a_i z_1 z_{2,i} N_i \frac{A_1}{A_1+A_{2,i}} \ (MeV/\ \ )$$

$$a_i = 4.6847\times10^{-9}(z_1^{2/3}+z_{2,i}^{2/3})^{-1/2}(cm).$$

Now to solve the integral in equation (2-23) it is required to develop $\frac{1}{\frac{dE}{dx}(v)}$ as a power series in v and determine the coefficients $x_1, x_2, \ldots x_5$ by least squares fit.

Thus
$$\frac{1}{\frac{dE}{dx}(v)} = x_1 v^{-1} + x_2 + x_3 v + x_4 v^2 + x_5 v^3 \qquad (2\text{-}29)$$

Dhaka University Institutional Repository

The range of the recoiling nuclei is given by

$$R = 1.0364\times10^{-2} A_1 (x_1 v_0 + \ldots\ldots \tfrac{1}{5} x_5 v_0^{\,5}) \qquad (2\text{-}30)$$

with $[v] = 10^8$ cm/sec., $\left|\frac{dE}{dx}\right| = \frac{MeV}{\mu}$, and A_1 = amu.

According to Blaugrund [19] and Strassheim [45] the average cosine of $\emptyset$, the angle of deflection is

$$\overline{\cos \emptyset(v,v_0)} = \exp\left\{ -\int_{v}^{v_0} \frac{1}{v} \frac{\sum_{i=1}^{N} \frac{A_{2,i}}{A_1} G_i \left(\frac{dE}{dx}\right)_n^i}{\sum_{i=1}^{n} \left(\frac{dE}{dx}\right)^i} dv \right\} \qquad (2\text{-}31)$$

The function G_i is given by Blaugrund [19]. We now develop the above integral as a power series in v.

$$\text{The Integral} = c_1 v^{-1} + c_2 + c_3 v + c_4 v^2 + c_5 v^3 \qquad (2\text{-}32)$$

and so

$$\overline{\cos \emptyset(v,v_0)} = \left(\frac{v}{v_0}\right)^{c_1} \exp \; c_2(v-v_0) + \ldots + \frac{1}{4} c_5 (v^4 - v_0^{\,4}) \qquad (2\text{-}33)$$

Now using equation (2-21), (2-22) and (2-33), the equation (2-23) can be written as

$$F(\tau) = \frac{M_1}{\tau v_0} \int_0^{v_0} g(v, v_0, \tau)\, dv \qquad (2\text{-}34)$$

Dhaka University Institutional Repository

with

$$g(v,v_0,\tau) = (x_1+x_2v+ \dots +x_5v^4)(v/v_0)^{\frac{x_1M_1}{\tau}} \exp \frac{M_1}{}(x_2v+\frac{1}{2}x_3v^2+\dots$$

$$\dots+\frac{1}{4}x_5v^4)-\frac{M_1}{}(x_2v_0+\frac{1}{2}x_3v_0^2+\dots+\frac{1}{4}x_5v_0^4) \times$$

$$(v/v_0)^{c_1} \exp \; c_2v+\dots+\frac{1}{4}c_5v^4)-(c_2v_0+\dots+\frac{1}{4}c_5v_0^4)$$

The attenuation factor $F(\tau)$ versus lifetime curve is obtained by a numerical integration of equation (2-34). The integration is done not from zero velocity but from a cut-off velocity V_{AB} where $V_{AB} = 0.1v_0$. In this work the attenuation factor has been calculated with a FORTRAN programme ELOSS.

2.9. The analysis

The analysis for the extraction of lifetime is done in the following way:

The average observed Doppler-shift $\overline{\Delta E_\gamma^{obs.}}$ is the difference of the γ-ray energies at the forward and backward angles. The ratio of this observed shift to maximum shift is termed as the experimental attenuation factor i.e.

$$F(\tau)^{exp.} = \overline{\Delta E_\gamma^{obs.}} / \Delta E_\gamma^{max.}$$

The experimental attenuation factor is then compared with the attenuation curve obtained by numerical integration of relation (2-34) to obtain the mean lifetimes.

Dhaka University Institutional Repository

2.10. Accuracy of the theory of slowing down

The theory of slowing down described in the previous subsections is rather approximate. So a comparison of the theory with results is required.

At low velocities, $v/c \leqslant 0.35\%$, the energy loss is dominated by nuclear scattering. As the velocities of the recoiling nuclei increase, the relative importance of the nuclear stopping decreases and the electronic stopping process becomes more important. However unexplained deviations have been observed [38,40] from the predicted [17] values of the electronic cross-sections for different z_1 values of the recoiling nuclei. Hvelplund and Fastrup [40] show that the amplitude of the oscillatory behaviour of the electronic stopping cross-section increases with increasing z_1. In fig. 2.4 is shown the electronic cross-section S_e for various ions with $z_1 < 40$ passing through an amorphous carbon foil at two velocities. The fluctuations are less at higher ion velocities. Similar effects have been observed by Hvelplund [46] for ^4He and ^{16}O ions moving in various media with $z_2 < 30$.

El-Hoshy *et al.* [47] studied the influence of the atomic shell effects and found that the behaviour of the electronic stopping power $S_e(z_1)$ can be described for materials showing crystalline structure. The crystalline structure has not been considered in the Thomas - Fermi model. According to the authors [46] the approach can be extended to amorphous materials.

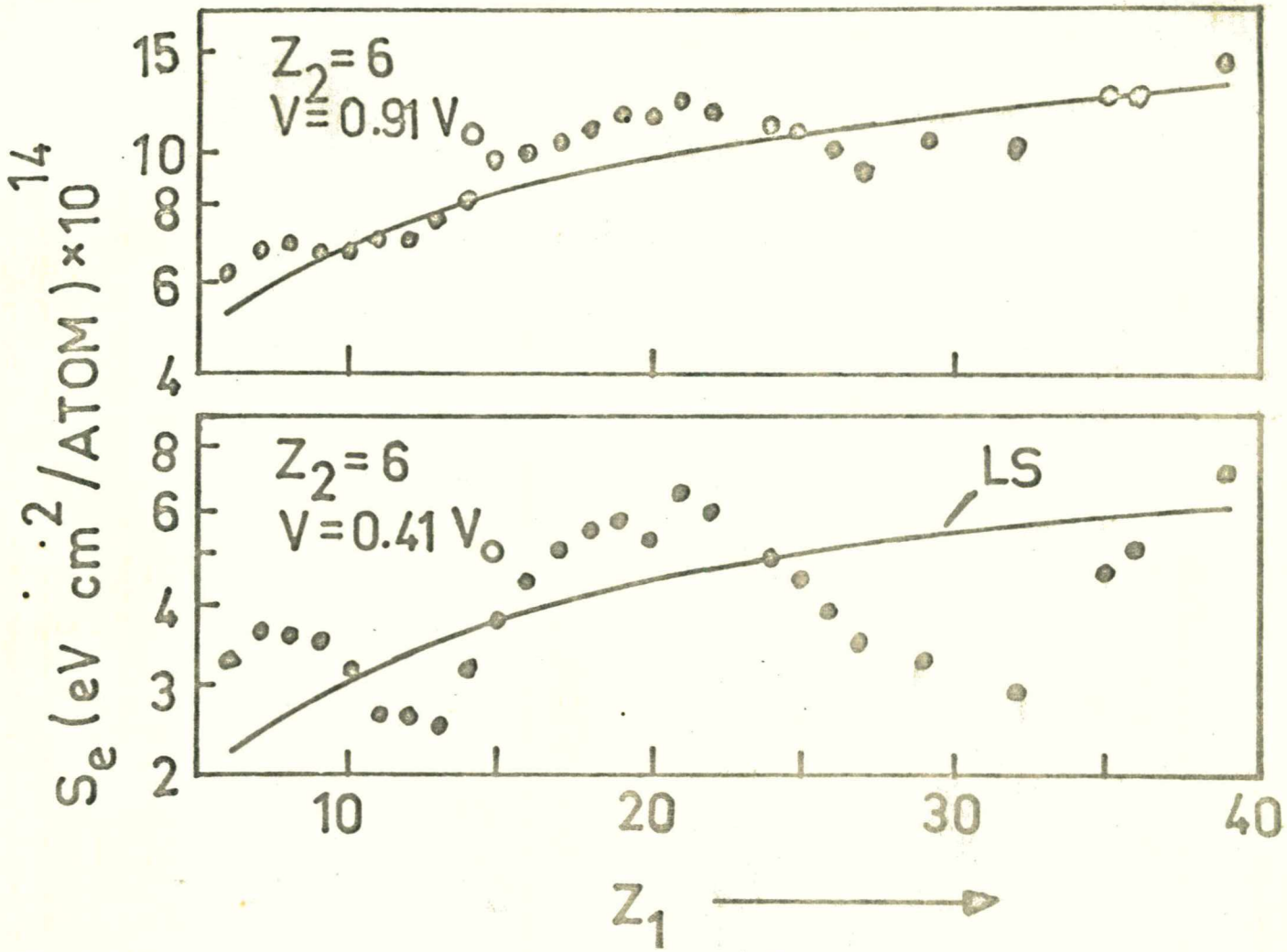

Fig. 2.4 The electronic stopping cross-section S_e in the carbon foil vs. z_1, the atomic number of the moving ion for two constant velocities. The solid curve is due to electronic stopping power from the theory of Lindhard et al.[17]. (Taken from ref. 40).

Dhaka University Institutional Repository

Dhaka University Institutional Repository

The dependence of the stopping power and so the lifetime on the backing material has been noted in many DSA measurements. The effect has been studied by several authors[48-53]. Hartman et al.[52] obtained a lower value of the lifetime of the 1.52 MeV state in ^{42}Ca using heavy backing material, for example, gold, than using ^{42}Ca as the self supporting target. Broude et al.[53] have systematically measured the lifetime of the 3.34 MeV state in ^{22}Ne using 39 different backing materials with $z_2 = 6-83$. The 3.34 MeV state in ^{22}Ne was excited by the $^{19}F(\alpha,p)^{22}Ne$ reaction at $E_\alpha = 6.0$ MeV. The target was 20 $\mu gm/cm^2$ LiF. The lifetime obtained by Broude et al.[53] for different backing materials is shown in fig. 2.5 (taken from ref. 53). The dashed line in this figure corresponds to the mean value of the data. The derived mean lifetimes vary by a factor of 1.85. There is no correlation between the data and the different physical parameters. Only an oscillatory behaviour of the data with atomic number is evident. Currie et al.[51] measured the lifetime of the first excited state of ^{30}Si by the $^{27}Al(\alpha,p)^{30}Si$ reaction and obtained results which vary by a factor of 1.45 for five different slowing materials. The lifetime of the 1.01 MeV level of ^{27}Al has been measured by Broude et al.[55]. Using six different backing materials the results obtained show similar departures[53] but with less variation than before. Recently Toulemonde et al.[54] carried out similar experiments as Broude et al.[53]. However these

Dhaka University Institutional Repository

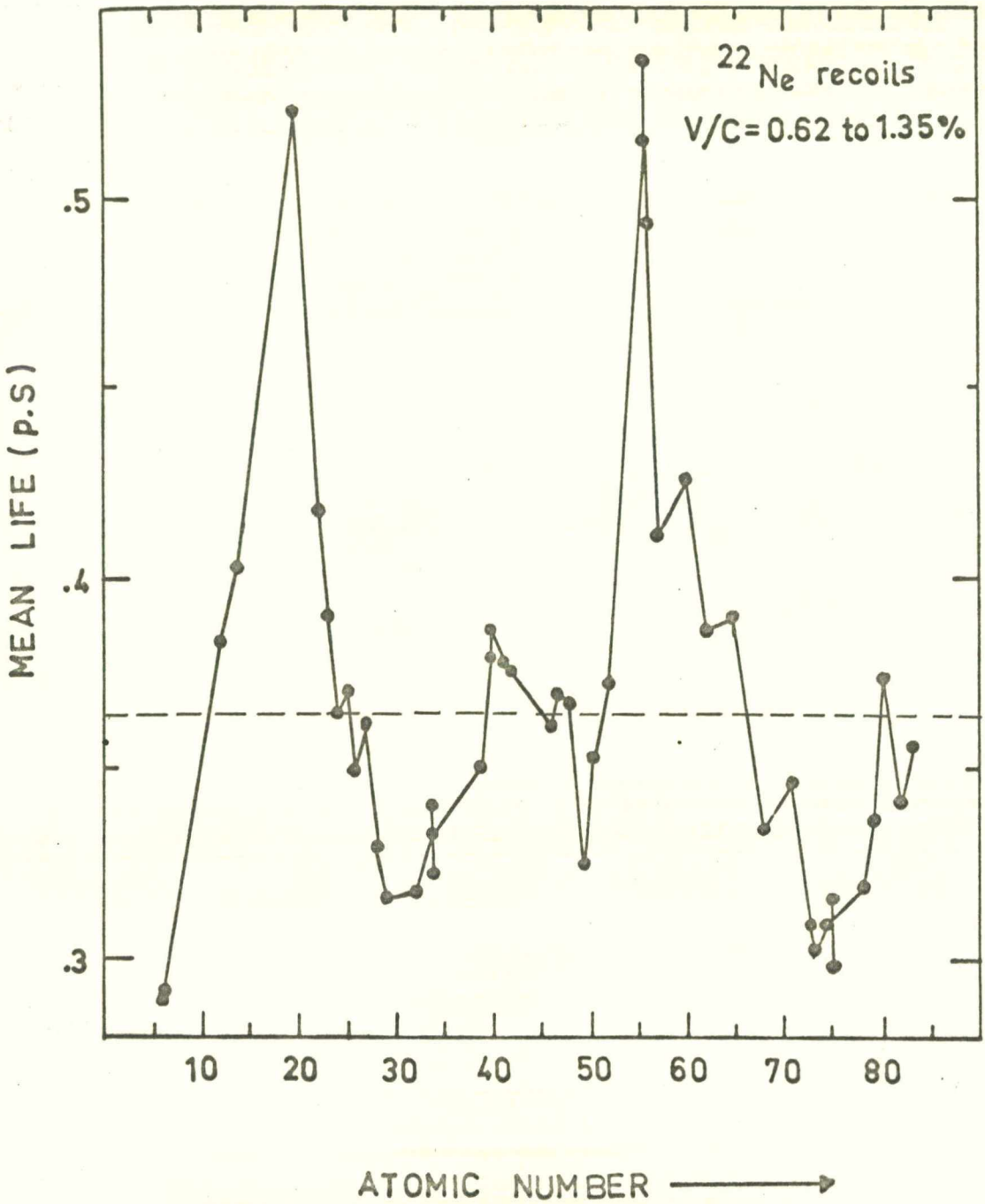

Fig. 2.5 Values of the mean lifetimes of the 3.34 MeV state in ^{22}Ne measured in different stopping materials (z_2 = 6 - 83). Taken from ref. 53.

Dhaka University Institutional Repository

authors [54] observed a correlation between the 'apparent' lifetime obtained with the Lindhard et al. [16] slowing down predictions and the electronic slowing-time τ which is related to the electron density distribution of the two colliding atoms.

An approximate and nearly universally adopted method is the treatment of Blaugrund [19] of the multiple scattering due to ion-atom collisions containing the approximation $\overline{v(t)\cos\phi(t)} \simeq \overline{v(t)}\,\overline{\cos\phi(t)}$ as discussed in section 2.7. The stopping of the ions involves many discrete collisions and an accurate evaluation of the process requires a statistical treatment such as the Monte Carlo method. But it involves lengthy computer time. As such the Monte Carlo method has been used [53,56] only to check the results with the LSS-Blaugrund calculations. The difference has been found to be $\leq 10\%$. In a special case where $A_1 = A_2$ and $S_n \gg S_e$, that is for small velocities, the value of 1 in relation (2-17) has to be reduced by 5-10%. Currie [56] checked this by applying Monte-Carlo procedure and found that for $A_1/A_2 < 1$ the deviation is negligible but for $A_1/A_2 = 1$, the difference increases. For the stopping of Si in Ni($A_1/A_2 \approx 0.5$) Currie obtained a deviation of 5-15% for the quantities $\overline{v(t)\cos\phi(t)}$ and $\overline{v(t)}\,\overline{\cos\phi(t)}$ in the velocity region $0.4 \leq \varepsilon^{1/2} \leq 1.4$. For the stopping of Si in Si with $v/c \approx 0.3\%$ ($\varepsilon^{1/2} \approx 1$), Latt et al. [57] obtained 10% higher values with Monte Carlo analysis than with Blaugrund approximation.

Dhaka University Institutional Repository

It is thus seen that there is a lot of spread in the results given by the DSA method. So long as no experimental information is available about the slowing down of the recoiling nuclei, large errors in lifetime measurements will only be natural. LSS [16] accepted an overall systematic error of 15-20% on the stopping cross-section; specially in the case of low recoil velocities uncertainties in the results may be of the order of 20 to 30%.

2.11. Other treatments of Ion-atom collisions

In the region of dominating nuclear stopping i.e. with $v/c < 0.2\%$ Kreger *et al.* [58] have treated the process by considering the first few ion-atom collisions as descrete events and noted that the $F(\tau)$ values are expected to decrease with increasing recoil velocity. This is just the opposite of LSS-B prediction. However, investigations by Robertson and Leslie [59] using ^{55}Fe ions with $v/c = 0.15-0.18\%$ disproved the prediction of Kreger *et al.* [58].

Using transport theory, Winterbon [60] has given an analysis of Doppler shifted gamma ray spectra. It has assumed the random binary collisions in an infinite medium and continuous electronic stopping uncorrelated with deflections. The difference with Blaugrund treatment is that in this case slowing and spreading of the beam of recoiling atoms are considered together whereas Winterbon [60] compared his results with

Dhaka University Institutional Repository

LSS-B theory with or without electronic stopping and showed that the Blaugrund treatment always underestimates the $F(\tau)$ value by upto 10%. That means the Blaugrund treatment will always give a lower lifetime than the Winterbon [60] theory when compared with the experimental $F(\tau)$ value.

Doerr et al. [61] derived lifetimes from $(p,p'\gamma)$ spectra of ^{90}Zr and ^{92}Mo at recoil velocity of $v/c \sim 0.25\%$ and using both the LSS-B and Winterbon [60] treatments for the calculation of $F(\tau)$ curves. From the attenuation curve using the Winterbon treatment they obtained lifetimes 25% higher which is in good agreement with other independent measurements[62,63]. Some more examples will be of interest to verify the Winterbon [60] treatment.

2.12: Limitations and uncertainties

Several limitations that come up in the application of DSA method are described below.

1) The measurements of lifetimes are generally limited by an attenuation factor of 95% and 5% for the lower bound and upper bound respectively. Below 5% and above 95% the attanuation curve is so flat that it gives lifetimes with a large uncertainty. With a backing material of low density the recoiling nuclei take longer time to stop and therefore the attenuation curve is shifted to the higher time values giving higher bound. Sometimes this is done by use of gases as backing

Dhaka University Institutional Repository

materials. If the backing used is too dense then only short lifetimes can be measured.

2) Another critical point is the necessity of good energy resolution of the Ge(Li) detector and gain stability of the electronics. Measurements of shifts depend on these factors. Now-a-days shifts of tenths of keV can be measured with Ge(Li) detectors with reasonable accuracy.

3) Using relations (2-4), (2-5) and (2-6) the Doppler shift is expressed by $E_0 F(\tau)(v_0/c)(\cos\theta_1 - \cos\theta_2)$. So a small v_0/c value means a small Doppler shift and thus the relative inaccuracy in the $F(\tau)$ value increases.

4) Target preparation is an important factor in the measurements by Doppler-shift attenuation method. The density and uniformity of the target depend on the way of preparation. If the density of the target is not uniform, then there will be an effect on the slowing down time of the recoiling nuclei which in turn gives an error in the determined lifetime. In the case of target-backing combination if there is vacuum in between the target and the backing then the recoiling nuclei will travel in vacuum for sometime which will again influence the slowing down time. Thus preferably thick and uniform targets are required to be used.

5) High background is another experimental problem. Because of high background the error in the shift sometimes becomes of

Dhaka University Institutional Repository

the same order as the shift itself. Therefore, a backing material with high Coulomb barrier is preferred. Impurities should be avoided.

6) Besides the above limitations the stopping theory used in the analysis of the measured shift results in an uncertainty in the lifetime. This uncertainty comes from the lack of knowledge of the time dependence of the velocity of the recoiling ions in the stopping medium. LSS [16] accepted an overall systematic error of 15-20% on the stopping cross-sections. The uncertainty can be reduced if the experimental values for the stopping are known. Thus in the measurements of lifetimes by DSA method the uncertainty comes both from the experimental inaccuracy and from the stopping power and as such errors of about 20% are quite natural.

Dhaka University Institutional Repository

CHAPTER-3

EXPERIMENTAL PROCEDURE

3.1. Principle of measurement

The main requirement for the measurement of lifetimes by Doppler-shift-attenuation method is the production of an ensemble of excited nuclei that are as unidirectional and monoenergetic as possible. Such a monoenergetic and unidirectional ensemble of excited nuclei recoiling along the beam axis is produced in capture reactions by accelerating a beam of particles and bombarding at a definite point of the target. Capture reactions are thus very suitable for the DSA method. In case of reactions in which a particle is emitted first, the analysis and the experimental arrangement is more complicated (see chapter 5 and 6).

In the DSA method the experimental difficulty is that in the proton induced reactions around $A \approx 50$ the Doppler shift of a gamma ray is very small. The shifts are sometimes much less than 2 keV for a gamma ray of energy 1 MeV. Now under the actual running conditions a Ge(Li) detector has a resolution of $\geqslant 2$ keV for the 1.33 MeV ^{60}Co line. That means the shifts are smaller than the energy resolution of the Ge(Li) detector.

The experimental method for determining the Doppler shift is that the gamma ray energy emitted by a decaying nucleus from a state of higher energy to a state of lower energy

Dhaka University Institutional Repository

is measured at two angles. The energy difference measured at these two angles gives the Doppler shift. These types of measurements require runs of many hours. In practice it has been seen that during these long hours of measurements there is a serious problem of gain drift in the gamma-ray spectra. The gain drift may occur due to the change in the values of the capacitance in the amplifier. Even a slight temperature difference in electronics and a slight movement in the cables may cause gain drift. Sometimes the gain drift is as large as the Doppler shift. But for the determination of lifetimes the peak positions should be determined accurately.

To get rid of the disturbing problem of gain drift a target chamber with two-target arrangement has been used in the present measurements. The principle is that both the spectra from the forward and backward angles can be accumulated simultaneously and the problem of gain drift can be avoided. Antilla et al. [20] used a special target chamber with two targets to determine the Doppler shift of the gamma-rays from a compound nuclear resonance in (p,γ) reactions. The two targets were placed in such a way that half of the beam hits one of the targets and the other half of the beam hits the other target. The Ge(Li) detector was placed in between the two targets and away from the beam axis. The $^{27}Al(p,\gamma)^{28}Si$ reaction at E_p = 1.364 MeV was used in the experiment to populate a compound level at 12.90 MeV which subsequently decays to the 9.32

Dhaka University Institutional Repository

and 9.38 MeV levels. These levels decay by 7.6 MeV gamma rays. The Doppler shift in this case was large. As a result, the two peaks from the two targets, the forward and backward shifted, could be separated very easily. The Doppler shift can then be read from the display of the multichannel analyser. The Ge(Li) detector remained at the same position during the whole experiment. This simple procedure adopted by Antilla et al. [20] is however, not, suitable for our measurements because the shifts are sometimes much smaller than the resolution of the Ge(Li) detector and so the forward and backward shifted peaks cannot be separated. In our measurements the two spectra have to be accumulated simultaneously but separately. This was achieved with the help of the target chamber with two-target arrangement and with a routing procedure. The target chamber is described in section 3.2 and the routing procedure in section 3.3. With this chamber, the accumulation of the two spectra from the two targets is possible only when one of the targets is taken out of the beam axis periodically by an electromagnet so that the beam falls on both the targets periodically for a prescribed period of time. The beam hits target 1 (fig. 3.1) for a time interval, say t_1 and target 2 for a time interval, say, t_2. To accumulate the two spectra separately, the memory of the multichannel analyser is split into two parts. The routing signal for the analyser is correlated with the position of the targets. Pulses from

Dhaka University Institutional Repository

the detector are accumulated in one 4k memory of the MCA for, say, for target 1 and in another 4k memory for target 2. During movement of the target, accumulation is prevented by a veto signal to the gate of ADC. Since the time intervals t_1 and t_2 are so short, say, 10-100 secs., compared with the total 15 measuring hours, both the spectra due to the forward and backward angles are affected by the possible gain drift in the same way. As a result there will be no effect of the gain drift on the derived mean lifetime.

3.2. The target chamber

The target chamber used in the present measurements makes possible the simultaneous DSA measurements at both the forward and backward angles and thus eliminates the problem of gain drift on the derived lifetime values. A diagram of the target chamber is shown in fig. 3.1. The chamber was constructed in the workshop of the Institut für kernphysik, University of Frankfurt. Four 5 mm thick pieces of steel were joined to form the chamber in such a way that the Ge(Li) detector could be placed at the middle of the chamber. At one side of the chamber, two transparent plexiglass windows were installed so that the inside of the chamber could be seen. The 520 mm long, 70 mm wide and 110 mm high chamber was nickel plated. It could stand a vacuum of the order of 5×10^{-6} cm of mercury. The horizontal dot and dash line in the figure

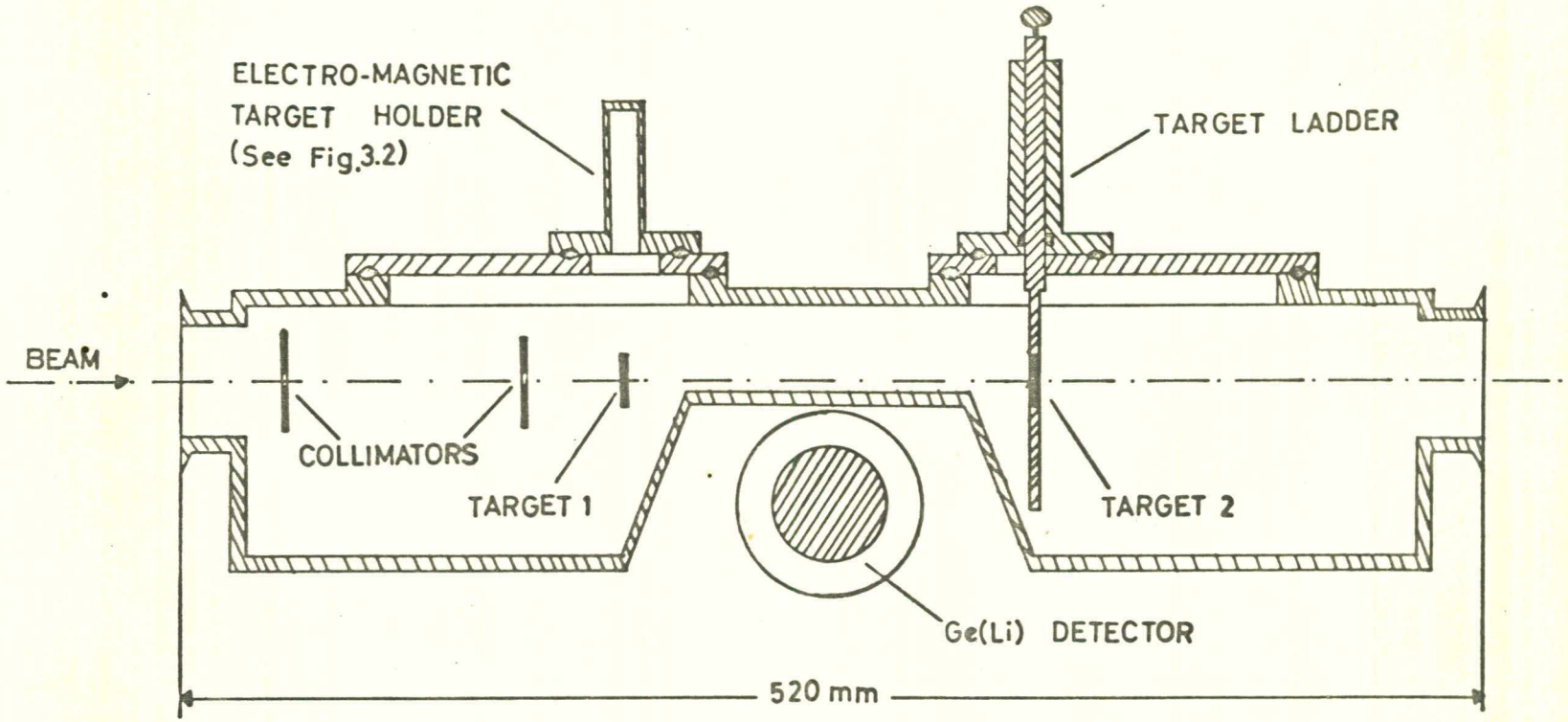

Fig. 3.1 Diagram of the target chamber with the two-target arrangement used to measure lifetimes by the DSA method in the present work.

Dhaka University Institutional Repository

Dhaka University Institutional Repository

indicates the path of the beam. The beam passes through 3 mm collimators placed inside the chamber before hitting target 1. The two targets are placed at a distance of 162 mm apart. Target 1 is removed out of the beam axis periodically with the help of an electromagnet. A diagram of the electromagnetic target holder is shown in fig. 3.2. On the top of the holder is placed a coil (100 , 2400 windings) which requires 24 volts. The upper part of the target is made of iron and insulated from the target. Target 2 is a normally fixed target placed on a ladder which can contain upto three targets. The position of these targets can be adjusted with the help of a sliding O-ring. A quartz placed on one of the positions of the target ladder is used to see the beam spot for beam alignment.

When there is no power in the coil, the target 1 remains at the normal position in the beam axis and the beam falls on it. In this position the Ge(Li) detector detects gamma rays from target 1. When the coil is magnetised by a 24 Volt power supply, target 1 is attracted and removed upwards away from the beam axis. As a result the beam falls on the second target i.e. target 2 and so the detector in this case detects gamma rays from target 2 only. The principle of this measurement is shown in fig. 3.3. In this way the beam is allowed to fall on both the targets alternatively and for a prescribed period of time which is controlled by a control unit. The Ge(Li) detector is placed symmetric to both the targets and away from the beam

Dhaka University Institutional Repository

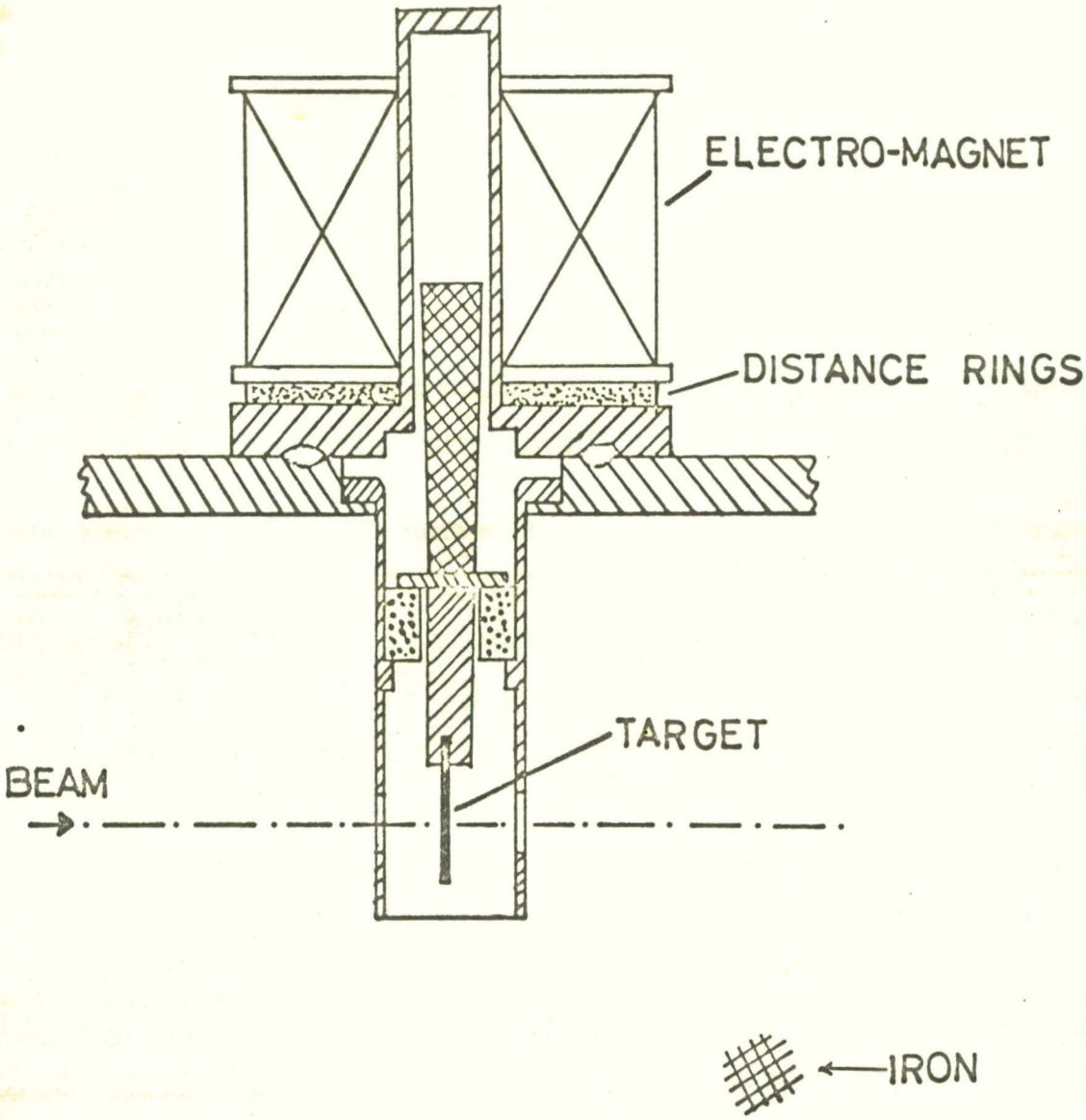

Fig. 3.2 A schematic side view of the electromagnetic target holder. The upper part of the target is made of iron and insulated from the target.

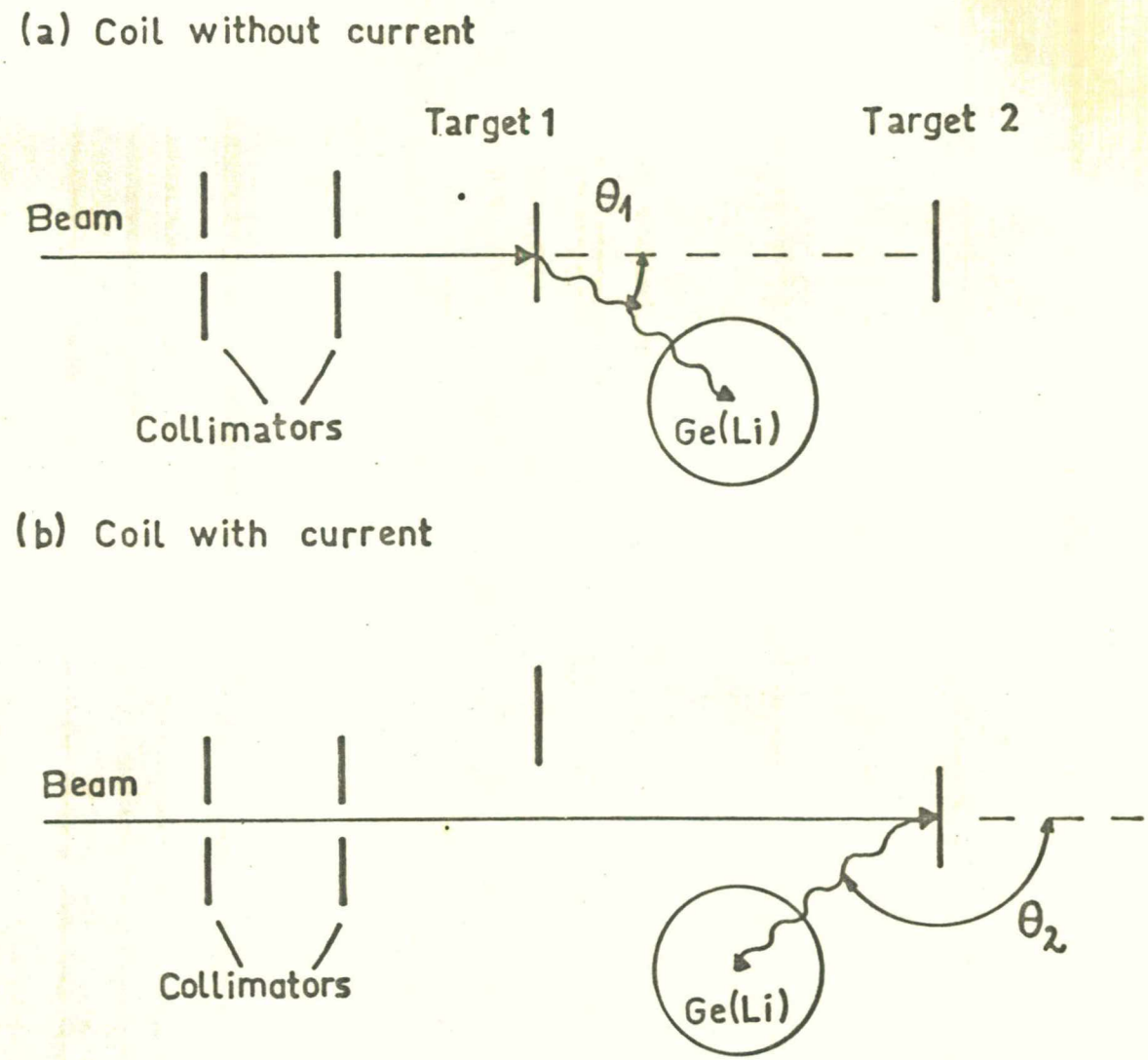

Fig. 3.3 Principle of measurement of the γ-ray spectra with the two-target arrangement.

Dhaka University Institutional Repository

Dhaka University Institutional Repository

axis. The detector is thus situated at a forward angle with respect to the first target (target 1) and at a backward angle with respect to the second target (target 2). The angles are approximately 31° and 149°. By changing the positions of the target holders measurements at 18° (162°) are also possible. The angle of inclination of the walls of the chamber (fig.3.1) just on the right and left side of the Ge(Li) detector was so chosen that the gamma rays meet them at 90°. This made the angular dependence of absorption of the gamma rays minimum. The inside part of the target chamber was covered with tantalum sheet to avoid unwanted reactions with the chamber walls.

The following are the advantages of the two-target chamber used in this work.

1) This chamber makes possible the measurement of gamma-ray spectra at both the forward and backward angles simultaneously and thereby eliminates the problem of gain drift. Since the two targets are in the beam axis alternatively only for a short time (10-100 sec.), both the spectra are affected by possible gain drift in the same way and as such it does not affect the final result.

2) The Doppler shift is determined by comparing the two spectra and no calibration line is required.

3) A large angular difference for measuring the two spectra is obtained and it is not required to change the position of

Dhaka University Institutional Repository

the detector which sometimes causes gain drift due to disturbance of the cables.

4) If the two spectra are accumulated in a PDP 15 computer, they can be displayed at the same time one above the other. One can see and compare the shift within a few minutes of the measurements which is not possible in a normal measurement.

5) The shift can be determined at each moment of the experiment and so measurement time is not wasted in case of a breakdown during measurement.

3.3. The electronics

The block diagram of the experimental setup used in the present DSA measurements is shown in fig. 3.4. Singles spectra were measured for the targets placed at forward and backward angles with respect to the detector. The output signals from the Ge(Li) detector were amplified by an ORTEC preamplifier (Model 120-4) and a main amplifier (spectroscopy amplifier, Canberra 1413). The amplified pulses were then used as an input to the signal of the ADC to be analysed by an ND 4096 pulseheight multichannel analyser (MCA). The two spectra from the two targets were stored separately in the two memories, called the External and the Internal memory of the multichannel analyser. A control unit and a router were used for this purpose. The separation of the two spectra were done in the following way.

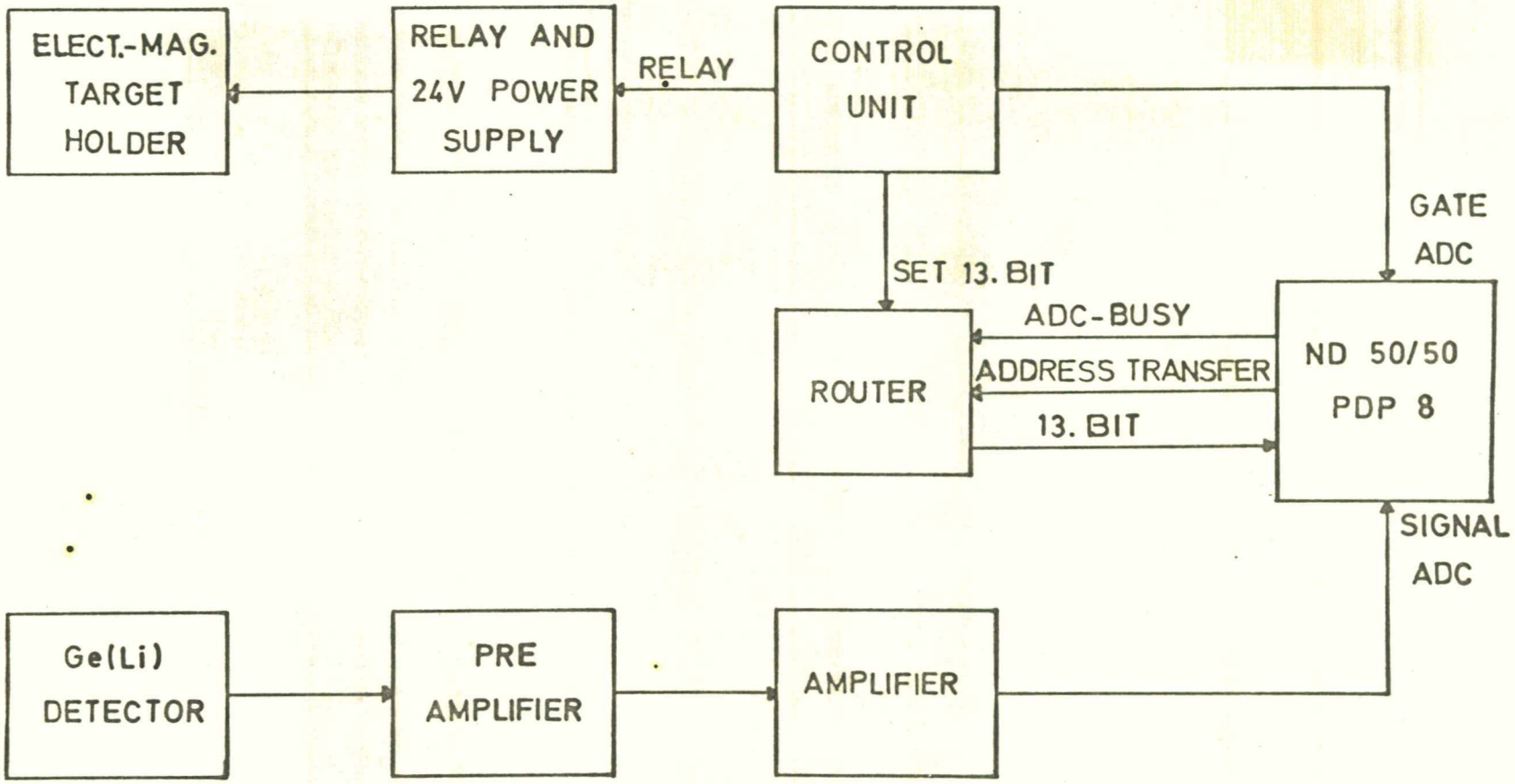

Fig. 3.4 Block diagram of the electronic set-up used in the DSA measurements with the two-target arrangement.

Dhaka University Institutional Repository

Dhaka University Institutional Repository

The outgoing pulses from the control unit are shown in fig. 3.5. The control unit is a TTL-logic. The control unit periodically produces 'Relay' pulse, say for t_2 seconds and stops producing for t_1 seconds. The duration can be controlled by a knob on the front panel of the unit. This 'Relay' pulse switches the relay on, which in turn supplies 24 volts to the coil of the electromagnetic target holder. Thus when there is no relay-pulse (relay pulse is low) from the control unit, there is no power in the coil. The target 1 is then down and in the beam axis. The 'Set' pulse is then high and a 13th Bit is added to the analog-signal, which is converted into 12 Bits (4096 channels). All events, where the 13th Bit is set, are stored in the external memory for t_1 seconds. Similarly when the relay pulse is high, the coil gets power and the target 1 goes up. The beam then falls on target 2. The set-pulse is then low (13 Bit 0) and the gamma rays from target 2 are accumulated for t_2 seconds in the internal memory of the multichannel analyser. Thus the routing signal for the analyser is correlated with the position of the targets. During the movement of target 1 there is a veto signal to the gate of ADC for a short time (0.1 sec.) and the accumulation of the spectra during this period remains stopped.

In the ND 50/50 PDP 8 system, an on-line analysis of the peak centre and so the determination of the energy of the peak is possible for the internal memory. But for external

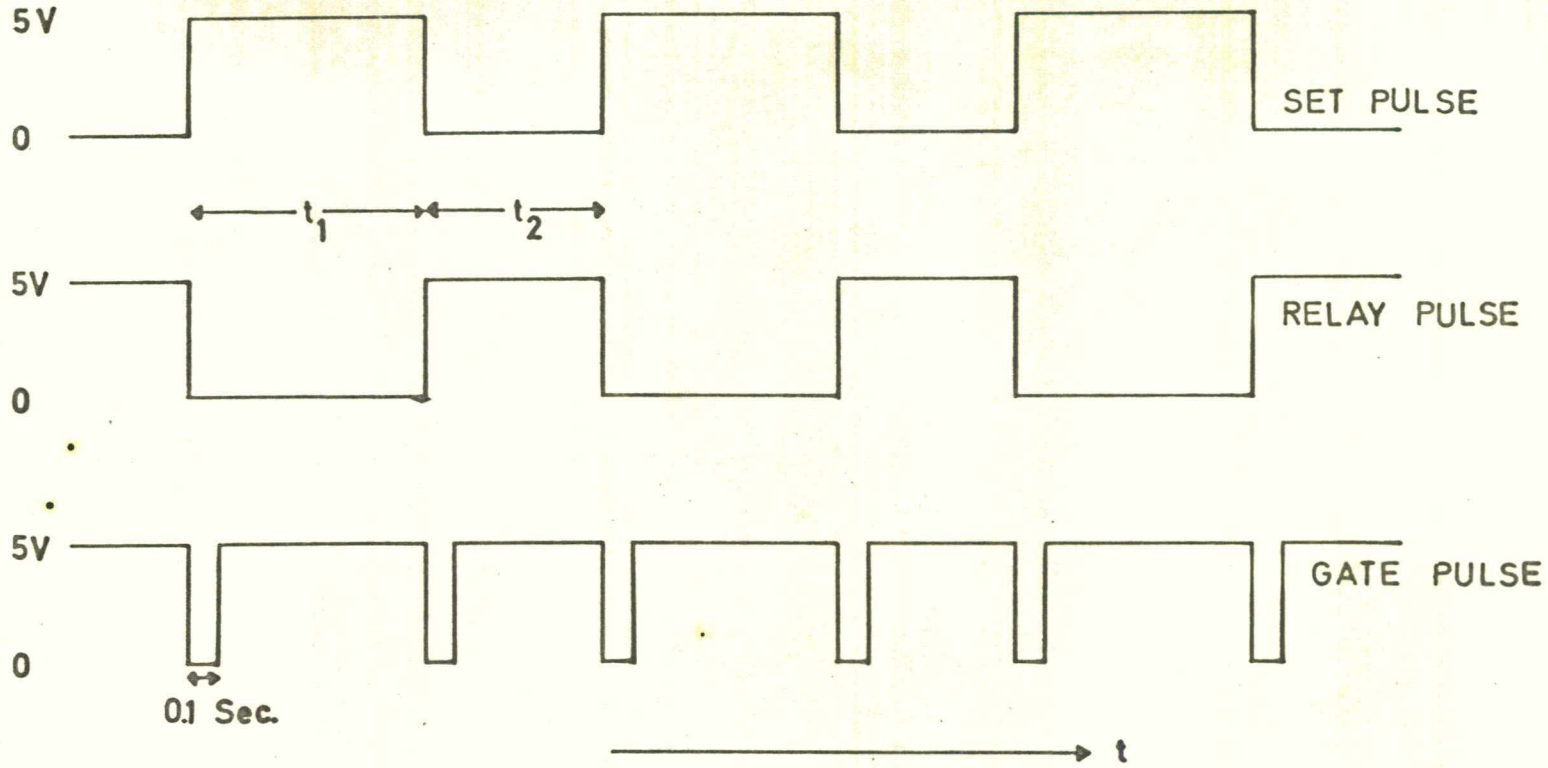

Fig. 3.5 The outgoing pulses from the control unit. The horizontal arrow indicates time axis.

Dhaka University Institutional Repository

Dhaka University Institutional Repository

memory the accumulation must be stopped. Energy calculations in both the spectra during measurements were done to check the Doppler shift. This helped to control the experiment. At the end of experiment the spectra were written on a magnetic tape for further analysis in a PDP 15 and a UNIVAC 1108 computer.

3.4. Determination of the mean value of cosθ

The formula (2-1) for Doppler shift is valid only for a point detector. An average over the solid angle must be made for a detector of finite size. In a normal arrangement for DSA measurements, the axis of the detector which is supposed to be cylindrical points to the target. So a measurement of the average cosine of the detection angle θ does not involve complication. But as discussed earlier (section 3.2), in our measurements with the two-target arrangement, the beam and the detector axis are no more in the same plane. Therefore the measurement of the mean value of cosθ was done in a different way. The cosine of the angle θ could be measured from the distances a and b (fig. 3.6) but to avoid errors and to determine it more accurately a method was used as discussed below.

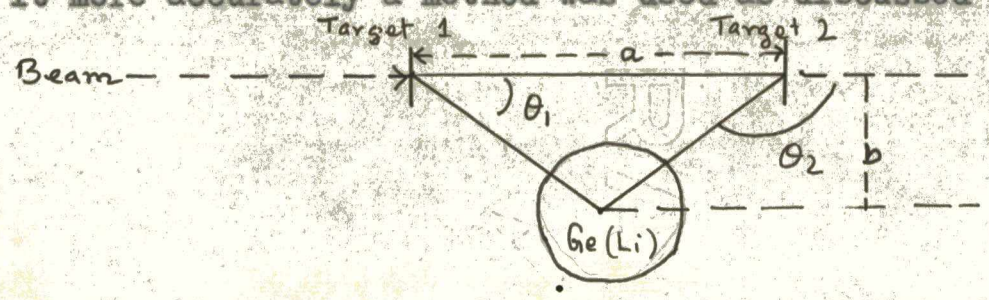

Fig. 3.6. Arrangement showing the geometry of the two-target arrangement and the detector.

Dhaka University Institutional Repository

It is well known that the mean lifetime of a compound nuclear state is smaller than the slowing down time of the recoiling nuclei in the stopping medium. So all the nuclei decay in flight with initial velocity and the corresponding emitted primary gamma rays have maximum Doppler shift. That means

$$F(\tau) = \frac{\overline{\Delta E_{\gamma}^{obs.}}}{(v_0/c)E_{\gamma_0}\ (\cos\theta_1 - \cos\theta_2)} = 1 \qquad (3\text{-}1)$$

So $$\cos\theta_1 - \cos\theta_2 = \frac{\overline{\Delta E_{\gamma}^{obs.}}}{(v_0/c)E_{\gamma_0}} \qquad (3\text{-}2)$$

where E is the unshifted gamma ray energy which is known and the initial velocity v_0 can be determined from reaction kinematics. The shift is obtained from the experiment. Since in our arrangement the detector is placed symmetric to both the targets, we have

$$\cos\theta_1 - \cos\theta_2 = 2\cos\theta \qquad (\theta_1 = \theta_2 = \theta \text{ say})$$

Equation (3-2) then becomes

$$\cos\theta = \frac{\overline{\Delta E_{\gamma}^{obs.}}}{(2v_0/c)E_{\gamma_0}} \qquad (3\text{-}3)$$

Dhaka University Institutional Repository

For the calibration experiment for measuring the mean value of cos θ the $^{27}Al(p,\gamma)^{28}Si$ reaction was chosen because it has a strong resonance at E_p = 992 keV and the width of the compound state Γ = 100 ± 15 eV [64]. This means the state has a lifetime of the order of $\tau \approx 8 \times 10^{-18}$ sec. This compound nuclear state in ^{28}Si decays through different excited states[64]. Observed shifts obtained from the 10.763 MeV gamma ray emitted in the decay of the compound state to the first excited state are summarized in table 3.1. The shifts were about the same for full energy, single escape and double escape peaks and did not show any difference. The weighted mean value of

Table 3.1

Observed Doppler shift of the 10.763 MeV gamma-ray energy from the $^{27}Al(p,\gamma)^{28}Si$ reaction.

Measurement no.	$E_{\gamma 0}$ (MeV)	Peaks	Measured shift $\Delta E_\gamma^{obs.}$ (keV)	cos θ
1	10.763	F.E.	30.18±0.31	0.845±0.009
		S.E.	30.51±0.28	0.854±0.008
		D.E.	30.41±0.34	0.851±0.010
2	"	F.E.	30.68±0.26	0.859±0.007
		S.E.	30.52±0.26	0.854±0.007
		D.E.	30.52±0.34	0.854±0.009
3	"	F.E.	30.69±0.51	0.859±0.014
		S.E.	30.72±0.40	0.860±0.012
		D.E.	30.65±0.39	0.858±0.012

F.E.=Full energy, S.E.=Single escape, D.E.=Double escape

Dhaka University Institutional Repository

the cosine of Θ was found to be

$$\cos\Theta = 0.855 \pm 0.001$$

which corresponds to a mean angle of

$$\Theta = (31.27 \pm 0.13)^{\circ}$$

This angle Θ was also calculated from the measured distances (fig.3.6) of a and b, where a = 162±1 mm and b = 46±1 mm. Cos Θ was then found to be

$$\cos\Theta = 0.870 \pm 0.005$$

and $$\Theta = (29.6 \pm 0.6)^{\circ}$$

It was found that the measurements of the distances was difficult and also not accurate enough as found from repeated measurements. Besides the diameter of the beam was about 3 mm, which also caused an error in b. So the value of cos Θ=0.855 ±0.001 obtained from the shift determination was used throughout this work.

3.5. The experiment in general

The experiments on the measurements of lifetimes were performed with protons provided by the 2.5 MeV and the 7.5 MeV Van de Graaff accelerator at the Institut fur Kernphysik, University of Frankfurt, West Germany. The 2.5 MeV accelerator was of horizontal type and the bending (25°) of the beam was achieved with an analysing magnet the field of which was

Dhaka University Institutional Repository

measured with a proton-spin resonance device. In this accelerator the beam was aligned by horizontal slits placed before the magnet and a number of tantalum collimators of various diameters placed inside the beamport tube. The beam was focussed by a quadrupole lens placed after the magnet. In the 7 MeV accelerator the bending of the beam was achieved first by a 90° magnet and then by a 25° magnet. The beam in this accelerator was focussed by two electrostatic quadrupole lenses, one placed after the 90° magnet and the other placed after the 25° magnet. A collimator of 3 mm diameter was used in the target chamber just before the beam fell on the target. A cold trap was used before the target chamber to reduce the background gamma radiation. The dirt and foreign materials inside the beam tube were trapped by the cold trap and this helped to reduce the background.

Targets were prepared by vacuum evaporation of target materials on tantalum backings. Tantalum was used as a backing material, since the gamma rays from Coulomb excitation of tantalum are low in energy [65]. Besides that the surface smoothness of tantalum is an advantage for preparing targets of uniform thickness. The thickness of the tantalum backing was 0.5 mm so that the proton beam could not pass through the target 1 (fig. 3.1). The target chamber was insulated from the beam tube and also from the collimators placed inside the target chamber. The whole chamber thus acted as a Faraday cup

Dhaka University Institutional Repository

and the beam was integrated by means of a current integrator. The deadtime in the analyser was kept at about 5% for better energy resolution. The gain of the amplifier was so adjusted that the full scale of 4096 channels in the pulse height analyser covered the required energy range. Accumulation and analyses of data were done with ND 50/50 MCA, PDP 8 and PDP 15 computers.

Since the introduction of high resolution Ge(Li) detectors, they have been frequently applied in the measurements of lifetimes by DSA method. A co-axial Ge(Li) detector (ORTEC) with an active volume of 85 cc has been used for the measurements reported here. The energy resolution of the detector was found to be 2.1 keV for 1.33 MeV gamma rays from ^{60}Co source.

The gamma rays are detected in a Ge(Li) detector by their ionizing properties. The high speed electrons produced by absorption or scattering of gamma rays within the intrinsic region lose their energy by creating hole-electron pairs or carriers. These carriers when collected by applying an electric field result in a pulse height which is proportional to the gamma-ray energy absorbed. The absorption of gamma rays in the detector takes place by three processes in which incident photons give up all or part of their energy in single events. These three processes are: photoelectric effect, Compton effect and pair production. The first two processes are dominant at low energy.

Dhaka University Institutional Repository

In photoelectric effect the photon energy is absorbed by a bound electron and appears as the kinetic energy of an electron as it is ejected and an X-ray or Auger electron is ejected by the residual ion. In Compton scattering the photon is scattered by an electron with a partial energy loss dependent on the angle of scattering. In the low-energy region the spectrum from monoenergetic gamma rays consists of the full energy absorption peak and a continuous Compton background up to an energy $E\,(1+\frac{m_0c^2}{2E})$, where E is the energy of the gamma ray and m_0 is the mass of the electron produced by Compton scattered gamma rays. Pair production becomes the dominant mode of interaction at an energy of about 2.50 MeV. The threshold energy for the pair production is 1.022 MeV which is equal to the combined positron-electron rest mass. When a gamma ray energy greater than 1.022 MeV is incident on a Ge(Li) detector it produces an electron-positron pair. The unstable positron annihilates with an atomic electron. The annihilation produces two gamma rays of 0.511 MeV emitted at 180^0 to each other. One or both the gamma rays may escape from the detector giving rise to two peaks corresponding to $(E_\gamma - 0.511)$ MeV and $(E_\gamma - 1.022)$ MeV and are called the single and double escape peaks respectively. Thus a spectrum of monoenergetic gamma rays consists of three peaks: one at E_γ (full energy peak/ photo peak) corresponding to the escape of neither photon and a Compton continuum, one at E_γ-0.511 MeV

Dhaka University Institutional Repository

(single escape peak) corresponding to the escape of one gamma ray and at E_γ-1.022 MeV (double escape peak) corresponding to the escape of both the gamma rays. The relative intensity with which each of them contributes to the spectrum depends on the energy of the incident gamma ray, the detector material and the size of the detector.

Energy calibration was done in order to determine the energies of the gamma rays observed in the spectrum. The energy calibration was done by using the 511 keV annihilation gamma ray, the 1461.2 keV ray from ^{40}K, the 2614.5 keV γ-ray from $^{228}ThC''$ and ^{56}Co and ^{60}Co sources.

3.6. Target preparation

The ^{45}Sc targets were prepared in the Institut für Kernphysik, University of Frankfurt. Natural target material of ^{45}Sc was procured from Johnson Mathey and Co. Ltd., U.K. Tantalum was used as the backing material. The thickness of the backing was 0.5 mm. The targets were prepared in a Speedivac-Coating unit (Model 12E6/1280) by evaporating the target material in vacuum onto tantalum backing from a directly heated tantalum boat. Both the target backing and the boat were cleaned by heating them in vacuum. It was done to make the targets dust free and of uniform density.

3.7. Analyses of spectra

The spectra were analysed in PDP 15 computer to determine

Dhaka University Institutional Repository

the peak centres with errors with the help of the programme GFIT [66]. Peak centres were determined after deducting the background counts represented by Polynomials up to third degree.

The peak centre is given by

$$C = \frac{1}{A}\sum_{i=I}^{I+M}(N_i - B_i).i, \quad i = I, I+1, I+2, \ldots I+M \qquad (3\text{-}4)$$

and the error in the peak centre is given by

$$\sigma_c = \frac{1}{A}\left[\sum_{i=I}^{M}(X(i)-C)^2\,(N_i+B_i)\right]^{1/2} \qquad (3\text{-}5)$$

where C = peak centre, σ_c = error in peak centre, N_i = peak count + Background count, B_i = Background count, X(i) = channel number, I = Initial channel number, I+M = Final channel number. The following was used for background fitting

$$U = \sum_{k=0}^{N} a_k X^k, \quad N = 1, 2, 3 \qquad (3\text{-}6)$$

For N=1, it means U_1 fit which represents a straight line and for N=2, it means a U_2 fit which represents a parabola and so on.

The G_1 and G_2 Gaussian fits were made for single and double peaks respectively. The function used for the single peak (G1 FIT) is given by

$$G1(X, A, X_0, {}_1, a_0, a_1)$$

Dhaka University Institutional Repository

peak (G1 FIT) is given by

$$G1(X,A,X_0,\sigma_1,a_0,a_1)$$

$$= \frac{A}{\sqrt{(2\pi)}\sigma_1} \exp\left\{-1/2\left(\frac{X-X_{01}}{\sigma_1}\right)^2\right\} + a_0 + a_1 X \qquad (3\text{-}7)$$

and the Gaussian fit for double peaks (G2 FIT) is given by

$$G2(X,A_j,X_{0j},\sigma_j,a_0,a_1)$$

$$= G1 + \frac{A_2}{\sqrt{(2\pi)}\sigma_2} \exp\left\{-1/2\left(\frac{X-X_{02}}{2}\right)^2\right\}, \; j=1,2 \qquad (3\text{-}8)$$

where X = channel number, X_0=peak centre, σ = width of the peak, A_j=peak area, a_0= intercept and a_1= slope. Peak centres were determined up to four decimal points for both the spectra obtained from target 1 and target 2. The difference in the channel number for the forward and backward shifted peaks of a particular γ-ray energy gives the Doppler shift.

3.8. Calculation of weighted mean

In cases where there were more than one gamma-ray energy deexciting the same level, a weighted mean of the $F(\tau)$ values resulting from the different gamma-ray energies was calculated to obtain the lifetime. The weighted mean is given by

$$\bar{X} = \frac{\sum_{i=1}^{n} X_i a_i}{\sum_{i=1}^{n} a_i} \quad \text{and} \quad \frac{1}{\overline{\Delta X}^2} = \sum_{i=1}^{n} \frac{1}{\Delta X_i^2} \qquad (3\text{-}9)$$

where $\bar{X}$ = weighted mean, $\overline{\Delta X}$ = error in weighted mean, $a_i = X_i^{-2}$, X_i= value from independent measurement, and ΔX_i= symmetric error in independent measurement.

Dhaka University Institutional Repository

CHAPTER-4

LIFETIME MEASUREMENTS IN ^{46}Ti

4.1. Introduction

The nuclei in the f-p shell region are of special theoretical interest. Electromagnetic decay properties of nuclei are necessary for comparison with nuclear models. Thus measurements of lifetimes are very important.

Lifetimes of levels in ^{46}Ti have been measured by a few authors. Durell *et al.* [22] measured the lifetimes of 10 states in this nucleus and set an upper limit for one state upto an excitation energy of 4.0 MeV by ^{43}Ca(α,n) ^{46}Ti reaction and using DSA method. Assimakopoulos *et al.* [23] using ^{46}Ti (p,p'γ) reaction and DSA method determined lifetimes of 7 states and set a lower limit for one state. There exists discrepancies among these two measurements by a factor of about 2. Dehnhardt *et al.* [24] studied the ^{32}S(^{16}O,2p) reaction and obtained lifetimes of 5 long lived states by recoil-distance Doppler-shift method. The lifetimes of the 889 and 2009 keV states were determined for the first time by these authors. With these results the present lifetime measurements in ^{46}Ti by (p,γ) reaction in ^{45}Sc and using DSA method were undertaken in an attempt to clear up the discrepancies existing in different measurements and to obtain electromagnetic decay rates for this nucleus.

Dhaka University Institutional Repository

Because of our limited knowledge of stopping power we used a calibrated $F(\tau)$ curve for the extraction of lifetimes in ^{46}Ti. The calibration of the $F(\tau)$ curve was obtained by measuring the lifetimes of a few levels in ^{45}Sc with DSA method and then comparing these results with those obtained by Metzger [25] by resonance fluorescence method. It may be mentioned that resonance fluorescence method is independent of slowing down process and the lifetime obtained by this method may be regarded as a reliable basis for the calibration of the $F(\tau)$ curve. This procedure of calibration is justified because the possible corrections to the slowing down theory will not change much by increasing the atomic number from 21 to 22 (^{45}Sc to ^{46}Ti). In both reactions the nuclear part of the stopping cross-sections is dominating. The calibration measurements along with lifetime results in ^{45}Sc are described in chapter 5.

The properties of the (p,γ) reaction in the A=40 mass region are somewhere between those of the (p,γ) reaction on light ($A \approx 20$) and medium heavy ($A \approx 90$) nuclei. The (p,γ) reaction on light nuclei populates usually a single compound resonance with defined spin and parity. As the decay of such a state is dominantly an electric dipole transition only a few low lying states are populated. The situation in the mass region of the medium heavy nuclei is completly different. Here typically several thousands of compound nucleus resonances

Dhaka University Institutional Repository

are excited and their decay leads to rather uniform population of low-lying states. Near $A \approx 40$ the level density is such that some resonances are excited in the (p,γ) reaction but the number is not at all sufficient to get a uniform population of low-lying states. That is why we did two measurements at proton bombarding energies of 1.75 and 1.80 MeV in the work reported here. At these energies different compound nucleus resonances are excited which decay to different low-lying states. This means in practice that the relative intensities of γ-transitions are changing rapidly with the bombarding energy.

It is known from previous excitation function measurements [67-69] in the $^{45}Sc(p,\gamma)^{46}Ti$ reaction that at this energy no sharp resonance exits. It is to be noted that the recoiling nuclei produced from a sharp resonance at the end of the target escape into the backing material which might give wrong information of the $F(\tau)$ curve. In a (p,γ) reaction in this mass region the spectra are simple and the analysis of most of the lines can be made. Besides, correction can be made if a low-lying state is fed in a cascade involving a long-living state.

4.2. The experiment

The experiment was performed with the 2.5 MeV Van de Graaff accelerator at the University of Frankfurt. The levels

Dhaka University Institutional Repository

of ^{46}Ti were populated by the $^{45}Sc(p,\gamma)^{46}Ti$ reaction at proton bombarding energies of 1.75 and 1.80 MeV. The relatively low bombarding energy was chosen to minimise the yield of the strong $^{45}Sc(p,p'\gamma)$ reaction. The principle of measurement and the experimental procedure in general has already been discussed in chapter 3. In this section only a short description of the experiment is given.

A collimated beam of protons was obtained with the help of a number of tantalum collimators of various diameters inside the beam port tube and slits in the target chamber. The specially designed two-target chamber was used in this experiment the details of which has been given in section 3.2. The inner part of the target chamber was covered with 0.2 mm thick tantalum sheet in order to be sure that the proton beam does not hit any part of the chamber. Insulated from the beam tube, the chamber worked as a Faraday cup. A beam current of the order of 400-500 nA was used. The targets were prepared by vacuum evaporation of natural Scandium on tantalum backings of 0.5 mm thickness. The thickness of the target was 400 μgm/cm^2. This thickness was sufficient for the stopping of the recoiling nuclei. The part of the recoiling nuclei escaping into the backing is neglisibly small.

An 85 cc Ge(Li) detector, the resolution of which was found to be 2.1 keV for 1.33 MeV gamma rays from ^{60}Co source, was used to detect the γ-rays. The Ge(Li) detector was placed

Dhaka University Institutional Repository

symmetric to both the targets and below the beam axis as shown in fig. 3.1. The detector was at a forward angle of about 31° with respect to target 1 and at a backward angle of 149° with respect to target 2. The measurement of the mean value of the cosine of θ (the angular difference of the position of detection of gamma rays) has been given in details in section 3.4. The electronic set-up used in this experiment is the same as that described in section 3.3.

Gamma-ray singles spectra measured from the two targets were separately stored in the two memories of the 4096 pulse height analyser. All spectra obtained contained 4096 channels. The gain of the amplifier was so adjusted that the 4096 channels covered approximately the energy range upto 4.0 MeV for the measurement at E_p=1.80 MeV and upto 2.0 MeV excitation energy for the measurement at E_p=1.75 MeV. The deadtime of the analyser was maintained at about 5% so that there was no deterioration of the resolution.

To obtain a reasonable statistics the gamma-ray spectra were measured for 12 hours. At the end of the measurement the spectra were written on a magnetic tape for further analysis. A γ-ray spectrum measured at E_p=1.8 MeV and at forward angle is shown in fig. 4.1.

4.3. Analysis

To obtain the observed Doppler shift in the gamma-ray energy, the peak centroids with errors were calculated for the

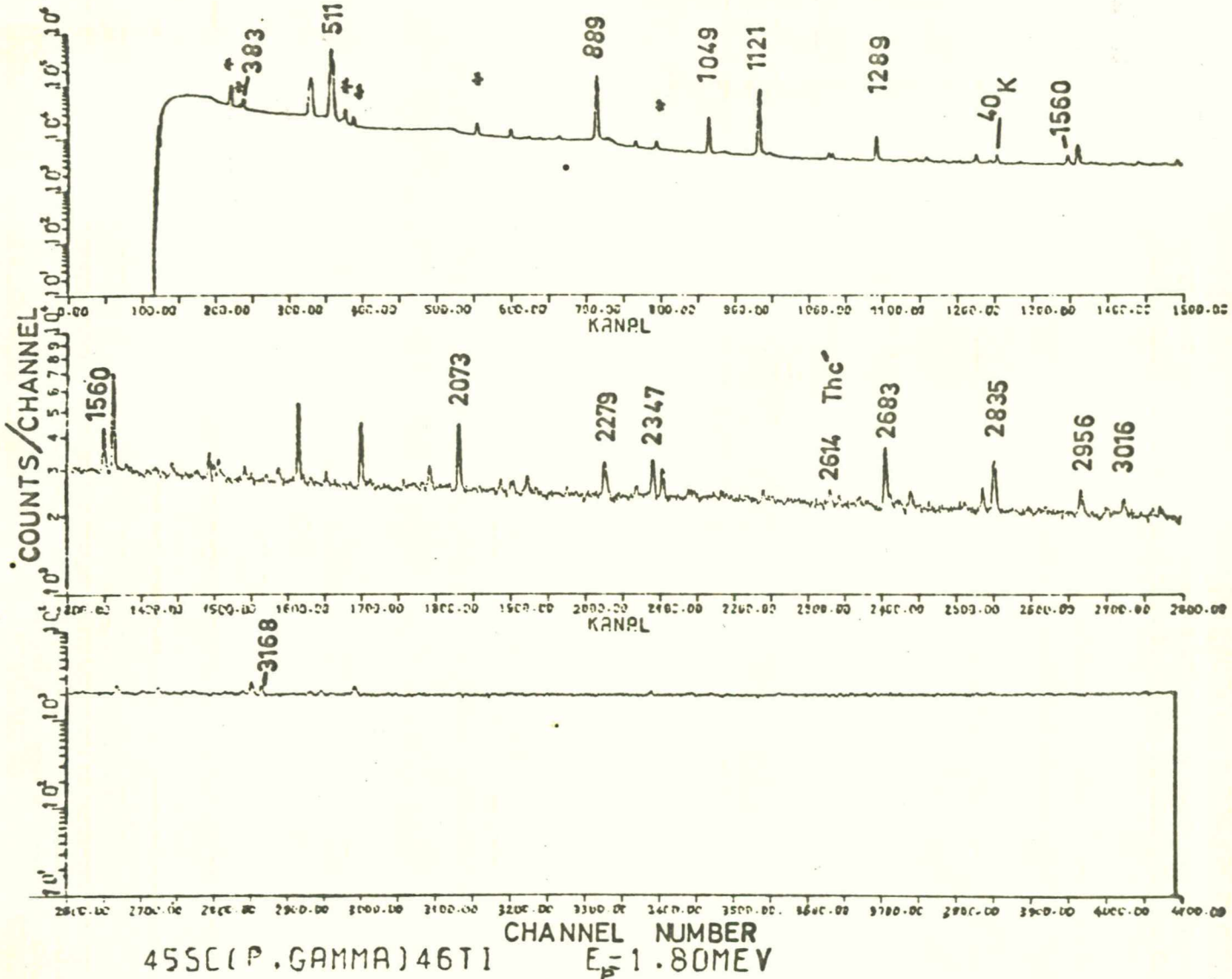

Fig. 4.1 Gamma-ray spectrum from the $^{45}Sc(p,\gamma)^{46}Ti$ reaction at E_p = 1.8 MeV and obtained at forward angle. Numbers over peaks are the energies in keV used for lifetime measurements. Peaks marked by star are from $(p,p'\gamma)$ reaction. Others were not identified.

Dhaka University Institutional Repository

Dhaka University Institutional Repository

peaks of interest. For the determination of peak centre the background was subtracted on either side of the peaks which was estimated by fitting a curve of the form given by expression (3-6). For the double peaks the G2 fit was employed according to relation (3-8) which yielded peak centres with errors for both the peaks. These analyses were carried out in PDP 15 computer. The difference in channels of the peak centroids for the forward and backward shifted peaks of a particular gamma-ray energy is the shift. This shift in channel numbers was multiplied by keV/ch. to obtain the observed shift in keV.

The energy calibration was done with the help of the radiation sources and well-known gamma rays, for example, the 511 keV annihilation γ-rays, the 1461.2 keV gamma rays from ^{40}K and the 2614.5 keV gamma rays from $^{228}ThC''$. It should be noted that for the extraction of lifetimes absolute energy calibration is not so critical, since only relative energies are needed for this purpose.

The experimental attenuation factor is the ratio of the observed to maximum shift. The maximum shift $E\gamma_0(v_0/c)\cos\theta$ was calculated using relation (2-5). The initial velocity for the ^{46}Ti nuclei recoiling in ^{45}Sc was obtained from the reaction kinematics and was found to be 0.136% of the velocity of light at E_p=1.80 MeV. It is to be noted that the initial velocity

Dhaka University Institutional Repository

of the recoiling nuclei from a (p,γ) reaction is the same as the velocity of the centre of mass and this type of reaction produces an almost perfectly defined beam of recoiling nuclei. The mean value of cos θ was obtained as discussed in section 3.4 and was found to be 0.855±0.001 which corresponded to an average angle of 31.27°.

Theoretical curves for the ratio of the attenuated shift to full shift, F(τ), as a function of mean lifetime were calculated. The details of the method of theoretical calculation of F(τ) versus lifetime τ curve have been described in section 2.8. In the absence of experimental information one has to apply the theoretical stopping powers of LSS [16] and the formalism of Blaugrund [19] to take into account the average change in direction of the recoiling nuclei. The density of ^{45}Sc used was 3.0 gm/cc.

Since our knowledge of the stopping power is still limited, a calibration of the theoretical attenuation curve was necessary for the extraction of lifetimes in ^{46}Ti. As discussed in the introduction of this chapter to obtain the calibration curve lifetimes of a few levels in ^{45}Sc were measured and compared with those obtained by the model independent resonance fluorescence method of Metzger [25] which may be regarded as a reliable basis. From the calibration measurements (chapter 5) it was found that when a correction factor of 0.9 ($f_e = f_n = 0.9$) was used in the calculation of

Dhaka University Institutional Repository

the attenuation curve then there was good agreement between our values and those of Metzger [25]. This correction factor of 0.9 was used in the attenuation curve calculation for ^{46}Ti recoiling in ^{45}Sc. The attenuation curve with correction factor $f_e = f_n = 0.9$ for ^{46}Ti recoiling in ^{45}Sc is shown in fig.4.2. The experimental attenuation factor was then compared with this curve for the lifetime extraction in ^{46}Ti.

The reduced transition probabilities $B(\sigma L)$ and the transition strengths $|M|^2_{W.u.}$ have been calculated for the levels. The $B(\sigma L)$ values for the first few electric and magnetic multipoles as calculated from equation (1-2) are

$$\begin{aligned} B(E1) &= 6.29\times10^{-16}\, E_\gamma^{-3} T(E1) \quad e^2 fm^2 \\ B(E2) &= 8.20\times10^{-10}\, E_\gamma^{-5} T(E2) \quad e^2 fm^4 \\ B(M1) &= 5.68\times10^{-14}\, E_\gamma^{-3} T(M1) \quad \mu_0 \\ B(M2) &= 7.41\times10^{-8}\, E_\gamma^{-5} T(M2) \quad \mu_0 fm^2 \end{aligned} \qquad (4\text{-}1)$$

If there is no mixture in the γ-transition to a final state then the lifetime is directly related to the transition probability $T(L)$ where L is the multipolarity. If a mixture of multipolarities does occur in a gamma trasition to a final state f, the transition probability is then equal to the intensity sum of both. In a particular case of say, M1 and E2 transition,

$$T = \frac{1}{\tau} = T(M1) + T(E2) \qquad (4\text{-}2)$$

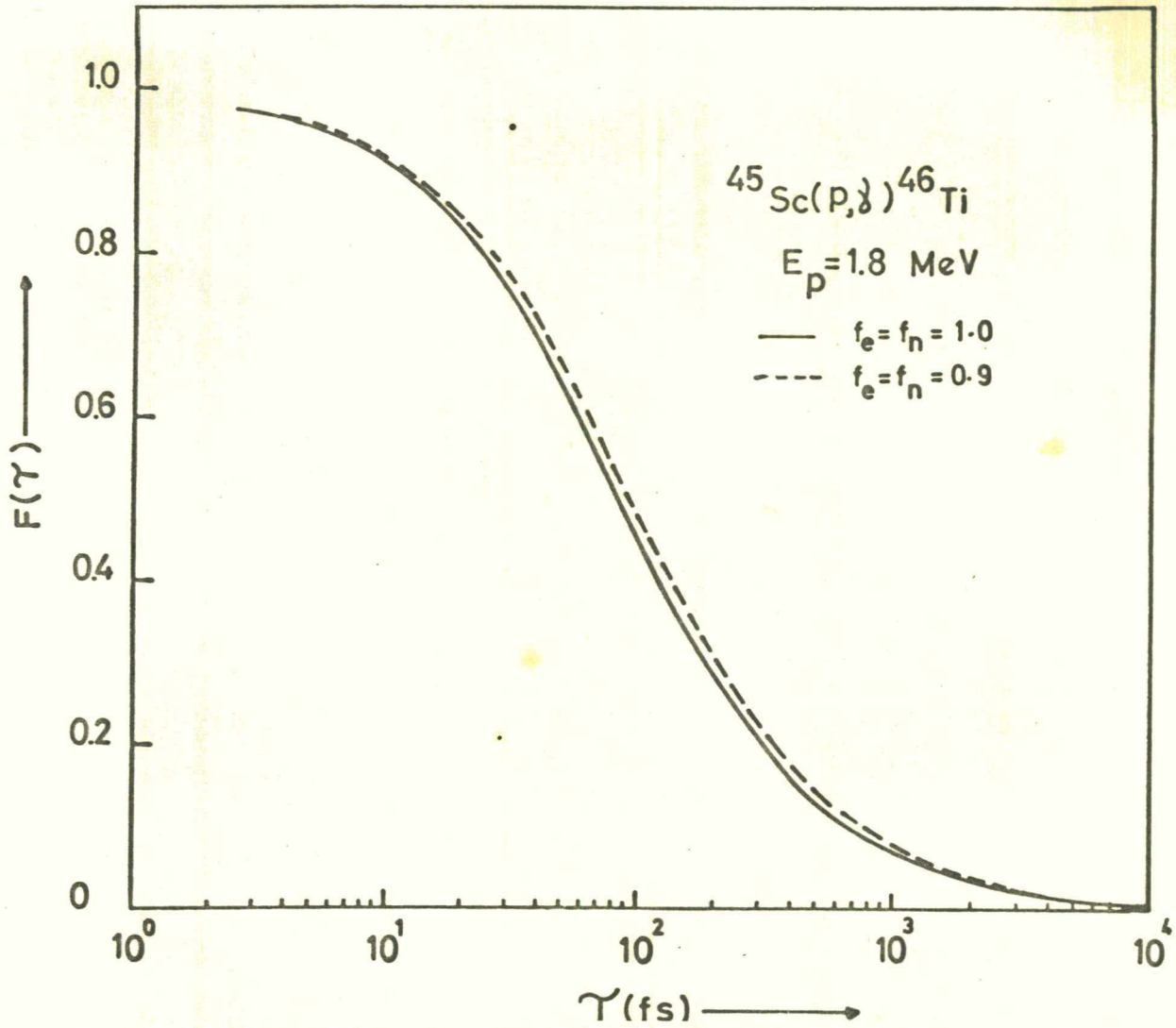

Fig. 4.2 The attenuation factor F(τ) vs. lifetime τ curve for ^{46}Ti nuclei recoiling in ^{45}Sc at E_p = 1.8 MeV. The solid curve refers to correction factor f=1.0 and the dashed curve refers to correction factor f=0.9.

Dhaka University Institutional Repository

Dhaka University Institutional Repository

and the mixing ratio is given by

$$\delta^2 = \frac{T(E2)}{T(M1)} \qquad (4\text{-}3)$$

The estimates of transition probability are called Weisskopf units and are

$$T(EL) = \frac{4.4(L+1)10^{21}}{L\left[(2L+1)!!\right]^2} \left(\frac{3}{L+3}\right)^2 \left(\frac{E}{197}\right)^{2L+1} R^{2L} \frac{1}{\text{sec.}} \qquad (4\text{-}4)$$

$$T(ML) = \frac{1.9(L+1)10^{21}}{L\left[(2L+1)!!\right]^2} \left(\frac{3}{L+3}\right)^2 \left(\frac{E}{197}\right)^{2L+1} R^{2L-1} \frac{1}{\text{sec.}} \qquad (4\text{-}5)$$

with $R = r_0 A^{1/3}$, $r_0 = 1.2$ fm.

If the observed transition probability can be quoted as a fraction or multiple of the single particle value or the 'Weisskopf Unit', then we say that the transition has a strength of

$$|M|^2_{W.u.} = \frac{\Gamma_{obs.}}{\Gamma_\gamma(\text{Weisskopf})} \qquad (4\text{-}6)$$

$|M|^2$ is some measure of the square of the matrix element of the actual transition relative to that of the extreme single particle transition where

$$\begin{aligned} \Gamma_\gamma(E1) &= 0.07\, E_\gamma^{\,3} A^{2/3} && \text{eV} \\ \Gamma_\gamma(M1) &= 0.021\, E_\gamma^{\,3} && \text{eV} \\ \Gamma_\gamma(E2) &= 4.9\times10^{-8}\, E_\gamma^{\,5} A^{4/3} && \text{eV} \\ \Gamma_\gamma(M2) &= 1.5\times10^{-8}\, E_\gamma^{\,5} A^{2/3} && \text{eV} \end{aligned} \qquad (4\text{-}7)$$

are the Weisskopf units with E_γ in MeV and are obtained when

Dhaka University Institutional Repository

the relations (4-4) and (4-5) are expressed in terms of radiative width

$$\Gamma^{obs.} = \frac{\hbar}{\tau} \cdot \frac{V}{1+\alpha} \qquad (4\text{-}8)$$

where $\hbar = 6.5819 \times 10^{-22}$ MeV sec., τ = mean lifetime in sec., V = branching ratio, and α = conversion factor which is negligibly small for $E_\gamma \geq 400$ keV.

From the experimental lifetime it is possible to give some restriction on the spin and parity of excited states when the spin and parity of the final state is known. One assumes that the M1, E1 and E2 are the most probable transition types. Higher multipole transitions occur in some special cases only, e.g., the well-known M4-isomers. The Nuclear Data Group has adopted empirical limits for the enhancement and hinderance of different radiation types compared to the Weisskopf estimate. The empirical criteria are

If the half life is:	The transition is not
$\frac{\tau_{exp.}}{\tau_W(M1)} < 0.1$	M1
$\frac{\tau_{exp.}}{\tau_W(M2)} < 1.0$	M2
$\frac{\tau_{exp.}}{\tau_W(M3)} < 0.1$	M3
$\frac{\tau_{exp.}}{\tau_W(M4)} < 0.033$	M4
$\frac{\tau_{exp.}}{\tau_W(E1)} < 1.0$	E1
$\frac{\tau_{exp.}}{\tau_W(E2)} < 0.001$	E2
$\frac{\tau_{exp.}}{\tau_W(E3)} < 0.01$	E3

Dhaka University Institutional Repository

4.4. Results and discussions

Levels in ^{46}Ti with spins upto J=6 could be populated in this (p,γ) work. Levels and transitions which were used only for the extraction of lifetimes are shown in fig. 4.3. The level energies and the spins have been taken from ref.23 except for the 3298 and 3441 keV levels which have been taken from ref. 24. Observed Doppler shifts for some of the gamma ray energies are shown in figs. 4.4a and 4.4b. The arrows in these figures show the shifts as obtained from the analyses in PDP 15 computer. Results of the DSA measurements obtained in this work at E_p=1.75 MeV are summarized in table 4.1 and those obtained at E_p=1.80 MeV are summarized in table 4.2. The lifetimes quoted in these two tables are given using the calibrated curves. It may be noted from the 4th column of table 4.2 that the measured shift is sometimes as high as 6 keV and as low as 0.025 keV. In the 5th column is given the experimental attenuation factor. We give the weighted average values in the experimental F(τ) value of the state having more than one gamma ray deexciting the level. The errors in the lifetime values are only experimental mainly coming from uncertainties in the peak determinations. Lifetimes obtained from the measurement at two different bombarding energies agree reasonably well. The adopted lifetime values along with the results of other authors are given in table 4.3 for the purpose of comparison. These adopted values are the

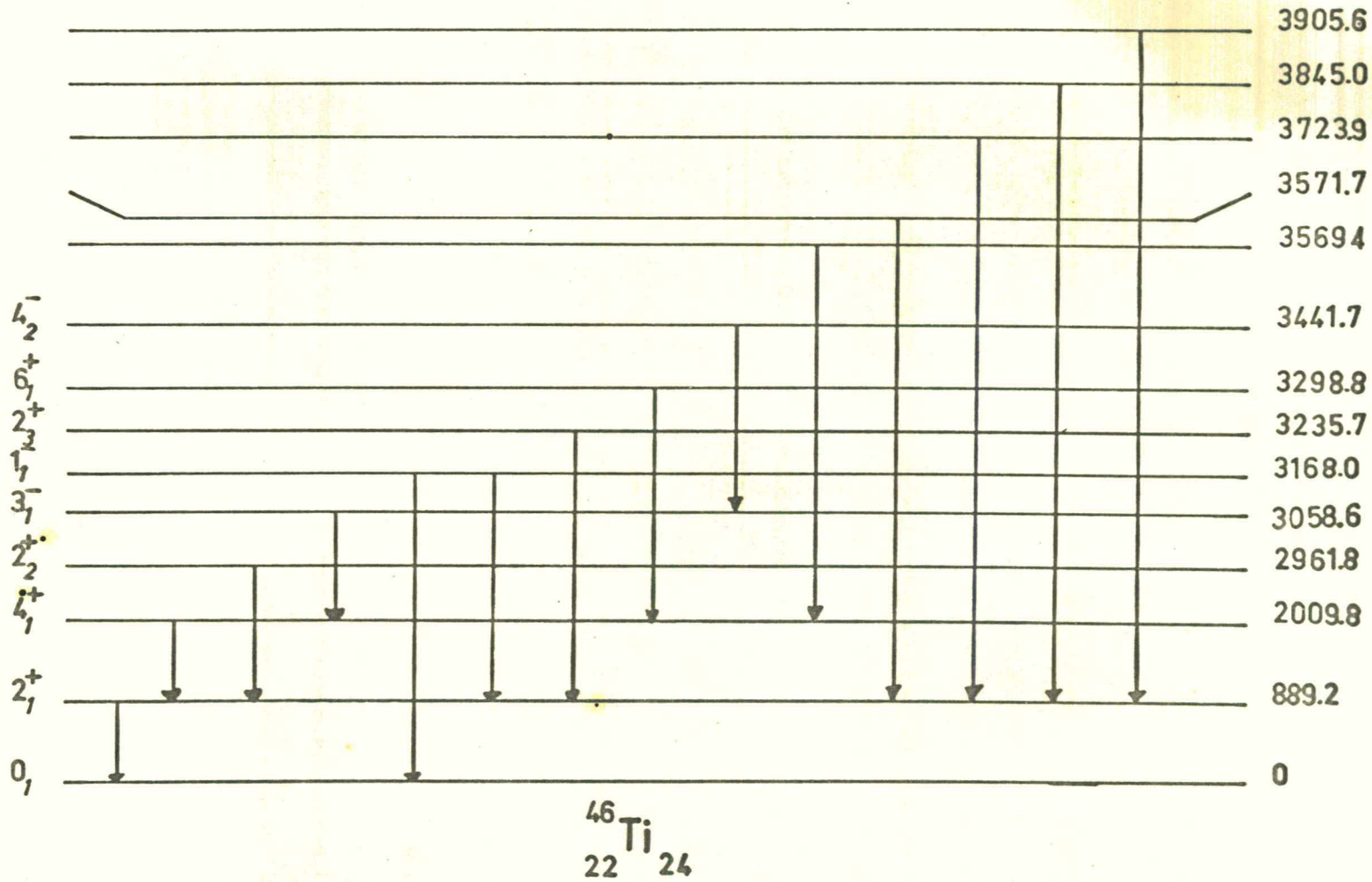

Fig. 4.3 Part of the level scheme in ^{46}Ti showing only those transitions which were employed in the extraction of lifetimes. Taken from ref. 23. (3298 and 3441 keV levels taken from ref. 24). The level schemes are not drawn to scale.

Dhaka University Institutional Repository

Dhaka University Institutional Repository

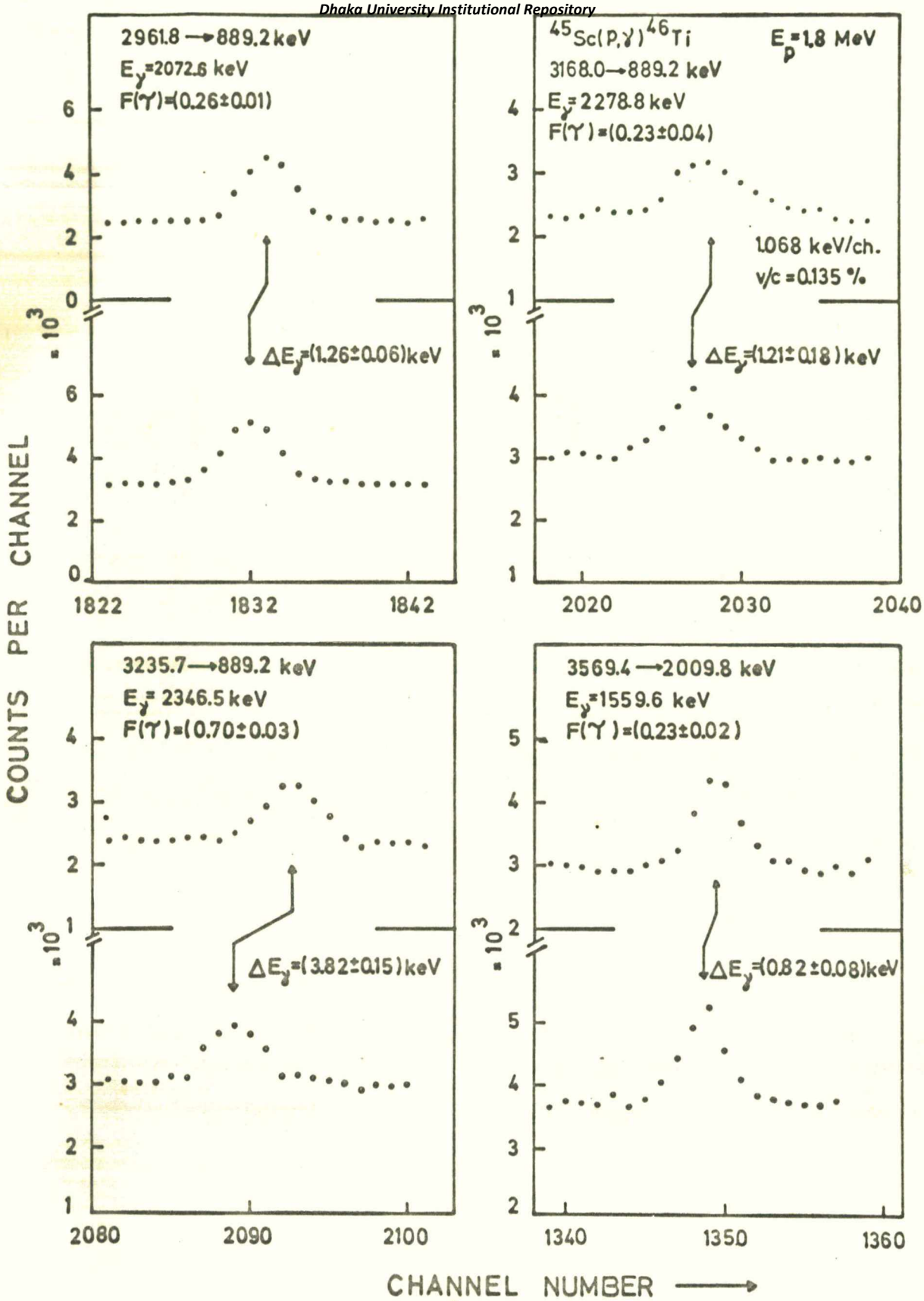

Fig. 4.4a Spectra of forward and backward Doppler-shifted γ-ray peaks from the $^{45}Sc(p,\gamma)^{46}Ti$ reaction at E_p = 1.8 MeV and measured with two-target arrangement. The arrows indicate the peak centres.

Dhaka University Institutional Repository

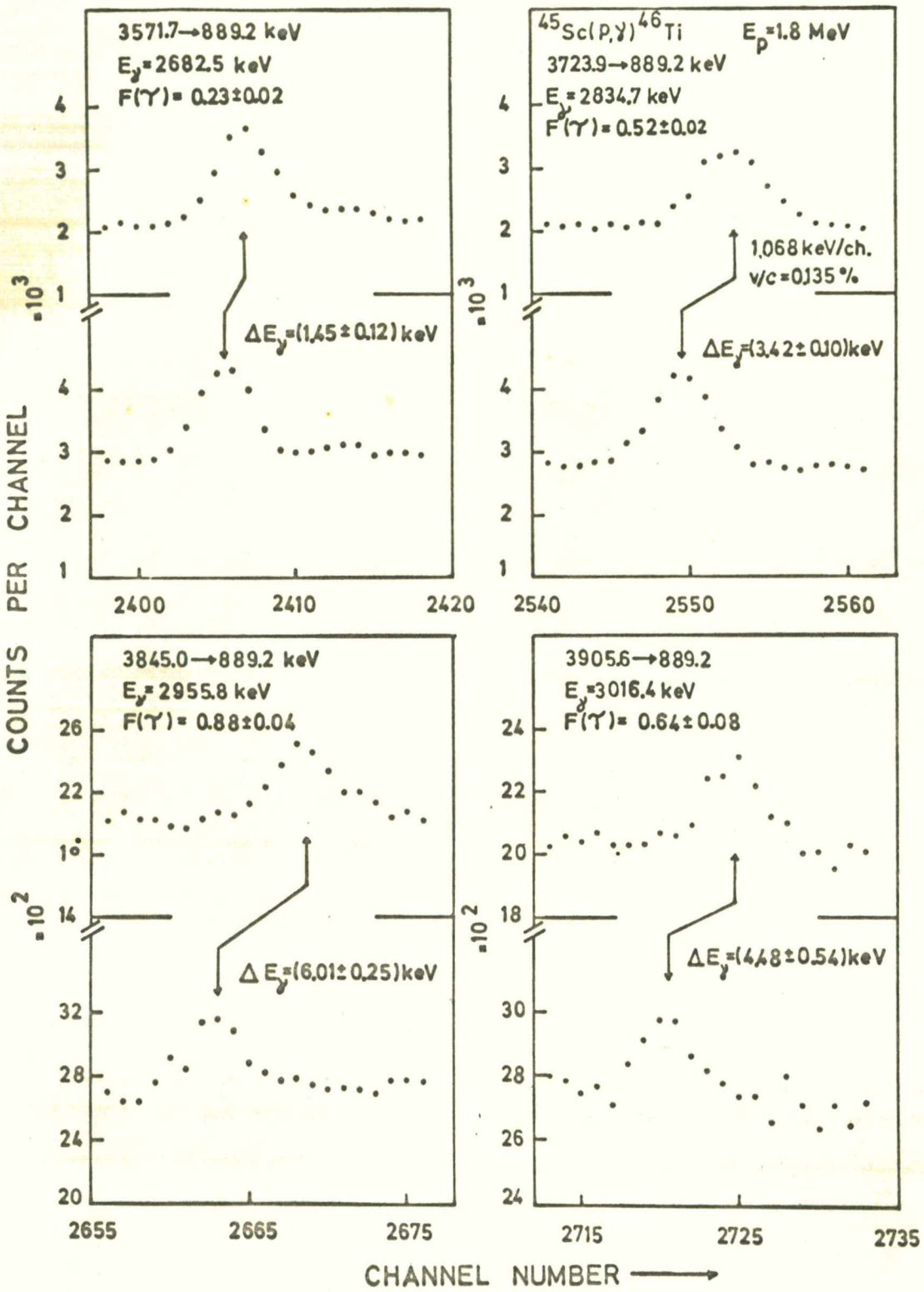

Fig. 4.4b Spectra of forward and backward Doppler-shifted γ-ray peaks from the $^{45}Sc(p,\gamma)^{46}Ti$ reaction at E_p = 1.8 MeV and measured with two-target arrangement. The arrows indicate the peak centres.

Table 4.1

Summary of lifetime results for ^{46}Ti from $^{45}Sc(p,\gamma)^{46}Ti$ reaction at E_p=1.75 MeV.

Level (keV)	E_{γ_0} (keV)	ΔE_γ^{max} (keV)	Measured shift $\overline{\Delta E_\gamma}$ (keV)	Attenuation factor $F(\tau)$ in ^{45}Sc in %	Mean lifetimes (fs)
889.2	889.2	2.035	0.008 ± 0.009	< 0.8	> 7500
2009.2	1120.6	2.565	0.046 ± 0.007	1.8 ± 0.3	2800^{+700}_{-400}
2961.8	2072.6	4.744	1.260 ± 0.064	26.6 ± 1.4	240 ± 15
3058.6	1048.8	2.401	0.011 ± 0.010	0.5 ± 0.4	> 6500
3298.8	1289.0	2.953	0.158 ± 0.026	5.3 ± 0.9	1450 ± 250
3441.7	383.1	0.875	0.001 ± 0.016	1.9	> 3100
3569.4	1559.6	3.570	0.726 ± 0.110	20.3 ± 3.1	330^{+70}_{-50}

Dhaka University Institutional Repository

Table 4.2

Summary of lifetime results for ^{46}Ti from $^{45}Sc(p,\gamma)^{46}Ti$ reaction at E_p=1.80 MeV.

Level (keV)	E_{γ_0} (keV)	ΔE_γ^{max} (keV)	Measured shift $\overline{\Delta E_\gamma}$(keV)	Attenuation factor $F(\tau)$ in ^{45}Sc in %	Mean lifetime (fs)
889.2	889.2	2.062	0.025±0.018	1.2±0.9	6000^{+9000}_{-2500}
2009.8	1120.6	2.599	0.078±0.018	3.0±0.7	1650^{+650}_{-350}
2961.8	2072.6	4.808	1.258±0.059	26.2±1.2	240^{+20}_{-10}
3058.6	1048.8	2.433	0.045±0.022	1.8±0.9	3900^{+2700}_{-1250}
3168.0	3168.0	7.349	1.918±0.353	26.1±4.8	
	2278.8	5.286	1.205±0.184	22.8±3.5	
				23.9±2.8 a)	275^{+45}_{-30}
3235.7	2346.5	5.443	3.823±0.152	70.2±2.8	42^{+10}_{-4}
3298.8	1289.0	2.986	0.170±0.026	5.7±0.9	1350^{+250}_{-150}
3441.7	383.1	0.887	0.007±0.023	3.3	>2500

Dhaka University Institutional Repository

Table 4.2 (Continued)

3569.4	1559.6	3.618	0.816 ± 0.084	22.5 ± 2.3	290^{+50}_{-30}
3571.7	2682.5	6.222	1.451 ± 0.119	23.3 ± 1.9	280^{+25}_{-20}
3723.9	2834.7	6.575	3.418 ± 0.102	52.0 ± 1.6	85 ± 5
3845.0	2955.8	6.856	6.013 ± 0.249	87.7 ± 3.6	15 ± 5
3905.6	3016.4	6.997	4.478 ± 0.537	64.0 ± 7.7	55^{+20}_{-13}

a) Mean life computed from weighted mean of estimated $F(\tau)$ values.

Dhaka University Institutional Repository

Table 4.3

Lifetime of levels in ^{46}Ti

Level (keV)	J^{π}	Mean lifetime τ (fs)				
		Present work $^{45}Sc(p,\gamma)$	Durell et.al.[22] $^{43}Ca(\alpha,n)$	Assimakopoulos et.al.[23] $^{45}Sc(p,p'\gamma)$ +	Assimakopoulos et.al.[23] $^{45}Sc(p,p'\gamma)$ ‡	Dehnhardt et.al.[24] $^{32}S(^{16}O, 2p)$
889.2	2_1^+	6000^{+9000}_{-2500}				6500 ± 700
2009.8	4_1^+	2200 ± 400				2600 ± 300
2611.0	0_2^+		110 ± 30			
2961.8	2_2^+	240 ± 10	220 ± 60	97^{+43}_{-33}	70 ± 11	
3058.6	3_1^-	3900^{+2700}_{-1300}	10000^{+3000}_{-2000}	> 650		< 83000
3168.0	1_1^-	275^{+45}_{-35}	210 ± 50	98^{+37}_{-31}	71 ± 12	
3235.7	2_3^+	42^{+10}_{-4}	41 ± 15	23^{+15}_{-9}	19 ± 3	
3298.8	6_1^+	1390 ± 155	1600 ± 400			1500 ± 700

Dhaka University Institutional Repository

Table 4.3 (Continued)

3441.7	4_2^-	2500	15000^{+10000}_{-5000}			83000 ± 9000
3569.4		302 ± 35		72^{+27}_{-23}		
3571.7		280^{+25}_{-20}	260 ± 60			
3723.9		85 ± 5	75 ± 20	47^{+27}_{-19}	47^{+23}_{-15}	
3845.0		15 ± 5	< 35	13^{+6}_{-4}	12.2 ± 3.5	
3892.0			55 ± 15			
3905.6		55^{+20}_{-13}		27^{+10}_{-9}	32 ± 6	

+ centroid shift, ‡ shape fitting

Dhaka University Institutional Repository

Dhaka University Institutional Repository

weighted averages of the two measurements and using the calibrated $F(\tau)$ curves with $f_e=f_n=0.9$. The correction for feeding to the 2009 keV state has been taken into account.

It may be noted from table 4.3 that lifetimes of 12 states have been determined and a lower limit for one state has been set in the present measurements. Our results for the 2_1^+ and 4_1^+ states agree quite well with the recoil distance data of Dehnhardt et al. [24] although these long lifetimes are close to the upper limit where the use of DSA method is no longer possible. It demonstrates, however, that the two-target arrangement used in this experiment is a powerful instrument for DSA work. The small energy shift of the $4_2^- \rightarrow 3_1^-$ transition allowed only to set the lower limit of the 3441 keV state. As such the discrepancy in this particular case could not be resolved. The present (p,γ) data decides clearly in favour of the results of Durell et al. [22] and shows that the ^{46}Ti $(p,p'\gamma)$ study of Assimakopoulos et al. [23] gives systematically too short lifetime values.

Information about γ-ray branching, mixing ratios, spin and parity is required in order to obtain absolute transition probabilities from nuclear lifetimes. But this information for this nucleus is available for a few levels from the measurements of Horoshko et al. [70], Church et al. [71], Lewis et al. [72] and Gallmann et al. [73]. The spins and parities are well established upto an excitation energy of 3298 keV.

Dhaka University Institutional Repository

Theoretical calculations for this nucleus are not much available. Müther et al. [74] and McCullen et al. [75] employed the generator coordinate method and the pure $(f_{7/2})^n$ configuration respectively, for the calculations of energy levels. The predictions from their calculations agreed quite well with experiment for the positive parity states up to 3.0 MeV.

Using the present mean lifetime values the reduced transition probabilities B(σL) and the transition strengths $|M|^2_{W.u.}$ have been calculated for some of the levels and are presented in table 4.4. The branching and mixing ratios have been used as quoted in ref. 23 which are the weighted average values of the references given therein. The branchings for the 3441 keV state were taken from ref. 24. The B(E1) value for the $3_1^- \rightarrow 2_1^+$ and $3_1^- \rightarrow 2_2^+$ decay from the 3058.6 keV level are reported here assuming a pure E1 transition. The values of $\delta = 0.0 \pm 0.1$ and $\delta = 0.0 \pm 0.04$ for the $3_1^- \rightarrow 4_1^+$ and $1_1^- \rightarrow 2_1^+$ decay respectively give only the uncertainty in δ value and as such the B(σL) value and the transition strength were calculated assuming a pure E1 transition.

The determinations of the lifetimes of the first three members of the ground state band, namely, $2_1^+ \rightarrow 0_1^+$, $4_1^+ \rightarrow 2_1^+$ and $6_1^+ \rightarrow 4_1^+$ made it possible to obtain their B(E2) values and transition strengths. These values for the electromagnetic transitions are summarized in table 4.5 along with the values of Muther et al. [74] and Dehnhardt et al. [24] for the

Electromagnetic decay properties in ^{46}Ti Table 4.4

Initial state (keV)	J^{π}	Transition to (keV)	J^{π}	Branching[a)] %	σ	δ[a)]	$B(\sigma L)$[c]	$\lvert M\rvert^2$ W.u.
2961.8	2_2^+	g.s.	0_1^+	4.2 ± 0.6	E2		0.62 ± 0.09	0.06 ± 0.01
		889.2	2_1^+	95.8 ± 0.6	E2	-1.29 ± 0.26	53.00 ± 18.0	5.31 ± 1.80
					M1		0.010 ± 0.002	0.005 ± 0.001
3058.6	3_1^-	889.2	2_1^+	3	(E1)		$\leq 0.7\times10^{-6}$	$\leq 0.8\times10^{-6}$
		2009.8	4_1^+	90 ± 3	E1	0.0 ± 0.1	$(1.26^{+0.63}_{-0.52})\times10^{-4}$	$(1.46^{+0.81}_{-0.62})\times10^{-4}$
		2961.8	2_2^+	10 ± 3	(E1)		0.018 ± 0.009	$0.020^{+0.010}_{-0.008}$
3168.0	1_1^-	g.s.	0_1^+	45.3 ± 0.9	E1		$(0.32^{+0.06}_{-0.05})\times10^{-4}$	$(0.38\pm0.06)\times10^{-4}$
		889.2	2_1^+	54.7 ± 0.9	E1	0.0 ± 0.04	$(1.06^{+0.17}_{-0.16})\times10^{-4}$	$(1.23^{+0.20}_{-0.19})\times10^{-4}$
3235.7	2_3^+	g.s.	0_1^+	16.8 ± 1.1	E2		$9.24^{+1.65}_{-2.27}$	$0.92^{+0.16}_{-0.22}$
		889.2	2_1^+	84.2 ± 1.1	E2	-0.01 ± 0.07	<0.27	<0.027
					M1		$0.088^{+0.010}_{-0.018}$	$0.048^{+0.006}_{-0.010}$
3441.7	4_2^-	2009.8	4_1^+	25 ± 3[b)]	E1	$-1.4\quad 0.1$	$<0.21\times10^{-4}$	$<0.24\times10^{-4}$
					M2		$<8.12\times10^{2}$	<37
		3058.6	3_1^-	75 ± 3[b)]	E2	$-1.0^{+0.42}_{-0.94}$	$<23.6\times10^{3}$	$<23\times10^{2}$
					M1		<0.22	<0.12

a) Taken from ref. 23 are the weighted average values of the references given therein
b) Taken from ref. 24,
c) The $B(\sigma L)$ values are in units of $e^2\,fm^{2L}$; $B(\sigma L)$ are in units of $\mu fm^{2(L-1)}$

Dhaka University Institutional Repository

Table 4.5

Electromagnetic transitions in ^{46}Ti

Transition			Muther et.al.[74]			Dehnhardt et.al.[24]		Present work(Expt)	
(keV)		J^{π}	$B\downarrow(E2)e^2fm^4$			$B\downarrow(E2)e^2fm^4$	$\|M\|^2$(W.u.)	$B\downarrow(E2)e^2fm^4$	$\|M\|^2$(W.u.)
			GCM	GCM+QP	Expt.	Expt.	Expt.	Expt.	Expt.
889.2	g.s.	$(2_1^+ \; 0_1^+)$	76	78	171 ± 8	217(17)	216(17)	245^{+175}_{-145}	24^{+18}_{-14}
2009.8	889.2	$(4_1^+ \; 2_1^+)$	106	102	177	177(20)	17.6(20)	210 ± 40	21 ± 4
3298.8	2009.8	$(6_1^+ \; 4_1^+)$	110	103		150(80)	15(8)	165 ± 15	16 ± 2

Dhaka University Institutional Repository

Dhaka University Institutional Repository

purpose of comparison. It is to be mentioned that Müther et al.[74] obtained the B(E2) values by employing the generator coordinate method including quasiparticle excitations. The calculated B(E2) values[74] are too small compared to the experimental value of the same authors[74] and our values.

The B↓(E2) values and the transition strengths obtained in this measurement (table 4.5) are in good agreement with those obtained by ref. 24. The transition strength for the $2_1^+ \rightarrow 0_1^+$ is observed to have a high value which indicates that the collective model is applicable to the ground state band. However collective character of the 6_1^+, 4_1^+ and 2_1^+ decreases with increasing angular momentum. Again the B↓(E2) values for the above transitions have been observed to decrease with increasing spin. This indicates that the high-spin states include shell-model configurations as well. This is observed from the energy position of the 6_1^+ state calculated from the $(1f_{7/2})^n$ model[75] which fits better than the 2_1^+ and 4_1^+ states.

From the criteria given by the Nuclear Data Group and using the lifetimes obtained in the present work, it was possible to put a range of possible spin and parity values for some of the levels for which no J^π value is known. They are summarized in table 4.6. Besides, some more restrictions are possible and are discussed in the following. The spins and parity of 1^- and 2^- for the 3723.9 and 3845.0keV states are less

Dhaka University Institutional Repository

likely than the other values because these J^{π} values involve an E1 transition to the 2_1^+ level. The 0^+ for 3905.6 keV level can be excluded because a ground state ($J^{\pi}=0^+$) branch is observed. The 4^+ for the same level may be excluded on the ground that then a ground-state transition will not be observed.

Table 4.6

Possible range of spins and parities in ^{46}Ti+

Level (keV)	J^{π}
3569.4	$2^+, 3^{\pm}, 4^{\pm}, 5^{\pm}, 6^+$
3571.7	$0^{\pm}, 1^{\pm}, 2^{\pm}, 3^{\pm}, 4^+$
3723.9	$1^{\pm}, 2^{\pm}, 3^{\pm}, 4^+$
3845.0	$0^+, 1^{\pm}, 2^{\pm}, 3^{\pm}, 4^+$
3905.6	$0^+, 1^{\pm}, 2^{\pm}, 3^{\pm}, 4^+$

+ The possible range of spin and parity assignments were made from the comparison of experimental and Weisskopf estimated lifetimes and using the criteria given by Nuclear Data Group. Further restriction are discussed in the text which are very tentative.

Finally it may be stated that the present measurements give a more complete set of lifetimes than any previous work. Using the calibrated curves our results decide in favour Durell et al.[22] and the discrepancy of a factor of 2 existing previously between the two measurements [22, 23] seems to have been resolved. That it was possible to measure small shift shows that the two-target arrangement used in this work is a useful instrument for the DSA measurements.

Dhaka University Institutional Repository

CHAPTER-5

LIFETIME MEASUREMENT IN ^{45}Sc

5.1. Introduction

The nucleus ^{45}Sc as a member of the f-p shell region is of theoretical interest and has been studied in several previous papers [28]. Investigations on lifetimes of excited states in this nucleus have been done by using different experimental methods. Lifetimes of 376, 720 and 1237 keV levels in ^{45}Sc have been deduced from transition probabilities obtained by Coulomb excitation [77-82] and inelastic scattering [83]. Metzger [25] and Arnold et al. [25a] measured the lifetimes of a few levels using the resonance fluorescence method which is independent of the slowing down process. Rust et al. [27] measured the lifetimes of 5 levels in ^{45}Sc using DSA method and $^{45}Sc(p,p'\gamma)$ reaction. Toulemonde et al. [28] and Chevallier et al. [29] employed the DSA method and used $^{42}Ca(\alpha,p\gamma)$ reaction. Schulte et al. [26] determined the lifetime of a number of states in ^{45}Sc with the DSA method and the $^{44}Ca(p,\gamma)$ reaction, and this is the only lifetime measurement for levels above 2092 keV. As can be seen from table 5.3, disagreements exist for the lifetime values determined by these different experiments. A summary of the properties of the levels in ^{45}Sc is given by Beene et al. [29a].

The original purpose of the present experiment was to obtain a calibration of the $F(\tau)$ curve for the stopping process

Dhaka University Institutional Repository

in ^{45}Sc by measuring the lifetimes of a few levels in ^{45}Sc and then comparing these values with those obtained by other methods. The lifetime data of Metzger [25] was regarded as the reliable basis for this purpose. This calibration we wanted to use for a (p,γ) experiment (chapter 4) on the same target leading to levels in ^{46}Ti. This procedure is justified because the properties of the target are identical and possible corrections to the slowing down process will not change much by increasing the atomic number from 21 to 22. In both the reactions the nuclear part of the stopping cross section is dominating. The calibration curve obtained from this measurement was used in our experiments on ^{46}Ti already described in chapter 4.

When running the $^{45}Sc(p,p'\gamma)$ experiment it was observed that many excited states in ^{45}Sc were populated. This led us to determine a complete set of lifetimes in ^{45}Sc, because new data could help to clear the already mentioned discrepancies (table 5.3). The other opportunity was to calculate the reduced transition probabilities and transition strengths from the measured lifetimes.

In a (p,γ) reaction the initial velocity of the recoiling nuclei is the same as the velocity of the centre of mass system and this type of reaction produces a unidirectional beam of nuclei. The DSA measurements with (p,p'γ) reaction are often done by proton-gamma coincidence measurements. But

Dhaka University Institutional Repository

as we did singles measurements the effect of the undefined kinematics and the Q-value dependence has to be considered. For example, a level directly populated at an excitation energy of 720 keV in ^{45}Sc at a proton bombarding energy of 4.5 MeV, yields for the recoiling nuclei an initial v/c value of 0.0039 and 0.0011 corresponding to an angle of emission of 30° and 150° respectively in the centre of mass system. In fig. 5.1 is shown the different $F(\tau)$ curves resulting from the different initial velocities corresponding to centre of mass angles of 150°, 120°, 90°, 60° and 30°. Thus an averaging over all initial v/c has to be done using the angular correlation function W as a weighting factor. For the influence of the angular correlation function and Q-value an averaging procedure was applied and a new averaged attenuation factor $\widetilde{F(\tau)}$ vs. τ curve calculated according to Moazed et.al.[11]. This new curve was used for the extraction of lifetimes. The procedure of calculation is described in section 5.3.

5.2. The initial velocity

The initial velocity of the recoiling nuclei can be calculated depending on the type of reaction and the experimental arrangement. In a reaction of the type

$$m_2(m_1,m_3)m_4^*$$

a target nucleus of mass m_2 is bombarded by a beam of particles of mass m_1 to form the nucleus of mass m_4 in an excited state

Dhaka University Institutional Repository

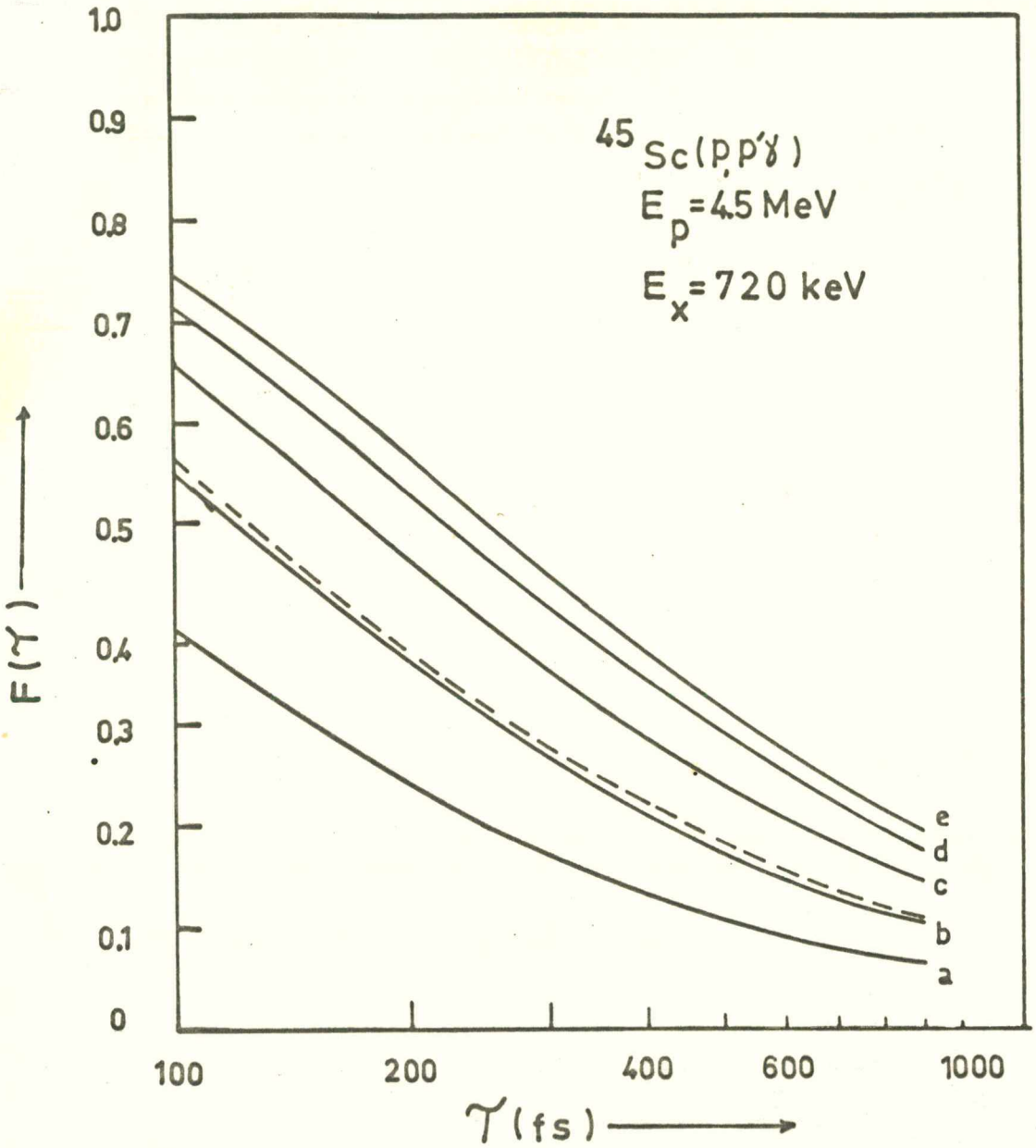

Fig. 5.1 Attenuation factor $F(\tau)$ vs. lifetime τ curves for ^{45}Sc nuclei recoiling in ^{45}Sc. The solid curves a, b, c, d and e refer to initial velocities of the recoiling nuclei corresponding to 150°, 120°, 90°, 60° and 30° respectively in the CM system. The dashed curve corresponds to $v_0 = v_{CM}$.

Dhaka University Institutional Repository

and a particle of mass m_3. Because of the emission of the particle m_3, the velocity of the recoiling nuclei in the lab. system is given by

$$\vec{v}_0 = \vec{v}^R_{lab.} = \vec{v}_{CM} + \vec{v}^R_{CM} \qquad (5\text{-}1)$$

where $\vec{v}_{CM}$ is the velocity of the centre of mass and $\vec{v}^R_{CM}$ is the velocity of the recoiling nuclei in the centre of mass system. From the simple application of mementum and energy conservation

$$v_{CM} = \left\{ \frac{2m_1 E_p^{lab.}}{(m_1+m_2)^2\ 931.5} \right\}^{1/2} \times c \qquad (5\text{-}2)$$

and

$$v^R_{CM} = \left\{ \frac{2m_3}{m_4(m_3+m_4)} \left[E_p^{lab.} \frac{m_2}{m_1+m_2} + Q \right] \right\}^{1/2} \left\{ 1/931.5 \right\}^{1/2} c \qquad (5\text{-}3)$$

where all masses are in atomic mass units and $E_p^{lab.}$ is the proton bombarding energy in the lab. system. The term in square bracket in relation (5-3) above is the total kinetic energy of the outgoing particle and the residual nucleus. Q is the Q-value. In case of a $(p,p'\gamma)$ reaction

$$Q = -E_x \qquad (5\text{-}4)$$

In case where m_3 is a gamma ray

$$\vec{v}^R_{lab.} = \vec{v}_{CM} \qquad (5\text{-}5)$$

Dhaka University Institutional Repository

5.3. Calculation of averaged attenuation factor $\widetilde{F(\tau)}$ vs. τ curve for recoiling nuclei having undefined initial velocity.

The determination of lifetimes from DSA method requires a defined direction and initial velocity of the recoiling nuclei. This is obtained by a (p,γ) reaction, particle-gamma coincidence measurements and by threshold measurements. The observed Doppler shift from relation (2-8) can then be written in the form

$$\overline{\Delta E_\gamma} = 1/c\ E_\gamma F(\tau)\ \vec{v}_0 . \vec{n} \qquad (5\text{-}6)$$

where $v(t=0)=v_0$ and the attenuation factor $F(\tau)$ is given by equation (2-7). In the above expression $\vec{n}$ denotes the direction of the emission and $\vec{v}_0$ the direction of the recoiling nuclei.

In $(p,p'\gamma)$ singles measurements the magnitude and direction of the v_0 of the recoiling nuclei are not precisely defined and are Q-value dependent. So in such experiments it is necessary to average over all initial v_0 using the angular correlation function W as a weighting function. The following symmetry relations for the angular correlation function W in the CM system [84] are given by the statistical theory for the compound nuclear reaction:

$$W(\theta_\gamma, \theta_R, \phi_R) = W(\theta_\gamma, \pi-\theta_R, \pi+\phi_R) \qquad (5\text{-}7)$$

$$= W(\pi-\theta_R, \theta_R, \pi+\phi_R) \qquad (5\text{-}8)$$

$$= W(\pi-\theta_\gamma, \pi-\theta_R, \phi_R) \qquad (5\text{-}9)$$

Dhaka University Institutional Repository

W is independent of azimuthal angle ϕ_R for $\theta_\gamma = 0, \pi$ or $\theta_R = 0, \pi$. θ_γ and θ_R are the angles of emission of the γ-ray and the recoiling nucleus with respect to the incident beam direction and ϕ_R is taken equal to zero.

The averaging of the term $\vec{v}_0 \cdot \vec{n}$ in equation (5-6) is one way to take into account all possible initial velocities with the assumption that the attenuation factor is independent of initial velocity (Method 1). Another way is to take into account the v_0 dependence of the attenuation factor $F(\tau)$ to define a new function $\widetilde{F(\tau)}$, called the averaged attenuation factor (Method 2). In this case equation (5-6) can be written as

$$\overline{\Delta E_\gamma} = 1/c \; E_\gamma \overline{F(\tau, v_0) \; \vec{v}_0 \cdot \vec{n}} \qquad (5\text{-}10)$$

For Method 1 the average is defined by

$$\overline{\vec{v}_0 \cdot \vec{n}} = \frac{\int \vec{v}_0 \cdot \vec{n} \; W^{lab} \; d\Omega_R^{lab}}{\int W^{lab} \; d\Omega_R^{lab}} = \int \vec{v}_0 \cdot \vec{n} \; W^{lab} \; d\Omega_R^{lab} \qquad (5\text{-}11)$$

where the normalisation of the correlation function is given by

$$W^{lab} \; d\Omega_R^{lab} = 1$$

For our experiment the difference in the quantities $\theta_\gamma, \vec{n}$ and $d\Omega$ in the CM system and lab. system can be neglected. From relation (5-1) one obtains

$$\overline{\vec{v}_0 \cdot \vec{n}} = \int \vec{v}_{CM} \cdot \vec{n} \; W \; d_R + \int \vec{v}_{CM}^{R} \cdot n \; W \; d\Omega_R \qquad (5\text{-}12)$$

The term $\vec{v}_{CM} \cdot \vec{n}$ above is independent of θ_R and ϕ_R and the

Dhaka University Institutional Repository

integration of the first term gives $\vec{v}_{CM}\cdot\vec{n}$. Integration of the second term gives

$$\int \vec{v}^{R}_{CM}\cdot\vec{n}\, W\, d_{R} = v^{R}_{CM} \quad (\sin\theta_{\gamma}\sin\theta_{R}\cos\phi_{R} + \cos\theta_{\gamma}\cos\theta_{R})W \sin\theta_{R}\, d\theta_{R}\, d\phi_{R} \qquad (5\text{-}13)$$

With the help of symmetry relations (5-7) the second term in equation (5-12) vanishes and so

$$\vec{v}_{0}\cdot\vec{n} = \vec{v}_{CM}\cdot\vec{n} = v_{CM}\cos\theta \qquad (5\text{-}14)$$

These results mean that the emission of the particle does not influence the Doppler shift but has an effect on the broadening of the line. The relative broadening is given by

$$\frac{\Delta v}{v} \doteq 2\left\{\frac{m_2 m_4}{m_1 m_3}\left[1 + \frac{m_1+m_2}{m_2}\,\frac{Q_0 - E_x}{E_{lab}}\right]\right\}^{1/2}$$

for the reaction of the type $m_2(m_1,m_3)m_4$

Method 2: Because of the change in $F(\tau)$ curves due to different initial velocities, the term $\overline{F(\tau,v_0)\,\vec{v}_0\cdot\vec{n}}$ has to be calculated according to Method 2. In this method an averaging procedure was applied according to Moazed et al.[11] for the calculation of the expression $\overline{F(\tau,v_0)\,\vec{v}_0\cdot\vec{n}}$. The authors define a new function by rewriting equation (5-6) as

$$\overline{\Delta E_{\gamma}} = 1/c\; E_{\gamma}\overline{F(\tau,v_0)\,\vec{v}_0\cdot\vec{n}} = 1/c\; E_{\gamma}\widetilde{F(\tau)}\;\overline{\vec{v}_0\cdot\vec{n}}$$
$$= 1/c\; E_{\gamma}\widetilde{F(\tau)}\;\vec{v}_{CM}\cdot\vec{n}$$

Dhaka University Institutional Repository

so that

$$\widetilde{F(\tau)} = \overline{F(\tau,v_0)\ \vec{v}_0.\vec{n}} \ / \ \vec{v}_{CM}.\vec{n} \qquad (5\text{-}15)$$

The initial velocity of the recoiling nuclei can be written as a function of the CM angles θ_R in the CM system as

$$v_0 = (v_{CM}^2 + v_{CM}^{R\,2} + 2\cos\theta_R . v_{CM} . v_{CM}^R)^{1/2} \qquad (5\text{-}16)$$

The initial velocity dependence of the attenuation factor $F(\tau)$ can be expressed as a power series in $\cos\theta_R$ as

$$F(\tau,v_0) = \sum_{k=0}^{4} a_k\ (\tau)\ (\cos\theta_R)^k \qquad (5\text{-}17)$$

The coefficients $a_k(\tau)$ are to be determined by calculating $F(\tau)$ for $\theta_k = 1/6.\pi k$, $k=1,\ldots 5$. Assumptions have to be made to solve the integral

$$\overline{F(\tau,v_0)\ \vec{v}_0.\vec{n}} = \int F(\tau,v_0)(\vec{v}_{CM}+\vec{v}_{CM}^R).\vec{n}\ W\ d_{\Omega_R} \qquad (5\text{-}18)$$

It is known that the correlation function is weakly dependent on the azimuthal angle ϕ_R [84]. Therefore, the ϕ_R dependence of the correlation function can be neglected. The authors assume a function of the form

$$W = \frac{n+s\ \cos(2\theta_R)}{4\pi\,(n-1/3\ s)} \qquad (5\text{-}19)$$

which takes into account symmetry properties(eqns (5-7)-(5-9))

Dhaka University Institutional Repository

of the correlation function. The correlation function W is normalised which for n=s=1 has a minimum at $\theta_R=90^\circ$ and for n=1, s=-1 has a maximum at $\theta_R=90^\circ$. The limit $n \longrightarrow 10^3$ results in an isotropic function. This is demonstrated in fig.5.2.

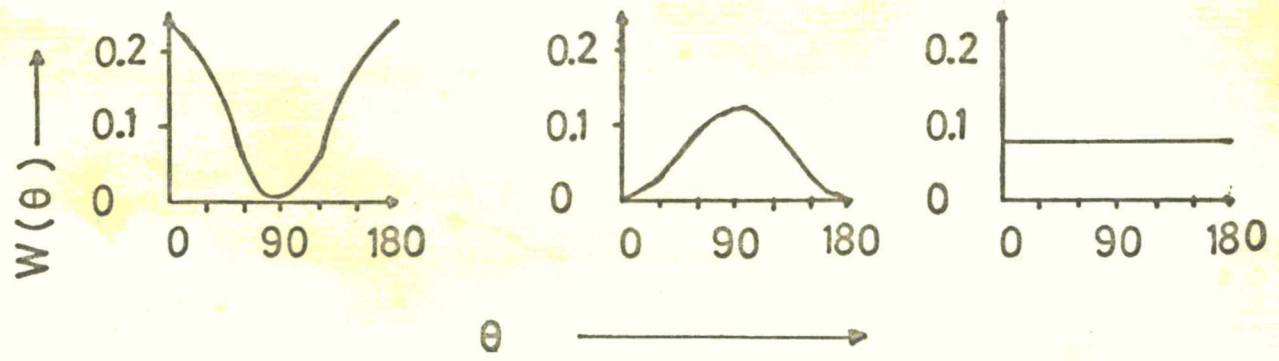

Fig. 5.2 The forms of the correlation function according to equation (5-19).

With these assumptions one obtains

$$\overline{F(\tau,v_0)\,\vec{v}_0\cdot\vec{n}} = \vec{v}_{CM}\cdot\vec{n}\sum_{k=0}^{4} a_k(\tau)(\cos\theta_R)^k \frac{n+s\cos(2\theta_R)}{4\pi(n-1/3\,s)}\sin\theta_R\,d\theta_R\,d\phi_R$$

$$+\,v^R_{CM}\sum_{k=0}^{4} a_k(\tau)(\cos\theta_R)^k \frac{n+s\cos(2\theta_R)}{4\pi(n-1/3\,s)}\sin\theta\,\sin^2\theta_R\cos\phi_R\,d\theta_R\,d\phi_R$$

$$+\,v^R_{CM}\sum_{k=0}^{4} a_k(\tau)(\cos\theta_R)^k \frac{n+s\cos(2\theta_R)}{4\pi(n-1/3\,s)}\cos\theta\,\cos\theta_R\,\sin\theta_R\,d\theta_R\,d\phi_R \qquad (5\text{-}20)$$

Because of the ϕ_R independence of W, the integration over ϕ of the first and third terms in the above expressions gives

Dhaka University Institutional Repository

a factor of 2π and the second term vanishes. Writing A and B in place of the first and third terms in equation (5-20) we get

$$\widetilde{F(\tau)} = 2\pi(A + v^{R}_{CM}/v_{CM}.B) \qquad (5\text{-}21)$$

The integrals A and B are solved numerically.

It is thus seen that the lifetimes of excited states can be obtained by measuring singles γ-ray spectra from a $(p,p'\gamma)$ reaction. Now one has to compare the experimental attenuation factor with the $F(\tau)$ vs. τ curve. The following were carried out for the calculation of $\widetilde{F(\tau)}$ curves.

1) Calculation of the initial velocity v_0 of the recoiling nuclei at 5 different angles in CM system.

2) Calculation of the $F(\tau)$ curves for the different initial velocities obtained from 1 above.

3) Calculation of the coefficients a_k for every τ.

4) Calculations of integrals A and B for every τ.

5) Calculation of $\widetilde{F(\tau)}$ curve according to equation (5-21).

5.4. The experiment

The measurements presented in this chapter were performed with protons from the 7.5 MeV vertical type accelerator of the Institut für Kernphysik, University of Frankfurt. The levels in ^{45}Sc were populated by the $^{45}Sc(p,p'\gamma)$ reaction at

Dhaka University Institutional Repository

proton bombarding energies of 3.0 and 4.5 MeV. A collimated proton beam was obtained by a number of tantalum collimators of various diameters and slits inside the beam port tube. The beam was focussed by two quadrupole lenses, one of which was situated after the 90° magnet and the other was after the 25° magnet. A cold trap was used before the target chamber for the suppression of background gamma rays. All other experimental apparatus including the target chamber, Ge(Li) detector and the electronic set-up were the same as used in the measurements described in the last chapter. The same targets were used for both the $^{45}Sc(p,\gamma)$ and the $^{45}Sc(p,p'\gamma)$ reactions as required by our calibration procedure.

Singles γ-ray spectra were measured for both the targets placed at forward and backward angles and stored separately in the two memories of the multichannel analyser. All 4096 channels were used for this purpose and the gain of the amplifier was so adjusted that the whole range of the analyser covered approximately 3.0 MeV for measurements at both bombarding energies. During the experiment γ-rays from a ^{60}Co source were recorded along with the reaction lines for the purpose of calibration. This also allowed to check if there was any shift in energy of γ-rays at two angles. The dead time of the analyser was maintained at about 5%. The γ-ray spectra were measured for 12 hours. The peak centre determinations were carried out in PDP 15 computer.

Dhaka University Institutional Repository

5.5. Analyses

For calculating the stopping cross-section the theory of Lindhard *et al.* [16] was used and the multiple scattering was treated in the way given by Blaugrund [19]. As we did singles measurements the effect of undefined kinematics was taken into account for the extraction of lifetimes from the experimental $F(\tau)$ values. As described in section 5.3 this was done by averaging the $F(\tau)$ curves over all initial velocities using the angular correlation function as a weighting factor [11]. It was checked by calculating the level density in ^{46}Ti that the application of statistical compound theory is justified. The v_0 dependence of the attenuation factor was applied to obtain an averaged attenuation factor $\widetilde{F(\tau)}$ versus τ curve in analogy with equation (5-6). Assumptions for the angular correlation function used were the same as Moazed *et al.* [11]. The effect of the shape of the correlation factor is not, of course, so large. The averaged curve from the isotropic function was used to fix the mean lifetime and the effect of the two extreme shapes given by Moazed *et. al.* [11], a minimum or a maximum at an angle of 90°, were used as an additional part to the statistical error. The $\widetilde{F(\tau)}$ curves due to the three forms of the correlation function for an excitation energy of 720 keV is shown in fig. 5.3.

It should be mentioned that the averaged attenuation curves are Q-value dependent. The $\widetilde{F(\tau)}$ curves for the three

Dhaka University Institutional Repository

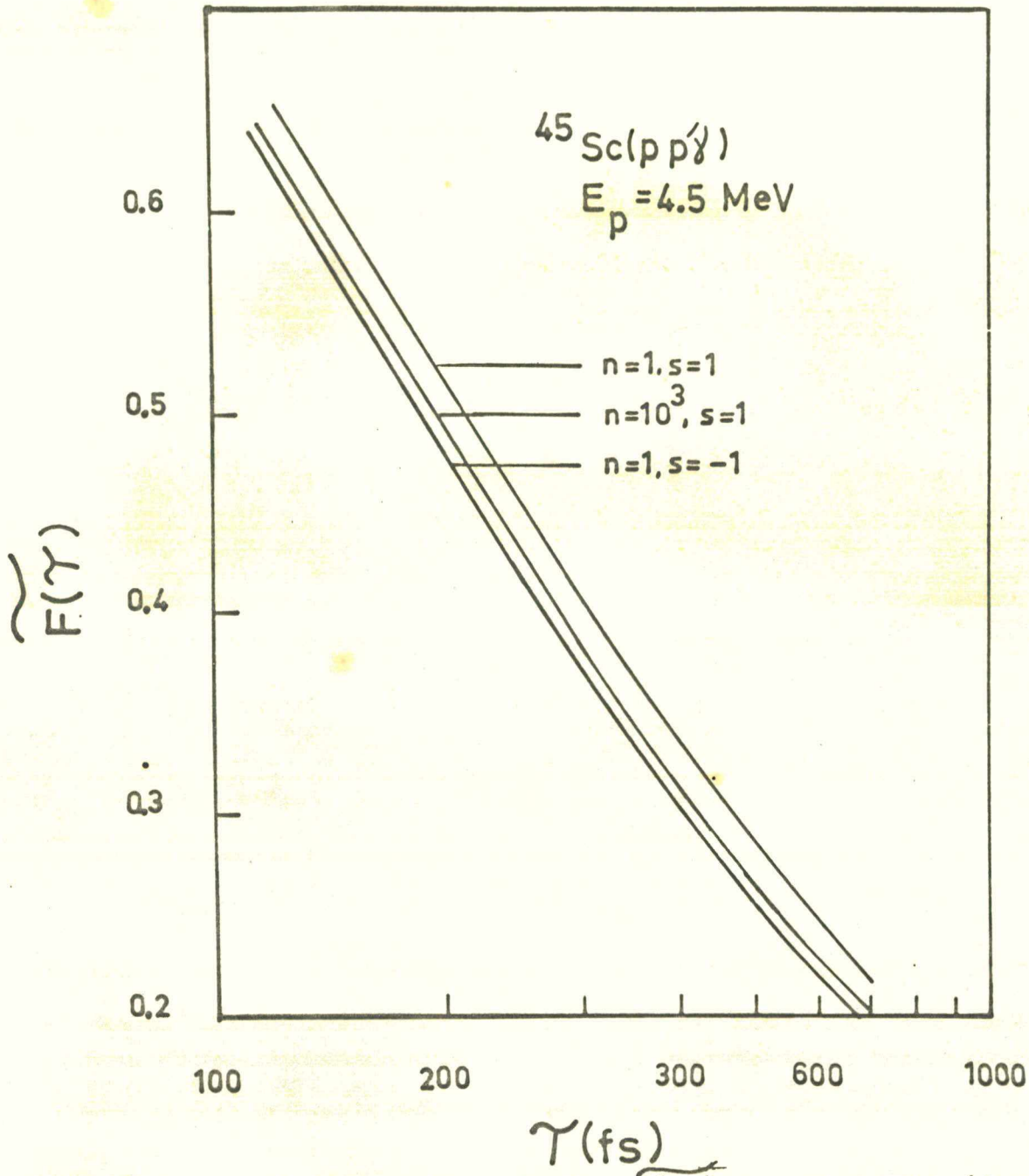

Fig. 5.3 Averaged attenuation factor $\tilde{F}(\tau)$ vs. τ curves (for the 720 keV level) showing the effect of the three forms of the angular correlation function. The middle one is due to isotropic function. The other two curves are due to extreme shapes of the correlation function (see section 5.3).

Dhaka University Institutional Repository

Q-values of -376, -1800 and -2778 keV are shown in fig. 5.4. It may be noted from fig. 5.4 that the Q-value has a considerable effect on the derived lifetime.

As mentioned in the introduction, the main purpose of this experiment was to obtain a calibration of the $F(\tau)$ curve for ^{46}Ti recoiling in ^{45}Sc. For this purpose the lifetime data of the 720, 1236, 1409, 1662 and 2092 keV levels obtained by the resonance fluorescence method by Metzger [25] were compared with our results. In fig. 5.5 our $F(\tau)$ values are compared with the lifetimes of Metzger [25]. The averaged $\widetilde{F(\tau)}$ curves using correction factor $f_e = f_n = 1.0$ are shown as solid curves for the 720 keV and 1662 keV levels. The dashed curve is due to 720 keV level and using correction factor of $f_e = f_n = 0.9$. It may be noted from the figure that the experimental points fit quite well with the curve obtained by using the correction factor of $f = 0.9$ to the stopping power. This factor has no general meaning and is valid for a special combination of recoiling nuclei and stopping atoms used in this experiment including possible deviations of the density of Sc from the value of 3.0 gm/cc. However the slowing down theory of Lindhard et al. [16] seems to overestimate the nuclear stopping cross section, which is the dominating part of the stopping cross section in this experiment.

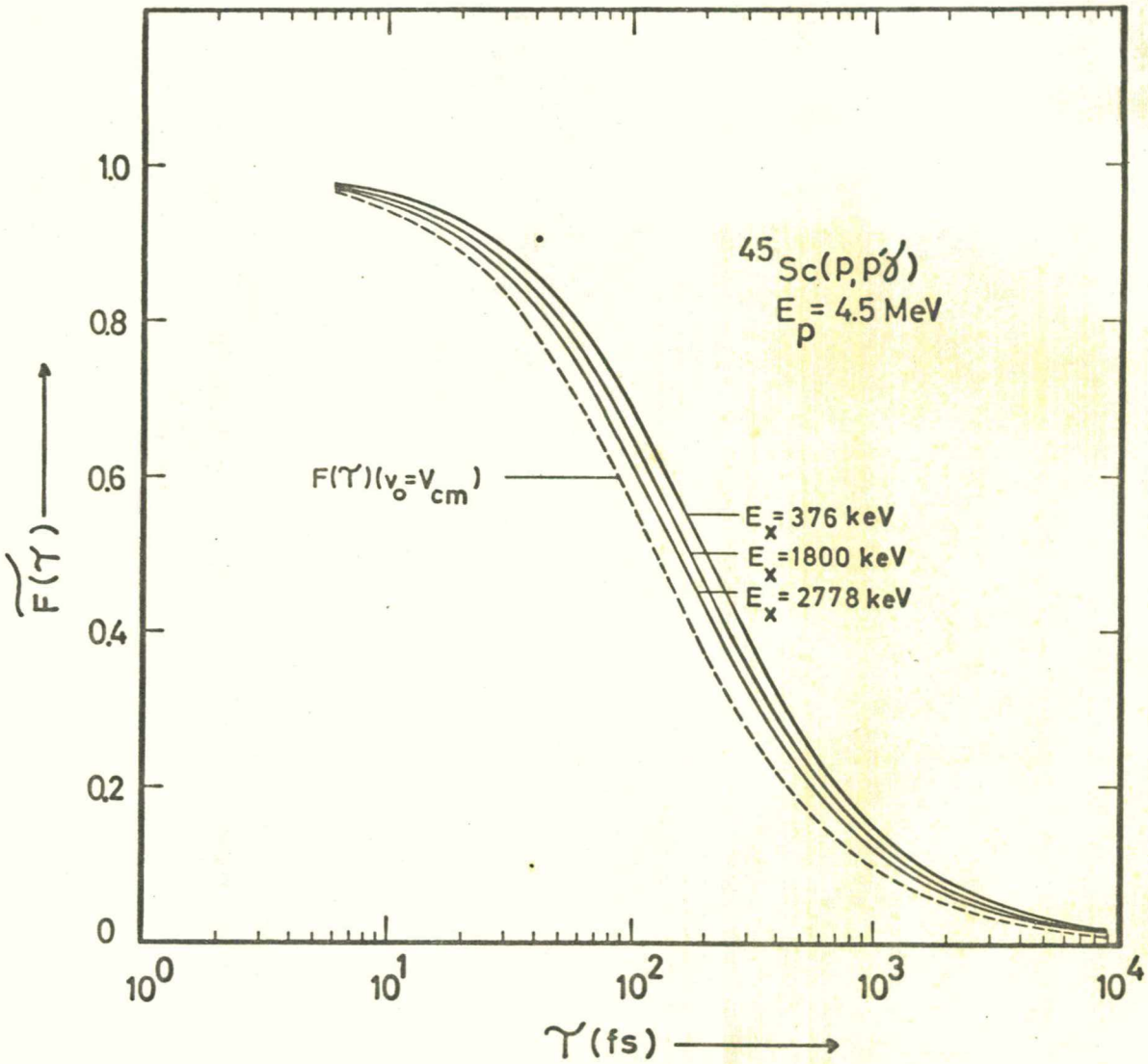

Fig. 5.4 Averaged attenuation factor $\widetilde{F(\tau)}$ vs. τ curves for ^{45}Sc nuclei recoiling in ^{45}Sc showing the Q-value dependence. The three curves are due to Q-values of -376, -1800 and -2778 keV. The dashed curve refers to $v_0 = v_{CM}$.

Dhaka University Institutional Repository

Dhaka University Institutional Repository

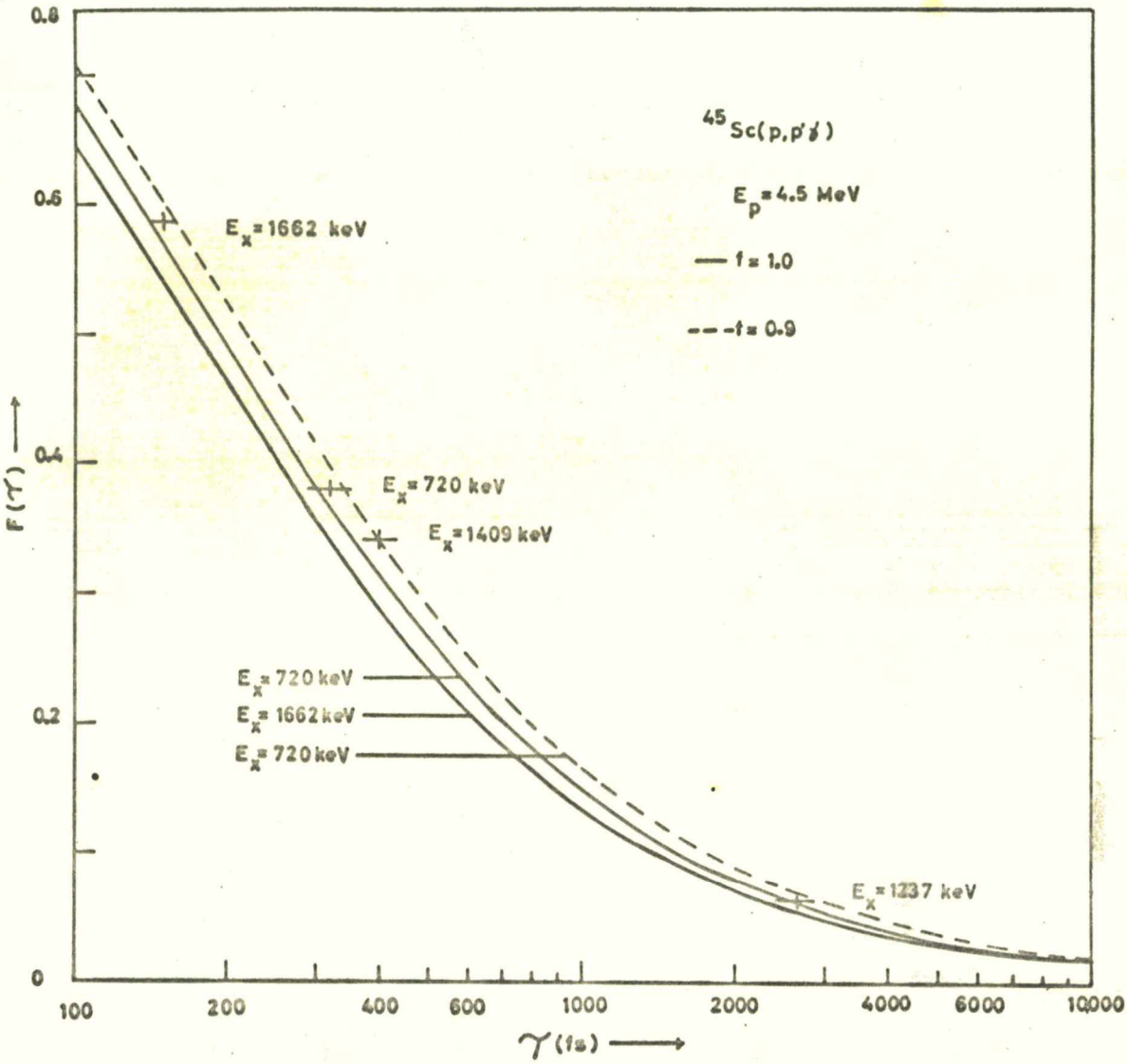

Fig. 5.5 Averaged $\widetilde{F(\tau)}$ vs. τ curves for the $^{45}Sc(p,p'\gamma)$ reaction for levels at E_x = 720 and 1662 keV. The solid curves are without any correction to the stopping cross-section. The dashed curve is for the 720 keV level and using a correction factor f = 0.9. The experimental points correspond to our measured $F(\tau)$ values plotted for the lifetime data of Metzger [25].

Dhaka University Institutional Repository

5.6. Results and discussions

The transitions in ^{45}Sc for which Doppler-shift-analysis was carried out are shown in fig. 5.6. The level energies and spins were taken from refs. 29d and 85. Examples of Doppler shifted spectra are shown in figs. 5.7a and 5.7b from the measurements at E_p = 4.5 MeV. The arrows in these figures show the peak centres of the Doppler shifted peaks. Levels up to E_x = 1662 keV and 2778 keV were populated at E_p=3.0 and 4.5 MeV respectively.

The results of the present measurements obtained at E_p = 3.0 and 4.5 MeV are (without using correction factor) respectively presented in tables 5.1 and 5.2. Excellent agreement was obtained in the experimental attenuation factors for the states that have two or more gamma rays. The 974 keV level is the best example of this. Lifetime values were extracted from the weighted averages of the experimental attenuation factors for the states that have more than one gamma ray deexciting the level.

Corrections for feeding into the low-lying states were done for both measurements at E_p = 3.0 MeV and E_p=4.5 MeV. The 376 keV state is fed from the 939 keV (not shown in fig. 5.6) state. The lifetime of the 2778 keV level is very short and since only a lower limit in lifetime was obtained for the 939 keV level, no feeding correction was done

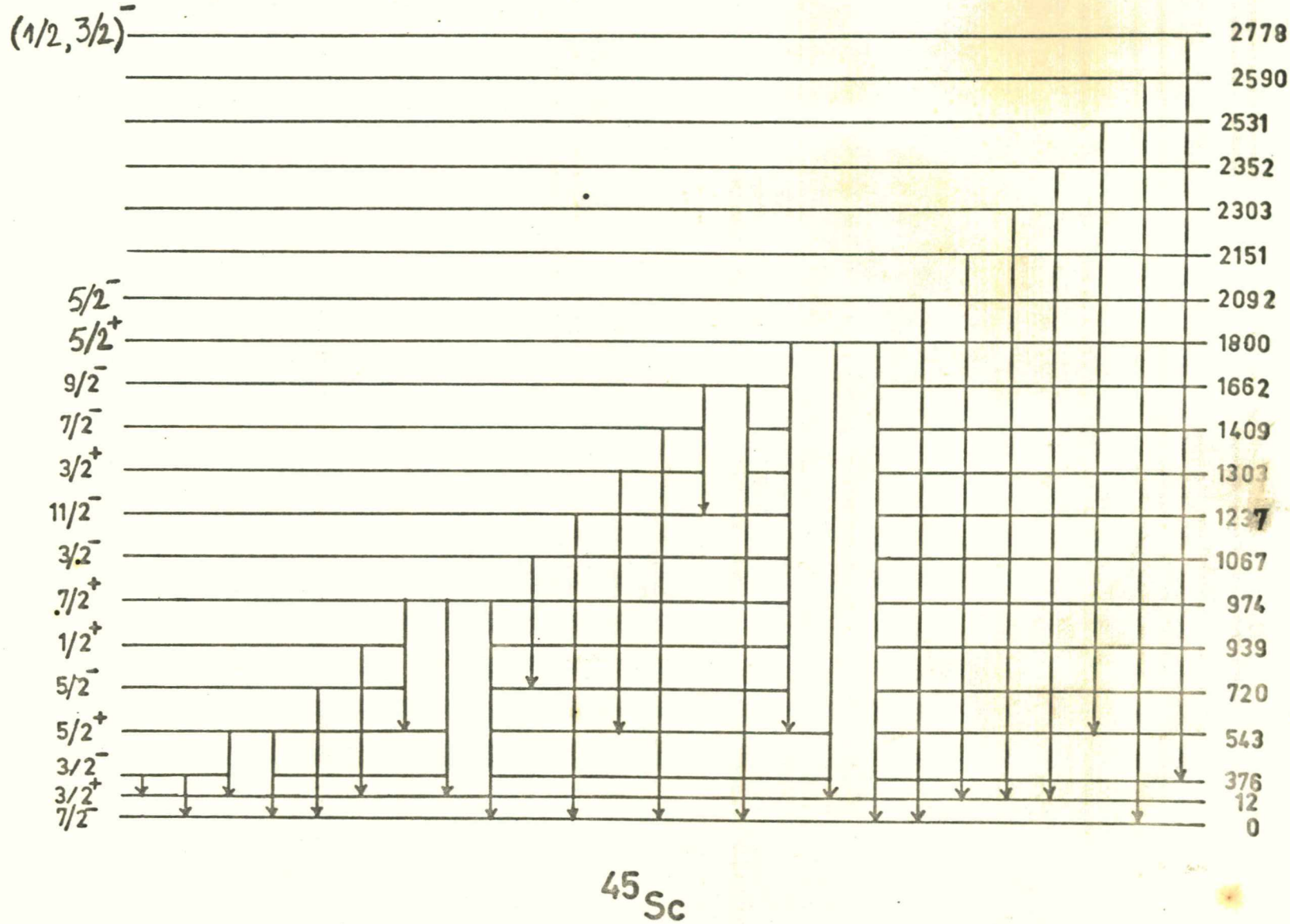

Fig. 5.6 Part of the level scheme in ^{45}Sc showing those transitions which were employed in the extraction of lifetimes. All energies are in keV. The energies and spin-parity values taken from refs. 29a and 85. The level schemes are not drawn to scale.

Dhaka University Institutional Repository

Dhaka University Institutional Repository

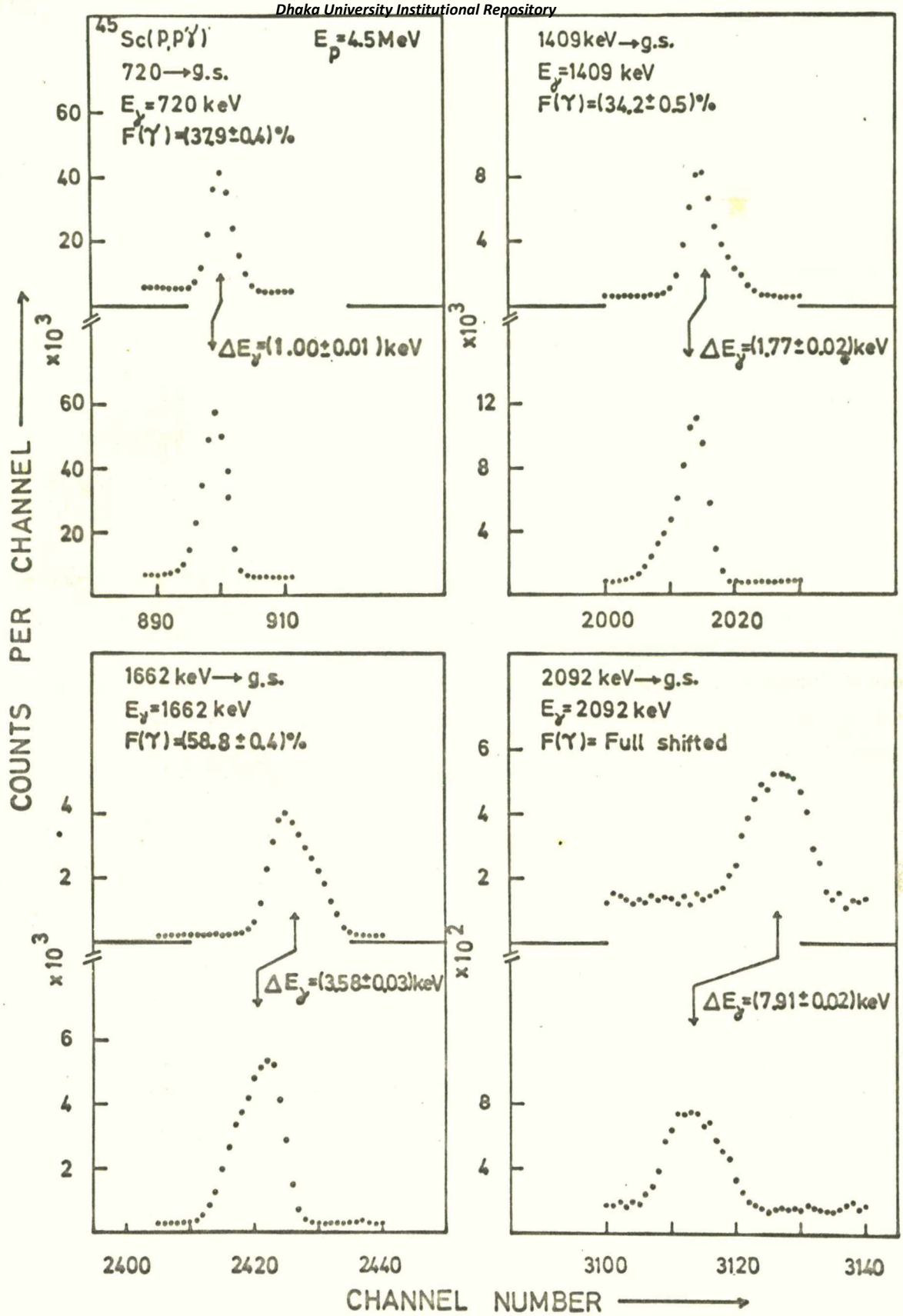

Fig. 5.7a Spectra of forward and backward Doppler-shifted γ-ray peaks of 720, 1409, 1662 and 2092 keV measured from the $^{45}Sc(p,p'\gamma)$ reaction at E_p=4.5 MeV using the two-target arrangement. Arrows indicate the shifts in energy.

Dhaka University Institutional Repository

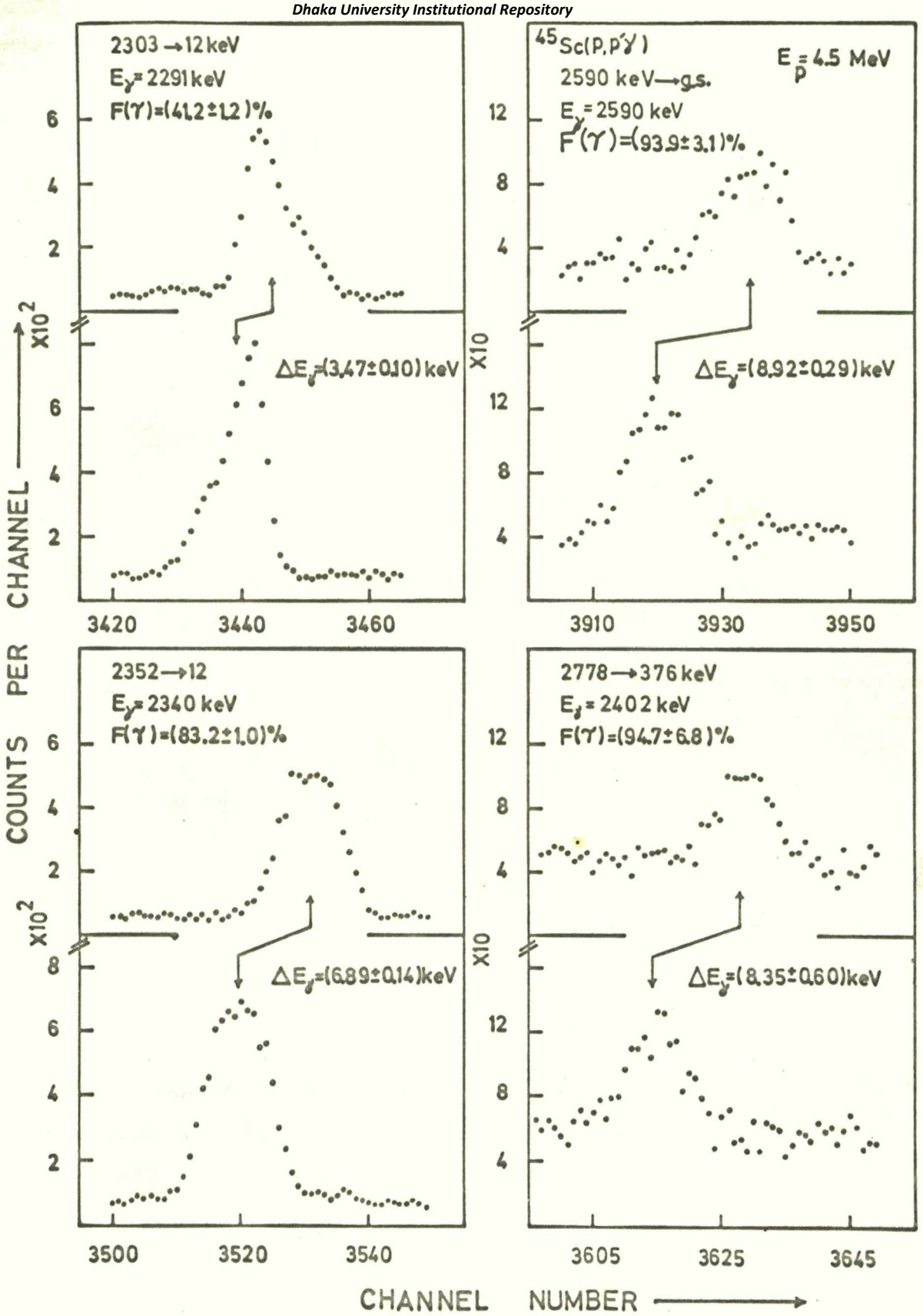

Fig. 5.7b Spectra of forward and backward Doppler-shifted γ-ray peaks of 2291, 2340, 2402 and 2590 keV measured from the $^{45}Sc(p,p'\gamma)$ reaction at E_p=4.5 MeV using the two-target arrangement. Arrows indicate shifts in energy.

Table 5.1

Summary of lifetime results in ^{45}Sc from $^{45}Sc(p,p'\gamma)$ reaction at E_p=3.0 MeV.

Level (keV)	E_{γ_0} (keV)	ΔE_γ^{max} (keV)	Measured shift $\overline{\Delta E_\gamma}$ (keV)	Attenuation factor $F(\tau)$ in %	Mean lifetime (fs)
376	376	1.127	0.048±0.029	4.3±2.6	
	364	1.091	0.024±0.017	2.2±1.5 / 3.6±1.3 a)	3700^{+2800}_{-1200}
543	543	1.627	0.036±0.011	2.2±0.7	
	531	1.591	0.033±0.009	2.1±0.6 / 2.1±0.5 a)	5800^{+1300}_{-1200}
720	720	2.157	0.766±0.014	35.5±0.6	260^{+20}_{-15}
939	927	2.778	0.070±0.012	1.2±2.5	>3400
974	974	2.919	0.133±0.022	4.6±0.8	
	962	2.883	0.125±0.022	4.3±0.8	
	431	1.291	0.070±0.026	4.5±2.0 / 4.5±0.5 a)	2700^{+600}_{-450}

Dhaka University Institutional Repository

Table 5.1 (Continued)

1067	691	2.071	0.637 ± 0.105	30.8 ± 5.1	
	347	1.040	0.344 ± 0.086	33.0 ± 8.3	
				31.4 ± 4.3 a)	290^{+90}_{-55}
1237	1237	3.704	0.226 ± 0.018	6.1 ± 0.5	1900^{+300}_{-200}
1409	1409	4.222	1.109 ± 0.047	26.3 ± 1.1	350^{+40}_{-30}
1662	1662	4.980	2.488 ± 0.193	50.5 ± 3.9	130^{+25}_{-20}

a) Mean lives computed from weighted means of estimated $F(\tau)$ values.

Dhaka University Institutional Repository

Table 5.2

Summary of lifetime results in ^{45}Sc from $^{45}Sc(p,p'\gamma)$ reaction at E_p=4.5 MeV.

Level (keV)	E_{γ_0} (keV)	ΔE_γ^{max} (keV)	Measured shift $\overline{\Delta E_\gamma}$ (keV)	Attenuation factor $F(\tau)$ in %	Mean lifetime (fs)
376	376	1.380	0.040 ± 0.040	2.9 ± 2.3	
	364	1.336	0.026 ± 0.014	2.0 ± 1.0 / 2.1 ± 0.9 a)	8000^{+6000}_{-2650}
543	543	1.993	0.014 ± 0.010	1.3 ± 0.6	
	531	1.949	0.032 ± 0.008	1.7 ± 0.4 / 1.6 ± 0.3 a)	9000^{+3000}_{-2000}
720	720	2.642	1.002 ± 0.010	37.9 ± 0.4	295^{+25}_{-20}
939	927	3.402	0.030 ± 0.028	0.9 ± 0.8	>10000
974	974	3.574	0.135 ± 0.025	3.8 ± 0.7	
	962	3.530	0.135 ± 0.024	3.8 ± 0.7	
	431	1.582	0.060 ± 0.020	3.8 ± 1.1 / 3.8 ± 0.5 a)	4100^{+1000}_{-600}
1067	347	1.273	0.335 ± 0.057	26.3 ± 4.5	490^{+180}_{-120}
1237	1237	4.536	0.297 ± 0.012	6.6 ± 0.3	2350^{+350}_{-250}
1303	760	2.789	0.147 ± 0.034	5.3 ± 1.2	2850^{+1200}_{-650}

Dhaka University Institutional Repository

Table 5.2 (Continued)

1409	1409	5.171	1.768±0.025	34.2±0.5	330^{+40}_{-30}
1662	1662	6.099	3.585±0.026	58.8±0.4	
	426	1.563	0.857±0.025	54.8±1.6	
				58.6±0.5 a)	135±10
1800	1800	6.605	4.431±0.319	67.1±4.8	
	1788	6.561	3.946±0.185	60.4±2.8	
	1257	4.613	3.259±0.125	70.7±2.7	
				65.9±1.8 a)	95^{+15}_{-8}
2092	2092	7.677	7.912±0.124	> 100	<10
2151	2139	7.850	2.436±0.681	31.0±8.7	350^{+160}_{-110}
2303	2291	8.407	3.467±0.097	41.2±1.2	225^{+25}_{-20}
2352	2340	8.587	6.896±0.143	80.3±1.0	46±3
2531	1988	7.295	6.412±0.230	87.9±3.1	26±7
2590	2590	9.505	8.924±0.290	93.9±3.1	13±7
2778	2402	8.815	8.348±0.601	> 88	< 25

a) Mean lives computed from weighted means of estimated F( ) values.

Dhaka University Institutional Repository

Dhaka University Institutional Repository

for the 376 keV level. The 543 keV level is fed by a 431 keV γ-ray (with a branch of 10%) from the 974 keV long-lived state and by a 760 keV γ-ray (with a strong branch of 70%) from the 1303 keV long-lived state. Correction for both of these feedings was done and was found to affect the lifetime by about 10%. The lifetimes of the two other states (1800 and 2590 keV) feeding the 543 keV state are short. The 720 keV state is fed by a gamma ray of 347 keV with a branch of 20% from the 1067 keV state. Correction for this feeding was done. Feeding corrections for other states which have lifetimes much larger than their parent states were not done.

The adopted lifetime values which are the weighted averages of the measurements at $E_p = 3.0$ and $E_p = 4.5$ MeV and using calibrated curves (with correction factor f=0.9) are presented in table 5.3 along with the results of other authors for the purpose of comparison. The adopted values contain only the experimental error mainly coming from the peak centre determination.

Using a calibration of $f_e = f_n = 0.9$ in the computation of attenuation F( ) the lifetime values of the 720, 1237, 1409, 1662 and 2092 keV levels obtained from the present measurements are in good agreement with the resonance fluorescence data [25]. But for the same levels the results of the DSA experiments by (p,p'γ) [27] and (α,pγ) [29] reactions do not agree with the present work nor with the resonance

Table 5.3

Lifetimes of levels in ^{45}Sc

Level (keV)	Mean lifetime (fs)						
	Present work (p,p'γ)	Metzger[25] (γ,γ)	Schulte et.al.[26] (p,γ)	Rust et.al.[27] (p,p'γ)	Chevallier et.al.[29] (α,pγ)	Toulemonde et.al.[28] (α,pγ)	C.E.[a]
376	5100 ± 1800			>1600	>6000		65000 ± 500
543	7600 ± 1300					9200^{+6800}_{-3300}	
720	313 ± 10	320 ± 30		220 ± 60	360^{+110}_{-80}		
939	> 3800					10500^{+8200}_{-4700}	
974	3600 ± 500					3200^{+800}_{-700}	
1067	380 ± 70				500^{+180}_{-120}		
1237	2400 ± 150	2630 ± 200		1100 ± 200	3400^{+1400}_{-900}		3100 ± 600
1303	3250^{+1200}_{-650}					3500^{+1700}_{-1000}	
1409	385 ± 20	400 ± 30	120^{+50}_{-30}	600 ± 300	620^{+180}_{-120}		

Dhaka University Institutional Repository

Table 5.3 (Continued)

1662	150 ± 10	151 ± 13		110 ± 30	200^{+70}_{-50}	
1800	110^{+15}_{-8}		95^{+90}_{-50}		< 50	160^{+60}_{-50}
2092	< 10	8 ± 1	12 ± 3			
2151	400^{+160}_{-110}		87^{+25}_{-17}			
2303	250 ± 25		80^{+50}_{-25}			
2352	52 ± 3		60^{+40}_{-25}			
2531	30 ± 7		117^{+55}_{-25}			
2590	15 ± 7		50 ± 12			
2778	< 25		19 ± 6			

a) The lifetime values have been calculated using the weighted average of the B(E2) values obtained from Coulomb excitation experiments. Quoted in ref. 29.

Dhaka University Institutional Repository

Dhaka University Institutional Repository

fluorescence experiment [25]. It may be noted that the lifetime of the 376 keV long-lived state obtained from the present measurement is in considerable disagreement with that obtained by Coulomb excitation (table 5.3). Previously only lower limits of lifetime for this level was quoted [27,29]. Our results for the long-lived states of 543, 939, 974 and 1303 keV are in good agreement with the $^{42}Ca\ (\alpha,p\gamma)^{45}Sc$ data of Toulemonde et al. [28]. The lifetime value for the 543 keV level is in complete agreement with the value 7400^{+2800}_{-1000} fs obtained by a resonance fluorescence experiment of Arnold et al. [25a]. For the 974 keV level the present value is within the experimental error of the value 2700 ± 400 fs obtained by the same experiment [25a]. The lifetime value for the 1067 keV level obtained by Chevallier et al. [29] though larger than the present value is within the experimental error. It is to be noted that the lifetime values obtained by Chevallier et al. [29] are larger than the resonance fluorescence data whereas the present data are in good agreement with the resonance fluorescence data.

The 2092 keV γ-ray deexciting the 2092 keV level is fully shifted and as such we assumed the lifetime of this level as less than 10 fs. Metzger also got a very short lifetime of 8 fs for this level. The upper limit of attenuation factor for the 2462 keV γ-ray deexciting the 2778 keV level exceeds 1 and as such an upper limit of lifetime for this level was quoted.

Dhaka University Institutional Repository

The comparison of the present results with those of Schulte et al. [26] shows an excellent agreement for some of the levels while for others there is complete disagreement. The lifetime values of 1800, 2092, 2352 and 2778 keV levels are in good agreement. But for the lifetimes of 2151 and 2303 keV levels our values are larger by factors of 4.6 and 3.1 respectively, while for the level at 2531 and 2590 keV our values are smaller than those of Schulte et al. [26] by factors of 3.9 and 3.3 respectively. We have no explanation for this. It should be mentioned that the lifetime of the 1409 keV level obtained by Schulte et al. [26] is smaller than the resonance fluorescence data of Metzger [25] by more than a factor of 3 whereas our result for this level is in good agreement with Metzger.

The low-lying odd-parity states in ^{45}Sc can be described by excited core model given by Lawson and Uretski [86] and de-Shalit [87]. This model considers a weak coupling of the odd nucleon to the remaining even-even core. The coupling of the $1f_{7/2}$ proton to the 2_1^+ state at 1156 keV of ^{44}Ca (ref. 88) nucleus may give rise to the 5 multiplet states. The observed levels 376 ($J^\pi = 3/2^-$), 720 ($J^\pi = 5/2^-$), 1237 ($J^\pi = 11/2^-$), 1409 ($J^\pi = 7/2^-$) and 1662 ($J^\pi = 9/2^-$) keV in ^{45}Sc are identified as the members of the multiplet. The lifetimes of these 5 multiplet states were used to calculate the E2 reduced transition probabilities for the ground state

Dhaka University Institutional Repository

transition. For this purpose the branching ratios given by Rust *et al.* [27] and dipole to quadrupole mixing ratios given by Zuk *et al.* [89] were used. The transitions for the 376 and 1237 keV states have pure E2 multipolarity as given in ref.89. The reduced transition probabilities B(E2)↓ for the above 5 states are presented in table 5.4 along with the results of Rust *et al.* [27] and previous works [76-80,82,83,90] as quoted in ref. 27.

Table 5.4

Reduced transition probability

Level (keV)	Transition	B(E2)↓ e^2fm^4		
		Present work[a]	Rust *et. al.* (ref. 27)	Previous[b]
376	$3/2^- \rightarrow 7/2^-$	1700±600	5400	150
720	$5/2^- \rightarrow 7/2^-$	22±2	31±10	89
1237	$11/2^- \rightarrow 7/2^-$	119±11	256±47	125
1409	$7/2^- \rightarrow 7/2^-$	34±3	21±10	
1662	$9/2^- \rightarrow 7/2^-$	53±5	73±20	55

a) Reduced transition probability calculated using branchings ratios given in ref. 27 and mixing ratio at χ^2 minimum given in ref. 89.

b) Average values derived from B(E2)↑ values given in references 76-80, 82, 83, 90. Taken from ref. 27.

The transition strengths have been calculated for 543 and 974 keV levels using the mixing ratio value determined by

Dhaka University Institutional Repository

Toulemonde *et al.* [28] and for 1067 and 1303 keV levels using the mixing ratio at χ^2 minimum determined by Zuk *et al.* [89]. They are presented in table 5.5.

Table 5.5

Transition strengths

E_i [c]	J_i	E_f	J_f	$B(E1)\times10^{-3}$ (W.u.)	$B(M1)\times10^{-2}$ (W.u.)	$B(E2)$ (W.u.)
543[a]	$5/2^+$	0	$7/2^-$	(0.26 ± 0.04)		
		12	$3/2^+$		(1.25 ± 0.35)	35^{+25}_{-15}
974[a]	$7/2^+$	0	$7/2^-$	(0.13 ± 0.01)		
		12	$3/2^+$			9 ± 1
		543	$5/2^+$		10 ± 2	8^{+16}_{-6}
1067[b]	$3/2^-$	376	$3/2^-$		(0.07 ± 0.01)	$(11\pm2)\times10^2$
1303[b]	$3/2^+$	376	$3/2^-$	(0.003 ± 0.001)		
		543	$5/2^+$		(1.48 ± 0.40)	(7.5 ± 2.0)

a) Transition strengths have been calculated using mixing ratio determined by Toulemonde *et al.* [28].

b) Transition strengths have been claculated using mixing ratio determined by Zuk *et al.* [89].

c) Branching ratios given by Rust *et al.* [27].

Dhaka University Institutional Repository

For the states above 2151 keV the reduced transition probabilities have been calculated assuming pure multipole radiation and using the lifetimes of the levels obtained from the present measurements. For this purpose the branching ratios were used from the measurements of Schulte et al. [85]. The E1, E2 and M1 transition strengths in Weisskopf units (W.u.) are presented in table 5.6.

Table 5.6

Transition strength for pure multipole transition in ^{45}Sc

Initial state[a] (keV)	Final state (keV)	E_γ (keV)	Branch (%)[a]	Transition strength (W.u.) E1 ($\times 10^{-3}$)	E2	M1 ($\times 10^{-2}$)
2151	12	2139	90	$0.17^{+0.06}_{-0.05}$	$4.2^{+1.6}_{-1.2}$	$0.72^{+0.27}_{-0.21}$
	1303	848	10	$0.30^{+0.12}_{-0.08}$	48^{+18}_{-14}	$1.28^{+0.49}_{-0.36}$
2303	12	2291	27	0.06±0.01	1.4±0.1	0.28±0.03
	376	1927	35	0.14±0.01	4.4±0.4	0.61±0.06
	1067	1237	38	0.59±0.06	44±4	2.53±0.25
2352	12	2340	25	0.28±0.02	5.7±0.33	1.17±0.06
	720	1632	45	1.48±0.08	63±4	0.62±0.36
	1067	1285	9	0.61±0.03	41±2	2.56±0.15
	1556	796	21	5.95±0.34	1060±61	25.07±1.44
2531	12	2519	36	0.56±0.13	9.9±2.3	2.35±0.55
	543	1988	50	1.57±0.37	45±11	6.65±1.55
	1303	1288	14	1.62±0.38	110±26	6.85±1.60
2590	0	2590	64	1.82±0.85	30±14	7.69±3.59
	376	2214	36	1.64±0.76	38±18	6.93±0.32
2778	376	2402	68	> 1.45	> 28	> 6.1
	720	2058	32	> 1.1	> 29	> 4.6

a) Transitions and branching ratios are taken from ref.85.

Dhaka University Institutional Repository

The possible range of spin and parity assignments were made from the comparison of experimental and Weisskopf estimated lifetimes and using the criteria given by Nuclear Data Group. They are presented in table 5.7.

Table 5.7

Possible range of spin and parity assignments

Level (keV)	J^{π} +
2151	$1/2^{\pm}$, $3/2^{\pm}$, $5/2^{\pm}$, $7/2^{+}$
2303	$1/2^{\pm}$, $3/2^{\pm}$, $5/2^{\pm}$, $7/2^{+}$
2352	$1/2^{\pm}$, $3/2^{\pm}$, $5/2^{\pm}$, $7/2^{+}$
2531	$1/2^{\pm}$, $3/2^{\pm}$, $5/2^{\pm}$, $7/2^{+}$
2590	$3/2^{-}$, $5/2^{\pm}$, $7/2^{\pm}$, $9/2^{-}$
2778	$1/2^{\pm}$, $3/2^{\pm}$, $5/2^{\pm}$, $7/2^{-}$

+ The possible range of spin and parity assignments were made from the comparison of experimental and Weisskopf estimated lifetimes and using Nuclear Data Group criteria.

Some more restrictions are possible on the spin and parity values as discussed below which are however rather very tentative. The M2 decay from the 2303 keV level is

Dhaka University Institutional Repository

very unlikely and so the spin 7/2 for this level may be excluded. The value of E1 for the transition from the 2352 keV level is very large and is unlikely. It is also not E2. The transition should therefore be M1 in nature excluding the possibility of J=7/2. The 2531 keV level decays only to the positive parity state so that this state should very likely have positive parity.

In conclusion, a complete set of lifetimes of 18 levels upto an excitation energy of 2778 keV have been obtained from the present measurements. Further work is necessary for the few levels where our results do not agree with those of Schulte et al. [26] only. However, a lot of lifetime data is now available for this nucleus. It is expected that these data will be useful for nuclear model calculations.

Dhaka University Institutional Repository

CHAPTER-6

LIFETIME MEASUREMENTS IN ^{45}Ti

6.1. Introduction

The structure of ^{45}Ti is of theoretical interest. The theoretical descriptions of McCullen *et al.* [91], Malik and Scholz [92] and Johnstone [93] predicted the negative parity states for this nucleus with spins as high as 11/2 for the low-lying levels. The nucleus ^{45}Ti has been studied by $^{46}Ti(^{3}He,\alpha)^{45}Ti$ (refs. 94, 95), $^{46}Ti(p,d)^{45}Ti$ (refs.96-98) and $^{45}Sc(p,n\gamma)^{45}Ti$ (refs.99-101) reactions. Decay schemes for the low-lying levels have been determined by Iyengar *et al.* [101]. Iyengar and Robertson [31], using the DSA method determined the lifetimes of 8 levels up to an excitation energy of 2016 keV through the $^{45}Sc(p,n\gamma)^{45}Ti$ reaction. Zuk *et al.* [30] determined the lifetimes of 6 levels up to an excitation energy of 1521 keV through the $^{45}Sc(p,n\gamma)^{45}Ti$ reaction and also using the DSA method. The agreement in the lifetime data of both authors is in general agreement. In both these work however only a lower limit for the 744 and 1266 keV levels were quoted. Blasi *et al.* [31a] determined the lifetimes of a few levels in ^{45}Ti by the recoil distance method using the $^{31}P(^{16}O,p,n\gamma)^{45}Ti$ reaction.

In view of these facts an attempt was made to measure the lifetimes of some of levels in ^{45}Ti. During the study of the $^{45}Sc(p,p'\gamma)$ reaction (chapter 5) at 4.5 MeV the levels in

Dhaka University Institutional Repository

^{45}Ti were also populated by the ^{45}Sc(p,nγ)^{45}Ti reaction. This afforded us an opportunity to determine the lifetimes of the levels in ^{45}Ti. The present information on lifetimes and the branching ratios and mixing ratios given by Iyengar et al. [31] was utilised for the calculation of transition strength for some of the levels. Possible spin values are quoted for some of the levels.

6.2. The experiment and analyses

The levels in ^{45}Ti were populated by the ^{45}Sc(p,nγ)^{45}Ti reaction at a proton bombarding energy of 4.5 MeV. This reaction was studied along with the measurements of ^{45}Sc(p,p'γ) reaction as described in chapter 5. Thus the experimental procedure including the targets, beam energy, beam current, all were identical. The Q-value for the ^{45}Sc(p,nγ)^{45}Ti reaction is -2846 keV. The levels up to an excitation energy of 1521 keV in ^{45}Ti were populated at E_p = 4.5 MeV. The levels in ^{45}Ti were not selectively populated. Singles γ-ray spectra were measured and no coincidence measurements were done. But because of the emission of neutrons there occurs a range of initial velocities of the recoiling nuclei at different angles. Thus to take into account of this, the $\widetilde{F(\tau)}$ curves were calculated as described in chapter 5. Averaged attenuation factor $\widetilde{F(\tau)}$ vs. τ curves for the 744 keV level and for the isotropic function is shown in fig. 6.1 where the solid

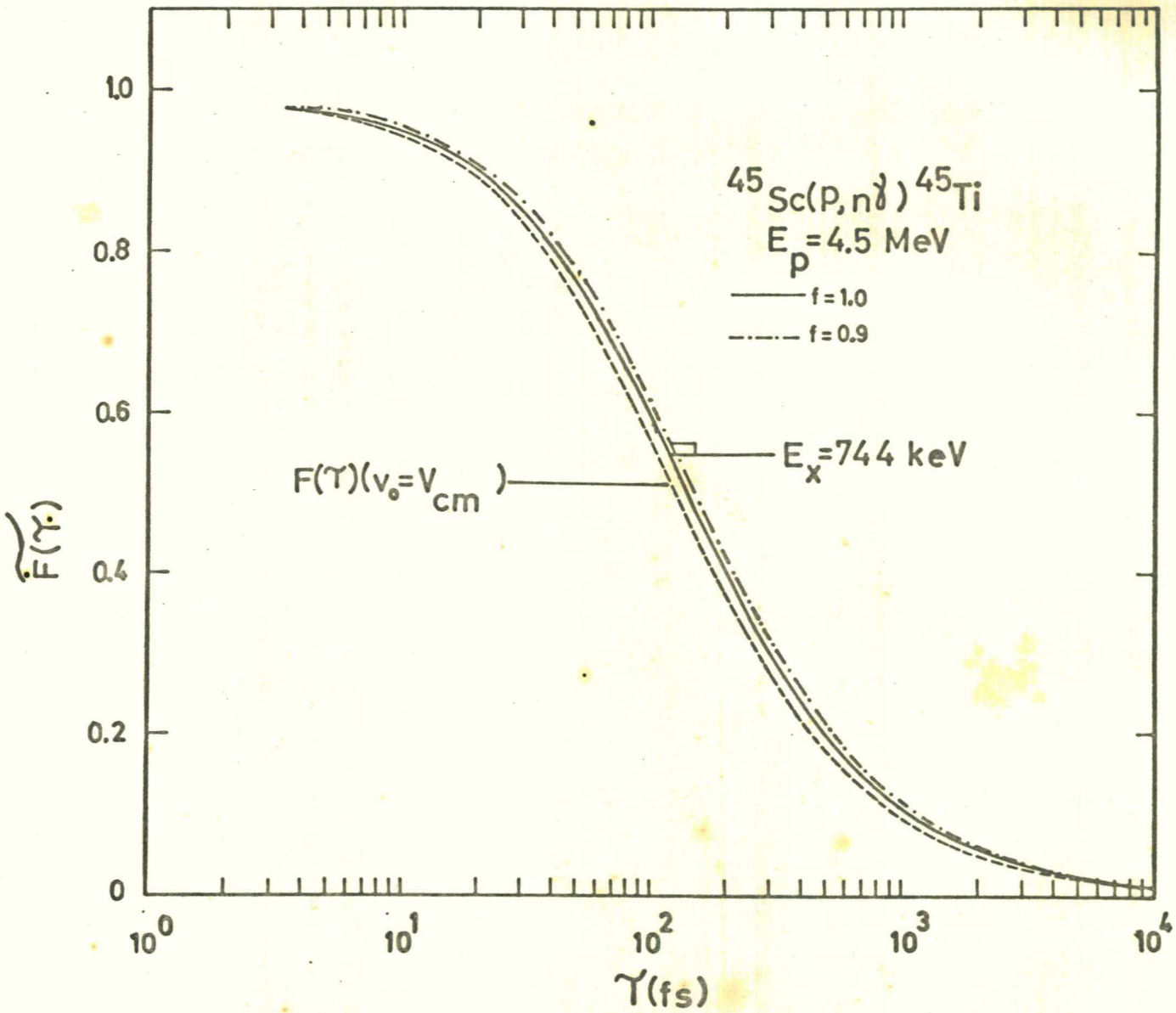

Fig. 6.1 Averaged attenuation factor $F(\tau)$ vs. τ curves for ^{45}Ti nuclei recoiling in ^{45}Sc for the 744 keV level. The solid and dot-dash curves refer to correction factor f=1.0 and f=0.9 respectively. The dashed curve is for $v_0=v_{CM}$.

Dhaka University Institutional Repository

Dhaka University Institutional Repository

curve refers to correction factor f = 1.0 and the dot-and-dash curve refers to correction factor of f = 0.9. The dashed curve in this figure is for $v_0 = v_{CM}$. Because of the negative Q-value of this reaction the effect of the Q-value dependence of the attenuation curves at different angles is small. The $\widetilde{F(\tau)}$ curves were calculated for each level of interest using f = 0.9 and were used for lifetime extraction.

6.3. Results and discussions

Transitions for which DSA measurements were carried out are shown in fig. 6.2. The level energies and spin-parity values were taken from ref. [29a]. Lifetimes of 5 states up to an excitation energy of 1521 keV have been determined. Examples of Doppler shifted γ-ray spectra deexciting the 1353, 1468 and 1521 keV levels are shown in figs. 6.3a and 6.3b. That the 1461 keV γ-ray from ^{40}K is unshifted at the two angles, as it should be, is also demonstrated in fig. 6.3a. Results of the present DSA measurements are summarized in table 6.1. It is to be noted from the table that an excellent agreement is obtained for the attenuation factors of the levels that have more than one γ-ray deexciting the level. The present lifetime data along with the results of other authors are presented in table 6.2 for a comparison. The errors in the mean lifetime values in this work are mainly from experimental uncertainties.

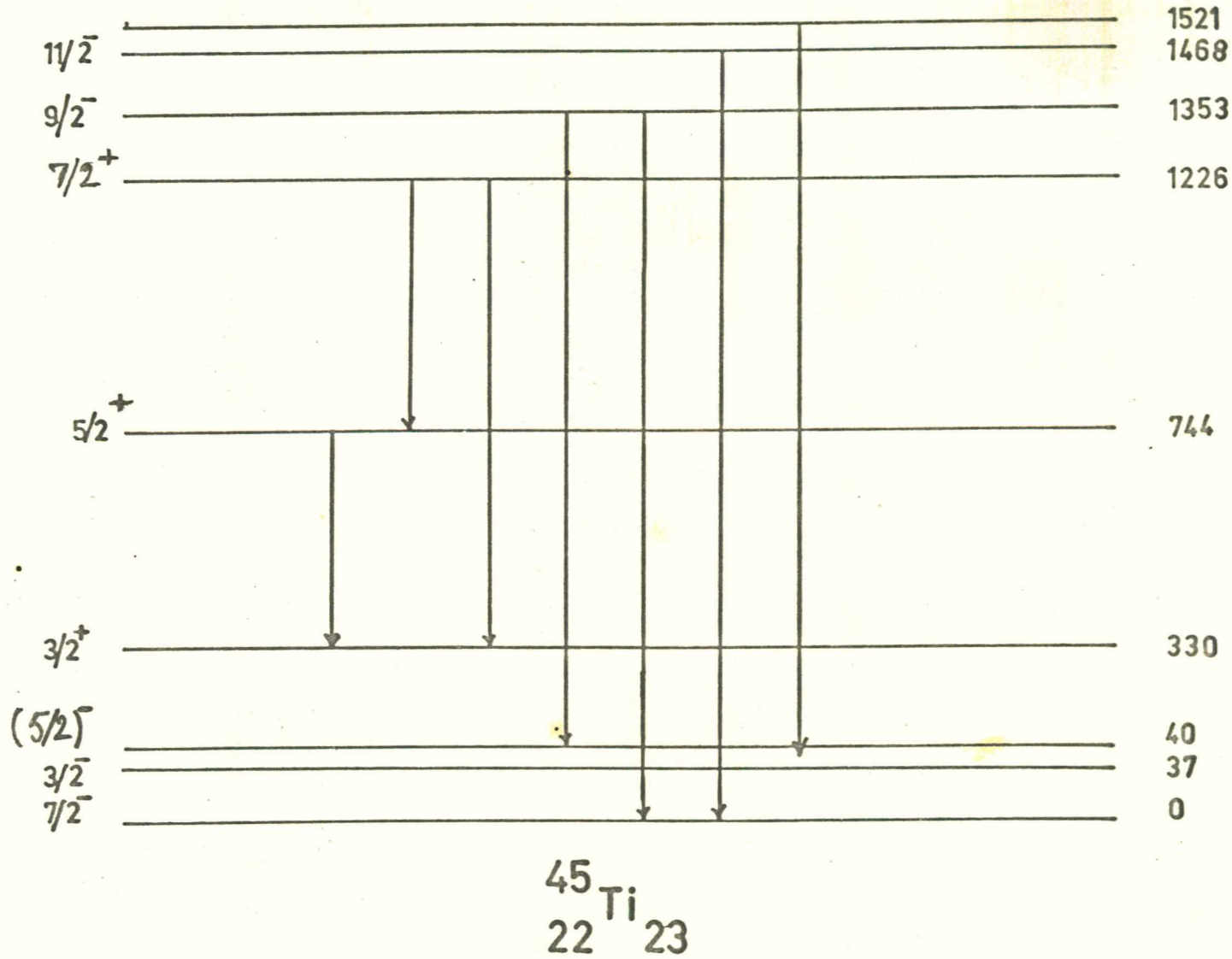

Fig. 6.2 Part of the level scheme in ^{45}Ti showing only those transitions which were employed for the extraction of lifetimes. The energies (keV) and spin-parity values taken from ref. [29a].

Dhaka University Institutional Repository

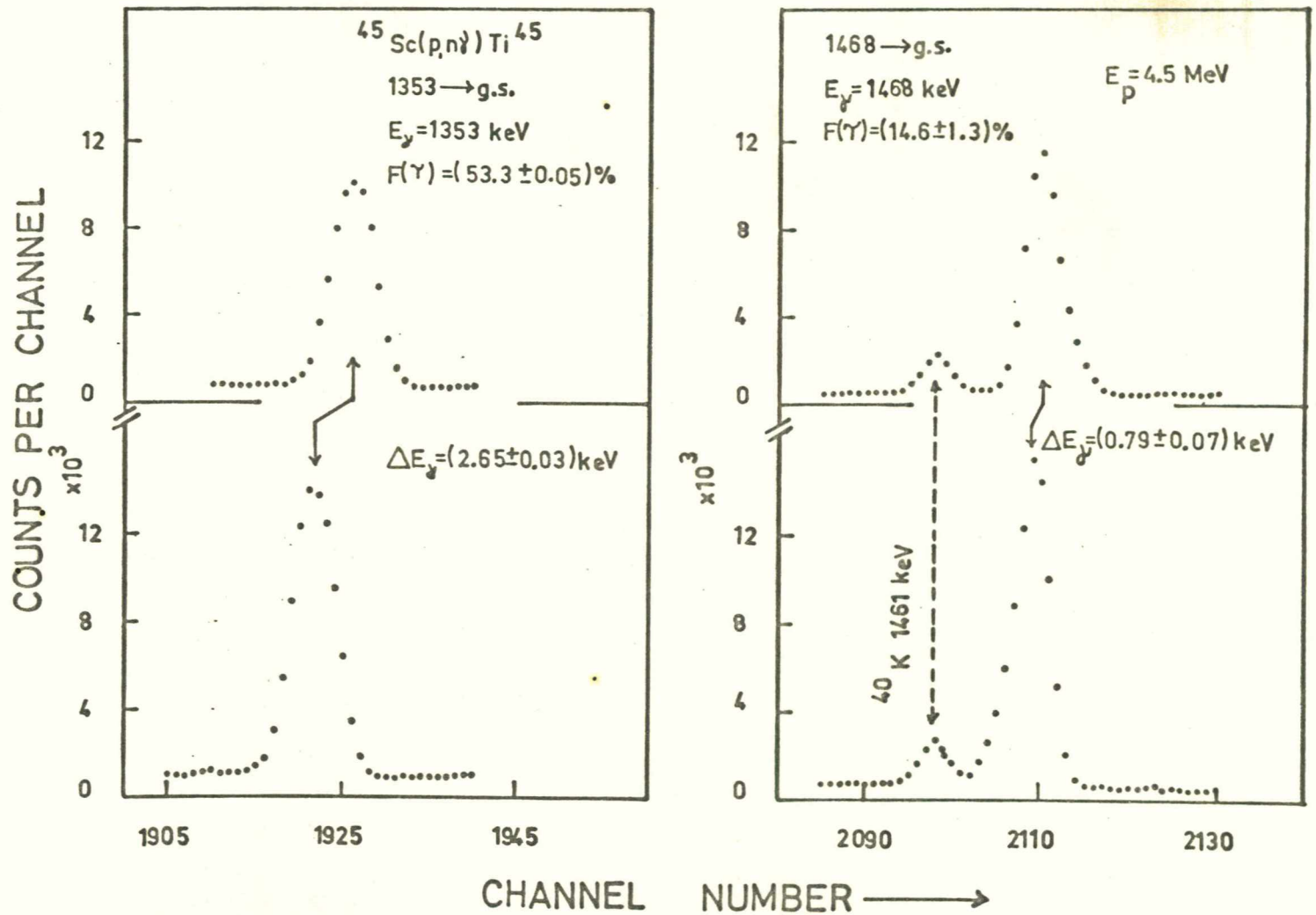

Fig. 6.3a Doppler-shifted peaks of 1353 and 1468 keV γ-rays from the $^{45}Sc(p,n\gamma)$ reaction at E_p=4.5 MeV using the two-target arrangement. That the 1461 keV γ-ray from ^{40}K should be unshifted is also demonstrated.

Dhaka University Institutional Repository

Dhaka University Institutional Repository

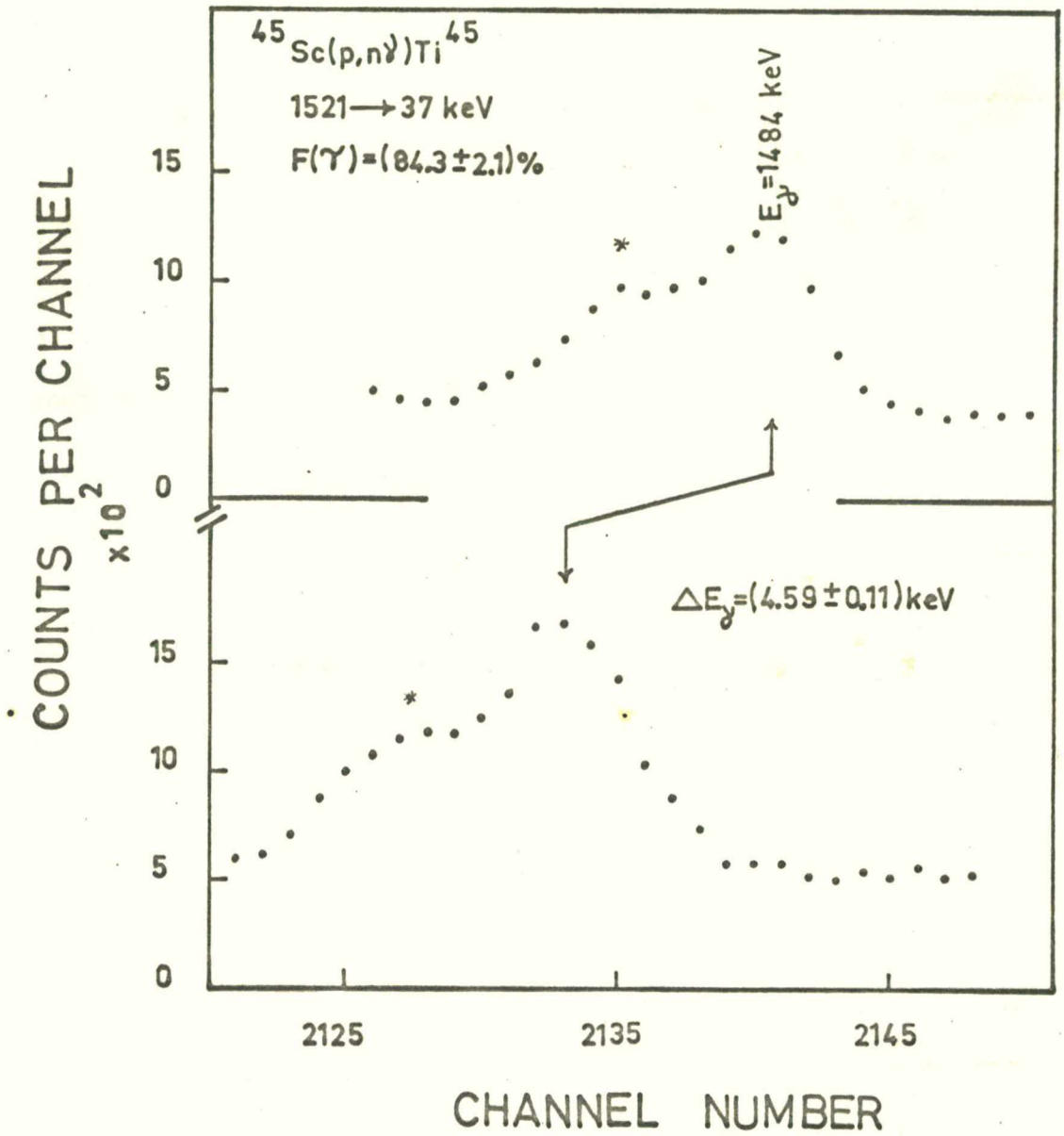

Fig. 6.3b Doppler-shifted peaks of 1484 keV γ-ray from the $^{45}Sc(p,n\gamma)$ reaction at E_p=4.5 MeV using the two-target arrangement. The peak marked with (*) is possibly from the background. A G2 analysis (see section 3.7) was done for this double peak.

Table 6.1

Summary of lifetime results in ^{45}Ti from $^{45}Sc(p,n\gamma)^{45}Ti$ reaction at E_p=4.5 MeV.

Level (keV)	E_γ (keV)	ΔE_γ^{max} (keV)	Measured shift $\overline{\Delta E}_\gamma$ (keV)	Attenuation factor $F(\tau)$ in %	Mean lifetime (fs)
744	414	1.519	0.015±0.010	1.0±0.7	9000^{+6600}_{-1650}
1226	896	3.288	0.110±0.035	3.4±1.1	
	482	1.769	0.055±0.027	3.1±1.5	3700^{+1250}_{-800}
				3.3±0.9 a)	
1353	1353	4.965	2.649±0.027	53.3±0.5	
	1313	4.818	2.558±0.058	53.1±1.2	125±6
				53.3±0.5 a)	
1468	1468	5.387	0.788±0.068	14.6±1.3	720±100
1521	1484	5.387	4.593±0.114	84.3±2.1	31±5

a) Mean lifetimes computed from weighted mean of $F(\tau)$ values.

Dhaka University Institutional Repository

Table 6.2

Lifetimes of levels in ^{45}Ti

Level (keV	Mean lifetime (fs)			
	Present work	Zuk *et al.*[30]	Iyengar *et al.*[31]	Blasi *et al.*[31a]
744	9000^{+6600}_{-1650}	> 1000	⩾ 1400	14500±2500
1226	3700^{+1250}_{-800}	> 1000	⩾ 2200	4000±800
1353	125±6	146±24	150±15	
1468	720±100	670^{+164}_{-128}	700^{+100}_{-90}	
1521	31±5	79±13	69^{+15}_{-16}	

ঢাকা বিশ্ববিদ্যালয় গ্রন্থাগার

387984

Dhaka University Institutional Repository

Dhaka University Institutional Repository

Zuk et al.[30] and Iyengar and Robertson[31] quoted only the lower limit of lifetimes for 744 and 1226 keV levels. The lifetime of the 744 keV level obtained by Blasi et al.[31a] is within the error of our value. The lifetime value of the 1226 keV level obtained in the present work is in good agreement with that obtained by Blasi et al.[31a]. The large error for the above two levels in the present work is consistent with the fact that the attenuation factor for these levels lie in the region where it is insensitive to τ. The 744 keV level is fed by a 482 keV γ-ray from the 1226 keV level. A correction was done for this feeding.

Lifetimes of 1353 and 1468 keV levels obtained in this work are in good agreement with those of refs.[30,31]. The lifetime obtained for the 1521 keV level is much small compared to these authors[30,31]. But it may be noted from fig.6.3b that the 1484 keV γ-ray deexciting 1521 keV level is a double peak and G2 analysis (section 3.7) was done which gave peak centres with errors for both peaks. The peak marked with star possibly comes from background. However the Doppler shift of the 1484 keV γ-ray is quite large which makes the short lifetime of the 1521 keV level possible.

Transition strengths have been calculated for the 744, 1226 and 1521 keV levels assuming a pure multipole radiation. The present mean lifetimes and the branchings from ref.[31]

Table 6.3

Transition strengths

Initial state (keV)	J_i	Transition to (keV)	J_f	E (keV)	Branch[a] (%)	Transition strength (W.u.) E1 ($\times 10^{-3}$)	E2	M1 ($\times 10^{-2}$)
744[c]	$5/2^+$	37	$3/2^-$	707	16	0.012 ± 0.006		
		330	$3/2^+$	414	94		720^{+162}_{-304}	$4.62^{+1.03}_{-1.96}$
1226[c]	$7/2^+$	0	$7/2^-$	1226	4	0.005 ± 0.001		
		40	$(5/2)^-$	1186	5	0.006 ± 0.001		
		330	$3/2^+$	896	45		18 ± 4	
		744	$5/2^+$	482	46		400 ± 99	3.48 ± 1.0
1353[b]	$9/2^-$	0	$7/2^-$	1353	93		14 ± 7	8.40 ± 0.60
1468[b]	$11/2^-$	0	$7/2^-$	1468	100		0.14 ± 0.02	
1521[c]		0	$7/2^-$	1521	17	1.150 ± 0.190	56 ± 9	4.87 ± 81
		37	$3/2^-$	1484	83	6.080 ± 0.980	312 ± 50	25.68 ± 4.13

a) Branching ratios have been taken from ref. 31.

b) Mixing ratios have been taken from ref.31.

c) Transition strength calculated assuming pure multipole radiation.

Dhaka University Institutional Repository

Dhaka University Institutional Repository

were used for this purpose. For the 1354 and 1468 keV levels transition strengths have been calculated using the mixing ratio given by ref. 31. The E1, E2 and M1 transition strengths in Weisskopf units (W.u) are presented in table 6.3. From the comparison of experimental and Weisskopf estimated lifetimes and using Nuclear Data Criteria the possible spin and parity values for 1521 keV levels was found to be $3/2^{\pm}$ and $5/2^{\pm}$.

Dhaka University Institutional Repository

CHAPTER-7

LEVEL SCHEME AND LIFETIMES MEASUREMENTS FOR ^{71}As

7.1. Level scheme

7.1.1. Introduction

Information on the nucleus ^{71}As is not much available uptil now and lifetime measurements have not been done at all. Broman and Rosner [32] studied the $^{70}Ge(^{3}He,d)^{71}As$ reaction and observed 11 levels up to an excitation energy of 2674 keV. Hundelshausen [34] investigated the radioactive decay of ^{71}Se and proposed a decay scheme of 6 levels up to an excitation energy of 1265 keV. Of these the 1265 keV level was a tentative identification. Betts *et al.*[33] studied the $^{70}Ge(^{3}He,d)$ reaction and determined 27 levels; the uncertainty in the energies of the levels in this work is ± 7 and ± 10 keV for $E_x < 2$ and $E_x > 2$ MeV respectively. During our measurements Heits *et al.* [35] have reported information on ^{71}As obtained from the $^{69}Ga(\alpha,2n)^{71}As$ reaction. Because of the large angular momentum in the incoming channel mostly the high-spin states were populated in this work. The (p,γ) reaction on nuclei around $A \approx 70$ has been rarely studied. The only work on $^{70}Ge(p,\gamma)^{71}As$ is due to Liu *et al.* [36]. These authors proposed a decay scheme up to an excitation energy of 1533 keV.

The proton capture reactions on light nuclei have extensively been used for the study of nuclear level schemes. But not so much has been studied with medium heavy nuclei. There

Dhaka University Institutional Repository

are many differences in (p,γ) studies between light and medium heavy nuclei. In light nuclei only isolated resonances are excited. The final states are populated quite selectively and the intensities for different primary transitions fluctuate strongly from one resonance to another. But in the medium heavy nuclei many compound nuclear states are excited simultaneously. All intermediate and low-lying states are populated by primary gamma transitions from the highly excited compound states. The secondary gamma rays following the primary transitions show decay modes of the low-lying states and help in constructing the level schemes. Some (p,γ) experiments [102,103] have shown that valuable information on the properties of the low-lying states in medium heavy nuclei around A$\approx$90 can be obtained. From these studies it may be inferred that the (p,γ) studies on nuclei around A$\approx$70 will also yield valuable information.

The ^{70}Ge(p,γ)^{71}As reaction has been studied in this work to extract information on level schemes and lifetimes in ^{71}As.

7.1.2. Experimental procedure

The ^{70}Ge(p,γ)^{71}As reaction was studied at a proton bombarding energy of 2.8 MeV. The proton beam was provided by the 7.5 MeV accelerator of the Institut für Kernphysik, University of Frankfurt, West Germany. The beam current used

Dhaka University Institutional Repository

was 600 nA. The beam was aligned with the help of slits and a number of tantalum collimators placed inside the beam port tube. Before falling on the target the beam passed through a tantalum collimator placed inside the target chamber. This collimator was 20 cm long and had a diameter of 3mm. The target chamber was made of brass and the inside part was covered with tantalum as a precaution from undesirable reactions. When required the beam spot on quartz target could be seen through the perspex glass fitted on the top of the target chamber. The target chamber was insulated from the beam tube. A cold trap was used before the target chamber to reduce the background gamma radiation.

Germaniun dioxide (GeO_2 with 98.9% enrichment of ^{70}Ge) target material was procured from Union Carbide Corporation of U.S.A. Targets of 80 $\mu gm/cm^2$ thickness were prepared by vacuum evaporation of the target material on 50 $\mu gm/cm^2$ carbon backing. These targets were used for measuring the γ-rays from primary transitions. Secondary γ-rays were measured by using targets of 400 $\mu gm/cm^2$ thickness and evaporated on 0.5 mm thick tantalum backing.

A co-axial Ge(Li) detector (ORTEC) with an active volume of 85 cc was used in this work. The resolution of the detector was 2.1 keV for 1.33 MeV γ-rays from ^{60}Co source. The target-detector distance during measurements was about 30 mm. During the measurements a 2 mm thick lead shielding

Dhaka University Institutional Repository

was in used in front of the detector face to suppress the low energy background γ-rays. The same shielding was used during the efficiency calibration of the detector.

The γ-ray energies observed at 90° are not influenced by the Doppler-effect. As such the measurements performed at 90° were used for the determination of the energy of gamma rays. Measurements at 55° were carried out for determining branchings of the γ-ray transitions. To be sure about the existence of levels, both primary and secondary γ-rays were recorded. Gamma ray singles spectra from the primary transitions were recorded at 90°. Singles spectra as well as Ge(Li) -NaI(Tl) coincidence spectra were measured from the secondary transitions. During the coincidence measurements the 5"x5" NaI(Tl) detector and the Ge(Li) detector were placed directly opposite to each other and at 90° to the beam direction. The purpose of the coincidence measurement was to determine which of the γ-rays really belonged to the decay of ^{71}As. It helped to reduce the background and a clear spectrum was obtained. The coincidence data were obtained when the pulses from the Ge(Li) detector were in coincidence with the pulses from the NaI(Tl) detector. The whole system had a resolving time of 50 nsec. The electronic set-up used in coincident measurement is discussed below.

Dhaka University Institutional Repository

7.1.3. The electronic setup

The electronic setup used in the Ge(Li)-NaI(Tl) coincidence measurements is shown in fig. 7.1. The two detectors placed opposite to each other were at an angle of 90° to the beam direction. The energy output pulses from the Ge(Li) detector were amplified by an ORTEC preamplifier (Model 120-4) and then by a main amplifier (Spectroscopy amplifier, Canberra 1413). The amplified positive signals were then used as an input to the linear gate and stretcher (ORTEC 442). The normal output pulses from the linear gate and stretcher were used as an input to the signal of ADC of the multichannel analyser. The function of linear gate and stretcher was to delay the analog signal. This effectively reduced the bandwidth requirement of the ADC in the multichannel analyser.

The negative time output of the preamplifier was fed to the input of the extrapolated zero strobe (Canberra 1426). Fast negative output of extrapolated zero strobe was then fed to the input of gate and delay generator (ORTEC 416 A). The amplitude and width adjusted pulses from gate and delay generator constituted the 'start' pulse of the time-to-pulse-height convert. Gamma rays detected by NaI(Tl) detector were obtained as a current signal from the 9th dynode of the photomultiplier tube and shaped in a preamplifier to be fed

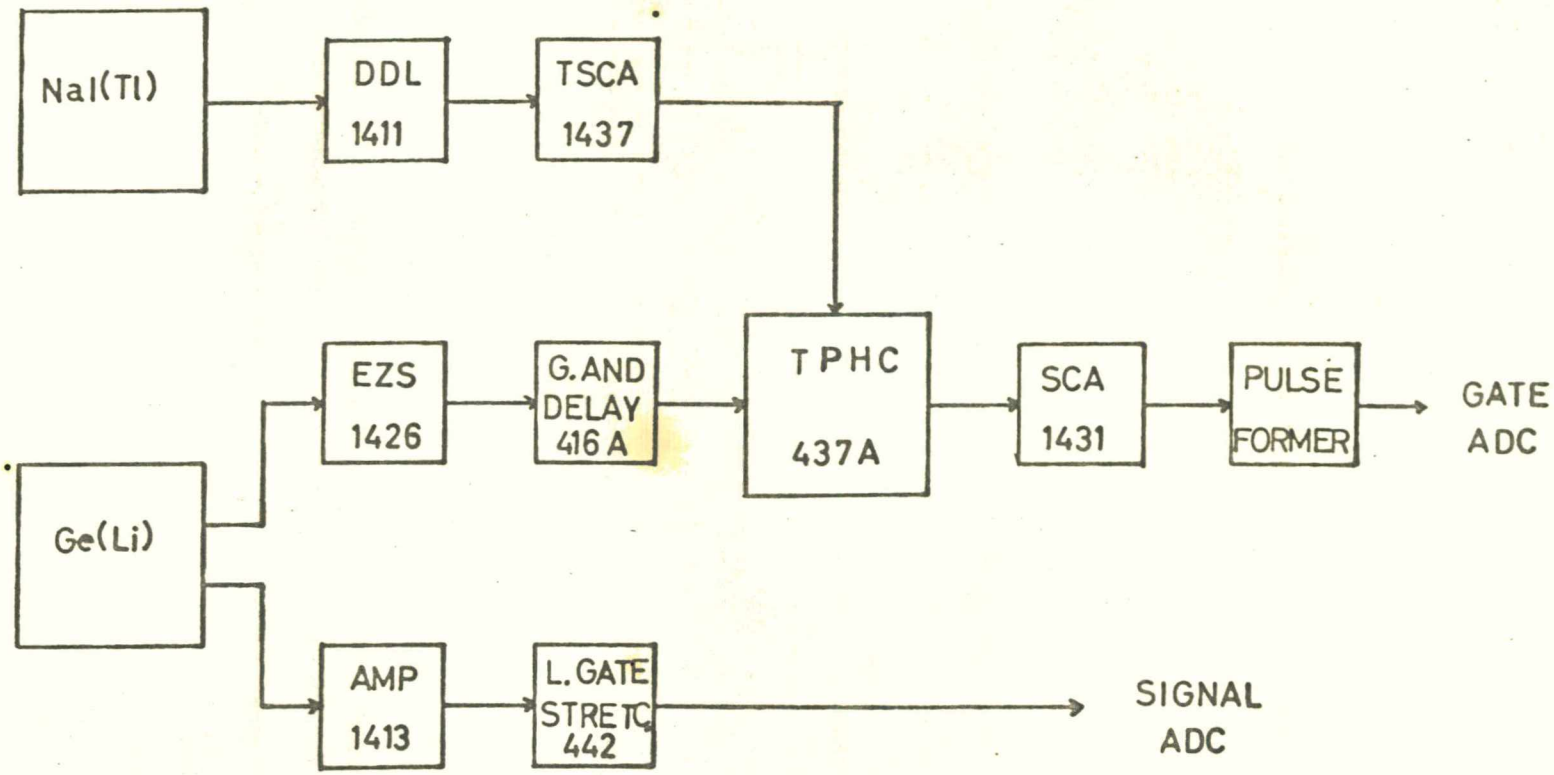

Fig. 7.1 Block diagram of the electronic set-up used in the Ge(Li)-NaI(Tl) coincidence measurements of $^{70}Ge(p,\gamma)^{71}As$ reaction.

Dhaka University Institutional Repository

Dhaka University Institutional Repository

to the input of a double delay line amplifier (Canberra 1411). The bipolar pulses obtained from double delay line amplifier were fed into the timing single channel analyser (Canberra 1437). Negative output of the timing single channel analyser constituted the stop pulse to the time-to-pulse-height converter. The bipolar output from time-to-pulse-height converter passing through single channel analyser and pulse former were used as an input to the gate of ADC. Thus the coincidence data were obtained when pulses from the Ge(Li) detector were in coincidence with pulses from the NaI(Tl) detector.

7.1.4. Efficiency calibration of Ge(Li) detector

Determination of the detection efficiency of a Ge(Li) detector is fundamental to quantative analyses of γ-ray spectra. In the present experiment it was sufficient to know the relative efficiency of the detector. The relative efficiency is given by

$$\text{Relative efficiency} = \frac{\text{Peak area}}{\text{Relative intensity}}$$

Knowing the peak area and relative intensity of a particular gamma ray, the relative efficiency can be calculated. Then the curve of relative efficiency as a function of gamma ray energy is drawn.

Dhaka University Institutional Repository

In the present measurements the detector efficiency for the energy range 344-3254 keV was measured using a ^{152}Eu source and a ^{56}Co source. The ^{56}Co source was prepared by bombarding a piece of iron with 7 MeV protons.

For determining branching ratios of the secondary transitions from the present measurements of the $^{70}Ge(p,\gamma)^{71}As$ reaction, the gamma-ray spectra were measured at an angle of 55° to the beam direction. After determining the yield with error of a gamma-ray, the intensity and hence the branching ratio was calculated.

The yield of each γ-ray was determined by substracting background counts from total counts under the peak. Thus

Yield = Total counts(T)-Background (B)

The error in yield is given by

$$Y = \left[(\Delta T)^2 + (\Delta B)^2\right]^{1/2}$$

7.1.5. <u>Energy calibration</u>

A pulse height versus gamma ray energy calibration is required for determining the energies of the deexciting gamma rays observed in a spectrum. For high energy γ-rays from the primary transitions this calibration was done by the internal or self calibration method. The dispersion (keV/channel) was obtained from full energy, single escape and double escape peaks.

Dhaka University Institutional Repository

For determining the energies of γ-rays from secondary transitions, the γ-ray spectra were measured twice. Once the reaction lines were accumulated along with the γ-lines from a ^{152}Eu source and next without the source. First the strong lines from the reaction (in singles spectrum) were calibrated using the the known γ-rays from ^{152}Eu source. The next step was to fix the energies of the weak γ-rays in the coincidence spectrum using these strong calibrated reaction lines. The 1461 keV γ-ray from ^{40}K was also utilized for energy calibration.

7.1.6. Results and discussions

A part of the γ-ray spectrum of the primary transitions from the $^{70}Ge(p,\gamma)^{71}As$ reaction at E_p = 2.8 MeV is shown in fig. 7.2. Numbers over peaks refer to level energies in keV. Peaks labelled B, (0), (1) and (2) refer respectively to background, full energy, single escape, and double escape respectively. Some of the weak lines in the spectrum were not identified. The differences to the ground state transition give directly the energies of the excited states.

A part of the spectrum of secondary transitions obtained from the Ge(Li)-NaI(Tl) coincidence measurement at E_p = 2.8 MeV is shown in fig. 7.3. The numbers over the peaks are the gamma ray energies. The decay scheme of ^{71}As as obtained in this work is given in fig. 7.4. In table 7.1 is given

Dhaka University Institutional Repository

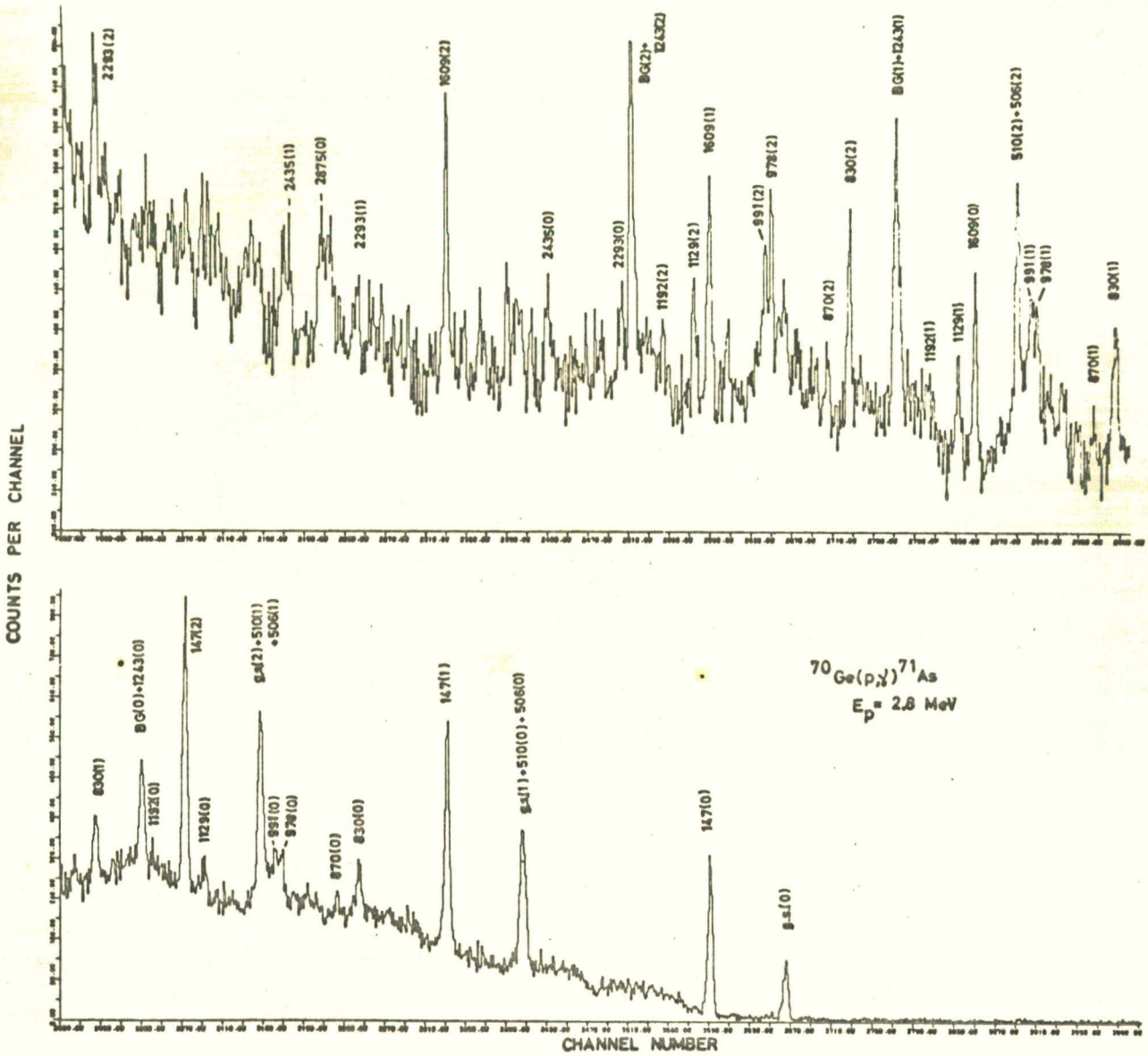

Fig. 7.2 A part of gamma-ray spectrum of the primary transitions from $^{70}Ge(p,\gamma)^{71}As$ reaction at E_p = 2.8 MeV. Numbers over peaks refer to level energies in keV. (0), (1) and (2) refer to full energy, single escape and double peaks respectively. B refers to background γ-ray.

Dhaka University Institutional Repository

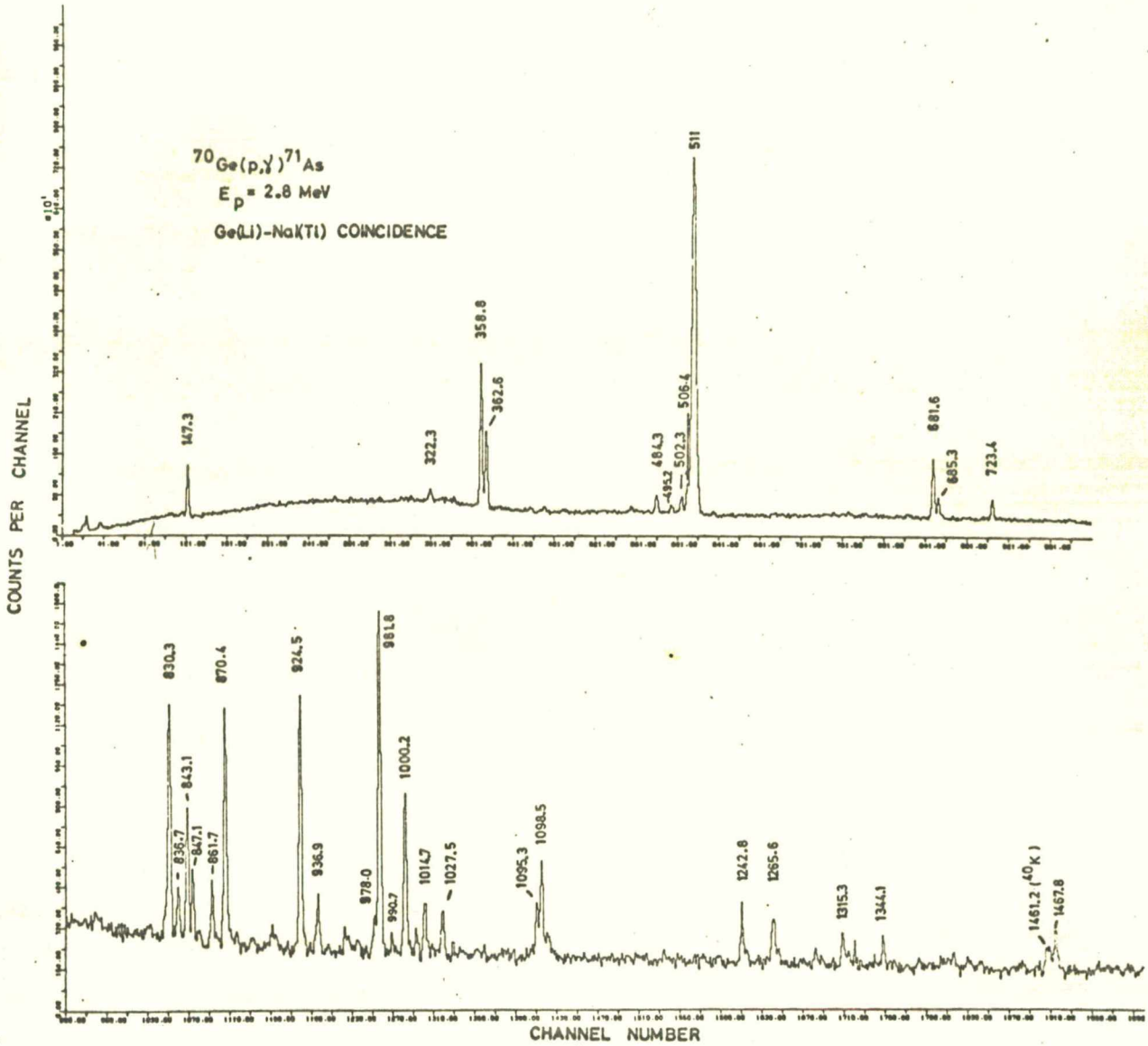

Fig. 7.3 A part of the gamma-ray spectrum of the secondary transitions from Ge(Li)-NaI(Tl) coincidence measurements from $^{70}Ge(p,\gamma)^{71}As$ reaction at E_p=2.8 MeV. Numbers over peaks refer to gamma-ray energies in keV.

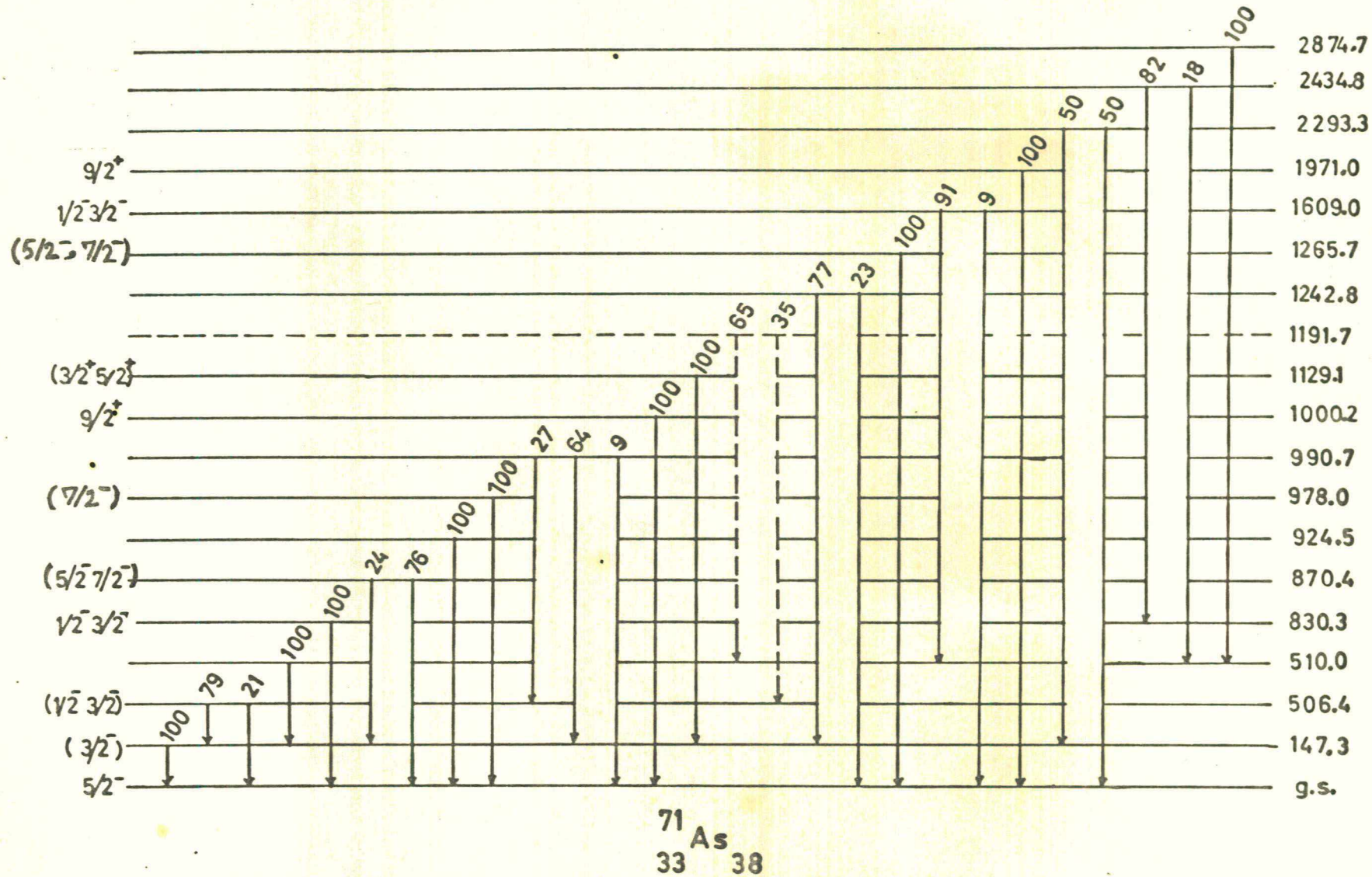

Fig. 7.4 The proposed decay scheme. The energies in keV and branchings ratios in % are given as obtained in this experiment. Spin and parity taken from refs. 33 and 35. The level schemes are not drawn to scale.

Dhaka University Institutional Repository

Dhaka University Institutional Repository

Table 7.1

Level energies, transition energies and branching ratios measured in the $^{70}Ge(p,\gamma)^{71}As$ reaction at E_p=2.80 MeV.

Level of origin (keV)	(Deexcitation) E_γ (keV)	Branching %	Level of origin (keV)	(Deexcitation) E_γ (keV)	Branching %
147.3±0.1	147.3	100	1191.7±0.1	685.3	35
				681.6	65
506.4±0.1	506.4	21			
	358.8	79	1242.8±0.1	1242.8	23
				1095.3	77
510.0±0.1	362.6	100			
			1265.7±0.2	1265.7	100
830.3±0.1	830.3	100			
			1609.0±0.1	1609.0	9
870.4±0.2	870.4	76		1098.5	91
	723.4	24			
			1971.0±0.3	1971.0	100
924.5±0.1	924.5	100			
			2293.3±0.6	2293.3	50
978.0±0.1	978.0	100		2145.9	50
990.7±0.5	990.7	9	2434.8±0.4	1924.2	18
	843.1	64		1604.4	82
	484.3	27			
			2874.7±0.5	2364.7	100
1000.2±0.1	1000.2	100			
1129.1±0.1	981.8	100			

Dhaka University Institutional Repository

the list of energy levels and deexcited γ-ray energies used in the construction of decay scheme. This table also contains the branching ratios of the secondary γ-transitions.

The identification of low-lying states of ^{71}As were based on the energy balance and energy consistency. This was taken into account up to 1 keV. That means wherever available two or more gamma ray energies were added together to give a certain level. The Ge(Li)-NaI(Tl) coincidence measurements were used for the construction of the decay scheme. The coincidence measurements helped to rule out γ-rays not belonging to $^{70}Ge(p,\gamma)^{71}As$ reaction. Above 1971 keV the deexitation -rays were very weak in the coincidence spectrum. As such gamma rays above 1971 keV were used from singles γ-ray spectrum. Most of the levels identified in the present experiment have their evidences in primary transitions also. The agreement between the energies of low-lying levels obtained from low energy gamma rays and the energies obtained as differences between high energy gamma rays is good. Some of the γ-rays in the coincidence spectrum did not fit into the decay scheme. A list of these γ-ray energies is given in table 7.2. In the present work 18 levels are reported and a complete decay scheme of these levels have been constructed. The level energies were determined to one decimal point. A level-by-level discussion of the results is given below.

Dhaka University Institutional Repository

Table 7.2

List of gamma ray energies in coincidence spectrum not identified.

No.	Gamma ray energy (keV)	No.	Gamma ray energy (keV)
1.	322.3±0.5	7.	936.9±0.2
2.	495.2±0.3	8.	1014.7±0.2
3.	502.3±0.1	9.	1027.5±0.2
4.	836.7±0.2	10.	1315.3±0.2
5.	847.1±0.1	11.	1344.1±0.5
6.	861.7±0.3	12.	1467.8±0.2

Dhaka University Institutional Repository

The 147.3 keV level.

This level was observed in (^{3}He,d) reaction by previous workers [32,33] and in the decay of ^{71}Se studied by Hundelshausen [34]. The state was also observed by Liu et al. [36] in the (p,) reaction but the energy of the level was determined as 145 keV. Recently Heits et al. [35] from ^{69}Ga(α,2n) reaction observed this level. In the present work transitions to and from this level are observed. The level decays 100% with a gamma ray of 147.3 keV to the ground state. The energy of the level as determined in this work is in good agreement with that of refs. [34,35] but not with the previous (p,γ) work. As can be seen from our primary spectrum this level is fed by primary gamma rays.

The 510.0 and 506.4 keV levels.

The 510 keV level was observed in (^{3}He,d)[32,33] and (p,γ) work [36] but not observed in ^{71}Se decay [34]. Recently a level has been observed at 506.4 keV by Heits et al. [35]. In the present experiment two levels were found at E_x=506.4 and 510 keV, which form a doublet. Transitions to and from both the levels are present. Liu et al. [36] observed a gamma ray of 360 keV (not resolved) which they assigned as a decay from the 870 keV state. But in our coincident spectrum it was clearly found to be a doublet with energies of 358.8 and 362.6 keV which are assigned as decays from 510 and 506.4 keV levels to the 147.3 keV state. The existence of the levels

Dhaka University Institutional Repository

is confirmed from the presence of the corresponding peaks in our primary spectrum.

The 830.3 keV level.

This level was observed in (^{3}He,d)[32,33] and (p,γ) works [36]. This level was not populated in the (α, 2n) reaction [35] at all. In ^{71}Se work a gamma ray of 830.9 keV was shown as a decay from the 978 keV level. In the present work transitions to and from this level are observed; the 830.3 keV level is found to decay 100% to the ground state. The existence of the level is also confirmed because it is fed by primary gamma rays as is observed in our primary spectrum. Liu *et al.* [36] observed two other branches decaying to 145 and 510 keV levels. We have similar gamma energies but with difference of more than 2 keV which do not fit well.

The 870.4 keV level.

This level was observed in all the previous works[32-36]. In the present work this level is also observed both in primary and secondary spectra. Transitions from this level occur via 870.4 and 723.4 keV γ-rays with branches of 76% and 24% respectively. This is in good agreement with that of ^{71}Se decay work but not with Liu *et al.* [36] who observed another branch to the 510 keV state.

Dhaka University Institutional Repository

The 924.5 keV level.

This level was not observed in any of the (^{3}He,d) work or the ^{71}Se decay work but observed in the (p,γ)[36] and the (α, 2n) reaction [35]. The presence of this level is also not observed in our primary spectrum. But we have a strong gamma ray of 924.5 keV in our coincidence spectrum which we suppose to stem from the decay of the 924.5 keV level to the ground state. That the primary transition to this level was not observed may be due to the fact that the target used in the measurements of the primary spectrum was very thin so that relatively few compound resonances contributed and there was a certain probability that not all low-lying states were populated strongly enough.

The 978.0 keV level.

This state is fed from the resonance state and decays straight to the ground state without branching. This level was not observed in previous (p,γ) work [36] or the (^{3}He,d) works. The level energy is in good agreement with that of ^{71}Se work and (α,2n) reaction.

The 990.7 keV level.

This level was observed only in the (^{3}He,d) work of Broman et al. [32] and in the previous (p,γ) work. It is also observed in our primary spectrum. Transitions from this level are found to the ground, 147.3 and 506.4 keV states.

Dhaka University Institutional Repository

The 1000.2 keV level.

A transition to this level is not observed in our primary spectrum. However, we observed a 1000.2 keV γ-ray. Heits et al. [35] in their (α,2n) reaction observed a level at 1000.8 keV. We also suppose that the 1000.2 keV γ-ray observed in our coincidence spectrum is a decay from the 1000.2 keV level to the ground state.

The 1129.1 keV level.

This state is fed from the capturing states. A strong γ-ray of 981.8 keV is observed from this level to the 147.3 keV state. This level was previously observed in the (^{3}He,d)[32,33] and (α,2n)[35] works but not observed in the ^{71}Se work or the other (p,γ) work [36].

The 1191.7 keV level.

This level is a new one and is tentatively assigned based on the following arguements. The energy difference between the 681.6 and 685.3 keV γ-rays is the same as that between the levels at 506.4 and 510.0 keV. It is supposed therefore that the two γ-rays are the decay branches of 65% and 35% respectively from the 1191.7 keV level to the 506.4 and 510 keV levels. Additional evidence comes from the primary spectrum where a weak peak of the corresponding energy is found. These two γ-rays were not resolved in the spectrum of Liu et al. [36]. They obtained a γ-ray with an

Dhaka University Institutional Repository

energy of 684 keV which they assigned as the decay of the 829 keV state to the first excited state.

The 1242.8 keV state.

This level has not been reported in (^{3}He,d) work but has been observed by other authors [34-36]. In this work transitions from this level are found to occur through 1242.8 and 1095.3 keV γ-rays with branches of 23% and 77%, respectively, and they are in good agreement with that of ^{71}Se work of Hundelshausen [34]. In the (p,γ) work of Liu et al. [36] another branch to the 870 keV state was observed which we did not observe. The level is also fed by primary γ-rays.

The 1265.7 keV level.

This level was tentatively assigned by Hundelshausen[34] and was later confirmed by Betts et al. [33]. In the present work this level is not fed by primary transitions but a 1265.7 keV γ-ray was observed in our coincidence spectrum. We therefore propose that this γ-ray is a decay from 1265.7 keV level to the ground state.

The 1609.0 keV level.

This level is fed by γ-rays from the capturing states. Transitions from the level are observed. The 1609 keV and 1098.5 keV gamma rays decay to ground state and 510 keV state respectively with 9% and 91% branches. The 1609 keV gamma

Dhaka University Institutional Repository

ray is not shown in the spectrum. The level was observed by Betts et al. [33] and Liu et al. [36] but not by other authors.

The 1971.0 keV level.

A γ-ray of 1971 keV is obtained in both the singles and coincidence spectra (not shown in fig.) which is proposed as a ground state decay. The level is not populated by primary γ-rays. This level was observed in the (^{3}He,d) works and also in the (p,γ) work of Liu et al.

The 2293.3 keV level.

A transition to this level is observed in the primary spectrum. From our singles spectrum of secondary transitions this level was found to decay through a 2293.3 keV γ-ray to the ground state with 50% branch and through 2145.9 keV γ-rays with the other 50% branch to the 147.3 keV state. This level is assigned new.

The 2434.8 keV level.

This level is fed by the primary γ-rays. The level decays to the 510 and 830 keV states. The 1604.4 keV γ-ray from the 2434.8 to the 510 keV state is observed in the coincidence spectrum (not shown in spectrum). The 1924.2 keV transition γ-ray to the 830.3 keV state is very weak in the

Dhaka University Institutional Repository

coincidence spectrum but quite prominent in the singles spectra. This level is also assigned new.

The 2874.7 keV level.

This level was not reported previously. We have found transitions from the capturing states to this state. As observed from singles spectra the level decays through a 2364.7 keV γ-ray to the 510 keV state.

In conclusion it may stated that the levels identified in ^{71}As in the present measurements are confirmed by their presence in both primary and secondary transitions. Agreement with previous authors is quite good. New levels at 2293.3, 2434.8 and 2874.7 are observed and the level at 1191.7 is assigned tentatively. The levels at 510.0 and 506.4 keV are found to form a doublet. Betts et al.[33] compared the experimentally observed and theoretically predicted level schemes of the isotopes in As. Systematics of these isotopes show that there should be a level below 700 keV in ^{71}As not previously found, which may be the new level at 506.4 keV as observed in the present work.

Dhaka University Institutional Repository

LIFETIMES MEASUREMENTS IN ^{71}As

7.2.1. Introduction

Before the present study no information was available on the mean lives of the states of ^{71}As. The reason for the lack of lifetime information is that levels and decay schemes for this nucleus are not well known. As discussed in the last section (7.1.1) levels were identified and a decay scheme was constructed for ^{71}As up to 2875 keV excitation energy. in the present work. With these results, measurements were carried out to determine lifetimes of levels in ^{71}As. Mean lives obtained from the present study were utilised to calculate transition strengths assuming pure multipole radiation.

7.2.2. Experimental procedure

The levels in ^{71}As were populated by $^{70}Ge(p,\gamma)^{71}As$ reaction at a proton bombarding energy of 2.8 MeV. The target chamber with two-target arrangement and the electronic set-up described in sections 3.2 and 3.3 respectively were used. The beam current was about 200 nA. Singles gamma ray spectra were measured at forward and backward angles simultaneously and stored separately in the two memories of the multichannel analyser. The mode of analysis is the same as that discussed in section 4.3 of chapter 4.

7.2.3. Density of germanium dioxide (GeO_2)

The density of GeO_2 is quoted as 4.228 and 6.239 for hexagonal and tetragonal crystalline structures respectively

Dhaka University Institutional Repository

by ref. 104. The structure of the material while making targets by evaporation is not known. But for calculating attenuation curves one has to know the density of the backing material as accurately as possible. The following procedure was adopted for determining the density of GeO_2.

The 1040 keV level of ^{70}Ge was excited by Coulomb excitation by bombarding a natural Ge target (density known) with a 9.0 MeV α-beam. The shift of the 1040 keV γ-ray deexciting the 1040 keV level was measured and the lifetime determined for the level. In the next step the enriched GeO_2 target(density to be determined) was bombarded with 9.0 MeV α-beam and the shift was measured. This shift was then compared with attenuation curves calculated with different densities. The curve that corresponds to the same lifetime as determined above gives the density of GeO_2.

In this way the density of the target was found to be 4.228, and this value was used for the calculation of attenuation curve. The curve is shown in fig. 7.5.

7.2.4. Results and discussions

Lifetimes of 10 states in ^{71}As have been obtained from the present measurements. The summary of these results are presented in table 7.3. Because of the large uncertainties in measured shift and attenuation factors, only limits in lifetime values for the 978.0, 1242.8 and 1609.0 keV levels could be quoted. Some of the states have large errors in

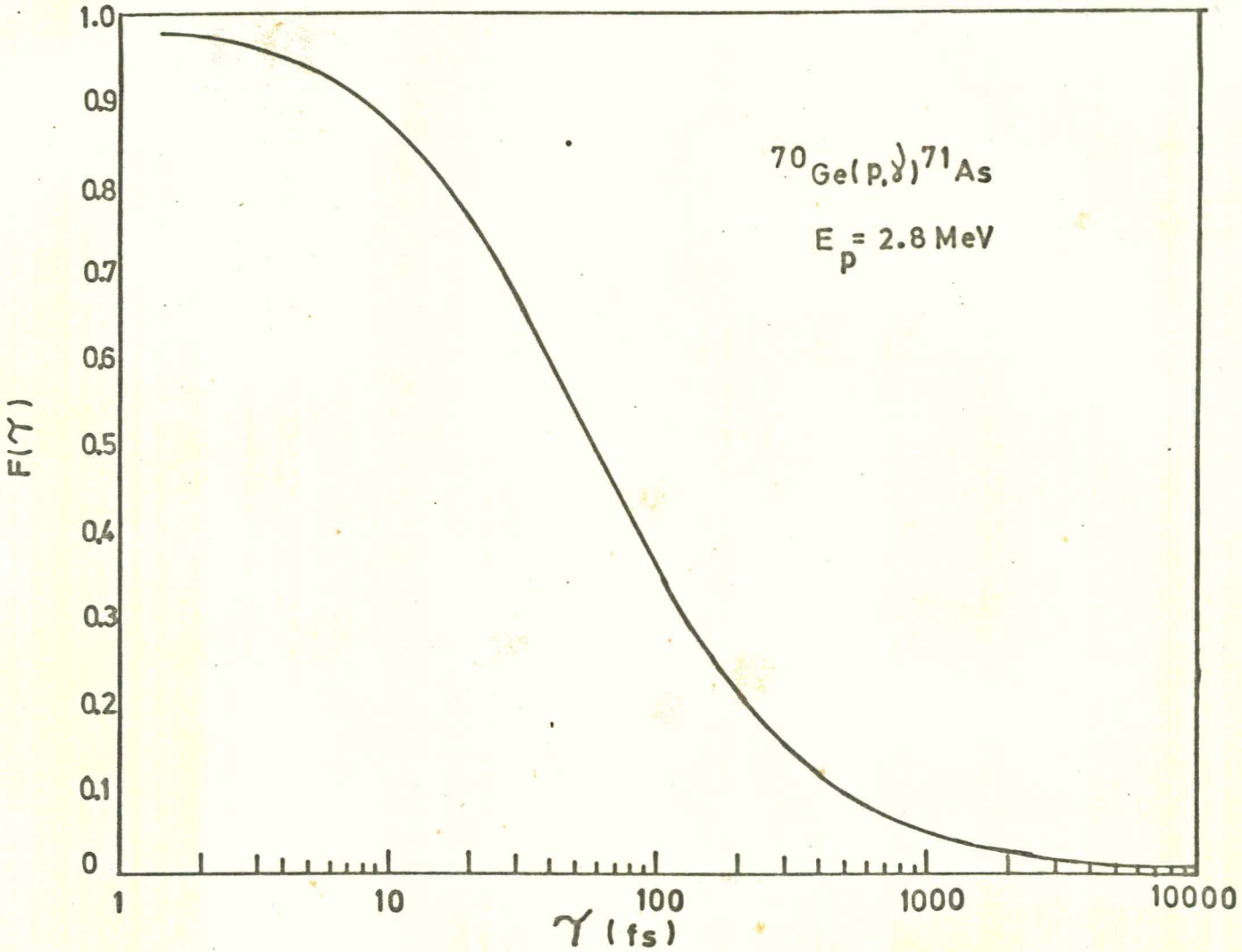

Fig. 7.5 The attenuation factor $F(\tau)$ vs. lifetime τ curve for ^{71}As nuclei recoiling in GeO_2 at E_p = 2.8 MeV. Density of GeO_2 used is 4.228 gm/cc.

Dhaka University Institutional Repository

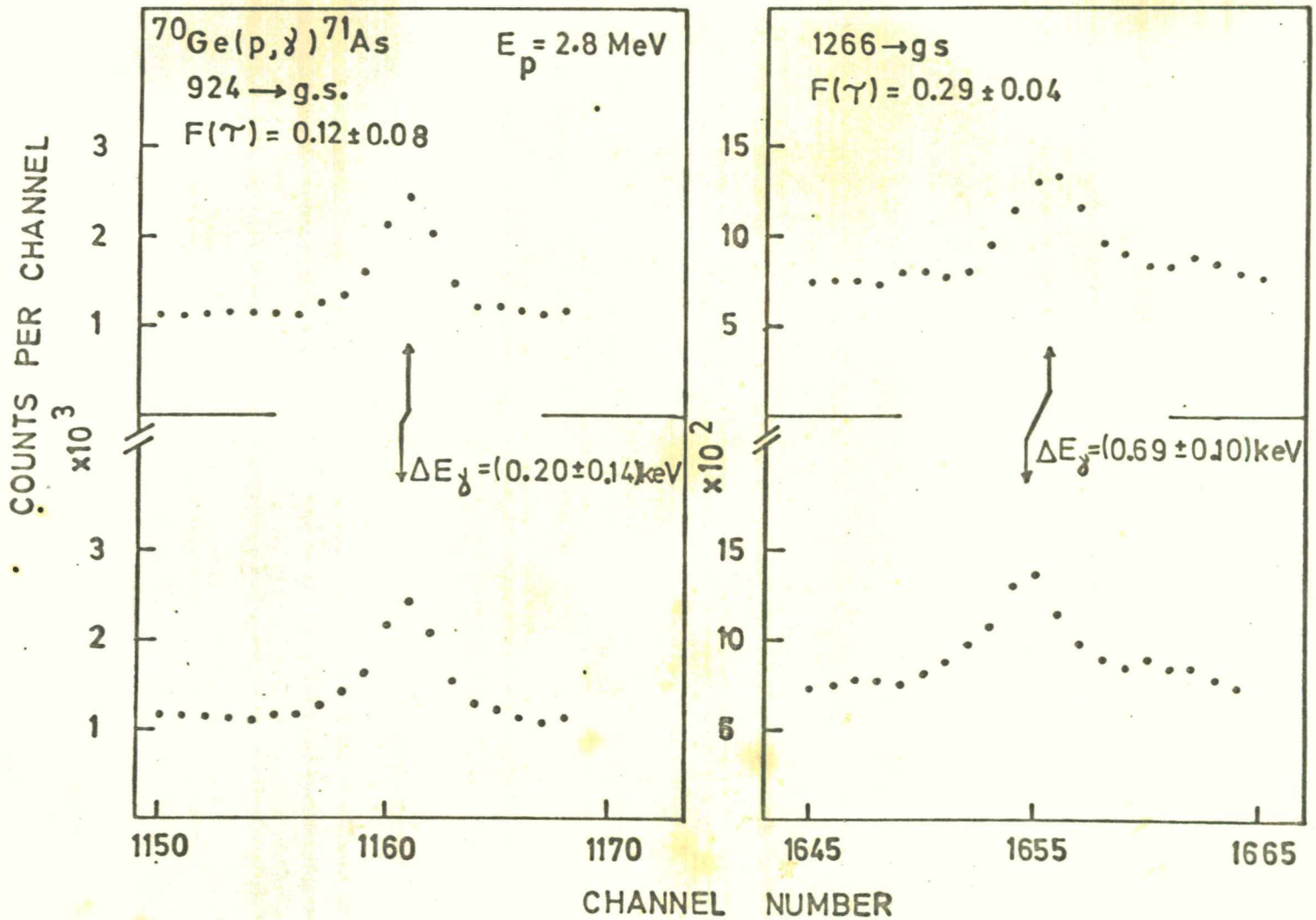

Fig. 7.6 Doppler-shifted γ-ray peaks of the 924 and 1266 keV from the $^{70}Ge(p,\gamma)^{71}As$ reaction at E_p = 2.8 MeV and using the two-target arrangement.

Dhaka University Institutional Repository

Table 7.3

Summary of lifetime results in ^{71}As from $^{70}Ge(p,\gamma)^{71}As$ reaction at E_p=2.8 MeV

Level ((keV)	E_{γ_0} (keV)	ΔE_γ^{max} (keV)	Measured shift $\overline{\Delta E}_\gamma$ (keV)	Attenuation factor $F(\tau)$ in GeO_2 in %	Mean lifetime (fs)
830.4	830.4	1.542	0.137±0.063	8.9±4.1	525^{+475}_{-175}
870.4	870.4	1.616	0.101±0.059	6.3±3.6	
	723.4	1.343	0.075±0.050	5.6±3.7	
				5.9±2.6 a)	800^{+700}_{-250}
924.5	924.5	1.717	0.197±0.142	11.5±8.3	400^{+1100}_{-185}
978.0	978.0	1.823	0.011±0.016	0.6±0.9	> 3500
990.7	843.1	1.567	0.110±0.045	7.2±2.8	650^{+450}_{-180}
1242.8	1242.8	2.308	0.079±0.140	< 9.4	
	1095.7	2.034	< 0.048	< 2.4	> 500
1265.7	1265.7	2.350	0.689±0.102	29.3±4.3	130^{+30}_{-20}
1609.0	1609.0	2.988	0.358	12.0	
	1098.5	2.039	0.066	4.8	
				< 12.0	> 260
1971.0	1971.0	3.660	1.474±0.980	40.3±26.8	85^{+235}_{-55}
2434.7	1604.4	2.979	0.294±0.179	9.9±6.0	480^{+720}_{-200}

a) Mean life computed from weighted average of the attenuation factors.

Dhaka University Institutional Repository

Dhaka University Institutional Repository

Table 7.4

Transition strength for pure multipole transition in ^{71}As

Initial state (keV)	Final state (keV)	E_{γ_0} (keV)	Branch %	Transition strength (W.u.) E1 ($\times 10^{-3}$)	E2	M1 ($\times 10^{-2}$)
830.3	0	830.3	100	$1.82^{+0.92}_{-0.86}$	220^{+110}_{-105}	1.0 ± 0.5
870.4	0	870.4	76	0.79 ± 0.36	87 ± 40	4.5 ± 2.1
	147.3	723.4	24	0.43 ± 0.20	69 ± 32	2.5 ± 1.1
924.5	0	924.5	100	$1.74^{+1.49}_{-1.27}$	169^{+145}_{-124}	$9.9^{+8.5}_{-7.3}$
978.0	0	978.0	100	< 0.16	< 14	< 0.9
990.7	0	990.7	9	0.08 ± 0.03	7 ± 3	0.4 ± 0.2
	147.3	843.1	64	0.90 ± 0.37	106 ± 42	5.2 ± 2.0
	506.4	484.3	27	2.00 ± 0.80	714 ± 280	11.5 ± 4.5
1242.8	0	1242.8	23	< 0.13	< 7	< 0.8
	147.3	1095.6	77	< 0.64	< 45	< 3.7
1265.7	0	1265.7	100	$2.08^{+0.4}_{-0.3}$	108^{+19}_{-15}	$11.9^{+2.2}_{-1.6}$
1609.0	0	1609.0	9	< 0.04	< 2	< 0.3
	147.3	1098.5	91	< 1.44	< 100	< 8.3
1971.0	0	1971.0	100	$0.84^{+1.56}_{-0.62}$	18^{+33}_{-14}	$4.8^{+8.8}_{-3.5}$
2434.8	510.0	1924.2	18	$0.03^{+0.02}_{-0.01}$	1 ± 0.5	0.2 ± 0.1
	830.3	1604.4	82	0.23 ± 0.15	7^{+5}_{-4}	$1.3^{+0.9}_{-0.8}$

Dhaka University Institutional Repository

lifetime values because the experimental situation in these cases is at the limit of $F(\tau)$ curve where DSA method is insensitive. The errors in the lifetime values contain only the experimental errors and do not contain contributions from the uncertainties in the stopping power theory. Two representative cases of Doppler shifts are shown in fig. 7.6.

Transition strengths calculated from the present lifetime values and branching ratios are presented in table 7.4. The E1, E2 and M1 transition strengths are in W.u.

From the comparison of experimental and Weisskopf estimated lifetimes and using the criteria of the Nuclear Data Group (section 4.3) the possible range of spin and parity values for some of the levels are obtained as follows:

Level (keV)	J^{π}
924.5	$3/2^{\pm}, 5/2^{\pm}, 7/2^{\pm}, 9/2^{-}$
990.7	$1/2^{\pm}, 3/2^{\pm}, 5/2^{\pm}, 7/2^{-}$
1242.8	$1/2^{-}, 3/2^{\pm}, 5/2^{\pm}, 7/2^{\pm}, 9/2^{-}$

No previous measurement on the lifetimes of the levels in ^{71}As exists. Theoretical calculations are also lacking. The lifetime values for the levels in ^{71}As have been determined in the present experiment for the first time which should be useful to a future theoretical calculation.

Dhaka University Institutional Repository

CHAPTER-8

LEVEL SCHEMES AND GAMMA-RAY ANGULAR DISTRIBUTION MEASUREMENTS IN ^{57}Co

8.1. Introduction

The energy levels in ^{57}Co have been studied by various authors through $^{54}Fe(\alpha,p)$, $^{56}Fe(p,\gamma)$, $^{56}Fe(d,n)$, $^{56}Fe(^{3}He,d)$, $^{57}Fe(p,n\gamma)$, $^{58}Ni(t,\alpha)$, $^{60}Ni(p,\alpha)$ and $^{58}Ni(d,\tau)$ reactions and also from $\beta^{\pm}$decay studies of ^{57}Ni. Decay schemes have also been measured in some of the above measurements. A summary of the above studies has been compiled very recently by Auble et al. [37]. The level scheme of ^{57}Co is of theoretical interest because the low-lying level structure is in some disagreement with the shell-model calculations of Gatrousis et al. [105] who assume an inert ^{40}Ca core and particles distributed in the $1f_{7/2}$, $2p_{3/2}$ and $1f_{5/2}$ orbits. This calculation gives only one low-lying $3/2^-$ level as against two observed around E_x=1.5 MeV. The unified-model calculations of Satpathy and Gujrathi [106] predict too few levels and also fail to give the lowest $1/2^-$ and $3/2^-$ energy levels. In a more recent shell-model calculation Horie and Ogawa [107] assume an inert ^{48}Ca core with a proton hole in $1f_{7/2}$ shell and the extra core neutrons in the 2p and $1f_{5/2}$ orbits. The $1/2^-$ and $3/2^-$ levels are not reproduced and also fewer levels are predicted than observed.

The $^{56}Fe(^{3}He,d)^{57}Co$ reaction has been studied by Rosner and Holbrow [108] who have reported energy levels up to

Dhaka University Institutional Repository

7.4 MeV. Hardie et al. [109] reported 69 energy levels in ^{57}Co up to 7.5 MeV and Banu et al. [110] up to 7.8 MeV. The $^{56}Fe(d,n)$ reaction has already been studied by Adam et al. [111] covering an excitation energy of 4.8 MeV. From the β^+-decay studies of ^{57}Ni Gatrousis et al. [105] determined the energies of the levels in ^{57}Co accurately up to 3.2 MeV. Dayras et al. [112] studied the $^{54}Fe(\alpha,p\gamma)$ reaction and determined the level energies up to 3.3 MeV. Energy levels and decay schemes up to 4 MeV have been given by Pietrzyk et al. [113] from the study of $^{57}Fe(p,n\gamma)^{57}Co$ reaction. The gamma decay of the low-lying and resonant levels has been studied by several authors through $^{56}Fe(p,\gamma)^{57}Co$ reaction. In all the works mentioned above there are some disagreements. For example, on the decay of 2883 keV level Hardie et al. [109], Dayras et al. [112] and Pietrzyk et al. [113] observed strong branches to the ground, 1758 and 1920 keV states, whereas Burton and McIntyre [114] did not observe a transition to the 1920 keV state but instead reported a branch to the 1378 keV state. While Leslie et al. [115] observed a transition from the 2984 keV state to the 1897 keV state, Hardie et al. [109] and Dayras et al. [112] observed only a branch to the 1758 keV state. In another work of $^{57}Fe(p,n\gamma)$ reaction Pietrzyk et al. [113] observed branches to the 1378 and 2133 keV levels in addition to the branch at 1758 keV state. O'Brien and Coote [116], Leslie et al. [115] and El-Kateb and Griffiths [117] observed a level

Dhaka University Institutional Repository

at 3993 keV which is possibly the same level as 4002 keV obtained by Hardie et al. [109]. Besides, γ-decays of some levels e.g. 3520, 3554, 3674 and 4238 keV observed by Pietrzyk et al. [113] have not been observed by others.

The gamma decay and the properties of the resonating states in ^{57}Co have been studied by a few authors through $^{56}Fe(p,\gamma)^{57}Co$ reaction. As can be seen from table 8.1 there exists discrepancy in the spin assignment of the resonance at E_p=1248 keV leading to the 7253 keV resonance state. The 3/2 spin value was assigned to this level by O'Brien and Coote [116], Leslie et al. [115] and El-Kateb and Griffiths [117]. The 1/2 spin value was assigned by Arnell and Persson [118], Abraham et al. [119], Brändle et al. [120] and Waymire [121]. The decay scheme of this resonance level is also not in agreement among the different authors. For example Leslie et al. [115] did not observe the ground state transition in disagreement with the observations of O'Brien and Coote [116] and El-Kateb and Griffiths [117]. El-Kateb and Griffiths [117] observed another branch to the 3268 keV level but this branch was not observed by other authors [115,116]. The spin assignment and decay of the 7650 keV resonating state (E_p=1652 keV) is due only to Leslie et al. [115] and it is considered worth-while to check the spin assignment. No information on the properties of the resonance at E_p=2065 keV leading to the 8056 keV resonanting state is available. It may be mentioned that in

Table 8.1

Comparison of J^{π} values of the previous and present work corresponding to resonances in ^{57}Co

E_p (keV)	Arnell and Persson[a)]	Abraham *et al.*[b)]	Brandle *et al.*[c)]	O'Brien and Coote[d)]	Leslie *et al.*[e)]	Waymire[f)]	El-Kateb and Griffiths[g)]	Present work
1248	$1/2^+$	$1/2^-$	$1/2^-$	$3/2^-$	3/2	$1/2^-$	$3/2^-$	3/2
1652					3/2			3/2
2065								3/2

a) Ref. 118, b) Ref. 119, c) Ref. 120, d) Ref. 116, e) Ref. 115, f) Ref. 121, g) Ref. 117.

Dhaka University Institutional Repository

Dhaka University Institutional Repository

our earlier work of excitation function measurement [122] we observed strong resonances at E_p=1248, 1652 and 2065 keV.

The present work of angular distribution measurement was undertaken in an attempt to remove the discrepancy in the spin assignment of 7253 keV resonating state, to check the spin assignment of 7650 keV resonating state, to assign spin to the 8056 keV state and to obtain level and decay schemes of the low-lying and resonance levels in ^{57}Co.

Measurements of the angular distributions of -radiation emitted from an excited nucleus can yield valuable information on multipole mixing ratios and nuclear level spins which in turn can be related to the model predictions. The spins of the low-lying states in ^{57}Co are well established and we have exploited these in assigning resonance spins.

The capture of a proton by a spin-zero target (^{56}Fe in this case) populates only the m = ±½ megnetic substates of the compound state. In such a case the analysis of the angular distributions of the deexciting gamma rays is rather simple. The theoretical γ-ray angular distributions are of the form

$$W(\theta) = A_0 + A_2Q_2P_2(\cos\theta) + A_4Q_4P_4(\cos\theta)$$

where $W(\theta)$ is the intensity of the γ-ray yield at an angle θ relative to the direction of the incident beam, Q_2 and Q_4 are attenuation factors of γ-rays due to finite size of the detector, the ratios $a_2 = A_2/A_0$ and $a_4 = A_4/A_0$ depend only

Dhaka University Institutional Repository

on the initial and final spins and on the multipolarity of the radiation. The values A_0, A_2 and A_4 are obtained by least squares analyses of the Legendre polynomial fit. The analyses of the angular distribution of gamma rays are carried out using the theoretical formulae derived by Rose and Brink [123]. The formula for the analysis of angular distribution of γ-rays emitted in the decay of an aligned initial state and making an angle θ with the beam direction which is an axis of symmetry is

$$W(\theta) = \sum_{k \text{ even}} B_k(J_1) \Big[R_k(LLJ_1J_2) + 2\delta R_k(LL'J_1J_2) + \delta^2 R_k(L'L'J_1J_2) \times Q_k P_k(\cos\theta)/(1+\delta^2) \qquad (8\text{-}1)$$

This formula is restricted to the case of γ-ray transition from the initial state of spin J_1 leading to the final state of spin J_2 and having definite parity and that the polarisation of γ-rays is not observed. L and L' =(L+1) are the two lowest multipolarities. The population parameter $B_k(J_1)$ describes the alignment of the initial state and contains information about the mode of formation of the initial state. The values of $B_k(J_1)$ are the same for all branches originating from the same initial level. The R_k contains the nuclear structure information of the transition from J_1 to J_2. The mixing ratio δ, i.e. the ratios of reduced matrix elements of different multipoles contributing to γ-ray transition

Dhaka University Institutional Repository

between two well defined nuclear states is

$$\delta = \frac{\langle J_1 \| T_L^{\langle \pi \rangle} \| J_2 \rangle / (2L+1)^{1/2}}{\langle J_1 \| T_{L'}^{\langle \pi \rangle} \| J_2 \rangle / (2L'+1)^{1/2}} \qquad (8\text{-}2)$$

where the symbol $\langle J_1 \| T_L^{\langle \pi \rangle} \| J_2 \rangle$ stands for the reduced matrix element of the multipole interaction parameter.

The values of the population parameters depend on the process by which the initial state $|J_1 M_1\rangle$ is formed. In the present experiment the initial state is aligned since the beam is unpolarized and target nuclei are randomly oriented. The beam axis is an axis of symmetry and may be taken as the quantization axis.

If two partial waves l and l' contribute to the formation of the initial state with definite parity and channel spin s then $B_k(J_1)$ is given by

$$B_k(J_1) = \sum_s \Big[S_k(llJ_1s)|A(l)|^2 + 2S_k(ll'J_1s)|A(l)|\,|A(l')|\cos(\phi_l - \phi_{l'}) + S_k(l'l'J_1s)|A(l')|^2 \quad T(s) \qquad (8\text{-}3)$$

Here A(l) and A(l') are the amplitudes for the formation of the initial state J_1 with partial waves l and l'. The normalization is given by

$$|A(l)|^2 + |A(l')|^2 = 1$$

Dhaka University Institutional Repository

The normalization of channel spin intensity is

$$\sum_{s} T(s) = 1$$

since only one l and one channel spin contribute to the formation of the compound level in case of spin-zero target, the expression for $B_k(J_1)$ is given by

$$B_k(J_1) = \sum_{s} S_k(llJ_1s)\ T(s) \qquad (8\text{-}4)$$

The allowed values of the multipolarity are

$$|J_i + J_f| \geq L \geq |J_i - J_f|$$

If the parity of the initial state is not known then by definition $B_k(J_1)$ is given by

$$B_k(J_1) = \sum_{M_1=J_1}^{J_1} w(M_1)(-)^{J_1-M_1}(2J_1+1)^{1/2}(J_1J_1M_1-M_1\ \ KO) \qquad (8\text{-}5)$$

with $B_0(J_1) = 1$

The sum over M_1 runs from $-J_1$ to J_1. The expression (8-5) for $B_k(J_1)$ can be simplified for the case of alignment. With the normalization $\sum_{M1} w(M_1) = 1$ and $w(M_1) = w(-M_1)$ we can replace the summation from $M_1 = -J_1$ to $M_1 = J_1$ by a summation from $M_1 = 0$ or $1/2$ to $M_1 = J_1$, then equation (8-5) becomes

Dhaka University Institutional Repository

$$B_k(J_1) = \sum_{M_1=0,\frac{1}{2}}^{M_1=J_1} w(M_1)(2-\ _{M_1 0})(-)^{J_1-M_1}(2J_1+1)^{\frac{1}{2}}$$

$$(J_1 J_1 M_1 - M_1 \mid K0)$$

$$= \ _{M_1} w(M)\ \ _k(J_1 M_1) \qquad (8\text{-}6)$$

$B_0(J_1) = 1$ and $B_k(J_1) = 0$ for odd k.

The coefficient $_k(J_1 M_1)$ is given by

$$\rho_k(J_1 M_1) = (2-\delta_{M_1 0})(-)^{J_1-M_1}(2J_1+1)^{\frac{1}{2}}(J_1 J_1 M_1 - M_1\ K0) \qquad (8\text{-}7)$$

The magnetic substates M_1 which can be populated are restricted by the condition

$$|M_1| = J_1 + s_1 + s_2 \qquad (8\text{-}8)$$

where J_1= spin of the target nucleus, s_1 is the spin of the incoming particle and s_2 is the spin of the outgoing particle. For the sake of convenience, a new population parameter $P(M_1)$ is defined by

$$P(M_1) = w(M_1)(2 - \ _{M_1 0})$$

where $0 \leqslant P(M_1 0) \leqslant 1$. It is assumed that the two lowest substates will be populated, i.e. $P(0)+P(1)=1$ where $P(0)$ is the population of the substates with lowest magnetic quantum

Dhaka University Institutional Repository

number and P(1) is the population of the next higher sub-state. Equation (8-6) then becomes

$$B_k(J_1) = \frac{P}{2-\delta_{M_1 0}} \rho_k(J_1 M_1) + \frac{1-P}{2} \rho_k(J_1 M_1 + 1) \qquad (8\text{-}9)$$

where M_1 is either 0 or 1/2.

Thus using the above expression for $B_k(J_1)$ the angular distribution can be obtained from equation (8-1).

For unpolarized protons bombarding a zero-spin target as in the present case of $^{56}Fe(p,\gamma)^{57}Co$ reaction only one parameter i.e. the mixing ratio δ enters the least squares fit of the experimental data to the theoretical expressions. The angular distribution results were analyzed to determine these spins and mixing ratios which minimize the function

$$\chi^2 = \frac{1}{n-1} \sum_{i=1}^{n} (Y_i - NW_i)/E_i^2 \qquad (8\text{-}10)$$

where n is the number of experimental points, Y_i and W_i are the experimental and theoretical distributions respectively at an angle θ and E_i is the error in experimental distribution.

The minimum condition is given by

$$N = \sum \frac{Y_i W_i}{E_i^2} \Big/ \frac{W_i^2}{E_i^2}. \qquad (8\text{-}11)$$

Dhaka University Institutional Repository

For each possible spin assignment the values of χ^2 are calculated for values of the multipole mixing ratio between -90° and $+90^\circ$. In actual practice the substitution $\emptyset = \arctan \delta$ was employed and values of χ^2 were calculated in steps of 5°. The values of R_k and S_k are taken from ref.124. The angular distribution data were analyzed with the aid of a computer programme. The values of χ^2 were plotted as a function of $\arctan \delta$ for a number of spin assignments. Acceptable solutions of spins are those for which χ^2 lie below a certain confidence limit. This confidence means the probability that the χ^2 would be smaller than a certain chosen χ_0^2. The probability depends on the number of degrees of freedom which is unity in our case. The value of confidence limit is taken from the graphs given by Wapstra et al.[125]. The fits below 0.1% confidence limit are considered as acceptable.

8.2. Experimental procedure

The reaction $^{56}Fe(p,\gamma)^{57}Co$ has been studied for the measurements of γ-ray angular distributions and level schemes at E_p=1248, 1652 and 2065 keV. The experiment was carried out using the proton beam from the 3 MeV Van de Graaff accelerator at the Atomic Energy Centre, Dacca. The beam was collimated by using slits and collimators. The diameter of the collimator just before the target holder was 2 mm. The beam energy

Dhaka University Institutional Repository

resolution was about 1 keV. A beam current of about 2.5 μA was used. A cold trap was used before the target chamber to reduce the background γ-radiation. Natural Iron targets of 20 μgm/cm^2 thickness were prepared by vacuum evaporation on tantalum backing.

Gamma rays were detected by a 30 cc Ge(Li) detector the resolution of which was about 3.2 keV for 1.332 MeV gamma rays from ^{60}Co source. The detector was placed on a rotating table at a distance of 3 cm from the target. Spectra were accumulated at laboratory angles of 0°,30°, 55° and 90° relative to the proton beam for 1248 and 1652 keV resonances and at 0°, 55° and 90° for the 2065 keV resonance. A 3"x3" NaI(TL) detector was placed at 90° which served as a monitor. The signal output of the Ge(Li) detector were amplified by a pre-amplifier and a main amplifier and then analysed in a Canberra 4096 pulse height analyser. The isotropy of the detection system was checked though the reaction ^{27}Al(p,γ)^{28}Si at E_p=992 keV. The resonance positions were checked by measuring the yield curve several times.

In the analyses of the spectra the peak areas were determined by adding counts in each channel under the peaks. The yield of a gamma ray at a particular energy was determined by removing the contributions of the background under the peak from the total number of counts. The relation is given in section 7.1.4. The peak areas were determined for

Dhaka University Institutional Repository

a particular gamma ray energy for all the angles of 0°, 30°, 55° and 90°. These areas were normalized with monitor counts. Anisotropy correction was taken into account.

8.3. Efficiency calibration

The intensities of gamma rays in a spectrum are obtained if the efficiency with which a particular gamma ray is detected is known. In the present measurements it was sufficient to know the relative efficiency of the detector. For this purpose the 55° spectrum from the $^{27}Al(p,\gamma)^{28}Si$ reaction at 992 keV was used. It may be mentioned that this resonance yields intense γ-rays of energy ranging between 1.522 and 10.763 MeV. The intensities of the known γ-rays have been taken from Azuma et al. [126]. Knowing the intensities and peak areas of the γ-rays, the relative efficiency for the full energy, single escape and double escape peaks were determined.

8.4. Energy calibration

The energies of the gamma rays in the measured spectra were determined from the regional energy dispersion (keV/channel) obtained from the 511 keV energy difference of the full energy, single escape and double escape peaks of the high energy gamma rays. The contamination reaction $^{19}F(p,\alpha\gamma)^{16}O$ provided convenient high energy calibration points in the

Dhaka University Institutional Repository

6129 keV γ-ray and its escape peaks. The other accurately known low-energy γ-rays e.g., 1461 keV γ-ray from ^{40}K, 1633 keV γ-ray from ($^{23}Na(p,\alpha\gamma)$) and the γ-rays from ^{60}Co were used for energy calibrations. Some of the levels in ^{57}Co are well established and the energies of the γ-rays emitted from these levels are accurately known. These γ-rays were also used for energy calibration.

8.5. Results and discussion

8.5.1. Level scheme in ^{57}Co

The resonances at E_p = 1248, 1652 and 2065 keV corresponding to the 7253, 7650 and 8056 keV excitation energy have been studied for the construction of decay scheme. These resonances are shown in fig. 8.1. To avoid Doppler-shift the gamma ray singles spectra measured at 90° were used to determine the γ-ray energies and are shown in figs. 8.2 - 8.4. Most of the gamma rays have been identified. The decay schemes of the levels in ^{57}Co excited by proton capture in ^{56}Fe have been proposed for all the three resonances mentioned above and are shown in figs. 8.5 - 8.7. The 55° spectra were used to determine the branching ratios on the assumption that the coefficient of $P_4(\cos\theta)$ was small. The energies, intensities and proposed transitions are given in tables 8.2 - 8.4. The intensities of the gamma rays have been normalized to the 1378 keV γ-ray peak.

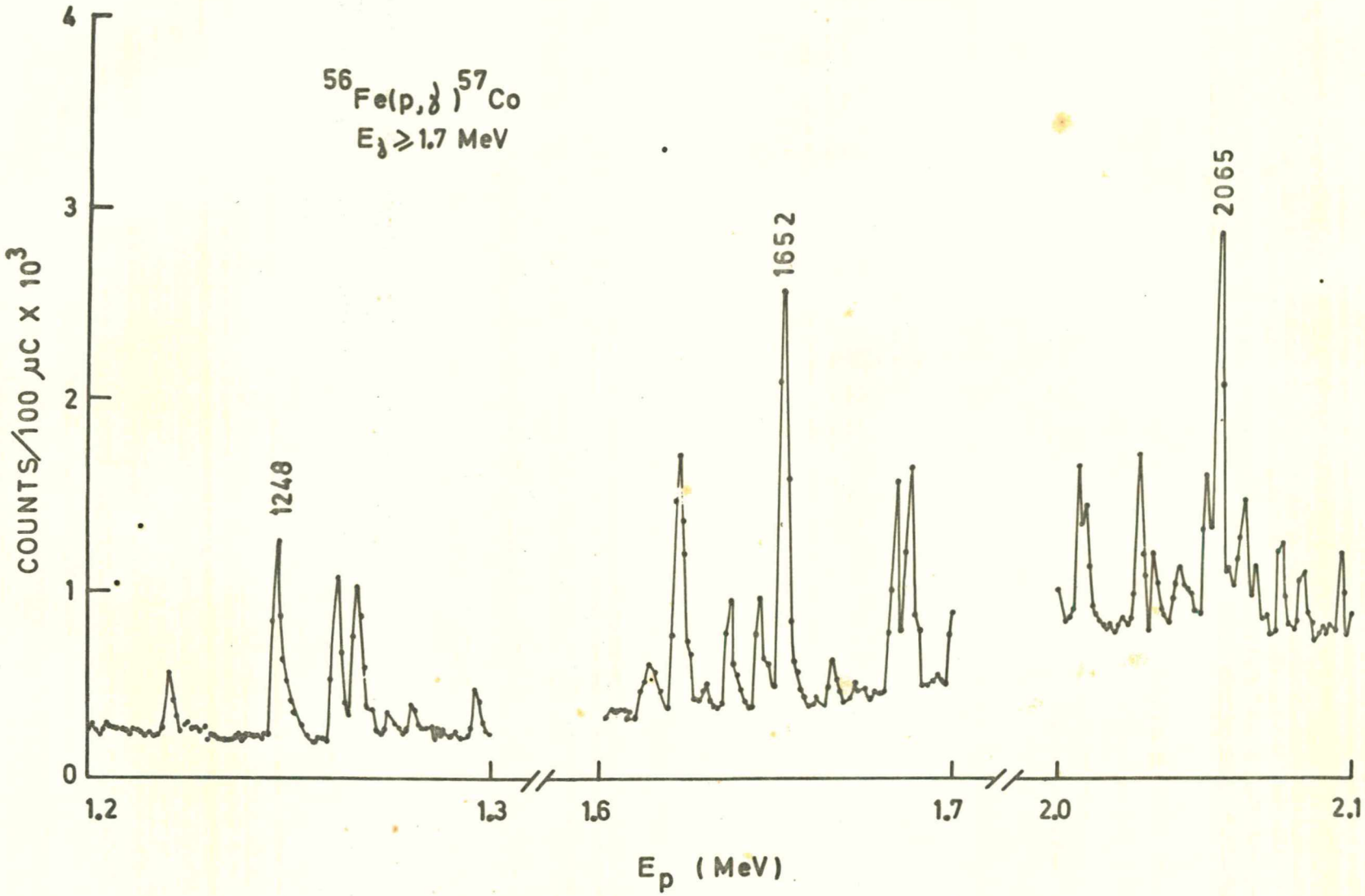

Fig. 8.1 Gamma-ray yield as a function of proton energy from the $^{56}Fe(p,\gamma)^{57}Co$ reaction. The resonances at E_p = 1248, 1652 and 2065 keV are labelled.

Dhaka University Institutional Repository

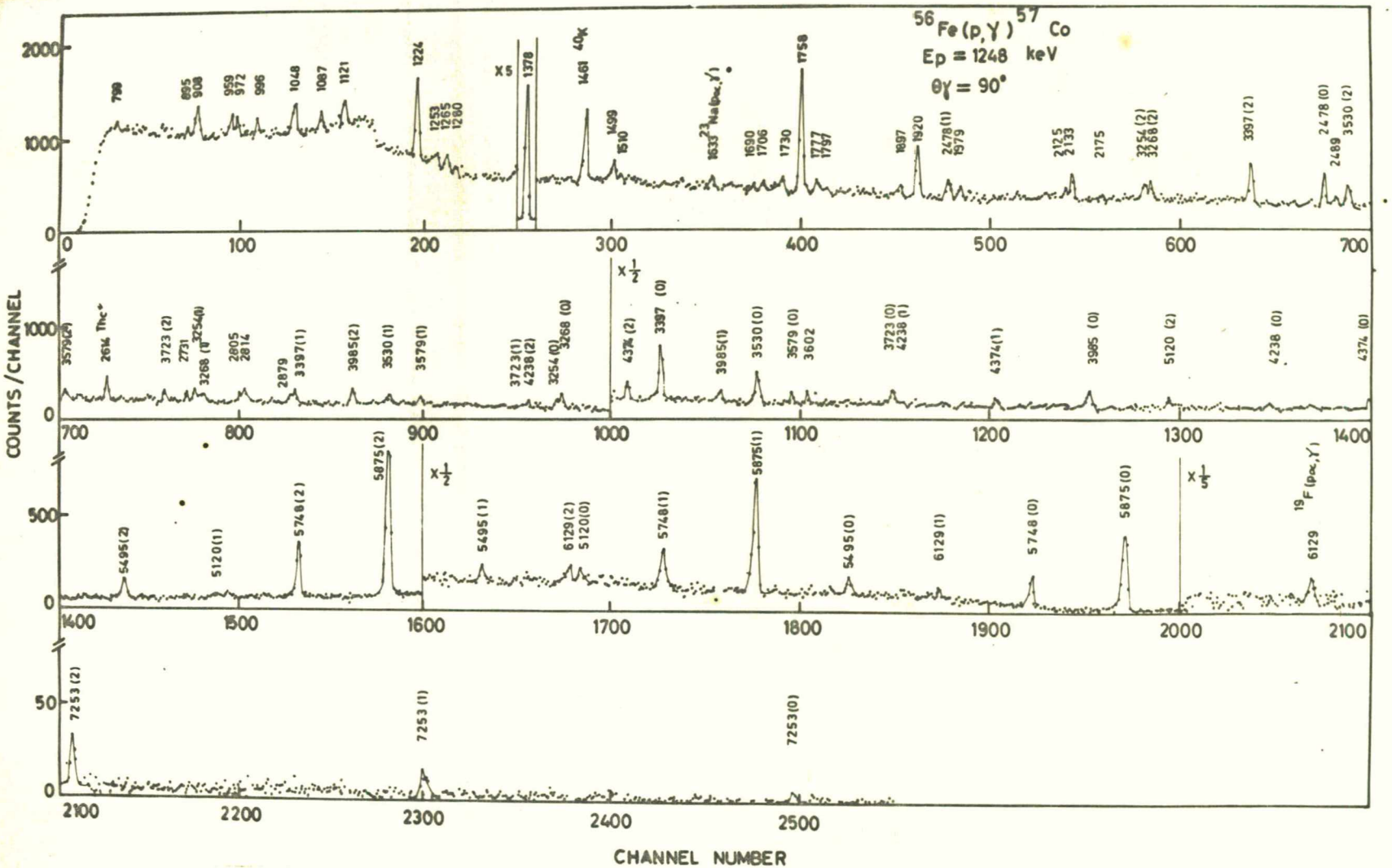

Fig. 8.2 A part of the γ-ray spectrum from the $^{56}Fe(p,\gamma)^{57}Co$ reaction at E_p=1248 keV. Numbers over peaks refer to γ-ray energies in keV. (0),(1) and (2) refer to full energy, single and double escape peaks respectively.

Dhaka University Institutional Repository

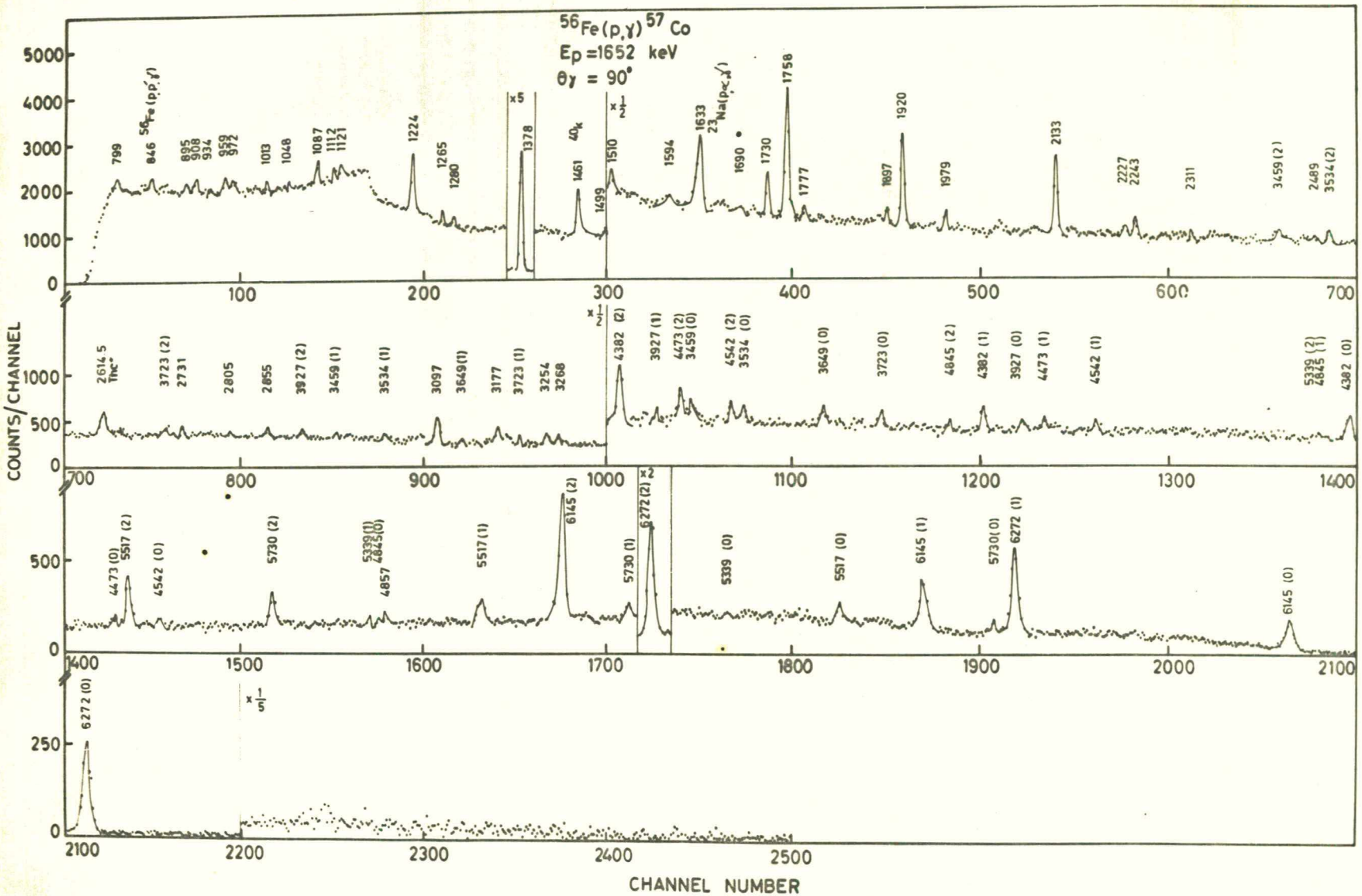

Fig. 8.3 A part of the γ-ray spectrum from the $^{56}Fe(p,\gamma)^{57}Co$ reaction at E_p=1652 keV. Numbers over peaks refer to γ-ray energies in keV. (0), (1) and (2) refer to full energy, single and double escape peaks respectively.

Dhaka University Institutional Repository

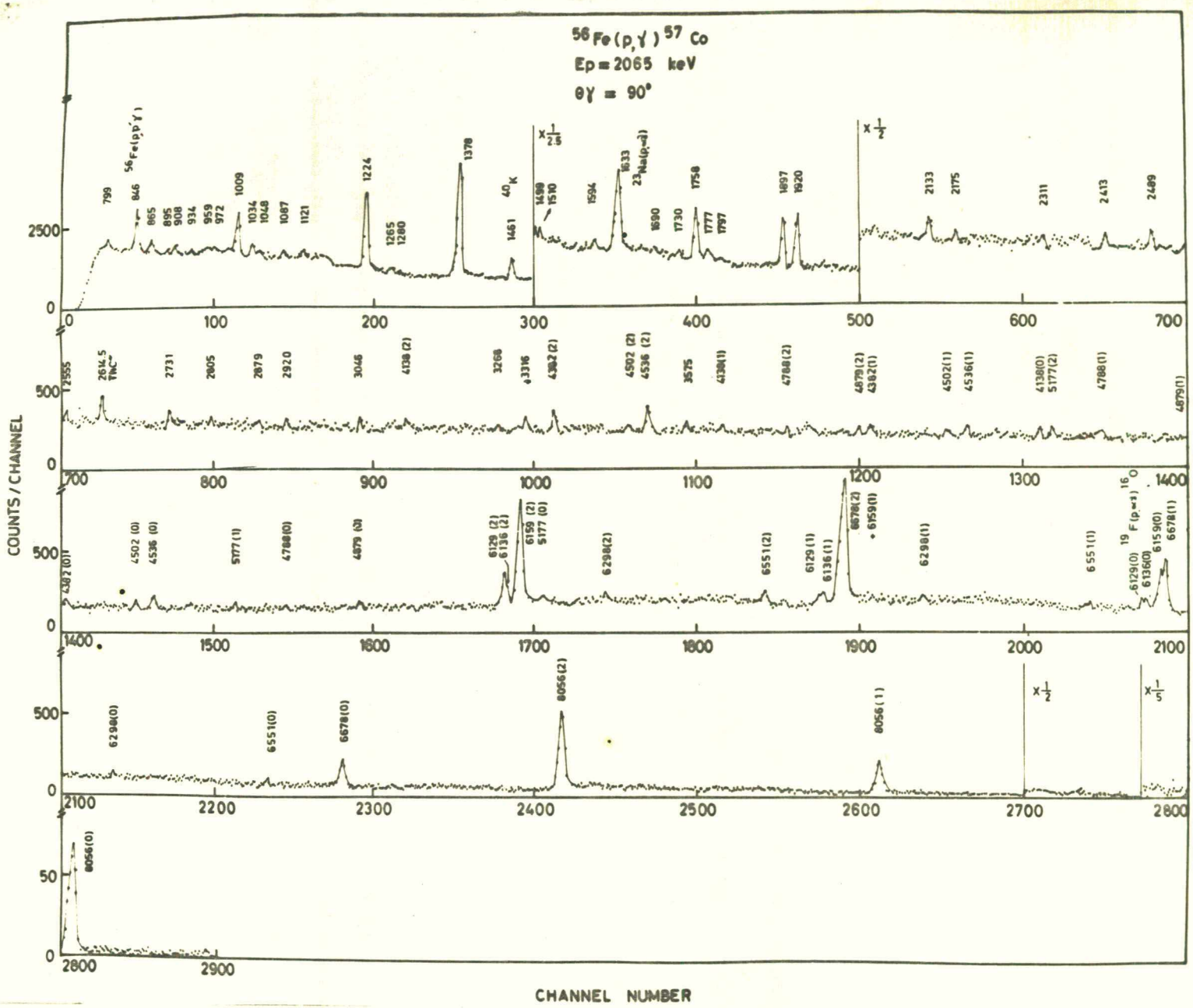

Fig. 8.4 A part of the γ-ray spectrum from the $^{56}Fe(p,\gamma)^{57}Co$ reaction at E_p=2065 keV. Numbers over peaks refer to γ-ray energies in keV. (0), (1) and (2) refer to full energy, single and double escape peaks respectively.

Dhaka University Institutional Repository

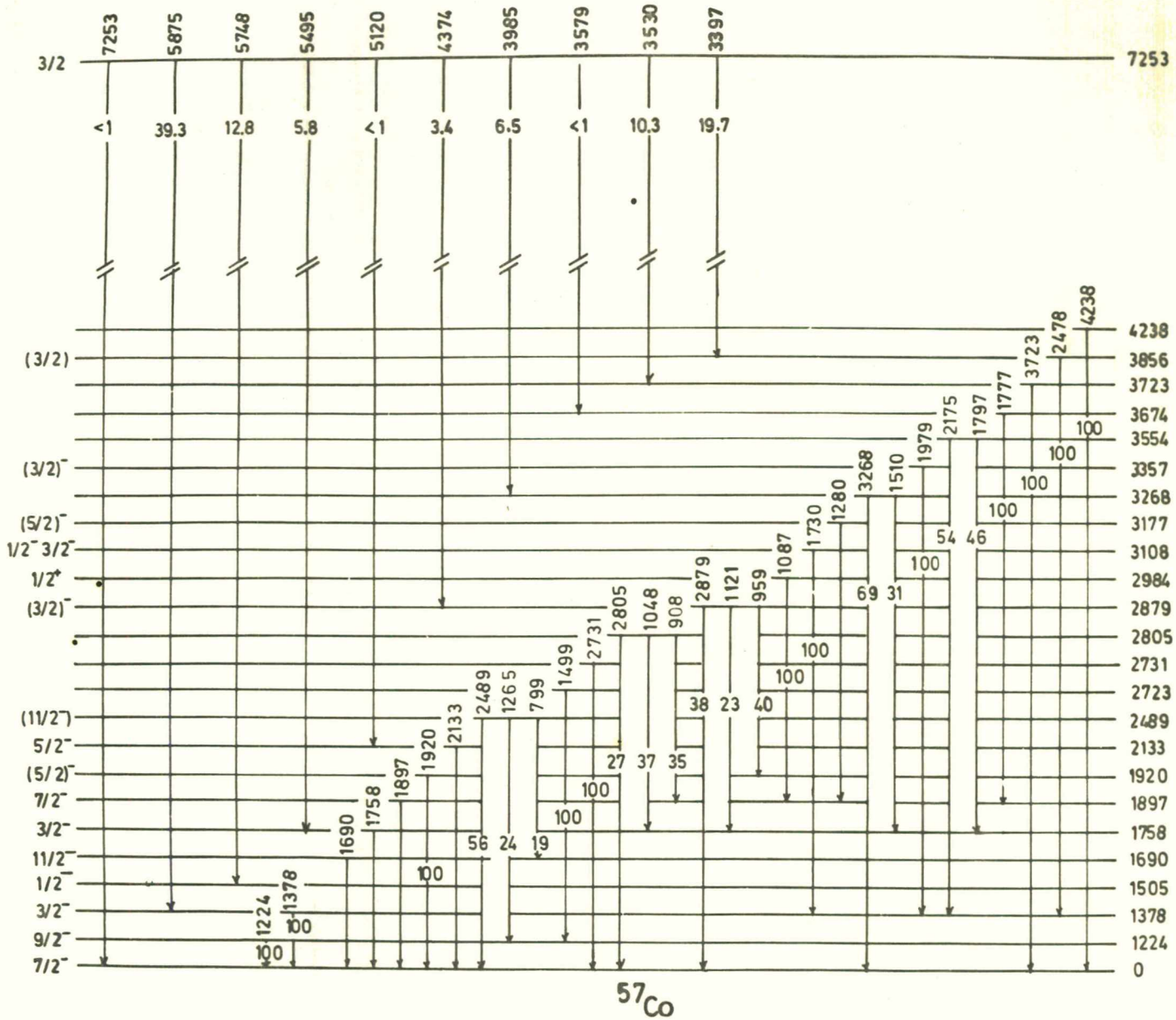

Fig. 8.5 The proposed decay scheme in ^{57}Co from the 1248 keV resonance. The energies in keV and branching ratios in % are given as obtained in this work. Spin and parity taken from ref. 37. Spin of the resonance level is from present work. Level schemes are not drawn to scale.

Dhaka University Institutional Repository

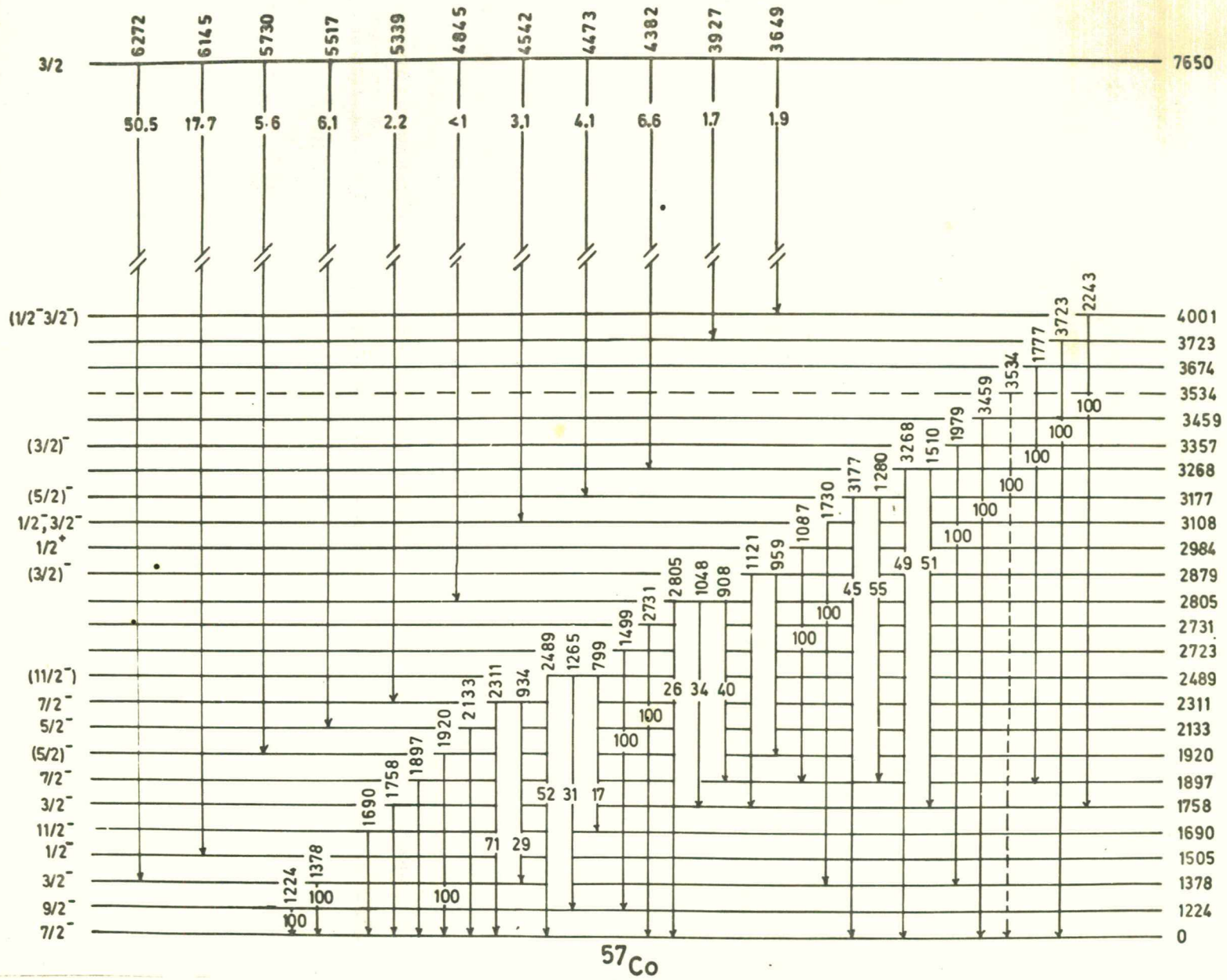

Fig. 8.6 The proposed decay scheme in ^{57}Co from the 1652 keV resonance. The energies in keV and branching ratios in % are given as obtained in this work. Spin and parity taken from ref.37. Spin of the resonance level is from present work. Level schemes are not drawn to scale.

Dhaka University Institutional Repository

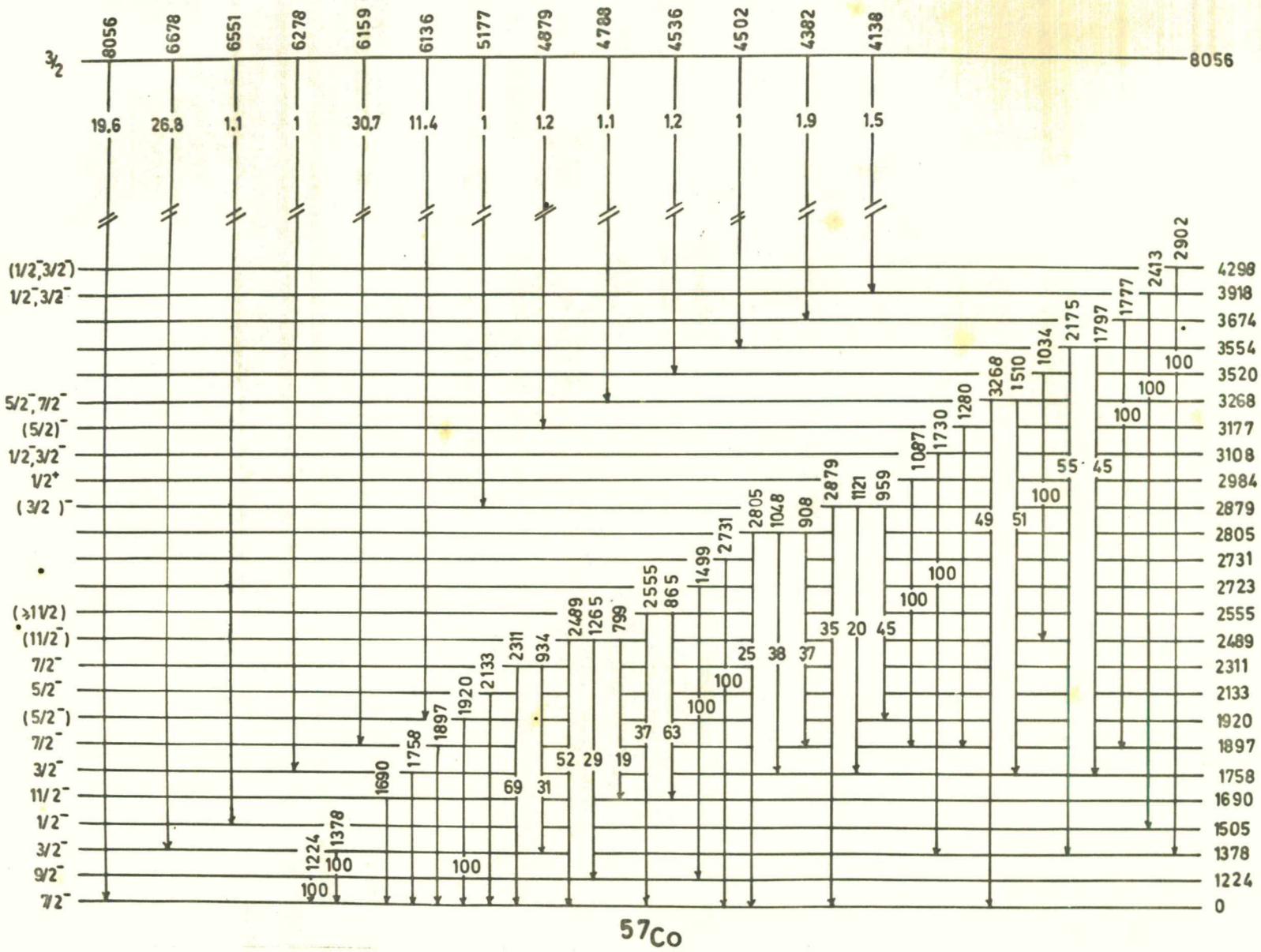

Fig. 8.7 The proposed decay scheme in ^{57}Co from the 2065 keV resonance. The energies in keV and branching ratios in % are given as obtained in this work. Spin and parity taken from ref. 37. Spin of the resonance level is from present work. Level schemes are not drawn to scale.

Dhaka University Institutional Repository

Dhaka University Institutional Repository

Table 8.2

The energies E_γ, relative intensities I_γ and proposed transitions observed at E_p=1248 keV resonance in the $^{56}Fe(p,\gamma)^{57}Co$ reaction.

E_γ (keV)	I_γ	Proposed transition E_i-E_f(keV)	E_γ (keV)	I_γ	Proposed transition E_i-E_f(keV)
7253		7253-0	1920	34	1920-0
6129		$^{19}F(p,\alpha\gamma)$	1897	22	1897-0
5875	373	7253-1378	1797	22	3554-1758
5748	122	7253-1505	1777	52	3674-1897
5495	55	7253-1758	1758	248	1758-0
5120		7253-2133	1730	55	3108-1378
4374	32	7253-2879	1706	36	
4238	16	4238-0	1690	17	1690-0
3985	62	7253-3268	1633		$^{23}Na(p,\alpha\gamma)$
3723	34	3723-0	1510	28	3268-1758
3602			1499	25	2723-1224
3579		7253-3674	1461		$^{40}K(\beta^+)$
3530	98	7253-3723	1378	1000	1378-0
3397	186	7253-3856	1280	12	3177-1897
3268	77	3268-0	1265	15	2489-1224
3254	57		1253	24	
2879	43	2879-0	1224	103	1224-0
2814	66		1121	26	2879-1758
2805	45	2805-0	1087	17	2984-1897
2614		^{228}ThC"	1048	62	2805-1758
2731	30	2731-0	996	10	^{55}Co
2489	35	2489-0	972		
2478	108	3856-1378	959	45	2879-1920
2175	25	3554-1378	908	58	2805-1897
2133	59	2133-0	895	10	
2125	42	^{58}Co	799	12	2489-1690
1979	14	3357-1378			

Dhaka University Institutional Repository

Table 8.3

The energies E_γ, relative intensities I_γ and proposed transitions observed at E_p=1652 keV resonance in the $^{56}Fe(p,\gamma)^{57}Co$ reaction.

E_γ (keV)	I_γ	Proposed transition E_i-E_f(keV)	E_γ (keV)	I_γ	Proposed transition E_i-E_f(keV)
6272	482	7650-1378	1920	129	1920-0
6145	169	7650-1505	1897		1897-0
5730	54	7650-1920	1777	24	3674-1897
5517	58	7650-2133	1758	148	1758-0
5339	21	7650-2311	1730	35	3108-1378
4845		7650-2805	1690		1690-0
4542	30	7650-3108	1633		$^{23}Na(p,\alpha\gamma)$
4473	39	7650-3177	1594	14	^{55}Co
4382	63	7650-3268	1510	23	3268-1758
3927	16	7650-3723	1499	25	2723-1224
3723	14	3723-0	1461		$^{40}K(\beta^+)$
3649	18	7650-4001	1378	1000	1378-0
3534	34	3534-0	1280	12	3177-1897
3459	15	3459-0	1265	11	2489-1224
3268	22	3268-0	1224	84	1224-0
3254	31		1121	24	2879-1758
3177	10	3177-0	1112	19	
3097	15		1087	19	2311-1224
2855	13	^{58}Co	1048	19	2805-1758
2805	11	2805-0	1013	14	
2731		2731-0	972	13	
2614		$^{228}ThC''$	959	12	2879-1920
2489	19	2489-0	934		2311-1378
2311	14	2311-0	908	16	2805-1897
2243	19	4001-1758	895	14	
2227	10		846		$^{56}Fe(p,p'\gamma)$
2133	120	2133-0	799		2489-1690
1979	11	3357-1378			

Dhaka University Institutional Repository

Table 8.4

The energies E_γ, relative intensities I_γ and proposed transitions observed at E_p=2065 keV resonance in the $^{56}Fe(p,\gamma)^{57}Co$ reaction.

E_γ (keV)	I_γ	Proposed transition E_i-E_f(keV)	E_γ (keV)	I_γ	Proposed transition E_i-E_f(keV)
8056	404	8056-0	1920	201	1920-0
6678	552	8056-1378	1897	157	1897-0
6551	23	8056-1505	1797	23	3554-1758
6298	19	8056-1758	1777	63	3674-1897
6159	632	8056-1897	1758	224	1758-0
6136	234	8056-1920	1730		3108-1378
6129		$^{19}F(p,\alpha\gamma)^{16}O$	1690		1690-0
5177	21	8056-2879	1633		$^{23}Na(p,\alpha\gamma)$
4879	25	8056-3177	1594	22	^{55}Co
4788	23	8056-3268	1510	17	3268-1758
4536	25	8056-3520	1499	18	2723-1224
4502	21	8056-3554	1461		$^{40}K(\beta^+)$
4382	39	8056-3674	1378	1000	1378-0
4138	30	8056-3918	1280		3177-1897
3575	19		1265	18	2489-1224
3316	80		1224	442	1224-0
3268	17	3268-0	1121	21	2879-1758
3046		^{58}Co	1087		2311-1224
2920	18	4298-1378	1048	22	2805-1758
2879	39	2879-0	1034	51	3520-2489
2805	15	2805-0	1009	308	^{58}Co
2731	34	2731-0	972	17	
2614		$^{228}ThC''$	959	50	2879-1920
2555	30	2555-0	934		2311-1378
2489	32	2489-0	908	22	2805-1897
2413	23	3918-1505	895		
2311	29	2311-0	865	51	2555-1690
2175	29	3554-1378	846		$^{56}Fe(p,p'\gamma)$
2133	10	2133-0	799		2489-1690

Dhaka University Institutional Repository

The gamma decay of the levels in ^{57}Co up to 2133 keV observed in the present work is almost the same as in previous works [109,112,113,115-117], above which there appears some discrepancies. A level by level discussion of the results up to 4298 keV is given below.

The levels up to 2133 keV

The level energies and J^{π} values in ^{57}Co are well established [37,105,106,109-113] for levels up to 2133 keV. The present results agree fairly well with the previous workers. The first excited state at 1224 keV is fed only from the low-lying levels. The spin and parity of the 1224 keV state is $J^{\pi} = 9/2^{-}$ [37]. Transitions from the resonant states to this level have not been observed. This confirms the low spin value of the resonant states as discussed in section 8.5.2. The 1378 and 1505 keV states are populated by primary transitions from all the three resonances studied. The 1378 keV state decays to the ground state without branching. The ground state ($J^{\pi} = 7/2^{-}$) decay of the 1505 keV state ($J^{\pi} = 1/2^{-}$) is not observed as it should be. A gamma ray of 1690 keV observed in all the spectra in the present work is proposed as a ground state decay from the 1690 keV level in agreement with the (p,nγ) work of Pietrzyk et al. [113]. The level ($J^{\pi} = 11/2^{-}$) is not populated by the proton capture states but is populated by secondary transitions. This again confirms the low spin value of the resonance levels (section

Dhaka University Institutional Repository

8.5.2.). The 1690 keV level has not been reported in previous (p,γ)[115-117] or (^{3}He,d)[108-110] measurements. The 1758 keV level is found to be populated by proton resonances at E_p = 1248 and 2065 keV. The level is not fed by the 1652 keV resonance in agreement with Leslie et al. [115]. The level decays to the ground state in agreement with the (p,γ) measurements [115-117]. The 1920 keV state is fed by proton resonances at E_p = 1652 and 2065 keV and the 1897 keV state is fed by the 2065 keV resonance. They are also fed by intermediate states. Both the states decay to the ground state. O'Brien and Coote [116] reported a weak transition from the 1248 keV resonance state to the 1920 keV state which is in disagreement with Leslie et al. [115] and El-Kateb and Griffiths [117]. The present work is in agreement with refs. 115 and 117. The 2133 keV level is populated by primary transitions from the 1248 and 1652 keV resonances and decays to the ground state. Some of the low energy γ-ray transitions were observed in the (p,nγ) work of Pietrzyk et al. [113]. This however could not be checked because of the energy threshold problem in the analyzer.

The 2311 keV level

The level is fed by 5339 keV γ-ray from the 1652 keV resonance. The level is probably fed by intermediate state in the 2065 keV resonance. The level decays to the

Dhaka University Institutional Repository

ground state via 2311 keV γ-ray and to the 1378 keV state via 934 keV γ-ray with branches of 70% and 30% respectively. In addition to the above two transitions Pietrzyk et al.[113] observed a third transition to the 1224 keV level via 1087 keV γ-ray. Hardie et al.[109] reported only the last decay. Leslie et al.[115] reported the 1087 keV γ-ray as a decay from the 2984 keV level to the 1897 keV level. However, a γ-ray of 1087 keV has been observed in all the spectra in the present work. We propose the 1087 keV γ-ray as a decay from the 2984 keV to the 1897 keV level in agreement with ref. 115 and not from the 2311 keV to the 1224 keV level. The arguements for this are as follows. The two transitions from the 2311 keV level mentioned above are not observed in the spectrum of E_p = 1248 keV resonance which indicate that the level is not excited at the 1248 keV resonance. In that case the 1087 keV γ-ray cannot be a decay from the 2311 keV level and it is therefore tentatively proposed as a decay from the 2984 keV level to the 1897 keV level.

The 2489 keV level

There are no γ-rays found feeding this level from the capturing states. The level is fed by 1034 keV γ-ray from the 3520 keV level as observed from E_p = 2065 keV spectrum. Transitions to this level from the capturing states were too weak to observe. The state decays to the ground, first and

Dhaka University Institutional Repository

the 1690 keV states through 2489, 1265 and 799 keV γ-rays in complete agreement with the (p,nγ) work of Pietrzyk et al.[113]. The 2489 keV level has not been reported by previous (p,γ) measurements [115-117].

The 2555 keV level

This level is identified in the 2065 keV resonance only and no gamma ray is found to feed this state. The level decays to the ground and 1690 keV state in agreement with the (p,nγ) work of Pietrzyk et al.[113]. Again no (p,γ) work reported this level.

The 2723 and 2731 keV levels

No transitions have been found to feed these levels from the capturing states or from any intermediate states probably because the transitions were very weak. The 2723 and 2731 keV levels decay to the first excited state and ground state respectively. These transitions are in agreement with the (p,nγ) work of Pietrzyk et al.[113]. The 2723 keV level has not been reported by the (p,γ) measurements[115-117]. Leslie et al.[115] in their (p,γ) work reported the 2731 keV level. The ground state transition from the 2731 keV level obtained in the present work is in agreement with the (p,γ) work reported by Leslie et al.[115]. Banu et al.[110] in a (^{3}He,d) work have assigned $J^\pi = (7/2^-)$ for the 2723 keV level and $J^\pi = 3/2^-, 5/2^-$ for the 2731 keV level.

Dhaka University Institutional Repository

The 2805 keV level

The level is weakly populated by primary γ-rays in the 1652 keV resonance and probably by very weak transitions from capturing and intermediate states in other resonances. In the present work the level decays through the 2805, 1048 and 908 keV γ-rays respectively to the ground, 1758 and 1897 keV states as suggested by the (p,nγ) work of Pietrzyk et al. [113]. Both Leslie et al. [115] and El-Kateb and Griffiths [117] reported only the ground state transition. Spin and parity of the level are suggested as $J^{\pi} = 3/2^{-}, 5/2$ [115]

The 2879 keV level

The level is found to be populated by the capturing states at E_p = 1248 and 2065 keV resonances. The level decays to the ground, 1758 and 1920 keV states as suggested by Hardie et al. [109] and Pietrzyk et al. [113]. Leslie et al. [115] observed only the ground state decay. The ground state branch is not observed in the 1652 keV resonance in the present work.

The 2984 keV level

The level is probably populated by very weak transition from capture state or some intermediate state. In the discussion of 2311 keV level it was mentioned that 1087 keV γ-ray is not a transition from this level. In agreement with Leslie et al. [115] the 1087 keV γ-ray is proposed as a 100%

Dhaka University Institutional Repository

transition from the 2984 to the 1897 keV level in the present work. The results do not agree with other works [109,112,113]. Spin and parity of the level is $J^{\pi} = 1/2^{+}$ [109].

The 3108 keV level

The level is fed by primary γ-rays in 1652 keV resonance and probably by intermediate states in other resonances. The level decays 100% to the 1378 keV level and agrees with the (p,nγ) work of Pietrzyk et al. [113] and (p,γ) work of Leslie et al. [115].

The 3177 keV level

The level is fed by the 1652 and 2065 keV resonances. The level decays to the 1897 keV state in all the resonances, but a ground state transition is observed only at E_p=1652 keV resonance.

The 3268 keV level

This level has been found to be populated by primary γ-rays in all the three resonances studied and decays to the ground and 1758 keV states. The results agree with those of Pietrzyk et al. [113]. Leslie et al. [115] and El-Kateb and Griffiths [117] observed only the ground state decay from (p,γ) experiments.

Dhaka University Institutional Repository

The 3357 keV level

No γ-rays from the capture states to this level are observed. The level was identified in the 1248 and 1652 keV spectra. The level decays to the 1378 keV level by a 1979 keV transition in agreement with other experiments [109,113,115]. However the energy assignment for the level by Hardie et al.[109] was 3369 keV. The level is probably populated from some intermediate state.

The 3459 keV level

No transition to this level from the proton capture state was found. A γ-ray of 3459 keV with intensity 15 identified in the spectrum of 1652 keV resonance is proposed as a ground state decay from the 3459 keV level. This does not agree with Pietrzyk et al.[113] and Hardie et al.[109] who instead have reported transitions to the 1378 and 1920 keV states. Hardie et al.[109] observed a level at 3467 keV which is probably the same level. Rosner and Holbrow [108] and Banu et al.[110] also observed the level. The spin of this level is not known.

The 3520 keV level

The level is fed from the 8056 keV resonance state (E_p = 2065 keV). The level has not been reported by previous (^{3}He,d)[108-110] or (p,γ)[115-117] works. Pietrzyk et al.[113] have tentatively shown a transition from this level to the

Dhaka University Institutional Repository

2489 keV level via 1034 keV γ-ray. In the present work the 1034 keV γ-ray was identified in the spectrum of 2065 keV resonance, thus confirming this as a transition to the 2489 keV level.

The 3534 keV level

A γ-ray of energy 3534 keV is identified in the spectrum of 1652 keV resonance. This γ-ray is proposed as a ground state decay from the 3534 keV level. No γ-ray was found to populate the level. The level is, therefore, assigned tentatively.

The 3554 keV level

The level is not fed by primary gamma-rays from the 1248 and 1652 keV resonances, but is fed weakly in the 2065 keV resonance. The level is also identified in the 1248 keV resonance. Transitions from this level occur via 2175 keV γ-ray (55%) and 1797 keV γ-ray (45%) to the 1378 keV and 1758 keV states respectively. The transitions agree with the (p,nγ) measurement of ref. 113. The level has not been reported by (^{3}He,d) or (p,γ) works. The J^π value for this state is not known.

The 3674 keV level

The level is fed by 3579 and 4382 keV γ-rays from the 1248 and 2065 keV resonances respectively. A 1777 keV γ-ray

Dhaka University Institutional Repository

is identified and is proposed as a decay from the 3674 keV to the 1897 keV state. Pietrzyk et al.[113] do not observe a transition to the 1897 keV state but report a transition to the ground state. Hardie et al.[109] and Banu et al.[110] observed the level, but it has not been reported by (p,γ) experiments [115-117]. The spin parity values are not known.

The 3723 keV level

The level is populated by 3530 and 3927 keV γ-rays from the proton capture states at E_p = 1248 and 1652 keV resonances respectively and decays directly to the ground state. The result is in agreement with the (p,γ) works of Leslie et al.[115] and El-Kateb and Griffiths [117]. Pietrzyk et al.[113] have not reported this level. The J^{π} value for this level is not known.

The 3856 keV level

This level is fed by 3397 keV γ-ray from the resonance at E_p = 1248 keV and decays to the 1378 keV level without branching. This agrees with Leslie et al.[115] and El-Kateb and Griffiths [117]. O'Brien and Coote [116] observed 50% transition to the 1378 and the 50% branch to the 1505 keV state. Pietrzyk et al.[113] observed still another branch to the ground state. In the present investigation no evidence for the ground state decay or a decay to the 1505 keV level is observed. Recently Banu et al.[110] have assigned $J^{\pi} = 3/2^{+}$ to this level.

Dhaka University Institutional Repository

The 3918 keV level

The level is fed by 4138 keV γ-ray from the proton capture state at E_p = 2065 keV and decays to the 1505 keV level via 2413 keV γ-ray. The 3918 keV level has been reported by Hardie et al. [109]. The (p,nγ) or (p,γ) measurements [113,115-117] do not observe this level. The decay of the level is observed in the present work only.

The 4001 keV level

The level is fed by 3649 keV γ-ray from the resonance state at E_p = 1652 keV. The level energy is consistent with that obtained by Hardie et al. [109] and Banu et al. [110]. The 3993 keV level indicated by (p,nγ) and (p,γ) measurements is probably the same level. There exists a confusion about the decay of this level. Hardie et al. [109] have tentatively shown a decay to the 1505 keV state. O'Brien and Coote [116] and El-Kateb and Griffiths [117] reported only the ground state decay. Pietrzyk et al. [113] have shown a tentative decay to the 1897 keV level in addition to the ground state decay. Leslie et al. [115] observed 90% decay to the ground state and 10% decay to the 1758 keV state. From the present measurements only a decay to the 1758 keV state via 2243 keV γ-ray is proposed. The spin-parity values are J^{π}=(1/2$^-$, 3/2$^-$)[117].

Dhaka University Institutional Repository

The 4238 keV level

The 4238 keV level is probably populated by some intermediate state or by a very weak primary transition which could not be observed. The level decays to the ground state which agrees with the (p,nγ) work of ref. 113. Rosner and Holbrow [108] and Hardie *et al.* [109] in the (^{3}He,d) reaction indicated a level at 4251 keV which may be the same level. The (p,γ) experiments [115-117] do not observe this level. The J^{π}- value of the level is not known.

The 4298 keV level

A 2920 keV γ-ray identified in the spectrum of 2065 keV resonance fits well as a decay from the 4298 keV level to the 1505 keV level. The level is also reported by Hardie *et al.* [109] and Banu *et al.* [110]. The decay of the level is observed new. Banu *et al.* [110] assigned J^{π}=(1/2$^-$,3/2$^-$).

The 7253 keV resonating state

The 7253 keV resonance state at E_p = 1248 keV decays to the ground (<1%), 1378 (39.3%), 1505 (12.8%), 1758 (5.8%), 2133 (< 1%), 2879 (3.4%), 3268 (6.5%), 3674 (< 1%), 3723 (10.3%) and 3856 (19.7%) keV states via 7253, 5875, 5748, 5495, 5120, 4374,3985, 3579, 3530 and 3397 keV γ-rays respectively. There exists anomally in the decay of the 7253 keV level among different (p,γ) measurements. O'Brien and Coote [116] do not

Dhaka University Institutional Repository

observe transitions to the 2879, 3268, 3674, 3723 and 3856 keV levels. The transition to the 2133, 3268 and 3674 keV levels have not been reported by Leslie et al. [115]. El-Kateb and Griffiths [117] do not observe transitions to the 2133 and 3674 keV levels. In the present investigation all the transitions mentioned above have been observed. In addition, a new transition to the 3674 keV (<1%) level is found. The J^{π}-value of the 7253 keV resonance state is obtained as J = 3/2 from the present measurements, as discussed in section 8.5.2.

The 7650 keV resonating state

The 7650 keV resonating state corresponding to the 1652 keV resonance has been previously studied only by Leslie et al. [115]. They observed transitions from the 7650 keV resonance to the 1378, 1505, 1920, 2133 and 3268 keV states. In addition to the above transitions, some weak transitions to the 2311 (2.2%), 2805 (<1%), 3108 (3.1%), 3177 (4.1%), 3723 (1.7%) and 4001 (1.9%) keV levels are observed in the present experiment. The spin value J = 3/2 obtained from the present work confirms the result of Leslie et al. [115] (section 8.5.2.).

The 8056 keV resonating state

The 8056 keV resonance state and the transitions from this state have not been reported earlier. The state decays

Dhaka University Institutional Repository

to the ground (19.6%), 1378 (26.8%), 1505 (1.1%), 1758 (1%), 1897 (30.7%), 1920 (11.4%), 2879 (1%), 3177 (1.2%), 3268 (1.1%), 3520 (1.2%), 3554 (1%), 3674 (1.9%) and 3918 (1.5%) keV levels. The spin assignment of J = 3/2 has been made from the present work (section 8.5.2.).

8.5.2. Gamma-ray angular distribution and spin assignments

Gamma-ray angular distributions have been measured for the assignment of spins to the resonances at E_p = 1248, 1652 and 2065 keV. Gamma-ray singles spectra measured at 0°, 30°, 55° and 90° have been analysed for spin determination. The theoretical fits to experimental angular distributions and plots of χ^2 versus arctan δ have been obtained using the relations (8.1), (8.10) and (8.11) for possible spin values and for various transitions. They are shown in figs. 8.8 - 8.10. The Legendre polynomial coefficients are summarized in table 8.5. Gamma-ray angular distributions, $\chi^2_{min.}$ and multipole mixing ratios for the resonances are summarized in table 8.6.

The E_p = 1248 keV resonance

The angular distribution data have been analysed for the determination of spin of the resonance at E_p = 1248 keV for the transitions from the 7253 keV resonating state to the ground (< 1%), 1378 (39.3%) and 1505 (12.8%) keV states. The

Dhaka University Institutional Repository

theoretical fits to experimental angular distribution and the plots of χ^2 as a function of arctan δ for the ground state transition (fig. 8A) show that all the assumed initial spins 1/2, 3/2, 5/2 and 7/2 are possible as they all lie below the 0.1% confidence limit. From the analyses of the transition to the 1378 keV state ($J^{\pi} = 3/2^-$) (fig. 8B) only the 7/2 spin can be ruled out. However the analysis of the transitions (fig. 8C) to the 1505 keV state ($J^{\pi} = 7/2^-$) indicates that 3/2 is the only acceptable spin value of 7253 keV state.

The E_p = 1652 keV resonance

Angular distributions of the 5730, 5517, 6272 and 6145 keV γ-rays emitted respectively in the decay of the 7650 keV resonating state (E_p = 1652 keV) to the 1920(5.6%), 2133 (6.1%), 1378 (50.5%) and 1505 (17.7%) keV states have been analysed. The theoretical fits to experimental distributions and χ^2 plots are shown in figs. 9A and 9B for the transitions to the 1920 ($J^{\pi} = 5/2^-$) and 2133 ($J^{\pi} = 5/2^-$) keV states respectively. From these figures it is found that all the 1/2, 3/2, 5/2 and 7/2 assumed spin values are acceptable. In the analysis of the transition to the 1378 ($J^{\pi} = 3/2^-$) (fig. 9C) keV it is found that (7/2 — 3/2) distribution lies above the confidence limit and thus 7/2 spin value is ruled out. From the analysis of the transition

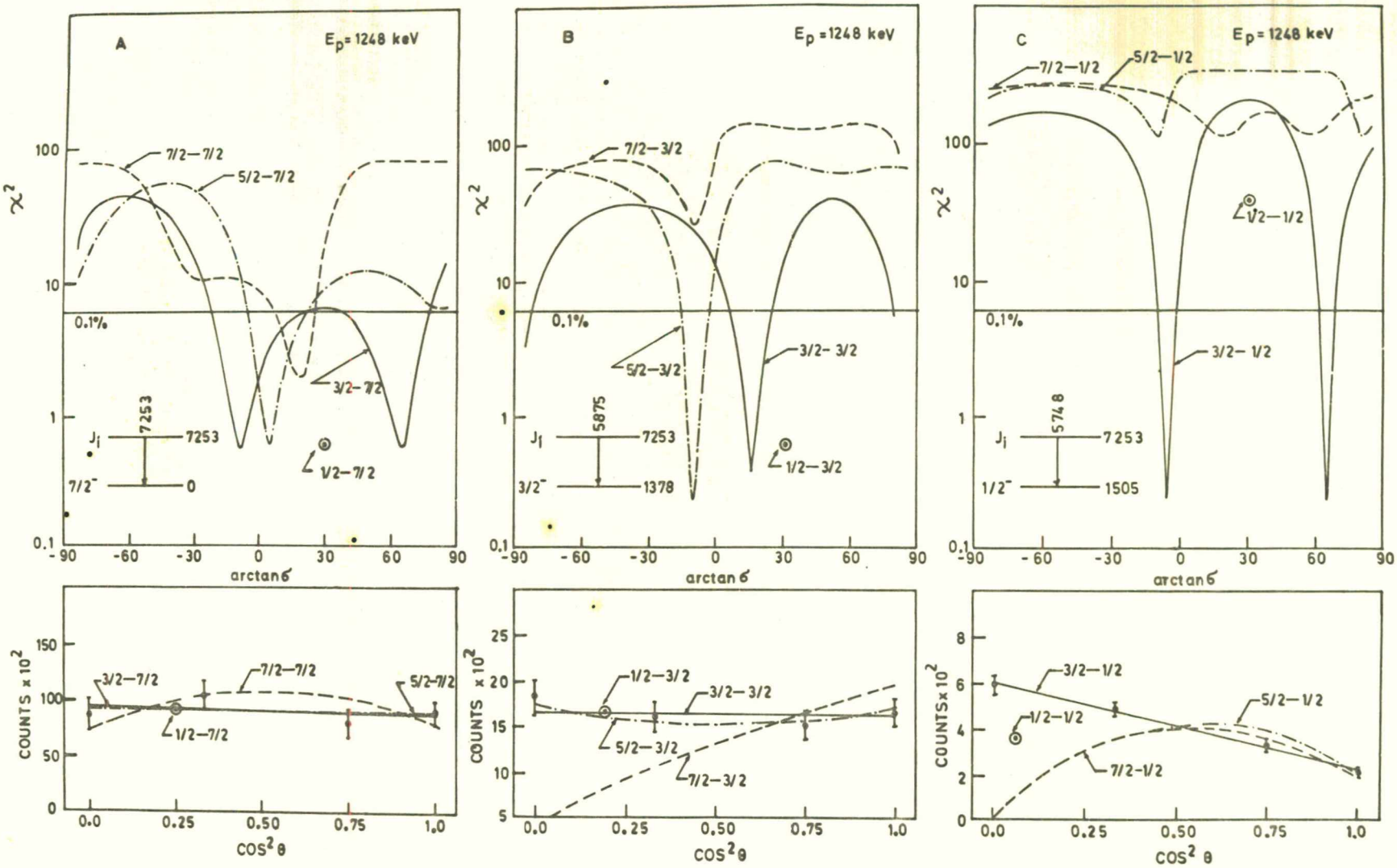

Fig. 8.8 Theoretical fits to experimental angular distributions and χ^2 plots of the (A) 7253 keV, (B) 5875 keV and (C) 5748 keV γ-rays from the E_p=1248 keV resonance.

Dhaka University Institutional Repository

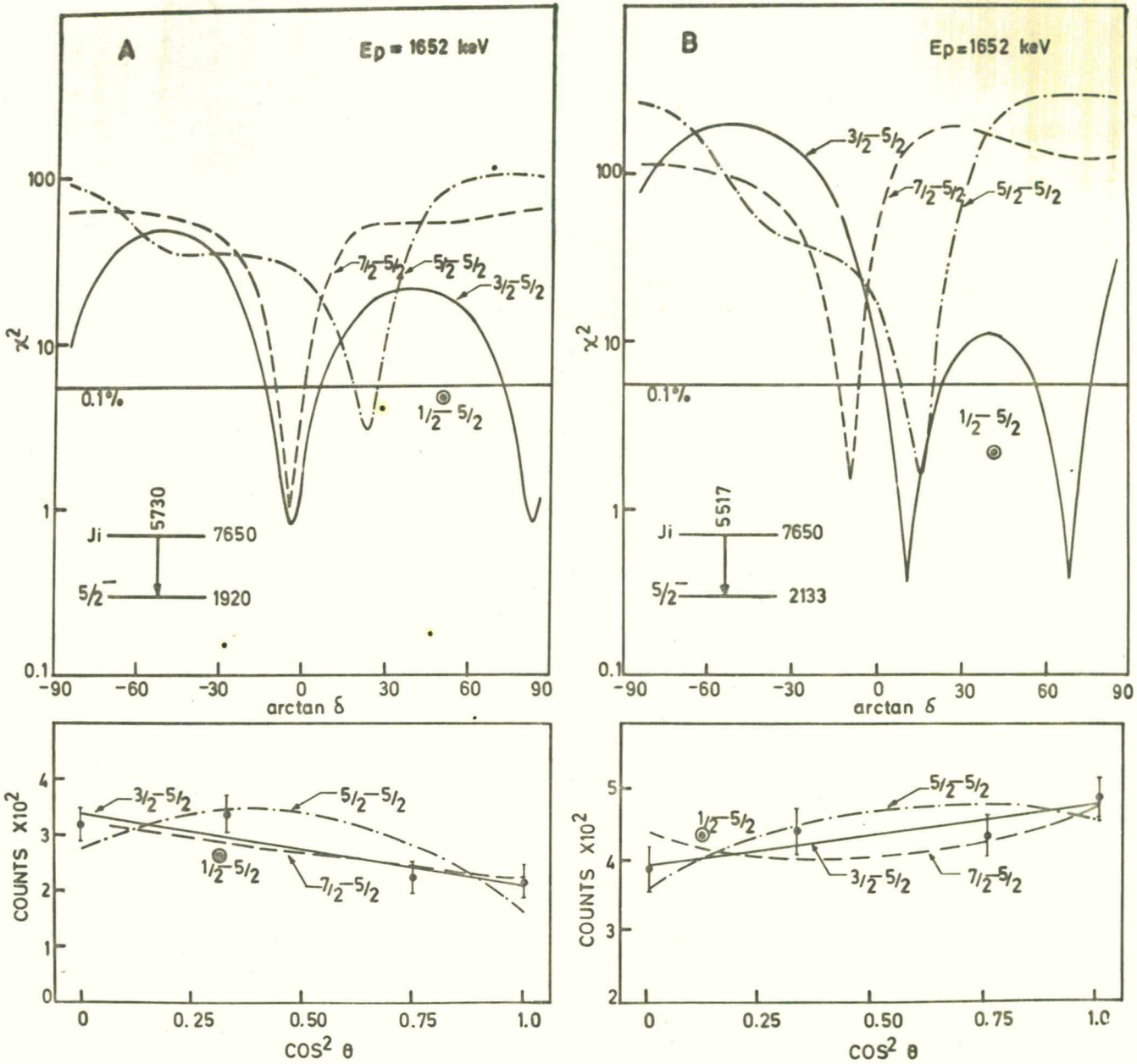

Fig. 8.9 Theoretical fits to experimental angular distributions and χ^2 plots of the (A) 5730 keV and (B) 5517 keV γ-rays from the E_p = 1652 keV resonance.

Dhaka University Institutional Repository

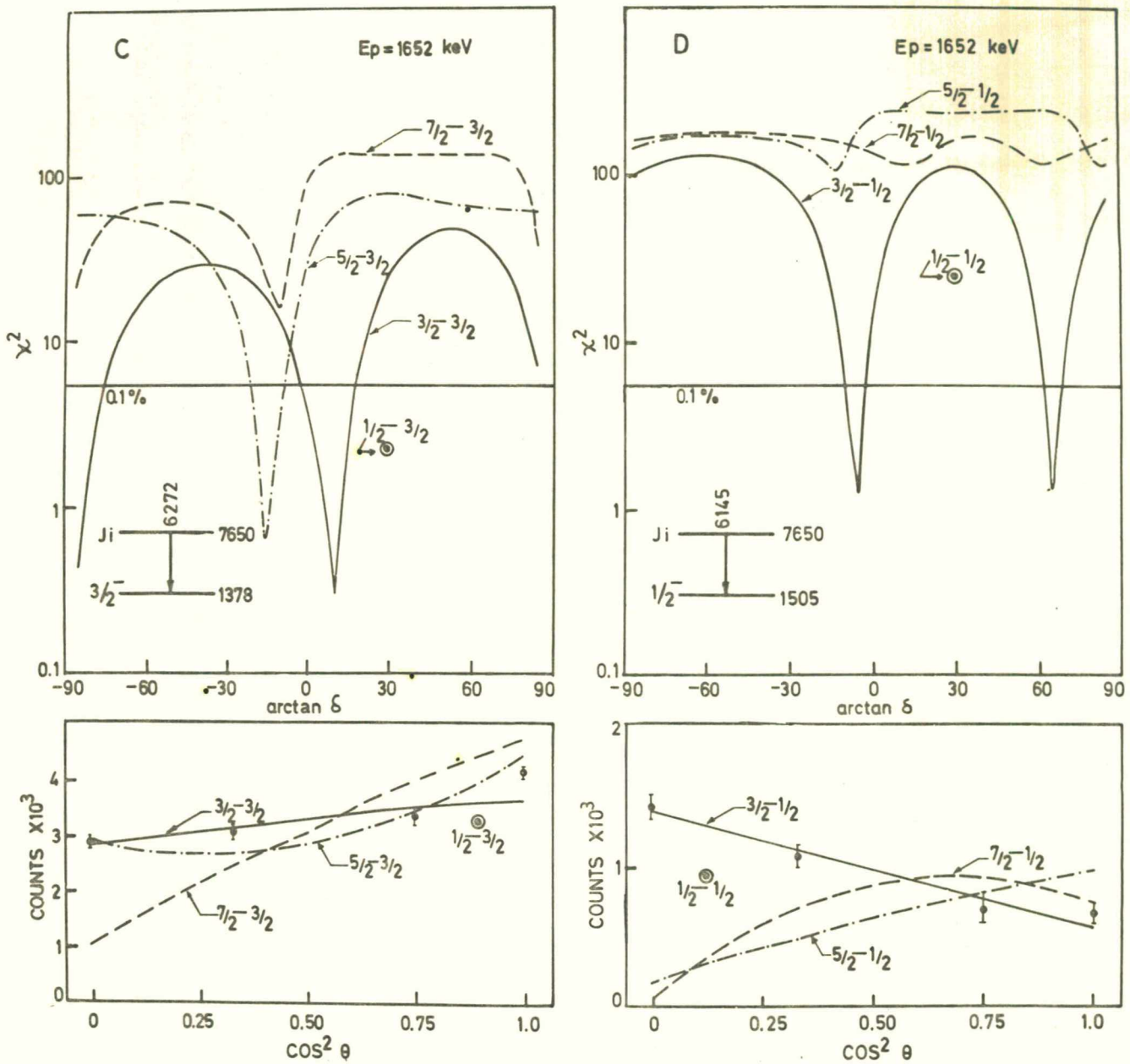

Fig. 8.9 Theoretical fits to experimental angular distributions and χ^2 plots of the (C) 6272 keV and (D) 6145 keV γ-rays from the E_p = 1652 keV resonance.

Dhaka University Institutional Repository

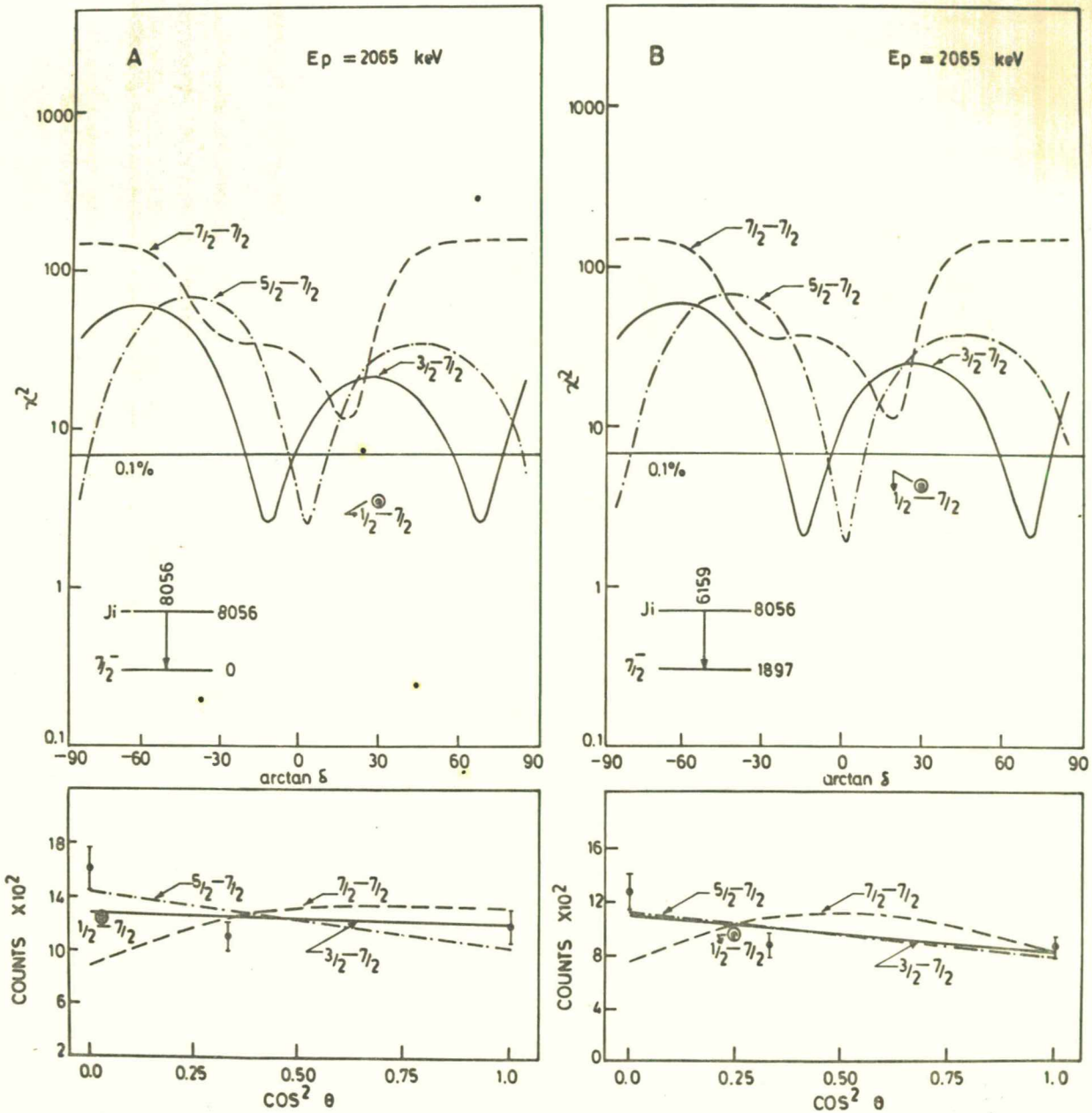

Fig. 8.10 Theoretical fits to experimental angular distributions and χ^2 plots of the (A) 8056 keV and (B) 6159 keV γ-rays from the E_p = 2065 keV resonance.

Dhaka University Institutional Repository

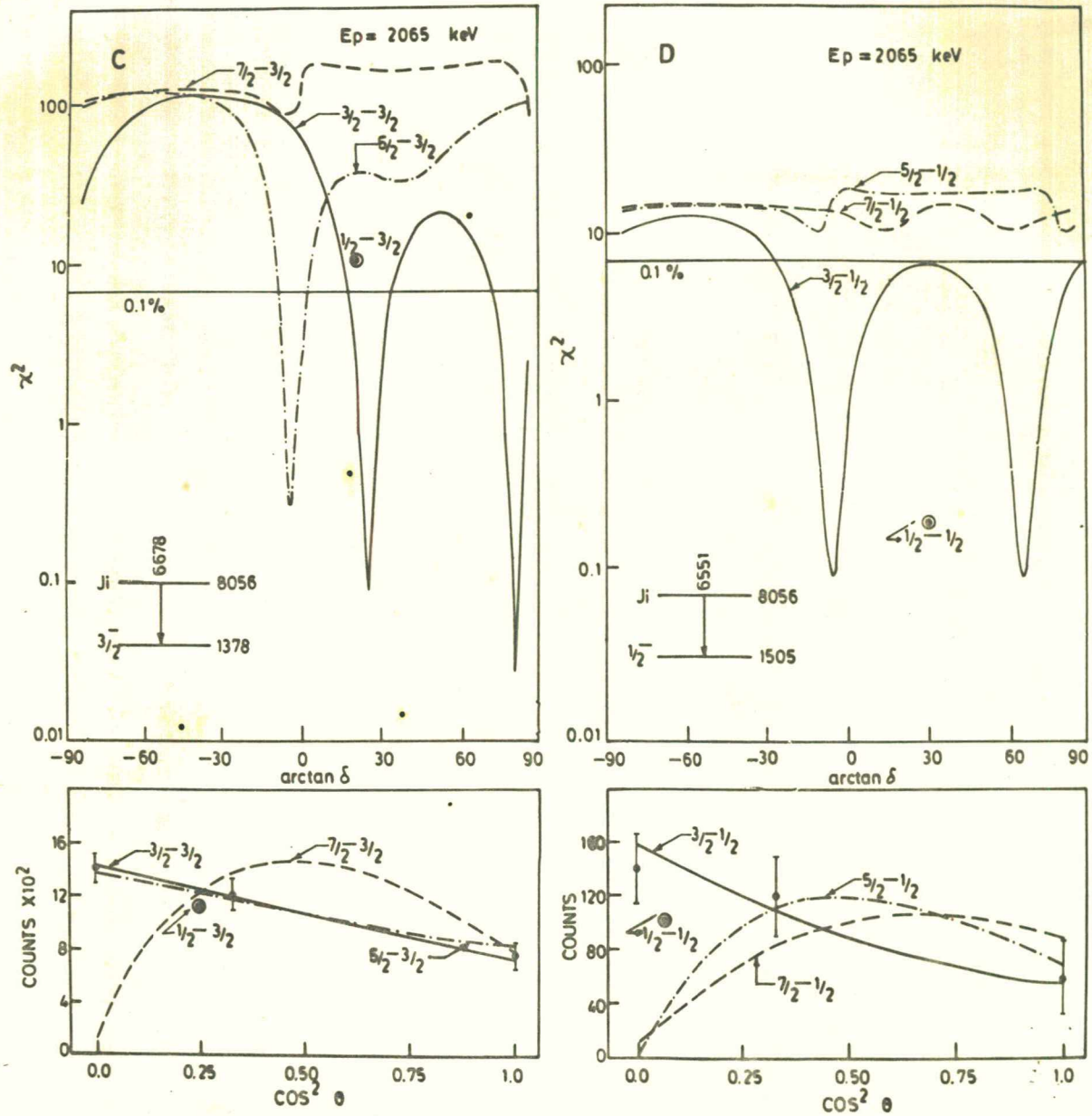

Fig. 8.10 Theoretical fits to experimental angular distributions and χ^2 plots of the (C) 6678 keV and (D) 6551 keV γ-rays from the E_p = 2065 keV resonance.

Dhaka University Institutional Repository

Dhaka University Institutional Repository

Table 8.5

Summary of Legendre polynomial coefficients for the resonances studied.

E_p(lab) (keV)	Primary transition (keV)	A_0	$a_2 = \frac{A_2}{A_0}$	$a_4 = \frac{A_4}{A_0}$
1248	7253	92±8	-0.01±0.14	-0.04±0.13
	5875	1654±96	-0.12±0.10	0.12±0.11
	5748	489±17	-0.48±0.06	-0.05±0.06
1652	6272	3096±176	0.19±0.10	0.11±0.12
	6145	1094±44	-0.55±0.07	0.13±0.06
	5730	295±18	-0.27±0.10	-0.54±0.12
	5517	419±18	0.14±0.07	0.01±0.08
2065	8056	1251±81	-0.35±0.14	0.30±0.13
	6678	1205±81	-0.35±0.10	-0.02±0.76
	6551	115±23	-0.37±0.31	-0.13±0.37
	6159	984±64	-0.40±0.14	0.27±0.13

Table 8.6

Summary of gamma ray angular distributions, $\chi^2_{min.}$ and multipole mixing ratios for the resonances studied.

E_p(lab) (keV)	Primary transition (keV)	Branching ratio %	Spin sequence	χ^2 (min.)	Mixing ratio δ at confidence limit 0.1%	min.	0.1%	
1248	7253	1	3/2−7/2	0.54	−0.40 0.84	−0.16 2.25	0.29 4.70	E2
	5875	39	3/2−3/2	0.36	0.12	0.27	0.47	E2/M1
	5748	13	3/2−1/2	0.22	−0.17 1.80	−0.10 2.14	−0.02 2.61	E2/M1
1652	6272	51	3/2−3/2	0.30	−0.02	0.19	0.32	E2/M1
	6145	18	3/2−1/2	1.30	−0.18 1.88	−0.09 2.14	−0.03 2.75	E2/M1
	5730	6	3/2−5/2	0.80	−0.24 2.90	−0.08 7.12	0.12 -	E2/M1
	5517	6	3/2−5/2	0.36	0.03 1.43	0.18 2.48	0.42 3.73	E2/M1
2065	8056	20	3/2−7/2	2.60	−0.38 1.53	−0.23 2.47	−0.03 4.16	E2
	6678	27	3/2−3/2	0.09	0.31 2.90	0.47 5.67	0.65 -	E2/M1
	6551	1	3/2−1/2	0.09	−0.51 0.58	−0.09 2.14	0.58 19.08	E2/M1
	6159	31	3/2−7/2	2.00	−0.42 1.63	−0.27 2.75	−0.06 5.14	E2

Dhaka University Institutional Repository

Dhaka University Institutional Repository

(fig. 9D) to the 1505 keV state ($J^{\pi} = 1/2^{-}$) it was found that 3/2 is the only acceptable spin value of the 7650 keV resonating state.

The E_p = 2065 keV resonance

The resonating state at 8056 keV (E_p = 2065 keV) and its spin have not been reported so far. Angular distributions for the transitions to the ground (19.6%), 1378 (26.8%), 1505 (1.1%) and 1897 (30.7%) keV states were analysed. From the theoretical fits to the measured angular distributions and χ^2 plots for the transitions to the ground ($7/2^{-}$) and 1897 ($7/2^{-}$) keV states (figs. 10A and 10B) spin assignments of 1/2, 3/2, 5/2 and 7/2 were found possible. However from the analyses of the transitions to the 1378 and 1505 keV states, the following were observed. The transition to the 1378 keV (fig. 10C) allows the 3/2 and 5/2 spin assignments rejecting 1/2 and 7/2 spin values. The transition to the 1505 keV (fig. 10D) indicates that the 1/2 and 3/2 are the possible spin values and rejects the 5/2 and 7/2 values which lie above 0.1% confidence limit. The J = 3/2 spin assignment is allowed in all the transitions. Therefore, the only consistent assignment of spin, J = 3/2 is given for this resonance level.

8.5.3. General remarks

Some more remarks on the results of level schemes and spin assignments are made below. Decay schemes have been

Dhaka University Institutional Repository

constructed and spin have been assigned for the 7253, 7650 and 8056 keV resonance levels at E_p = 1248, 1652 and 2065 keV resonances respectively. The decay scheme of the 2065 keV resonance is reported new. Many more levels than the previous (p,γ) measurements [115-117] have been observed from the present work. The decay scheme of the low-lying levels agrees fairly well with the (p,nγ) measurement of Pietrzyk et al. [113]. It may be mentioned that the 2311, 2489, 2555, 2723, 3459, 3520, 3534, 3554, 3674, 3918, 4238 and 4298 keV levels observed from the present work have not been reported by other (p,γ) measurements [115-117]. The tentative decay[113] of the 3520 keV level by a 1034 keV γ-ray is confirmed. Transitions observed from the 3918 and 4298 keV levels are new. Some weak transitions from the 1248 keV resonance to the 3674 keV (< 1%) state and from the 1652 keV resonance to the 2311 (2.2%), 2805 (< 1%), 3108 (3.1%), 3177 (4.1%), 3723 (1.7%) and 4001 (1.9%) keV levels are observed new. Pietrzyk et al. [113] from the (p,nγ) measurement indicated a limit for the spin of the 2555 keV state as $J \geq 11/2$. However since in the present work one of the branches from the 2555 keV state is found to decay to the ground state ($J^{\pi} = 7/2^-$), the only consistent spin value of the state is J = 11/2. The level at 3534 keV is tentatively identified. In agreement with previous experiments two established low-lying $3/2^-$ states have been observed below 1.8 MeV from the present experiment.

Dhaka University Institutional Repository

It is to be noted that the theoretical calculations [105,106] predict only one low-lying 3/2 state below 1.8 MeV.

A spin value of 3/2 is assigned to the 7253 keV resonance state and the confusion existing so far is removed. The spin assignment of J = 3/2 to the 7650 keV resonance level by the only (p,γ) work of Leslie et al. [115] is confirmed from the present work. The spin assignment of J = 3/2 to the 8056 keV resonance level from the present work is reported new. It is to be noted that transitions from the resonance levels to the established 1505 keV ($J^{\pi} = 1/2^{-}$) level in ^{57}Co have been found to be the most sensitive for spin assignment.

As mentioned above the spins of all the three resonances at E_p = 1248, 1652 and 2065 keV have been obtained as J = 3/2 from the present measurement. The 3/2 spin can be reached through the capture of an l = 1 or 2 proton partial waves. At these low proton bombarding energies the probability of a proton p-wave capture is more than a d-wave, in view of smaller centrifugal barrier for a p-wave. The parity of the resonance levels can then be assigned as negative.

With the spins of the capturing states known, it has been possible to limit the range of spin assignments of some of the low-lying levels namely the 3723, 3268, 3554, 3674 and 3520 keV levels as discussed below.

Dhaka University Institutional Repository

The 3723 keV level is fed from both the 7253 and 7650 keV resonance states and decays 100% to the ground state ($7/2^-$). It is, therefore, very likely that the spin of the 3723 keV level should be $3/2 \leq J \leq 7/2$. The spin $J = 9/2$ reported by Banu et al.[110] thus appears to be unlikely. About the parity of the level it may be mentioned that the level has been excited in the (^{3}He, d) and (d,n)[111] reactions with $l = 4$ and $l = (0)$ respectively. The parity of the 3723 keV level should thus positive.

Since the 3268 keV level is populated by all the three resonance levels ($J=3/2$) and decays to the ground ($J^\pi=7/2^-$) and 1758 keV states ($J^\pi=3/2^-$), it is again possible to limit the spin of the state to $3/2 \leq J \leq 7/2$. The level has been excited by $l=3$ proton transfer reactions as reported by various authors[108-111] and as such the parity of the level must be negative.

The 3554 and 3674 keV states are both populated by resonance states. The 3554 keV level decays to the 1378 ($J^\pi=3/2^-$) and 1758 keV states ($J^\pi=3/2^-$) and the 3674 keV state decays to the 1897 keV state ($J^\pi=7/2^-$). From the decay modes it is likely that the spin of the 3554 keV state is $J \leq 7/2$ and that of the 3674 keV state is $3/2 \leq J \leq 7/2$.

The 3520 keV is fed from the 8056 keV resonance level and decays to the 2489 keV level which has a spin of 11/2.

Dhaka University Institutional Repository

This decay mode is possible for a spin value of 7/2 for the 3520 keV level. But since the angular distribution relating this level could not be measured, the spin of the level is assigned tentatively as 7/2.

Dhaka University Institutional Repository

CHAPTER-9

CONCLUSIONS

Lifetime measurements have been performed in a number of nuclei using the Doppler-shift-attenuation method. Because of the scarce experimental information on the slowing down process of the recoiling nuclei, the stopping power theory of LSS [16] and the expression for multiple scattering given by Blaugrund [19] are employed in the calculation of the theoretical attenuation function $F(\tau)$.

To get rid of the serious problem of gain drift in the γ-ray spectra, a target chamber with two-target arrangement have been used for all lifetime measurements reported here. Using this chamber spectra from both the targets mounted at forward and backward angles are measured simultaneously and, using a routing procedure, are stored separately in the two memories of the multichannel analyser.

By studying the $^{45}Sc(p,\gamma)^{46}Ti$ reaction at proton bombarding energies of 1.75 and 1.80 MeV lifetimes of 12 states and a limit for one state up to an excitation energy of 3905 keV have been determined. A calibrated attenuation curve with a correction factor of $f_e = f_n = 0.9$ was used in the extraction of lifetimes. The small energy shift of the $4_2^- \rightarrow 3_1^-$ transition allowed only to set the lower limit for the 3441 keV level. Our results for the 889.1(2_1^+) and 2009.8(4_1^+) keV long-lived states are in good agreement with

Dhaka University Institutional Repository

the recoil distance data of Dehnhardt et al. [24] although these long lifetimes are close to the region where DSA method is not so sensitive. It demonstrates, however, that the two-target arrangement used in this experiment is a useful apparatus for the DSA work. The systematic discrepancy by a factor of about 2 in the lifetime results existing previously between Durell et al. [22] and Assimakopoulos et al. [23] is resolved in the present experiment. The present results favour the results quoted by Durell et al. [22]. Reduced transition probabilities ($B(\sigma L)$) and transition strengths $|M|^2$(W.u.) for 2961.8, 3058.6, 3168.0, 3235.7 and 3441.7 keV levels are obtained. The $B(E2)\downarrow$ values obtained for the $(2_1^+ \rightarrow 0_1^+)$, $(4_1^+ \rightarrow 2_1^+)$ and $(6_1^+ \rightarrow 4_1^+)$ transitions belonging to the ground state band are compared with theoretical values calculated by Müther et al. [74] and the experimental results of Dehnhardt et al. [24]. Possible spin and parity values for the 3569.4, 3571.7, 3723.9, 3845.0 and 3905.6 keV states are quoted using the criteria set by Nuclear Data Group. (Information obtained from this criteria is not so meaningful).

The $^{45}Sc(p,p'\gamma)$ reaction has been investigated to obtain a calibration of the attenuation curve for the stopping process in ^{45}Sc in addition to determination of lifetimes in ^{45}Sc. This calibration was used for determining

Dhaka University Institutional Repository

the lifetimes in ^{46}Ti using the same ^{45}Sc target. The calibration has been done by comparing the lifetimes of the 720, 1237, 1409, 1662 and 2092 keV levels in ^{45}Sc obtained by Metzger [25] by the resonance fluorescence method which is independent of the slowing down process. A correction factor of $f_e = f_n = 0.9$ obtained from the calibration experiment has been used for the calculation of the attenuation curves. The effect of the undefined kinematics due to singles-spectra measurements of the $^{45}Sc(p,p'\gamma)$ reaction was taken into consideration for extracting lifetimes from the experimental $F(\tau)$ values. This has been done by averaging the $F(\tau)$ curves over all initial velocities and using the angular correlation function as a weighting factor. The formalism is given by Moazed et al. [11]. The new averaged attenuation factor $\widetilde{F(\tau)}$ vs. τ curve was used for the extraction of lifetimes. A complete set of lifetimes of 18 levels in ^{45}Sc is obtained in this work.

Present results for the 720, 1237, 1409, 1662 and 2092 keV levels are in good agreement with the resonance fluorescence data of Metzger [25]. But for the same levels the lifetime values obtained by Chevallier [29] et al. [29] and Rust et al. [27] do not agree with the resonance fluorescence experiment. The lifetime values for the 543, 939, 974, 1303 and 1800 keV levels derived from the present experiment are in good agreement with those obtained by

Dhaka University Institutional Repository

Toulemonde et al. [28] through $^{42}Ca(\alpha,p\gamma)^{45}Sc$ reaction. The lifetime value of the 543 keV level is also in complete agreement with the value 7400^{+2800}_{-1000} fs deduced from the resonance fluorescence experiment of Arnold et al. [25a]. The lifetime value of 2700±400 fs for the 974 keV level by the same resonance fluorescence experiment [25a] is within our experimental error. The comparison of present results with the (p,γ) work of Schulte et al. [26] for levels above 2092 keV shows an excellent agreement for some of the levels while for others there is a complete disagreement. We have no explanation for this. It should, however, be mentioned that the lifetime value for the 1409 keV level obtained by Schulte et al. [26] is smaller than the resonance fluorescence data [25] by a factor of about 3 whereas our result for this level is in good agreement with resonance fluorescence experiment. Now since the present lifetime values for the 543, 720, 974, 1237, 1409, 1662, 1800 and 2092 keV levels are in good agreement with those obtained by the resonance fluorescence data [25,25a], present lifetime values for the other levels may be regarded as more reliable than those of Schulte et al. [26].

Lifetimes of 5 levels in ^{45}Ti have been obtained from the $^{45}Sc(p,n\gamma)^{45}Ti$ reaction at E_p = 4.5 MeV. Mean lifetimes for the 744 and 1226 keV levels are in good agreement with those obtained by Blasi et al. [31a]. Except for the 1521 keV state, lifetimes of other levels are in

Dhaka University Institutional Repository

good agreement with those given by Zuk et al. [30] and Iyengar and Robertson [31].

By the (p,γ) reaction on ^{70}Ge, singles and Ge(Li)-NaI(Tl) coincidence spectra in ^{71}As have been measured. A complete decay scheme with branching ratios of 18 levels obtained in this work is proposed. New levels at 2293, 2435 and 2875 keV have been found and a level at 1192 is tentatively assigned. The previously known 510 keV level is found to be a doublet, with another level at 506.4 keV. Results of other workers are mostly in good agreement with our results.

No lifetime measurements in ^{71}As had been done previously. In this work the lifetimes of 10 states are reported. Possible spin-parity values for some of the levels are given.

Angular distributions of the γ-rays have been measured and decay schemes have been constructed from the ^{56}Fe(p,γ)^{57}Co reaction at E_p = 1248, 1652 and 2065 keV resonances. The decay schemes in ^{57}Co obtained from the present work agree fairly well with the previous workers, particularly with the (p,nγ) measurement of Pietrzyk et al. [113]. Transitions from the 3918 and 4238 keV levels are observed for the first time. A level at 3534 keV has been assigned tentatively. The transitions from the

Dhaka University Institutional Repository

7253 keV(E_p = 1248 keV) resonance state to the 3674 keV level is new. Some weak transitions from the 7650 keV resonance (E_p = 1652 keV) state to the 2311, 2805, 3108, 3177, 3723 and 4001 keV levels have been observed which were not reported in the only previous (p,γ) measurement of Leslie et al.[115] on this resonance. The level scheme of the E_p=2065 keV proton resonance has been studied for the first time in the present experiment.

From the angular distribution measurements of the γ-rays, spins have been assigned to the resonances studied in ^{57}Co. The spin J = 3/2 assigned to the 7253 keV resonance state (E_p = 1248 keV) has removed the discrepancy that existed so long. The spin value J = 3/2 assigned to the 7650 keV (E_p = 1652 keV) resonance state by Leslie et al.[115] has been confirmed by the present work. The spin value J = 3/2 has been assigned to the 8056 keV resonance (E_p = 2065 keV) state for the first time by the present work. With the spins of the proton capture states known and from the mode of population and decay, the spin value of the 3554 keV state should be limited to $J \leq 7/2$ and those of the 3268, 3674 and 3723 keV states should be limited to $3/2 \leq J \leq 7/2$. The spin of the 3520 keV state has been tentatively assigned as 7/2.

Dhaka University Institutional Repository

REFERENCES

1. S.A. Moszkowski, α, β, γ-Ray Spectroscopy edited by K. Siegbahn (1968)

2. E.K. Warburton, in Nuclear Research with Low Energy Accelerators, edited by J.B. Marion and D.M. Van Patter (Academic Press, New York, 1966), p.43

3. A.Z. Schwarzschild and E.K. Warburton, Ann. Rev. Nucl. Sc. 18 (1968)265

4. C. Broude, in Proc. Int. Conf. Properties of Nuclear states, Montreal, edited by M. Harvey, R.Y. Cusson, J. Geiger, and J.M. Pearson (Univ. of Montreal, 1969), p.221

5. D.B. Fossan and G.K. Warburton, in Nuclear Spectroscopy and Reactions, Part C, edited by Joseph Cerny (Academic Press, New York, 1974), p.307

6. S. Devons, G. Manning and D.St.P. Bunbury, Proc. Phys. Soc. (London) A68 (1955)18

7. D.St.P. Bunbury, S. Devons, G. Manning and J.W. Towle, Proc. Phys. Soc. (London) A69 (1956)165

8. S. Devons, G. Manning and J.W. Towle, Proc. Phys. Soc. (London) A69 (1956)173

9. A.E. Litherland, M.J.L. Yates, B.M. Hinds and D. Eccleshall Nucl. Phys. 44 (1963)220

10. E.K. Warburton, D.E. Alburger and D.H. Wilkinson, Phys. Rev. 129 (1963)2180

11. Cyrus Moazed, T. Becker, P.A. Assimakopoulos and D.M. Van Patter, Nucl. Phys. A169 (1971)651

12. P. Paul, J.B. Thomas and S.S. Hanna, Phys. Rev. 160 (1967)774

13. E.K. Warburton, J.W. Olness and A.R. Poletti, Phys. Rev. 160 (1967)938

14. J.R. MacDonald, D.F.H. Start, R. Anderson, A.G. Robertson and M.A. Grace, Nucl. Phys. A108 (1968)6

15. M.G. Bertin, N. Benczer-Koller, G.G. Seaman and J.R. MacDonald, Phys. Rev. 183 (1969)964

Dhaka University Institutional Repository

16. J. Lindhard, M. Scharff and H.E. Schitt, Mat. Fys. Medd. Dan.Vid. Selsk. 33, No. 14(1963)

17. J. Lindhard and M. Scharff, Phys. Rev. 124 (1961)128

18. J. Lindhard, V. Nielsen and M. Scharff, Mat. Fys. Medd. Dan. Vid. Selsk. 36, No. 10(1968)

19. A.E. Blaugrund, Nucl. Phys. 88 (1966)501

20. A. Antilla, J. Keinonen and M. Bister, Nucl. Instr. & Meth., 124 (1975)605

21. H.P. Nottrodt, F. Rauch and P. Hubener, Nucl. Instr. & Meth., 133 (1976)581

22. J.L. Durell, G.D. Dracoulis and W. Gelletly, J. Phys. A: Math., Nucl. Gen., 7 (1974)1448

23. P.A. Assimakopoulos, T. Becker, Cyrus Moazed and Van Pater, Nucl. Phys. A180 (1972)131
and references therein

24. W. Dehnhardt, O.C. Kistner, W. Kutschera and H.J. Sann Phys. Rev. C7 (1973)1471

25. F.R. Metzger, Phys. Rev. C12 (1975)312

25a. R.G. Arnold, E.C. Booth and W.J. Alston, Phys. Rev. C7 (1973)1490

26. R.L. Schulte, J.D. King and H.W. Taylor, Phys. Rev. C9 (1974)1436

27. N.J.A. Rust, W.J. Naude, J.W. Koen and W.L. Mouton, Nucl. Phys. A219 (1974)232

28. M. Toulemonde, J. Chevallier, B. Haas, N. Schulz and J. Styczen, Nucl. Phys. A262 (1976)307
and references therein

29. J. Chevallier, B. Haas, N. Schulz and M. Toulemonde, J. Phys. (Paris) 37 (1976)303

29a. J.R. Beene, Nuclear Data Sheets 22 (1977)1

30. W.M. Zuk, W.F. Davidson, L.E. Carlson and M.R. Najam Nucl. Phys. A187 (1972)501

31. K.V.K. Iyengar and B.C. Robertson Nucl. Phys. A171 (1971)73

Dhaka University Institutional Repository

31a. P. Blasi, M. Morando, P.R. Maurenzig and N. Taccetti, Lett. Nuovo Cimento 2 (1971)63

32. L. Broman and B. Rosner, Nucl. Phys. A114(1968)237

33. R.R. Betts, S. Mordechai, D.J. Pullen, B. Rosner and W. Scholz, Nucl. Phys. A230 (1974)235

34. Ulrich Frhr. V. Hundelshausen, Z. Phys. 225 (1969)125

35. B. Heits, H.G. Friedrichs, A. Rademacher, K.O. Zell and P. von Brentano and C. Protop, Phys. Rev. C15 (1977)1742

36. Y.C. Liu, T.H. Hsu, E.K. Lin, P.K. Tseng, C.C. Hsu and C.W. Wang, J. Phys. Soc. Jap. 39(1975)1

37. R.L. Auble, Nuclear Data Sheets 20 (1977)327

38. J.H. Ormrod and H.E. Duckworth, Can. J. Phys.41(1963)1424

J.H. Ormrod, J.R. MacDonald and H.E. Duckworth, Can. J. Phys. 43 (1965)275

39. J.R. MacDonald, J.H. Ormrod and H.E. Duckworth, Z. Naturforschung, 21a (1966)130

40. P. Hvelplund and B. Fastrup, Phys. Rev. 165 (1968)408

41. B. Fastrup, P. Hvelplund and C.A. Sautter, Mat. Fys. Medd. Dan. Vid. Selsk, 35 (1966), no. 10
and references therein

42. S. Goudsmit and J.L. Saunderson, Phys. Rev. 57 (1940)24, 58 (1940)36

43. H.W. Lewis, Phys. Rev. 78 (1950)526

44. G.A.P. Engelbertink, H. Lindeman and M.J.H. Jacobs, Nucl. Phys. A138 (1969)588

45. W. Strassheim, Thesis, Frankfurt University, 1971

46. P.Hvelplund, Mat. Fys. Medd.Danm.Vid.Selsk 38 (1971)no.4

47. A.H. El-Hoshy and J.F. Gibbons, Phys. Rev. 173 (1968)454

48. M. Bister, A. Anttila, A. Fontell and E. Leminen, Z. Phys. 250 (1972)82

49. A. Antilla, M. Bister, and M. Piiparinen, Nucl. Ins. & Meth. 96 (1971)141

Dhaka University Institutional Repository

50. M. Bister and A. Anttila, Nucl. Ins. & Meth. 77(1970)315

51. W.M. Currie, L.G. Earwaker and J. Martin, Nucl. Phys. A135 (1969)325

52. R. Hartmann and H. Grawe, Nucl. Phys. A164 (1971)209

53. C. Broude, P. Engelstein, M. Popp and P.N. Tandon, Phys. Letts., 39B (1972)185

54. M. Toulemonde and F. Haas, Phys. Rev. C15 (1977)49

55. C. Broude, F.A. Beck and P. Engelstein, Nucl. Phys. A216 (1973)603

56. W.C. Currie, Nucl. Instr. & Meth. 73 (1969)173

57. B.M. Latta, P.J. Scanlon, Nucl. Instr. & Meth 114 (1974)179

58. M. Kreger, P. Kump, M. Pavsic and M. Vakselj Nucl. Instr. & Meth. 109 (1973)109

59. B.C. Robertson and J.R. Leslie, Nucl. Instr. & Meth. 114 (1974)389

60. K.B. Winterbon, Can. J. Phys. 50 (1972)3147

61. R. Doerr, F. Rauch, W. Schafer and D.M. Van Patter, International conference on Gamma-ray Transition Probabilities, Delhi (1974)

62. F.R. Metzger, Phys. Rev. C9 (1974)1525
Nucl. Phys. A182 (1972)213

63. P. H. Stelson and L. Grodzins, Nucl. Data, 1 (1965)21

64. Nuclear Physics A214, edited by P.M. Endt and C. Van Der Leun, page 195

65. E.L. Chupp, J.W.M. Dumond, F.J. Gordon, R.C. Jobson and Hans Mark, Phys. Rev. 112 (1958)518

66. Th. Weber, Annual Report, Univ. Frankfurt, IKF-32(1973)43

67. B. Erlandsson and K. Valli, Arkiv fur Fysik 24(1962)31

68. J. Dubois and S. Maripuu, Arkiv fur Fysik, 24 (1963)127

69. M.A. Rahman, M. Rahman and H.M. Sen Gupta, Nucl. Sci. & Appl. 7 (1974)21

70. R.N. Horoshko, P.F. Hinrichsen and H.L. Scott., Nucl. Phys. A118 (1968)609

Dhaka University Institutional Repository

71. D.J. Church, R.N. Horoshko and G.E. Mitchell Phys. Rev. 160 (1967)894

72. C.W. Lewis, J.N. Mo, C.F. Monahan, M.F. Thomas and P.J. Twin, Nucl. Phys. A107 (1968)273

73. A. Gallmann, G. Guillaume, N.E. Davison, P. Wagner and G. Franck, Nucl. Phys. A166 (1971)271

74. H. Muther, K. Goeke, K. Allaart and Amand Faessler, Phys. Rev. C15 (1977)1467

75. J.D. McCullen, B.F. Bayman and L. Zamick Phys. Rev. 134 (1964)B515

76. A.E. Blaugrund, R.E. Holland and F.J. Lynch Phys. Rev. 159 (1967)926

77. D.A. Eastham and W.R. Phillips, Nucl. Phys. A146 (1970)112

78. D. Alkhazov, A. Grinberg, G. Gusenskii, E. Erokhina and I.K. Lemberg, Sov. Phys. - JEPT, 10 (1960)1086

79. N. Imanishi, F. Fukayawa, M. Sakisaka and Y. Uemura, Nucl. Phys. A101 (1967)654

80. O.F. Afomin, A.P. Grinberg, I.K. Lemberg and I.N. Chugunov, Sov. J. Phys. 6 (1968)160

81. D.S. Andreev, O.F. Afomin, V.K. Bonderev, A. Grinberg, K.I. Erokhina and I.K. Lemberg, Bull. Aca. Sci. USSR Phys. Ser. 32 (1968)1543

82. M.D. Goldberg and B.W. Hooton, Nucl. Phys. A132 (1969)369

83. R.J. Peterson and D.M. Perlman, Nucl. Phys.A117 (1968)185

84. E. Sheldon, Revs. Mod. Phys. 35 (1963)795

85. R.L. Schulte, J.D. King and H.W. Taylor, Can. J. Phys. 52 (1974)131

86. R.D. Lawson and J.L. Uretski, Phys. Rev. 108(1957)1300

87. A. de-Shalit, Phys. Rev. 122 (1961)1530

88. P.M. Endt and C. Van der Leun, Nucl. Phys. A105 (1967)1

89. W.M. Zuk, G.D. Symons and D.J. Baugh, Aust. J. Phys. 24 (1971)13

Dhaka University Institutional Repository

90. P. Blasi, T.F. Fazzini, P.R. Maurenzig, N. Tacetti and R.A. Ricci, Nuovo Cimento 68 (1970)49

91. J.D. McCullen, B.F. Bayman and L. Zamuck Phys. Rev. 134 (1964)B515

92. F.B. Malik and W. Scholz, Phys. Rev. 150 (1966)919

93. I.P. Johnstone, Phys. Letts. 28B (1969)643

94. J.L'Ecuyer and C. St-Pierre, Nucl. Phys. A100 (1967)401

95. H.F. Lutz and T.S. Bohn, Nucl. Phys. A116(1968)112

96. E. Kashy and T.W. Conlon, Phys. Rev. 135 (1964)B389

97. G.D. Jones, R.R. Johnson and J.H. Jett, Nucl. Phys. A111 (1968)449

98. P.J. Plauger and E. Kashy, Nucl. Phys. A152 (1970)609

99. F.J. Lynch, K.E. Nysten, R.E. Holland and R.D. Lawson Phys. Letts. 32B (1970)38

100. J.H. Jett, G.D. Jones and R.A. Ristinen Phys. Letts. 28B (1968)111

101. K.V.K. Iyengar, E. Wong and G.C. Neilson Nucl. Phys. A155 (1970)582

102. F. Rauch, Z. Physik 243 (1971)105

103. C.J. Umbanger, C.A. Close, W.L. Sievers and R.C. Bearse, Phys. Rev. C3 (1971)199

104. Handbook of Chemistry and Physics, edited by Robert C. Weast (CCR Press, 1974-1975)P. B93

105. C. Gatrousis, R.A. Meyer, L.G. Mann and J.B. McGrory, Phys. Rev. 180 (1969)1052

106. L. Satpathy and S.C. Gujrathi, Nucl. Phys. A110 (1968)400

107. H. Horie and K. Ogawa, Nucl. Phys. A216 (1973)407

108. B. Rosner and C. Holbrow, Phys. Rev. 154(1967)1080

109. G. Hardie, T.H. Braid, L. Meyer-Schutzmeister and J.W. Smith, Phys. Rev. C5 (1972)1600

Dhaka University Institutional Repository

110. Hamida Banu, H.M. Sen Gupta and F. Watt, Nucl. Phys. A307 (1978) 106

111. A. Adam, O. Bersillon and S. Joly, Phys. Rev. C14 (1976)92

112. R. Dayras, M. Toulemonde, B. Cujec, B. Heusch, J.N. Mo and I.M. Szoghy, Nucl. Phys. A173 (1971)49

113. P. Pietrzyk, K.D. Buchs, E. Finckh, W. Fritsch and B. Schreiber, Z. Physik 262 (1973)239

114. K.S. Burton and L.C. McIntyre, Phys. Rev.C3 (1971)621

115. J.R. Leslie, W. McLatchie, C.F. Monahan and J.K. Thrasher, Nucl. Phys. A170 (1971)115

116. B.J. O'Brien and G.E. Coote, Nucl. Phys. A153 (1970)593

117. S. El-Kateb and G.M. Griffiths, Nucl. Phys. A240 (1975)120

118. S.E. Arnell and P.O. Persson, Ark. Fys. 26 (1964)193

119. D.R. Abraham, L.D. Ellsworth, S. Hechti, D.G. Megli and J.C. Legg, Bull. Am. Phys. Soc. 14 (1969)1234

120. H. Braondle, W.R. Wylie, and F. Zambori and W. Zuch, Nucl. Phys. A151 (1970)211

121. D.R. Waymire, Phys. Abs. 75 (1972)3772

122. M.A. Awal, M.A. Rahman, M. Rahman and H.M. Sen Gupta, Nucl. Sc. and Appln. 9B (1976)1

123. H.J. Rose and D.M. Brink, Rev. Mod. Phys.39(1967)306

124. O. Hausser, J.S. Lopes, H.J. Rose and R.D. Gill, Nuclear Physics Laboratory Report (Oxford, 1966)

125. A.H. Wapstra, G.J. Nijgh and R. Van Lieshout, Nuclear spectroscopy tables (North-Holland Publishing Company, Amsterdam, 1959)

126. R.E. Azuma, L.E. Carlson, A.M. Charlesworth, K.P. Jackson, N. Anyas-Weiss and B. Lalovic, Can. J. Phys. 44 (1966)3075